Title
LIGHT INTERFERENCE IN ELECTROLYTE FILMS ON METALS

Author
Sand, Michael L.

Publication Date
1975-06-01

LBL-3589

LIGHT INTERFERENCE IN ELECTROLYTE FILMS ON METALS

Michael L. Sand
(M. S. thesis)

June 1975

Prepared for the U. S. Energy Research and
Development Administration under Contract W-7405-ENG-48

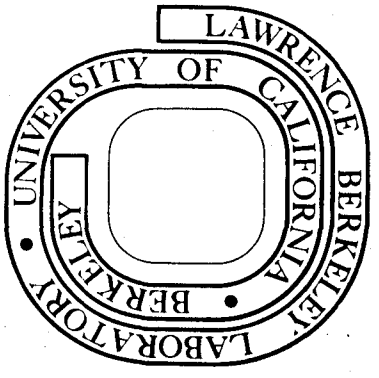

LBL-3589

DISCLAIMER

LIGHT INTERFERENCE IN ELECTROLYTE FILMS ON METALS

Contents

LIGHT INTERFERENCE IN ELECTROLYTE FILMS ON METALS

Michael L. Sand

Inorganic Materials Research Division, Lawrence Berkeley Laboratory and
Department of Chemical Engineering; University of California
Berkeley, California 94720

ABSTRACT

The colorimetry of interference colors has been examined for the purpose of optically determining the thickness of transparent films on metal substrates. Interference color series for arbitrary phase change in reflection and surfaces of different reflectivities have been computed. Optimum angles of incidence for the observation of thin film interference have been determined based on the criterion of maximum color purity and compared to that based on monochromatic fringe visibility. Computations for the optimum angle of incidence and sequences of interference colors have been verified with film-substrate combinations of different phase change and reflectivity. As an application, the thickness profiles of aqueous potassium hydroxide films on a platinum surface have been measured.

I. INTRODUCTION

The current-voltage characteristics of gas diffusion electrodes in electrochemical fuel cells have been of increasing interest during the past 20 years. Mechanisms have been proposed by which the charge transfer can occur. Observed currents have been calculated by assuming the existence of a thin electrolyte film above the meniscus of an electrolyte in contact with the electrode.

Will's observations and theory,[1,2] written in 1963, formed a sound basis for subsequent research. From electrical measurements he deduced the existence of a thin film above the meniscus at a platinum electrode partially immersed in acidic solution. Electrochemical oxidation of hydrogen occurred mainly in a narrow zone in the thin film adjacent to the upper edge of the meniscus. He discounted the theory of Justi et al.[3] that surface diffusion of hydrogen atoms along the electrode to a reaction zone below the top of the meniscus was the rate determining step.

Other authors[4-8] have found the main source of current to be localized in a relatively small region above the meniscus. Film thicknesses were found to be on the order of 1 micron.[6,8] Some studies have used smooth platinum electrodes to investigate factors that alter the thin films. Burshtein[9,10] has shown that the electrolyte film depends on the properties of the surface of the electrode and on the composition of the solution. As did Burshtein, Shepelin[11] observed both film and lens formation. He said that the question of film stability was not altogether clear. A distinction should be made between the "capillary" film, which forms on a rough surface independent of the current, and the stability of current-formed films. He suggested that the upward

stretching of a film under current could be caused by positive surface tension gradients.

Studies that showed experimental evidence for the existence of stable films of electrolyte solutions above the meniscus in gas diffusion electrodes prompted Lightfoot[12-14] to investigate the source of their stabilization. In one of his articles,[14] he chose to discuss the Marangoni effect, which is the movement of liquid due to surface tension gradients. He proposed a model of a dynamic thin film whose internal motion was due to surface tension gradients caused by concentration or temperature gradients. These effects have been analyzed elsewhere.[15-19] Lightfoot said that some observations were still left unexplained. He cited the article of Muller,[20] which reported the existence of stable films with thicknesses on the order of a micron in the apparent absence of surface tension gradients and the upward growth of a concentrated electrolyte film over a dilute one against a downward directed surface tension gradient.

Other attempts have been made to explain the existence of thin liquid films on vertical surfaces. Bascom et al.[21] wrote an excellent article in 1964 describing their study of spreading of oils on solids. They observed oil spreading mainly on vertical surfaces and developed a mechanism that included both a primary film advancing largely by surface diffusion and a secondary film advancing as a result of surface tension gradients. Microroughness was found to affect the spreading rate. Bikerman[22,23] felt that not enough attention has been focused on the contribution of surface roughness to the formation of thin films. He drained oils from stainless steel plates with different roughnesses. The

theory of drainage[24] was approximately fulfilled by the smoothest plates. However, on the rough plates, an apparently stagnant liquid layer existed whose thickness was nearly equal to the average heights of hills on the solid surface. Read and Kitchener [25] attempted to explain the existence of wetting films (0.1 micron) of water on silica in terms of Deryagin's "disjoining pressure" concept, which was briefly discussed in an article of Deryagin's.[26] The surface free energy is no longer independent of the form of the liquid, when the thickness becomes comparable to the range of action of surface forces. The gradient of surface tension must balance the hydrostatic pressure.

Much work has been performed under the supervision of Muller[20,27,28] on the formation of thin electrolyte films on vertical metal surfaces in the absence of any externally applied gradients of temperature or concentration. He has established the geometry of stable electrolyte films on polished metal surfaces partially immersed in aqueous caustic solutions. Using optical methods of thin film interference[20,27] and ellipsometry,[28] he found thicknesses on the order of 1 micron. After initial drainage, a stationary film was established after a period on the order of 10 hr. Film geometries have not changed over periods of several weeks. It was found that the thickness of stable films increases with increasing concentration. Thus, a 3.5N potassium hydroxide film could be grown upward on a nickel surface covered by a film of distilled water.[20]

A smooth, planar and vertical electrode is an idealized geometry for the observation of liquid films and is well suited for both electrochemical analysis and optical thickness measurements. Light

interference is a method that has been used in other investigations and in this one. It has an advantage over mechanical and electrical techniques in that it creates a minimal amount of disturbance in the film. In this study, the computationally involved method of white-light interference[20,27] was employed. It has an advantage over ellipsometry[28] in that the thicknesses over an extended region can be recorded simultaneously in a photograph. It is to be preferred over monochromatic interference due to the fact that the observer can distinguish several hues in the same interference order and differentiate between orders. Therefore, thickness measurements can be made with a greater degree of certainty.

Distinct interference fringes must be observable if one is to make accurate thickness measurements of thin transparent films on metal surfaces. Fringe contrast of both monochromatic and white-light interference fringes can be significantly improved with the use of polarized light and the proper choice of the angle of incidence. The colorimetry of interference colors of dielectric films on metal surfaces has received little attention since the review of Kubota[29] in 1961. Under the supervision of Muller, "generalized" color charts were developed[27] and checked experimentally.[30] The concept of an "optimum angle of incidence" to maximize the color purity of white-light interference fringes was investigated[27] as an extension of the work of Muller[31] in monochromatic interference.

In the present study, the colorimetry of interference colors is examined in great detail. Concepts expressed in previous work[27,30,31] are developed further. Color charts for surfaces of specified reflectivities

are presented as part of a graphical representation of white-light interference. Also, results of computations of the optimum angle of incidence are presented graphically for both monochromatic and white-light interference. A more exact analysis of interference for a specific film and substrate can be obtained with the computer programs given in the Appendix. The present analysis of white-light interference clarifies uncertainties in the calculations of Turney[27] and Brown.[30] Computer programs in the Appendix are both revised and corrected versions of programs[27] used by both of these investigators.

Experimental verification of calculated color series has been undertaken by Brown, who made several independent thickness measurements of the same dielectric films on metal surfaces. A few film thickness profiles measured by different techniques, however, showed some disagreement. The present work has uncovered errors that are sources of much of the disagreement. Also, colorimetrically determined thickness profiles of cryolite films on chromium and aluminum have been compared with ellipsometrically measured profiles. The agreement is generally very good. The experimentally observed angles of incidence at which the interference colors appeared most saturated were compared with the calculated values. Agreement between calculated and observed optimum angles is very good.

An investigation of the thickness profiles of thin films of aqueous solutions on vertical electrodes was undertaken as a continuation of previous work.[20,27] Aqueous potassium hydroxide solutions were used as the liquid film material, while optically polished platinum was used as the metal substrate. The number of valid experimental results

was very limited. Only the results for the drainage of two potassium hydroxide solutions are reported. Contrary to the previous work, film drainage continued at times much longer than 1 day following the lowering of the meniscus. Viscosities much greater than those of the bulk solutions must be assumed in order to obtain agreement between experimental and theoretical thickness profiles during drainage.

II. OPTICAL INTERFERENCE IN THIN FILMS

Optical interference is a useful technique for determining the thickness of thin films. It affords minimal disturbance to a film and at the same time it allows one to measure the thickness over an extended region. In monochromatic interference, the interference fringes alternate between dark and light regions. In white-light interference, one may observe continuously changing colors as the thickness changes. White-light interference has a distinct advantage over monochromatic interference in that the eye is much more sensitive to a change in color than to a change in shade. Also, different interference orders with monochromatic light appear identical, while with white light they can be distinguished. The following paragraphs are presented to introduce the development of the equations and the application of the theory.

The basis for interference lies in the sinusoidal wave nature of light in which any number of superimposed waves of the same wavelength but arbitrary phase can combine vectorally to produce a resultant wave of the same wavelength. Its amplitude varies from a value of zero to one with a value equal to the sum of the amplitudes of the individual waves. Consequently, the amplitude of the resultant wave at each wavelength throughout the spectrum can be established. Thin film interference is a special case in which reflection and refraction of light waves at the interfaces of a film produce multiple waves from a single, polarized and monochromatic incident wave in a beam of light that is temporally and spatially coherent. Phase differences among these multiple waves can be described quantitatively. They stem from phase changes due to reflection at the interface between one medium and

another as well as from differences in optical path length traveled by each wave. The amplitude of the reflected and refracted waves at each interface are quantitatively described, too, in the equations for the amplitude reflection and transmission coefficients. An infinite number of monochromatic light waves of known amplitude and relative phase thus comprise the multiple-beam model for interference in thin films. Although the incident waves enter the film at different distances from the point of exit, their interference represents the thickness very close to the point of exit because of the very small thickness of the film.

The use of white light as the source of incident light enhances the value of the interference technique, but interpretation of fringes requires more computational effort. It should be noted that a fringe is a dark or bright region in monochromatic interference, while in white-light interference it is a colored region that can be clearly distinguished from an adjacent region of a different hue. In order to use a light source for colorimetric analysis, one must know its spectral intensity distribution. The intensity distribution of the reflected beam can be calculated by applying the interference equation to each wavelength. As the thickness of a film on a substrate is varied, the intensity of every resultant monochromatic wave passes through minima and maxima at film thicknesses characteristic of each wavelength. Thus, the wavelengths that are dominant in the spectral intensity distribution change with film thickness. Wavelength intervals in the spectrum are represented by different colors. As the dominant color changes with film thickness, the hue of the interference color changes. As opposed to monochromatic interference, sequences of hues within each color

order can be observed. This particular fact points to the advantage of using a white-light source, which is that absolute thicknesses can be measured with a greater degree of certainty. Similar white-light interference colors can result from different film thicknesses. However, the spectral energy distribution of the reflected light is different. An approach that can be more clearly defined is to use a color theory that can quantitatively represent every color. Each color is considered to be composed of three primary colors, all of which vary in magnitude through the spectrum. A beam of light with a known spectral intensity distribution can be assigned a color according to the fractional content of the primary colors.

The ability of an observer to identify interference fringes from a film-substrate combination is of critical importance in determining film thicknesses. In monochromatic interference, fringe contrast depends on the intensity variation with film thickness. A measure of the fringe contrast is the Michelson fringe visibility, which is calculated from the maximum and minimum intensities. In white-light interference, the ability of an observer to identify a hue depends on the color saturation. Both the fringe contrast and color saturation are dependent on the optical constants of the film and substrate, the polarization of light and the angle of incidence and are highest at the "optimum angle of incidence." The optimum angles to observe monochromatic and white-light interference fringes do not necessarily coincide.

Spectral analysis at selected points along a film is another method of determining the thickness. The interference spectrum is measured as a ratio of reflected to incident intensity through the spectrum. Of

special interest are the wavelengths at which the maxima and minima of intensity occur. At the monochromatic optimum angle of incidence, complete destructive interference can occur and the minimum intensities are zero.

A. Sign Conventions and Definitions

Phase changes due to reflection at interfaces between two media necessitate the consistent use of a sign convention for the direction of the positive electric field vectors. Although it is not crucial which sign convention is used, it must be reflected in the equations for the amplitude reflection(r) and transmission(t) coefficients. A reflection coefficient is the ratio of the electric field amplitude, E", of reflected light to the electric field amplitude, E, of incident light, while a transmission coefficient is the ratio of the electric field amplitude, E', of refracted light to the amplitude of incident light. Subscripts, n, on amplitudes, phase changes and coefficients may represent either the interface at which transmission and reflection occur or the polarization of light. The subscripts, s and p, refer to light polarized perpendicular and parallel, respectively, to the plane of incidence. The plane of incidence is one which contains the propagation vector for the incident, reflected and refracted waves. These terms are more clearly defined in Fig. 1. The propagation direction is defined according to the angle it makes with the normal to the interface. These angles are represented in Fig. 2. The incident and refracting dielectric media have refractive indices, n_0 and n_1, respectively.

A convenient way of expressing the amplitude and phase of a light wave relative to a specified reference light wave is through the use

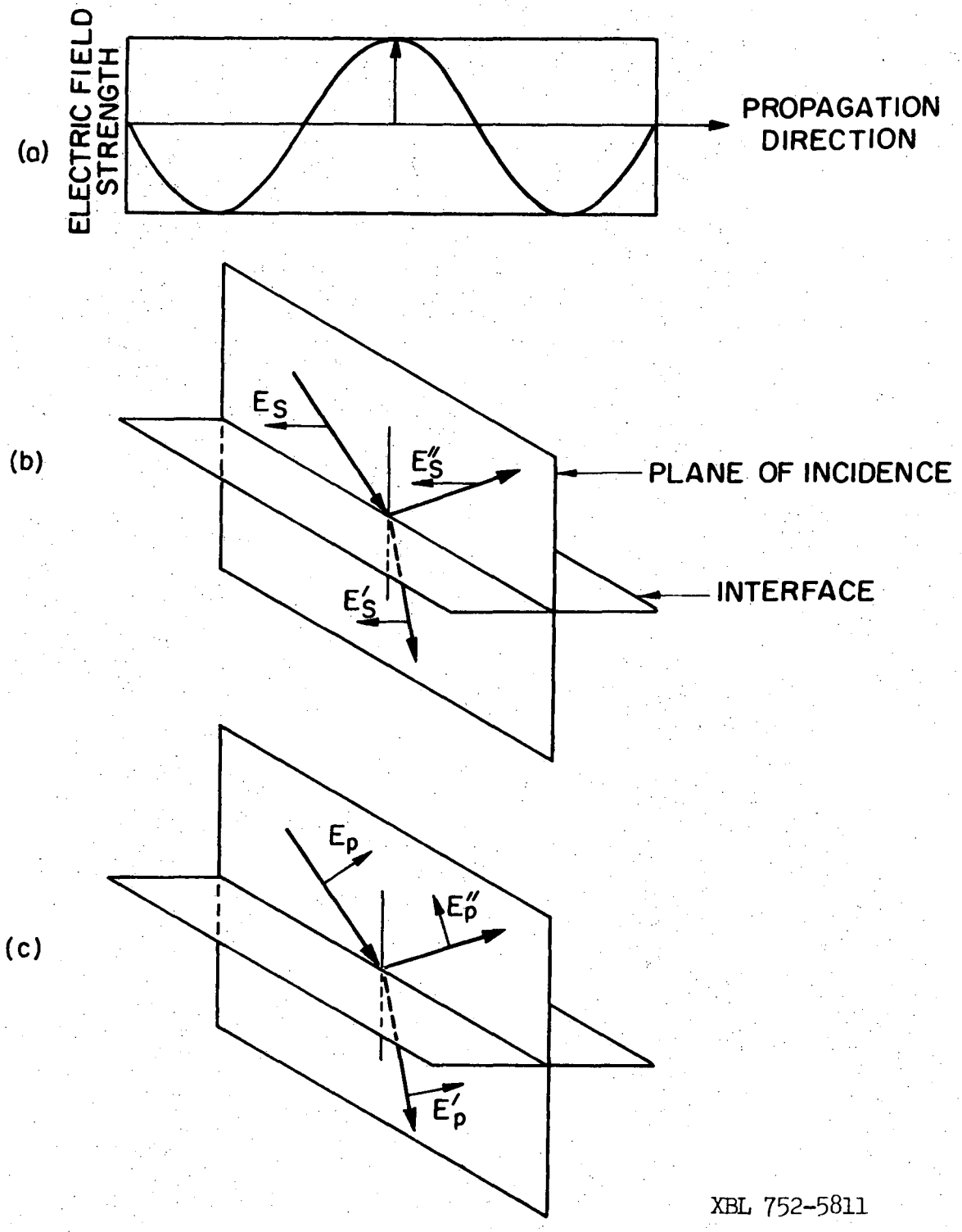

Fig. 1. (a) Electric field strength of linearly polarized light at fixed time and as a function of space. (b) Positive electric field vectors for incident (E_s), reflected (E''_s) and refracted (E'_s) waves for light polarized perpendicular to the plane of incidence. (c) Positive electric field vectors for incident (E_p), reflected (E''_p) and refracted (E'_p) waves for light polarized parallel to the plane of incidence.

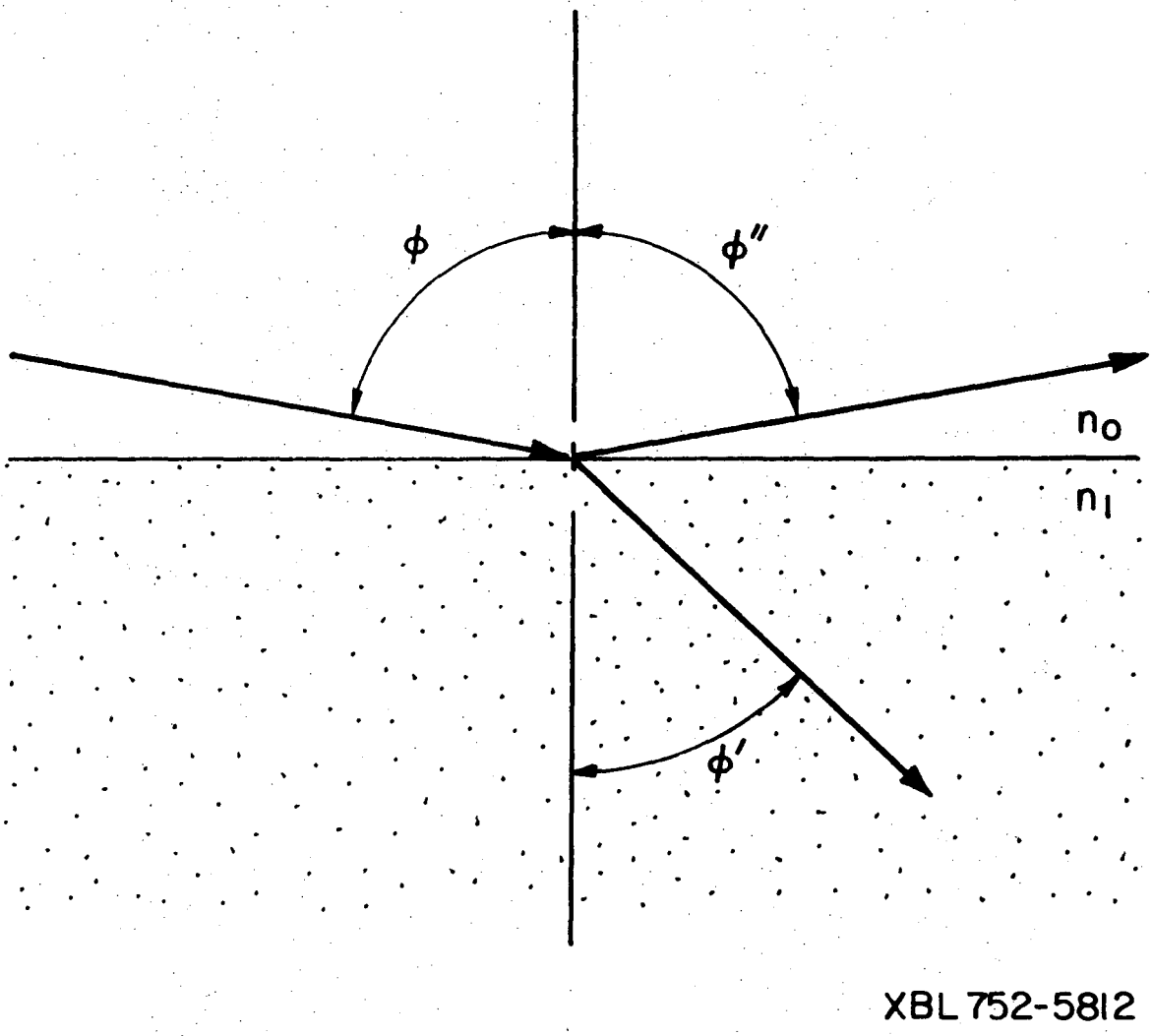

Fig. 2. Propagation directions defined by angle of incidence (ϕ), refraction (ϕ') and reflection (ϕ'').

of complex numbers.[32] The amplitude, E_n, and relative phase, δ_n, of a light wave are both contained in the complex amplitude $\hat{E}_n$ where

$$\hat{E}_n = E_n e^{i\delta n} \quad .$$

Equation (1) is written in the complex notation. A reference phase, δ_r, is an arbitrary quantity and can be taken equal to zero. The time dependent phase, ωt, equals the product of the angular frequency, ω, and time, t. The spatial dependent phase, $\vec{k}\cdot\vec{x}$, equals the dot product of the propagation vector, $\vec{k}$, and the position vector, $\vec{x}$. The quantity, i, is the imaginary unit $\sqrt{-1}$ in the complex plane. The use of the complex notation is most quickly understood, when it is shown that the addition of two vectors in the complex plane is equivalent to the trigonometric addition of the corresponding waves. The general form of the equation that describes a light wave incident onto an interface is

$$\hat{E}_n = E_n e^{i(\omega t+\delta_r-\vec{k}\cdot\vec{x})} = E_n\cos(\omega t+\delta_r-\vec{k}\cdot\vec{x}) + iE_n\sin(\omega t+\delta_r-\vec{k}\cdot\vec{x}) \quad . \qquad (1)$$

A complex reflection coefficient, $\hat{r}_n$, is defined as being the ratio of the complex amplitude of reflected light to the complex amplitude of incident light. δ_n is the phase change due to reflection. A phase change caused by a difference in optical path length traversed by interfering waves is designated by δ without a subscript.

$$\hat{r}_n = \frac{E_n'' e^{i(\omega t+\delta_r+\delta_n-\vec{k}\cdot\vec{x})}}{E_n e^{i(\omega t+\delta_r-\vec{k}\cdot\vec{x})}}$$

$$= \frac{E_n''}{E_n} e^{i\delta_n} \qquad (2)$$

$$= r_n e^{i\delta_n}$$

For unit incident amplitude, Eq. (2) represents the amplitude and phase of reflected light. Since transmission has no associated phase change, a complex transmission coefficient, $\hat{t}_n$, equals the real coefficient, t_n, which is the ratio of E'_n to E_n. For unit incident amplitude, the transmission coefficient, t_n, is the amplitude of a refracted light wave. Both t_n and r_n are always positive numbers.

B. Reflection and Transmission Coefficients

The amplitude reflection coefficients for a dielectric-dielectric interface for light polarized perpendicular(s) and parallel(p) to the plane of incidence are given by the Fresnel equations.[33] The terms within the absolute value signs are the complex quantities, $\hat{r}_n$. A negative $\hat{r}_n$ signifies that the phase change, δ_n, in Eq. (2) is 180° (π radians), since $e^{i\pi} = -1$.

$$r_s = \frac{E''_s}{E_s} = \left|\frac{n_0\cos\phi - n_1\cos\phi'}{n_0\cos\phi + n_1\cos\phi'}\right| \equiv \left|\frac{-\sin(\phi - \phi')}{\sin(\phi + \phi')}\right| \qquad (3)$$

$$r_p = \frac{E''_p}{E_p} = \left|\frac{n_1\cos\phi - n_0\cos\phi'}{n_1\cos\phi + n_0\cos\phi'}\right| \equiv \left|\frac{\tan(\phi - \phi')}{\tan(\phi + \phi')}\right| \qquad (4)$$

The amplitude transmission coefficients are

$$t_s = \frac{E'_s}{E_s} = \frac{2n_0\cos\phi}{n_0\cos\phi + n_1\cos\phi'} \qquad (5)$$

$$t_p = \frac{E'_p}{E_p} = \frac{2n_0\cos\phi}{n_1\cos\phi + n_0\cos\phi'} \qquad (6)$$

Directions of reflected and transmitted waves at an interface have been defined in Fig. 2 by the angles they make with the normal to the interface. For reflection, the angles of incidence and reflection are equal.

$$\phi = \phi'' \tag{7}$$

For refraction, Snell's law is obeyed.

$$n_0 \sin\phi = n_1 \sin\phi' \tag{8}$$

The angle of incidence at which the reflection coefficient for p-polarized light becomes zero is called Brewster's angle. At this angle, the sum of the angles of incidence and refraction is equal to 90°. Under this condition, the equation used to calculate Brewster's angle ϕ_p, can be derived from Eq. (8).

$$\phi_p = \tan^{-1}\left(\frac{n_1}{n_0}\right) \tag{9}$$

In agreement with the present convention, the reflection coefficients are taken to be positive. The phase changes upon reflection from a dielectric have a value of 180 or 360 (or 0) degrees. When light is incident from a dielectric medium of refractive index, n_0, onto a dielectric medium of higher refractive index, n_1, it undergoes a phase change upon reflection as shown in Fig. 3(a). At Brewster's angle, the amplitude of the reflected p-polarized light is zero, and the phase change at higher angles differs from that at angles lower than Brewster's angle by 180°. However, when n_0 is greater than n_1, the phase changes are as shown in Fig. 3(b). The difference of 180° between the phase changes in the two cases can be derived from Eqs. (3) and (4). If n_1 is substituted for n_0 and ϕ' for ϕ, the terms within the absolute value signs retain the same magnitude but are opposite in sign.

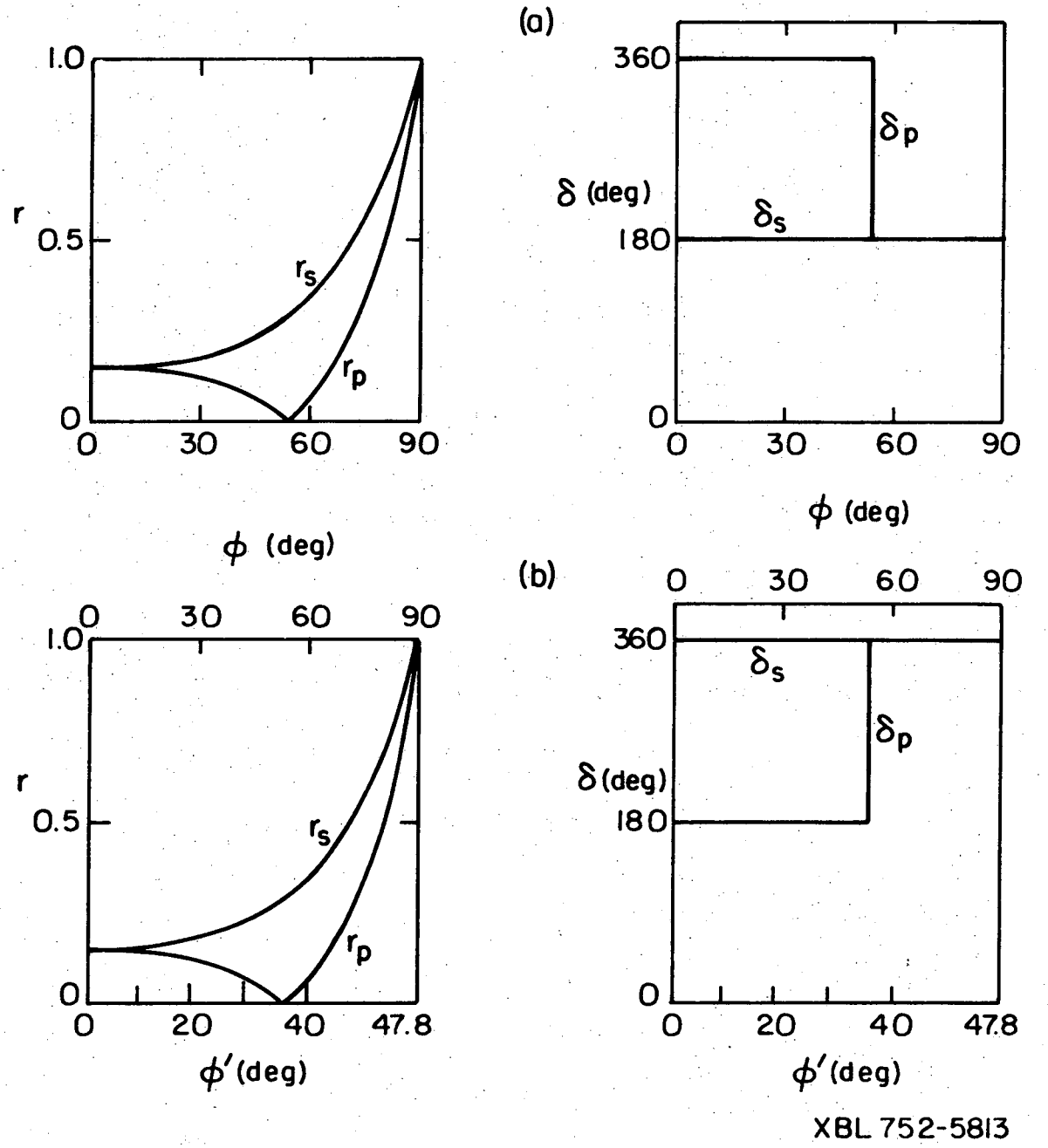

Fig. 3. Amplitude reflection coefficients for internal and external reflection from a dielectric film and associated phase changes. Diagrams are based on refractive indices 1 (air) and 1.35 (dilute aqueous solution). $\sin\phi = 1.35 \sin\phi'$.
(a) external reflection, $n_1 > n_0$.
(b) internal reflection, $n_0 > n_1$.

The reflection and transmission coefficients of Eqs. (3) through (6) are related by the following equations. Since the reflection coefficients are taken to be positive numbers, the phase change must be specified.

$$t_s - r_s = 1 \text{ (for } \delta_s = 360°) \quad t_s + r_s = 1 \text{ (for } \delta_s = 180°) \tag{10}$$

$$\frac{n_1}{n_0} t_p - r_p = 1 \text{ (for } \delta_p = 360°) \quad \frac{n_1}{n_0} t_p + r_p = 1 \text{ (for } \delta_p = 180°) \tag{11}$$

For the case of reflection from an absorbing medium, the index of refraction is complex:

$$n_c = n - ik \quad , \tag{12}$$

where k is called the extinction index. The Fresnel equations can still be used but in a complex form. These can be expressed differently by the following equations for reflection from an absorbing medium in contact with a dielectric medium of refractive index, n_0.[33,34] Their distinct advantage is that they are expressed in terms of real arithmetic. They reduce to the equations for reflection from a dielectric medium when the extinction index is zero.

$$r_s = \frac{E_s''}{E_s} = \sqrt{\frac{A^2 + B^2 - 2A\cos\phi + \cos^2\phi}{A^2 + B^2 + 2A\cos\phi + \cos^2\phi}} \tag{13}$$

$$r_p = \frac{E_p''}{E_p} = r_s \sqrt{\frac{A^2 + B^2 - 2A\sin\phi\tan\phi + \sin^2\phi\tan^2\phi}{A^2 + B^2 + 2A\sin\phi\tan\phi + \sin^2\phi\tan^2\phi}} \quad , \tag{14}$$

where

$$A = \sqrt{\frac{1}{2n_0^2}\left[\sqrt{(n^2 - k^2 - n_0^2\sin^2\phi)^2 + 4n^2k^2} + (n^2 - k^2 - n_0^2\sin^2\phi)\right]} \qquad (15)$$

$$B = \sqrt{\frac{1}{2n_0^2}\left[\sqrt{(n^2 - k^2 - n_0^2\sin^2\phi)^2 + 4n^2k^2} - (n^2 - k^2 - n_0^2\sin^2\phi)\right]} . \qquad (16)$$

Phase changes for reflection from absorbing media in contact with a non-absorbing medium have also been derived.[33,34] They are

$$\delta_s = \tan^{-1}\left(\frac{-2B\cos\phi}{A^2 + B^2 - \cos^2\phi}\right) \qquad 0 \leq \delta_s \leq \pi \qquad (17)$$

$$\Delta = \tan^{-1}\left(\frac{-2B\sin\phi\tan\phi}{A^2 + B^2 - \sin^2\phi\tan^2\phi}\right) \quad 0 \leq \Delta \leq \pi \qquad (18)$$

$$\delta_p = \Delta + \delta_s \qquad (19)$$

$$\delta_p = \tan^{-1}\left[\frac{2B\cos\phi(A^2 + B^2 - \sin^2\phi)}{A^2 + B^2 - \frac{1}{n_0^4}(n^2 + k^2)^2\cos^2\phi}\right] . \qquad (20)$$

The application of these equations to a specific dielectric film on an absorbing substrate is presented in Fig. 4.

C. Multiple-Beam Interference

1. Physical Model

Figure 5 represents the physical model for multiple-beam interference in thin films. A series of parallel and coherent light waves is incident from a medium of refractive index, n_0, onto a film of refractive index, n_1, at an angle, ϕ. The interfaces are mathematically both plane and parallel to each other. Line segments $\overline{AB}$ and $\overline{BC}$ in Fig. 5 represent

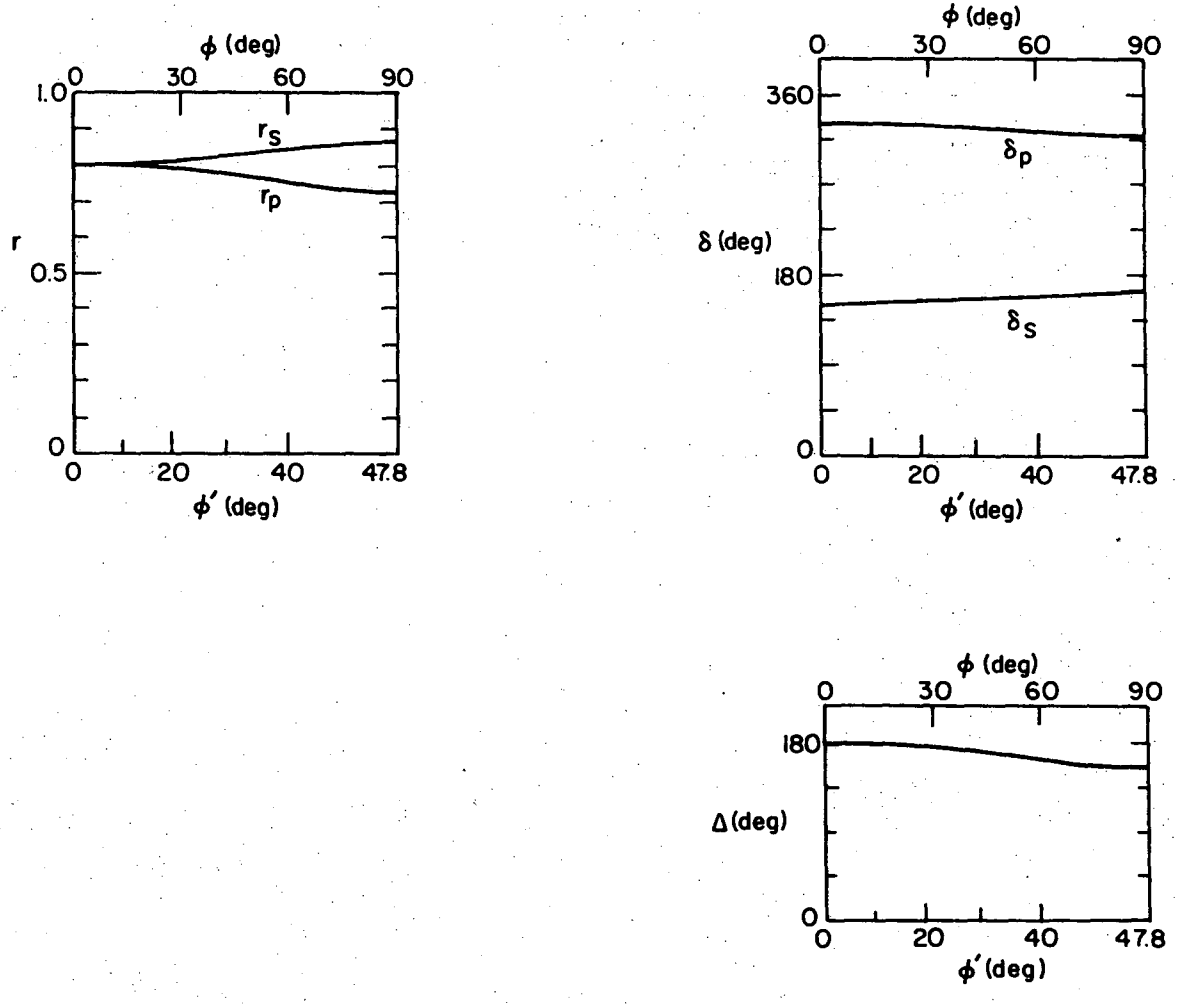

Fig. 4. Reflection coefficients for an absorbing substrate (refractive index=2.07-i(4.40)) in contact with a dielectric film (refractive index = 1.35) as a function of the angle of incidence ϕ or ϕ' on the film or substrate. Air is incident medium in contact with film. Modulus of reflection coefficients (r_s,r_p), absolute phase changes (δ_s,δ_p) and relative phase change ($\Delta = \delta_p - \delta_s$).

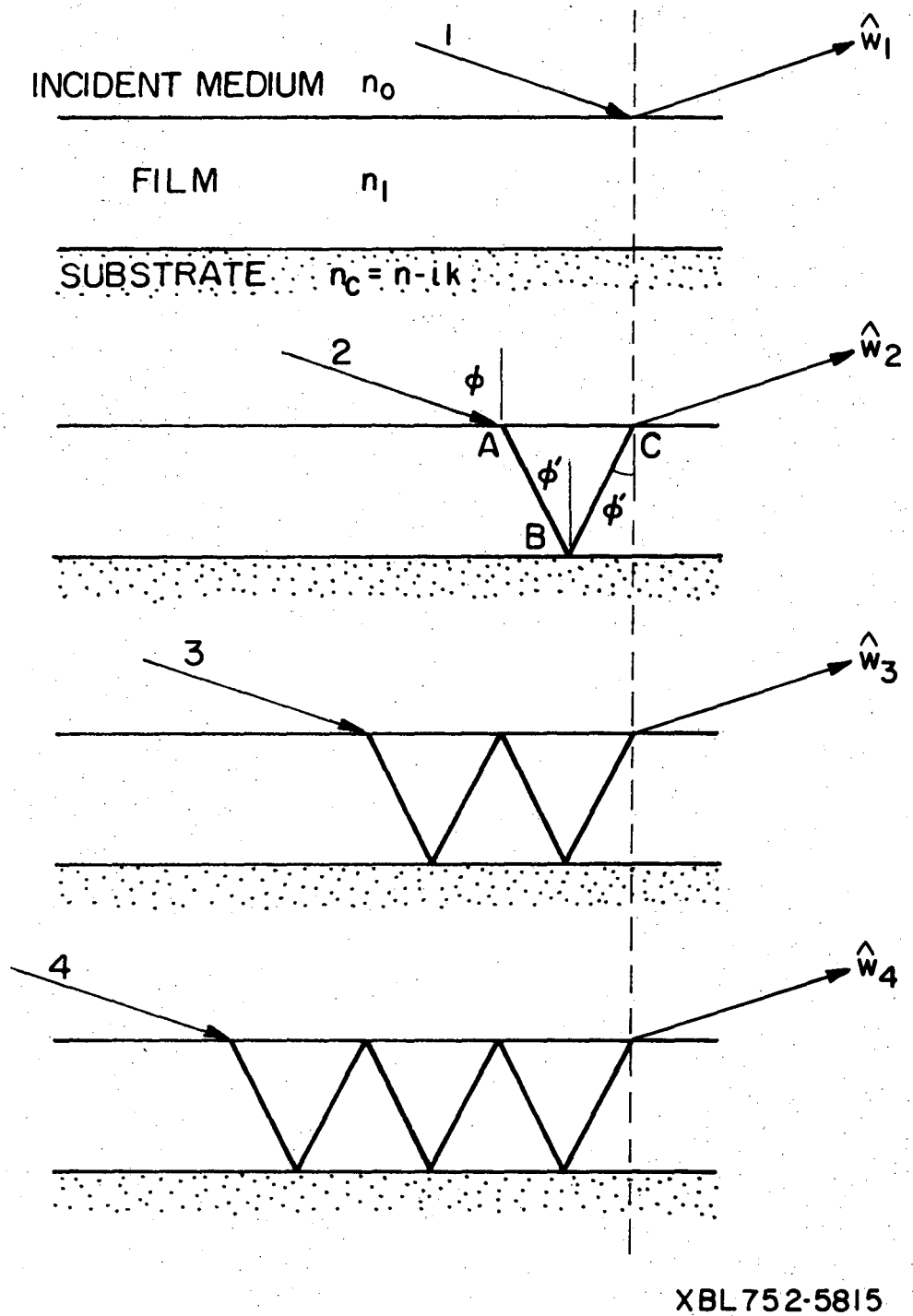

Fig. 5. Multiple-beam interference model. The reflected wave is the resultant of an infinite number of interfering waves, each of which originates from a different incident wave. The first four interfering waves ($\hat{w}_1, \hat{w}_2, \hat{w}_3, \hat{w}_4$) are shown.

light waves which are incident at an angle, ϕ', onto the lower and upper interfaces within the film. The angle of refraction, ϕ', in the film can be calculated from Eq. (8). All light that is absorbed or transmitted by the substrate is lost and does not enter directly into the equations.

Equations for multiple-beam interference are applicable to either polarization. For this reason, the use of the subscripts, s and p, will be discontinued. Subscripts that denote the interface from which a wave is reflected and changed in phase and through which transmission occurs will be employed. They are presented in Fig. 6.

Since each incident wave is divided into reflected and refracted waves at every interface, the waves emanating from the film which result from one incident wave are mathematically infinite in number. Each wave has undergone a different number of reflections within the film so that each one is characterized by its own amplitude and phase. The phase shift of one wave with respect to another is caused not only by phase changes at the two interfaces but also by phase differences due to the optical path length difference between interfering waves. The difference in optical path length, ΔS, can be derived from the geometry of Fig. 7. More than one derivation occurs in the literature.[35,36] Waves 1 and 2 are in phase at points D and A, which are in a plane perpendicular to the propagation direction, and interference occurs at point C. Wave 1 travels an optical path length given by the length of line segment $\overline{DC}$ times the refractive index, n_0, of the incident medium. The fraction of wave 2 that is refracted at A travels an optical path length given by the sum of the lengths of line segments $\overline{AB}$ and $\overline{BC}$ times the refractive index, n_1, of the film. Geometric substitutions are given in the second line. The symbol for film thickness is "d".

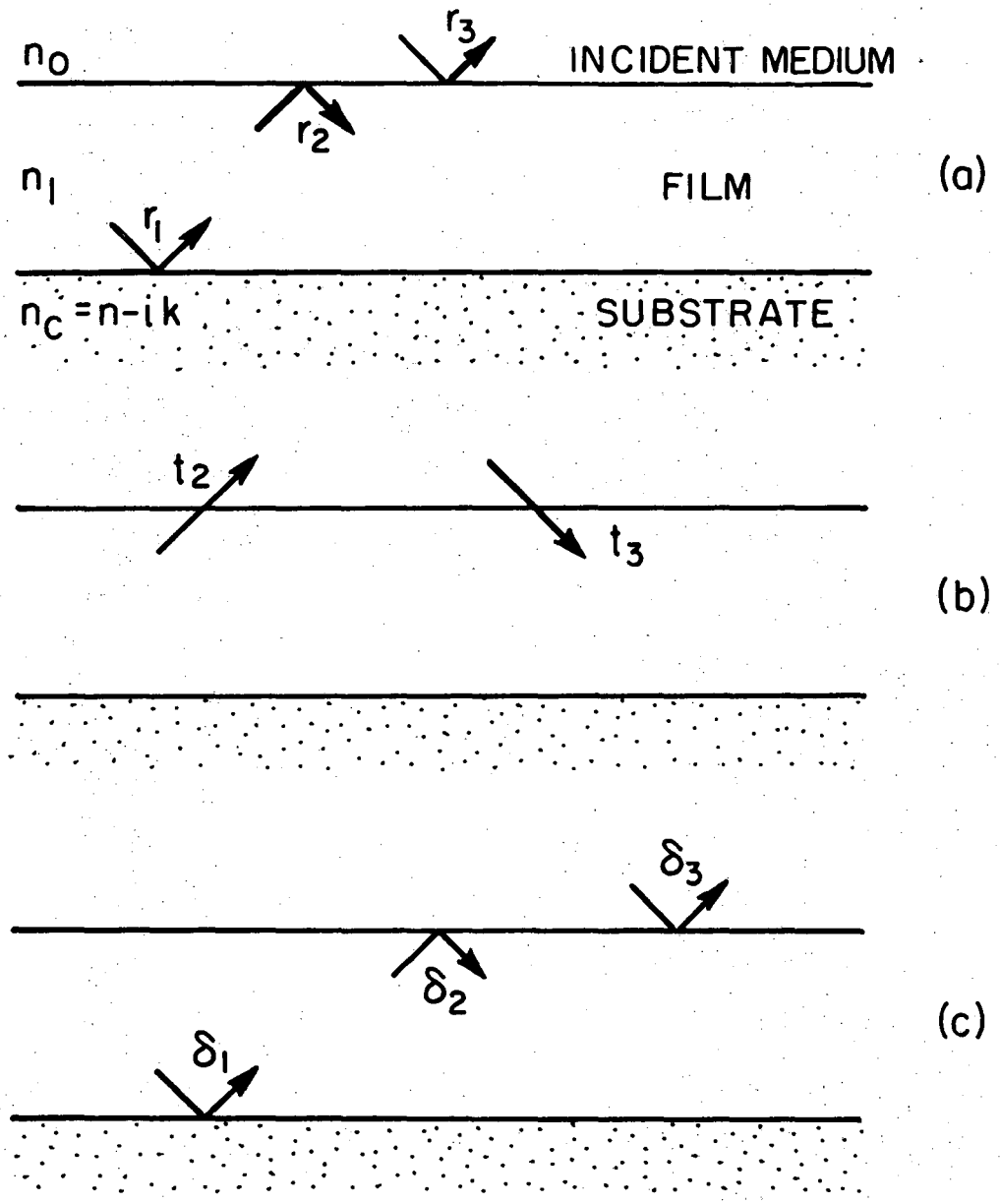

Fig. 6. Notations for dielectric film-covered substrate.
(a) Reflection coefficients and refractive indices.
(b) Transmission coefficients.
(c) Phase changes upon reflection.

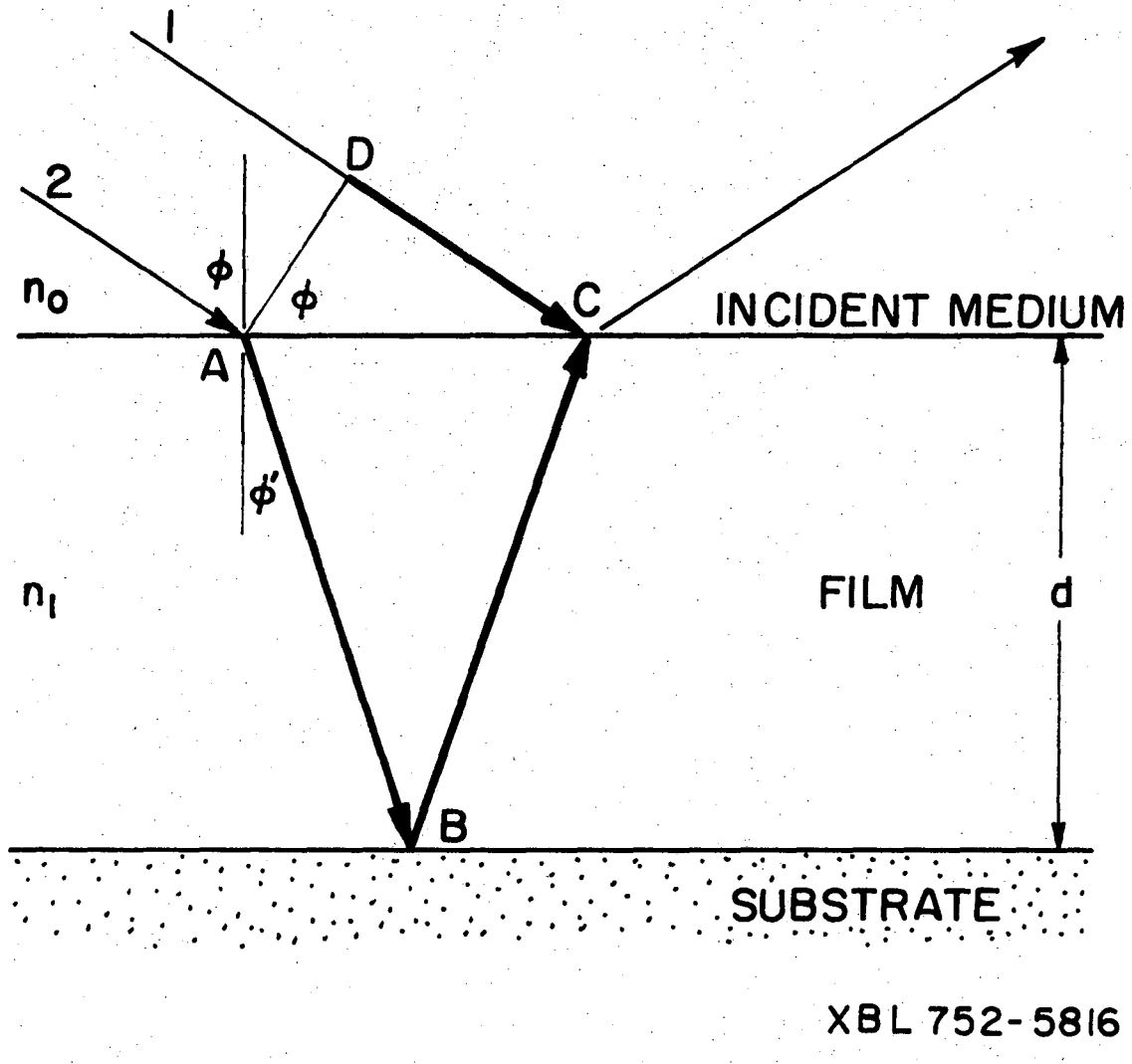

Fig. 7. Refer to Fig. 5. Construction to calculate difference in optical path length between successive interfering waves.

$$\Delta S = (\overline{AB} + \overline{BC})\, n_1 - (\overline{DC})\, n_0$$

$$\overline{AB} = \overline{BC} = \frac{d}{\cos\phi'} \qquad \overline{AC} = 2d\tan\phi' \qquad \overline{DC} = \overline{AC}\sin\phi$$

$$\Delta S = \frac{2n_1 d}{\cos\phi'} - 2n_0 d\tan\phi'\sin\phi$$

According to Snell's law of refraction, Eq. (8), $n_1\sin\phi'$ can be substituted for $n_0\sin\phi$. The equation then becomes

$$\Delta S = \frac{2n_1 d}{\cos\phi'} - 2d\,\frac{\sin\phi'}{\cos\phi'}\,(n_1\sin\phi')$$

$$= \frac{2n_1 d}{\cos\phi'}\,(1 - \sin^2\phi') = \frac{2n_1 d}{\cos\phi'}\,(\cos^2\phi') \quad ,$$

and the optical path difference is

$$\Delta S = 2n_1 d\cos\phi' \quad . \tag{21}$$

The associated phase shift is

$$\delta = \frac{\Delta S}{\lambda}\cdot 2\pi = \frac{4\pi n_1 d\cos\phi'}{\lambda} \quad . \tag{22}$$

2. Derivation of Equations

One should understand that each member of the infinite number of waves that are interfering at each point originates from a different incident wave. The amplitude and phase of the interfering waves can be derived from the geometry of Figs. 5 and 7 and from the definitions in Fig. 6. The complex amplitude of just the first four waves will be shown in order to establish the mathematical trend in the series. Since δ in Eq. (22) corresponds to a delay in time as does the dot product, $\vec{k}\cdot\vec{x}$ in Eq. (1), it must be preceded by a negative sign.

$$\hat{w}_1 = r_3 e^{i(\delta_3)} \tag{23a}$$

$$\hat{w}_2 = t_3 r_1 t_2 e^{i(-\delta+\delta_1)} \tag{23b}$$

$$\hat{w}_3 = t_3 r_1 r_2 r_1 t_2 e^{i(-\delta+\delta_1+\delta_2+\delta_1-\delta)} \tag{23c}$$

$$\hat{w}_4 = t_3 r_1 r_2 r_1 r_2 r_1 t_2 e^{i(-\delta+\delta_1+2(\delta_2+\delta_1-\delta))} \tag{23d}$$

The infinite series of complex amplitudes can be expressed in this manner:

$$\hat{W} = \hat{w}_1 + \hat{w}_2 + \hat{w}_3 + \hat{w}_4 + \ldots = \sum_{n=1}^{\infty} \hat{w}_n \quad ,$$

and

$$\hat{W} = r_3 e^{i\delta_3} + t_2 t_3 r_1 e^{i(-\delta+\delta_1)} \left[1 + r_1 r_2 e^{i(-\delta+\delta_1+\delta_2)} + (r_1 r_2)^2 e^{2i(-\delta+\delta_1+\delta_2)} + \ldots \right] \quad . \tag{24}$$

The bracketed terms form a converging series and can be replaced by an equivalent expression, so that

$$\hat{W} = r_3 e^{i\delta_3} + \frac{t_2 t_3 r_1 e^{i(-\delta+\delta_1)}}{1 - r_1 r_2 e^{i(-\delta+\delta_1+\delta_2)}} \quad . \tag{25}$$

The phase change, δ_2, can be eliminated from this equation by using the relationship between δ_2 and δ_3, the phase changes for internal and external reflection at the film-incident medium interface. Their values depend on the angle of incidence and the polarization. The sign of δ_3 can be either positive or negative, since the difference between $+\delta_3$ and $-\delta_3$ is either 2π or 4π radians.

$$\delta_3 = \pi \text{ or } 2\pi \qquad \delta_2 = \delta_3 \pm \pi \tag{26}$$

It can be further simplified by Eqs. (27) and (28), the first of which can be derived from either Eq. (3) or (4) upon consideration of the propagation directions of light reflected from interfaces 2 and 3. Equation (27) states that in a thin film the reflection coefficients for light reflected from either side of the dielectric film-incident medium interface are equal.

$$r_2 = r_3 \tag{27}$$

Equation (28) is derived by applying the conditions of Eq. (26) to either Eq. (10) or (11). For s-polarized light, $\delta_3 = \pi$ ($n_0 < n_1$) and

$$t_2 - r_2 = 1 \quad \text{and} \quad t_3 + r_3 = 1 \quad .$$

For p-polarized light, $\delta_3 = \pi$ or 2π and

$$\frac{n_1}{n_0} t_3 + r_3 = 1 \quad \text{and} \quad \frac{n_0}{n_1} t_2 - r_2 = 1$$

or

$$\frac{n_1}{n_0} t_3 - r_3 = 1 \quad \text{and} \quad \frac{n_0}{n_1} t_2 + r_2 = 1 \quad .$$

With Eq. (27) as a condition, each of the preceding three pairs of equations can be solved to yield the following relationship:

$$t_2 t_3 = 1 - r_3^2 \quad . \tag{28}$$

Equation (25) can now be rewritten as

$$\hat{W} = r_3 e^{i\delta_3} + \frac{\left(1 - r_3^2\right) r_1 e^{-i(\delta-\delta_1)}}{1 + r_1 r_3 e^{-i(\delta+\delta_3-\delta_1)}} \quad .$$

After the two terms are combined over a common denominator, the complex amplitude is

$$\hat{W} = \frac{r_3 e^{i\delta_3} + r_1 e^{-i(\delta-\delta_1)}}{1 + r_1 r_3 e^{-i(\delta+\delta_3-\delta_1)}} \quad . \tag{29}$$

Equation (29) can be converted to a well-known equation called the Drude equation[36] by making the following substitutions:

$$\hat{r}_3 = r_3 e^{i\delta_3} \qquad \hat{r}_1 = r_1 e^{i\delta_1} \quad .$$

The Drude equation is

$$\hat{W} = \frac{\hat{r}_3 + \hat{r}_1 e^{-i\delta}}{1 + \hat{r}_1 \hat{r}_3 e^{-i\delta}} \quad . \tag{30}$$

The first step in finding the intensity of reflected light with respect to unit incident intensity is to multiply the numerator and the denominator of Eq. (29) by the complex conjugate of the denominator in order to make the denominator real. The whole expression for the amplitude is then multiplied by its complex conjugate in order to derive the intensity. After the terms in the numerator are expressed as the product of two factors, an intermediate equation is

$$I = \hat{W}(\hat{W}^*) = \left(r_3^2 + r_1^2 + r_3 r_1 e^{i(\delta+\delta_3-\delta_1)} + r_3 r_1 e^{-i(\delta+\delta_3-\delta_1)}\right)$$

$$\left(1 + r_3^2 r_1^2 + r_3 r_1 e^{i(\delta+\delta_3-\delta_1)} + r_3 r_1 e^{-i(\delta+\delta_3-\delta_1)}\right) \Big/$$

$$\left(1 + r_3^2 r_1^2 + r_3 r_1 e^{i(\delta+\delta_3-\delta_1)} + r_3 r_1 e^{-i(\delta+\delta_3-\delta_1)}\right)^2 .$$

The numerator and denominator can be divided by a factor common to both. Equation (1) is used along with identities between cos(x) and cos(-x) and between sin(-x) and -sin(x) to reduce the multiple-beam intensity equation to its most understandable form.[36]

$$I = \frac{r_3^2 + r_1^2 + 2r_3 r_1 \cos(\delta + \delta_3 - \delta_1)}{1 + r_3^2 r_1^2 + 2r_3 r_1 \cos(\delta + \delta_3 - \delta_1)} \tag{31}$$

It can be expected that the intensity calculated from the multiple-beam model is closely approximated by considering a limited number of reflections within the film. Interference of only the first two waves comprises the two-reflection approximation. The sum of the complex amplitudes, $\hat{w}_1$ and $\hat{w}_2$, in Eqs. (23a) and (23b) is multiplied by its complex conjugate. Equation (28) is used again to eliminate the transmission coefficients.

$$I = \left(r_3 e^{i\delta_3} + r_1\left(1 - r_3^2\right) e^{-i(\delta-\delta_1)}\right)\left(r_3 e^{-i\delta_3} + r_1\left(1 - r_3^2\right) e^{i(\delta-\delta_1)}\right)$$

$$= r_3^2 + \left(1 - r_3^2\right)^2 r_1^2 + 2\left(1 - r_3^2\right) r_3 r_1 \cos(\delta + \delta_3 - \delta_1) \tag{32}$$

The two-reflection intensity equation, Eq. (32), is valid as an approximation to the multiple-beam equation only when the reflection coefficients are small compared to 1. Under this condition, the equation becomes

$$I = r_3^2 + r_1^2 + 2r_1r_3\cos(\delta + \delta_3 - \delta_1) \quad . \tag{33}$$

Equation (33) will be referred to as the double-beam intensity equation. It is identical to the numerator of the multiple-beam equation, Eq. (31), but only represents the superposition of two light waves of amplitude r_3 and r_1. It has no physical meaning in thin film interference.

When only the first n waves in the infinite number of interfering waves are considered to be interfering, the sum of the first n complex amplitudes in Eq. (24) is multiplied by its complex conjugate to derive the intensity. The intensity of reflected light with respect to unit incident intensity for interference of three beams or more ($n > 2$) is

$$I = r_3^2 + \sum_{m=1}^{n-1} \left(1 - r_3^2\right)^2 r_1^2(r_3r_1)^{2m-2} + \sum_{m=1}^{n-1} 2\left(1 - r_3^2\right) r_3r_1(-r_3r_1)^{m-1} \tag{34}$$

$$\cos(m(\delta + \delta_3 - \delta_1)) + \sum_{m=1}^{n-2} \left[\sum_{L=m+1}^{n-1} 2\left(1 - r_3^2\right)^2 r_1^2(-r_3r_1)^{2L-2-m} \cos(m(\delta + \delta_3 - \delta_1)) \right] \quad .$$

The intensity for the multiple-beam model can be expressed as an infinite series as in Eq. (35) by employing Eq. (34) with n equal to infinity. Equation (35) is of the same form as that employed by

Kubota[29] to demonstrate the effect of considering only a limited number of reflections within the film when calculating the color of reflected light. For this purpose, however, Eq. (34) is the correct equation to use.

$$I = \frac{r_1^2 + r_3^2 - 2r_1^2r_3^2}{1 - r_1^2r_3^2} - \sum_{m=1}^{\infty} \frac{2\left(1 - r_1^2\right)\left(1 - r_3^2\right)}{1 - r_1^2r_3^2}$$

$$(-r_1r_3)^m \cos(m(\delta + \delta_3 - \delta_1)) \qquad (35)$$

3. Monochromatic Optimum Angle of Incidence

Monochromatic interference fringes should be observed or recorded under conditions at which the maxima and minima of intensity are in highest contrast. Fringes occur in multiple-beam interference when the intensity given by Eq. (31) varies with film thickness. For observing the interference fringes produced by a given dielectric film on a specific metal substrate with polarized light, the fringe contrast can be changed only by changing the viewing direction. At normal incidence, the reflection coefficient of the film-metal interface is much greater than that of the air-film interface, so that complete destructive interference cannot occur and fringe contrast is low. Note that at an angle of incidence of 90° the incident light is totally reflected from the air-film interface and fringe contrast is totally absent. At some angle between these two extremes, the amounts of light reflected from a film-covered substrate with and without penetration of the film are equal and the result is that the intensity minima are zero and fringe contrast is at a maximum.[31]

Light polarized parallel and perpendicular to the plane of incidence has different reflection coefficients at either interface for all angles of incidence between 0 and 90°. For this reason, it is unlikely that the angle of maximum fringe contrast would be the same for p and s polarized light. Also, above Brewster's angle for the dielectric film, the values of $\delta_3 - \delta_1$ in Eq. (31) differ by approximately 180° for the two polarizations. δ_3 is the same for both polarizations, and since the range of values of the angle of incidence onto the film-metal interface is limited by refraction at the air-film interface, the difference in the values of δ_1 for the two polarizations does not depart significantly from 180°. The magnitude of the difference can be estimated from Fig. 4. Because 180° is the spacing between a maximum and a minimum of intensity, the fringe contrast for unpolarized light would be significantly less than for polarized light. Observations should be made with polarized light, because for most film-metal combinations the angle at which the highest contrast occurs is above Brewster's angle.

A well-established criterion for fringe contrast is the Michelson fringe visibility, V.[37]

$$V = \frac{I_{max} - I_{min}}{I_{max} + I_{min}} \quad , \tag{36}$$

where I_{max} and I_{min} are the intensity maxima and minima of interference fringes. The angle of incidence at which the intensity minima are zero is the optimum angle to observe a film. The fringe visibility according to Eq. (36) is then equal to one. When the intensity maxima and minima are equal, the visibility is zero. This result occurs at Brewster's

angle for light polarized in the plane of incidence and at 90° angle of incidence for both polarizations.

The equations for the multiple-beam intensity maxima and minima can be derived from Eq. (31). If the intensity is differentiated with respect to δ, the condition for a maximum or a minimum is that $\sin(\delta + \delta_3 - \delta_1)$ equals zero. That is, $\delta + \delta_3 - \delta_1$ equals zero or a multiple of π radians. From the second derivative, one can determine that the condition for a maximum is that $\cos(\delta + \delta_3 - \delta_1) = 1$ and for a minimum that $\cos(\delta + \delta_3 - \delta_1) = -1$. Equivalently, $\delta + \delta_3 - \delta_1$ equals zero or an even multiple of π for a maximum and an odd multiple of π for a minimum. Substitution of these values in Eq. (31) yields[36]

$$I_{max} = \left(\frac{r_1 + r_3}{1 + r_1 r_3}\right)^2 \tag{37}$$

$$I_{min} = \left(\frac{r_1 - r_3}{1 - r_1 r_3}\right)^2 \tag{38}$$

The condition for the optimum angle of incidence in multiple-beam interference can be readily established by examining Eq. (38) for the intensity of the interference minima. When the reflection coefficients, r_1 and r_3, are equal, the magnitude of the intensity minima is zero and the Michelson fringe visibility, Eq. (36), has its maximum value of one.

CONDITION FOR OPTIMUM ANGLE OF INCIDENCE $\qquad r_3 = r_1 \qquad (39)$

A specific example of the variation of the fringe visibility with direction of observation is given in Figs. 8 and 9. The curves represent Eqs. (36) through (38). At the optimum angle, the intensity minima are zero and the fringe visibility is equal to one. If the reflection

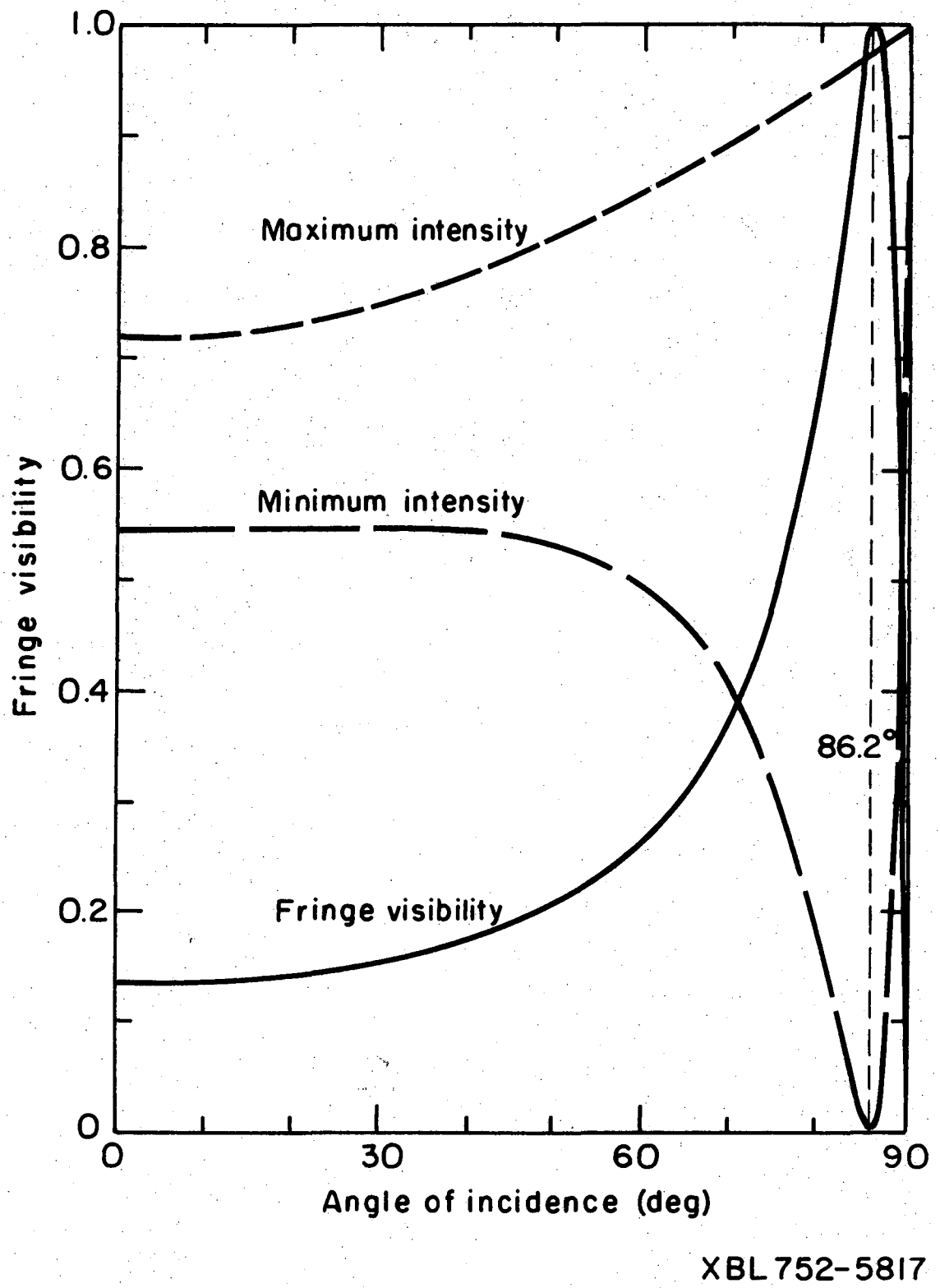

XBL752-5817

Fig. 8. Variation of monochromatic fringe visibility and intensities of interference maxima and minima with angle of incidence for light incident from air onto a film-covered (n_1 = 1.35) absorbing substrate (n_c = 2.07 - i(4.40)). s-polarized light.

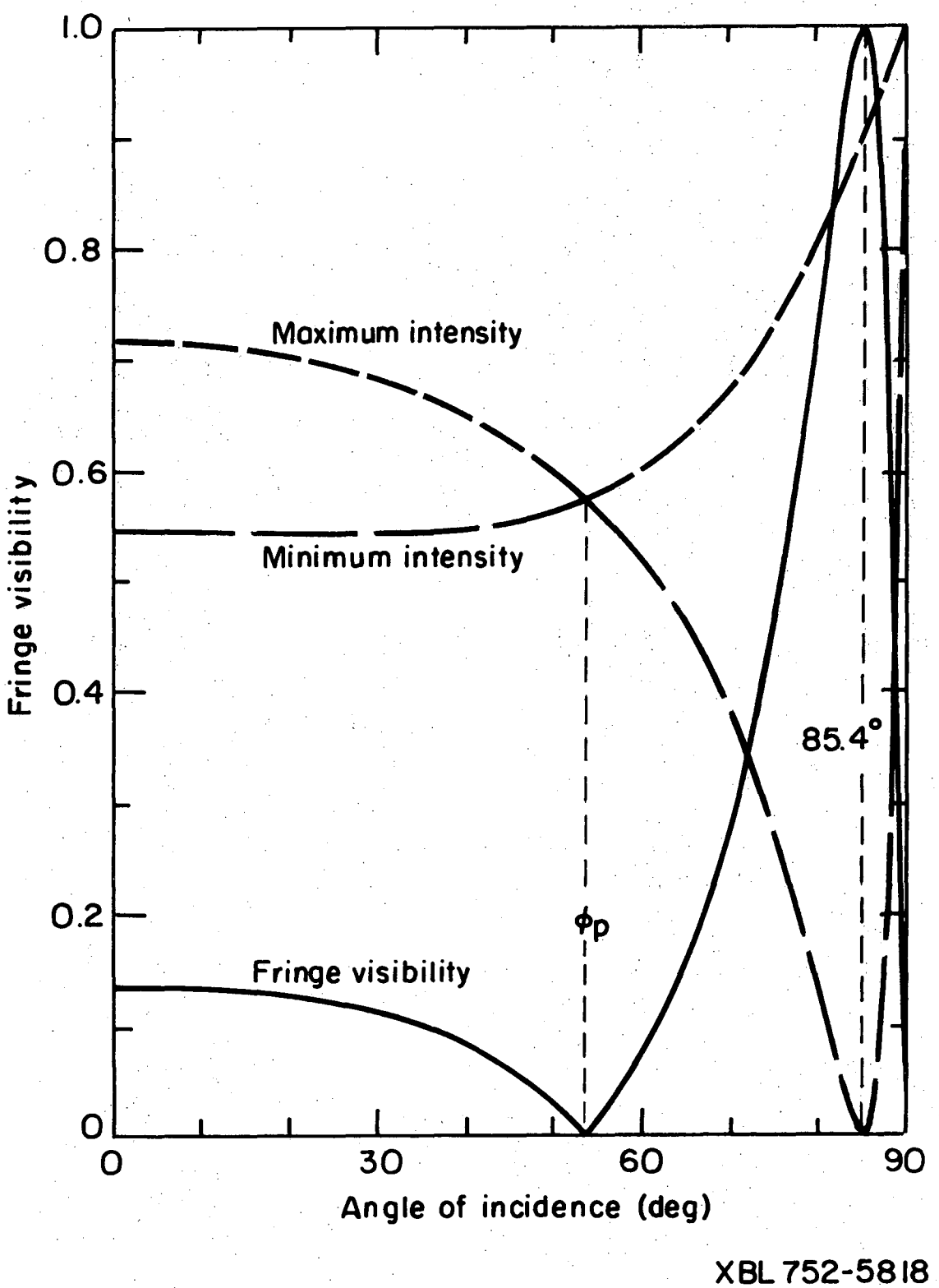

Fig. 9. See Fig. 8. p-polarized light.

coefficients at both interfaces in Figs. 3 and 4 are compared at this angle, they are found to be equal.

The criterion for the optimum angle given by Muller[31] can be confirmed by introducing the conditions for a zero minimum of intensity into the amplitude equation, Eq. (25). The first and second terms can be regarded as the amplitude and phase of the light reflected from the film-covered substrate without and with penetration of the film. They both have amplitudes equal to r_3 but differ in phase by 180°.

The two-reflection intensity equation, Eq. (32), can be used as an approximation to the multiple-beam intensity, Eq. (31), when the reflection coefficients of the two interfaces is small. The conditions for a maximum or minimum of intensity are found by inspecting each term in the equation. The cosine term is the only one that can vary with film thickness. As in the multiple-beam equation, maxima occur when $\cos(\delta + \delta_3 - \delta_1) = 1$ and minima occur when $\cos(\delta + \delta_3 - \delta_1) = -1$. However, the condition for which the intensity minima are zero is not the same as for the multiple-beam equation. When the minima for the two-reflection intensity equation are zero, Eq. (32) becomes

$$r_3^2 + \left(1 - r_3^2\right)^2 r_1^2 - 2\left(1 - r_3^2\right) r_1 r_3 = 0 \quad .$$

After the left side of the equation is factored, the condition for a zero intensity miminum for the two-reflection approximation is shown to be

$$r_3 = \left(1 - r_3^2\right) r_1 \quad . \tag{40}$$

When the reflection coefficients are small compared to 1, the double-beam equation, Eq. (33), is applicable. It does not physically represent thin film interference. Nevertheless, it has a mathematical similarity to the multiple-beam equation in that the conditions for the interference maxima or minima are the same in the two equations. Also, in both equations the intensity minima equal zero when r_1 and r_3 are equal. This result has already been derived in Eq. (39) for the multiple-beam model. It can be derived for the double-beam equation, Eq. (33), in the same manner that Eq. (40) was derived from the two-reflection approximation.

D. Colorimetry of Interference Colors

1. Principles of Colorimetry

The basis for colorimetry lies in the observation that the visual stimulus of light of any spectral composition can be duplicated by the proper mixture of three "primary" colors. Two such mixtures, each of which has been selected to match a color, will, when mixed additively, match a similar addition of the original colors.

In 1931, the Commission Internationale de l'Eclairage (C.I.E.) adopted a color matching system for 2° foveal vision. In 1964, it adopted a color system for an annular zone of the retina around the fovea that subtends an angle of 10°.[38] The former system is used in this study. The systems were chosen to match each color of a single wavelength in the spectrum with a specified amount of three radiations. These amounts are $\bar{x}_\lambda$, $\bar{y}_\lambda$ and $\bar{z}_\lambda$. Figure 10 shows their distributions on the basis of equal energy through the visible spectrum. They are called the distribution coefficients for an equal-energy stimulus.

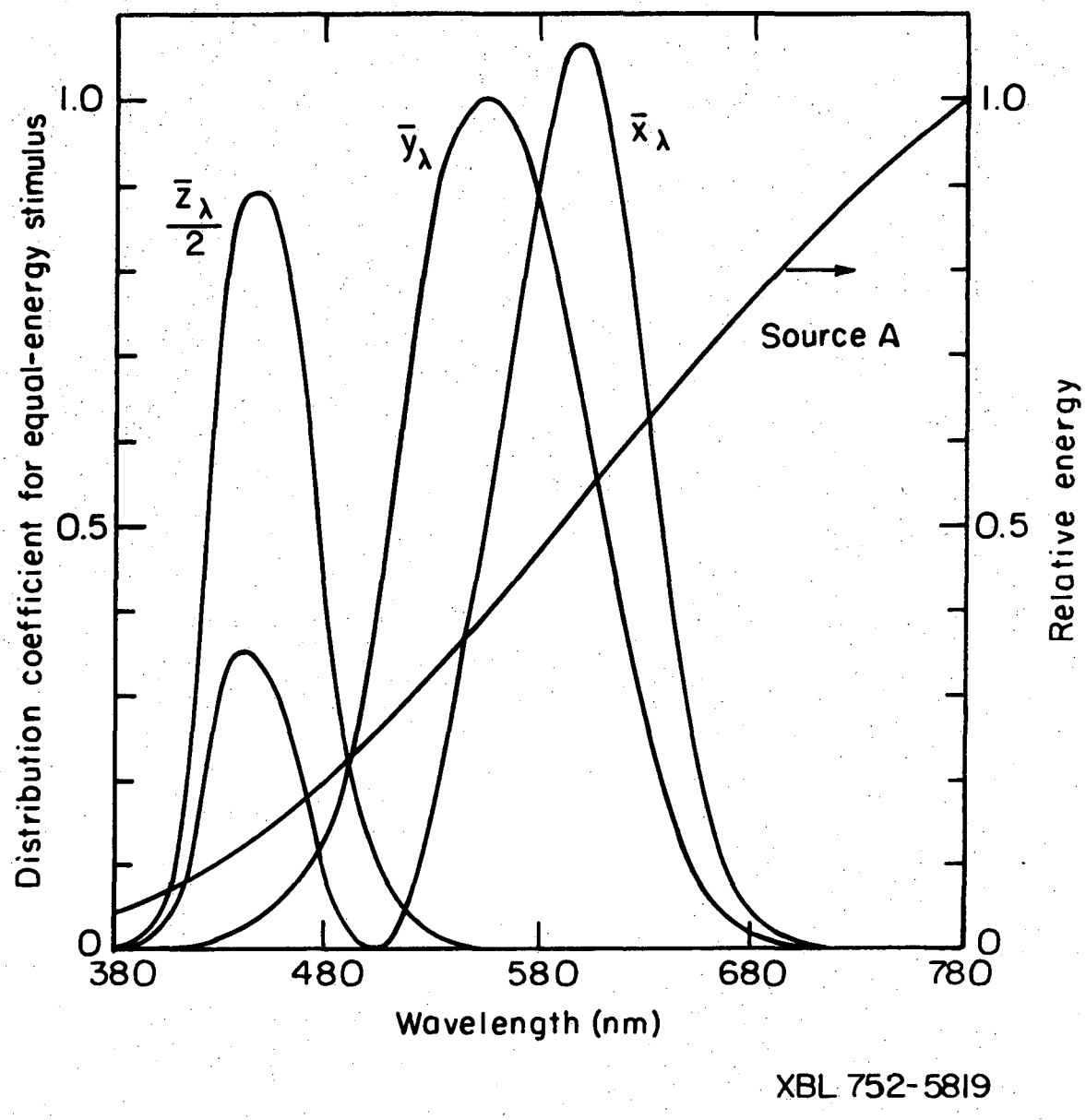

Fig. 10. Relative intensity of 1931 C.I.E. primaries (X), (Y) and (Z) in spectrum colors. These are distribution coefficients for an equal-energy spectrum (Wright).[38] Energy distribution of standard tungsten source A included.

Wright[38] has tabulated them for wavelength intervals of 5 nm from 380 to 780 nm. Since practical sources of illumination do not have an equal-energy distribution, Wright has tabulated the energy distribution, P_λ (again in intervals of 5 nm over the visible range) for three standard sources A, B and C. Source A, a tungsten lamp with a color temperature of 2854°K, represents average artificial illumination. Sources B and C correspond to two phases of daylight. The spectral energy distribution, P_λ, has been multiplied by the tristimulus coefficients, $\bar{x}_\lambda$, $\bar{y}_\lambda$ and $\bar{z}_\lambda$ to obtain distribution coefficients weighted by energy values of the standard illuminants. Wright has tabulated these weighted coefficients in 5 nm intervals for the 1931 C.I.E. values.

The curves of $\bar{x}_\lambda$, $\bar{y}_\lambda$ and $\bar{z}_\lambda$ have been adjusted so that the amount, designated by the tristimulus values (X, Y, Z), of the three tristimulus primaries ((X), (Y), (Z)) are equal in a match on an equal-energy stimulus. The tristimulus values of a sample of light with an energy distribution, P_λ, are

$$X = \Sigma P_\lambda \cdot \bar{x}_\lambda \tag{41a}$$

$$Y = \Sigma P_\lambda \cdot \bar{y}_\lambda \tag{41b}$$

$$Z = \Sigma P_\lambda \cdot \bar{z}_\lambda \tag{41c}$$

The summations are intended to closely approximate integrations. For the tabulated intervals, they can be regarded as equivalent. The distribution of $\bar{y}_\lambda$ has been selected to be identical to the spectral sensitivity curve of the eye, V_λ, while the tristimulus primaries, (X) and (Z), have been chosen to have zero luminous efficiencies (they make no contributions to the luminous sensation). V_λ is a measure of the relative contribution to the luminous sensation that each wavelength makes

in an equal-energy spectrum. The spectral sensitivity curve has a maximum value of $V_\lambda = 1$ at a wavelength of about 555 nm and values of zero for wavelengths outside the visible range. Values of $P_\lambda \cdot \bar{y}_\lambda$ for the standard illuminants have been multiplied in Wright's tables by a constant factor in order that Y is equal to 100.0. Values of $P_\lambda \cdot \bar{x}_\lambda$ and $P_\lambda \cdot \bar{z}_\lambda$ had to be multiplied by this same factor to maintain the same relative amounts of the primary colors. The percentage luminance, which is defined with respect to the luminance of the incident light for surface colors, is given directly by the value of Y. In this case, however, P_λ, the spectral composition of the reflected light, is a product of the spectral composition of the source and I_λ, the intensity of the reflected light as a function of the wavelength with respect to unit incident intensity.

Color is described by the three visual responses that a sample of light evokes: hue, saturation and brightness. In the Munsell system, color is specified by what is called its hue, chroma and value.[39] Corresponding terms in the C.I.E. color system are dominant wavelength, purity and intensity. In the C.I.E. system, color is represented by the amounts of the tristimulus primaries. A method of expressing the relative amounts of the primaries independent of the intensity is to calculate the chromaticity values x, y and z, which are defined as

$$x = \frac{X}{X + Y + Z} \tag{42a}$$

$$y = \frac{Y}{X + Y + Z} \tag{42b}$$

$$z = \frac{Z}{X + Y + Z} \tag{42c}$$

Since the sum of the chromaticity values is equal to one, the hue and saturation are defined by only two variables. The 1931 chromaticity diagram is shown in Fig. 11 with the ordinate and abscissa being y and x, respectively. The coordinates for single wavelengths comprise the curved section of the boundary or the spectrum locus. They can be found by calculating the chromaticity coordinates from $\bar{x}_\lambda$, $\bar{y}_\lambda$ and $\bar{z}_\lambda$ at each wavelength. Wright has tabulated these chromaticity coordinates. A straight line in the lower part of the diagram connects the two ends of the visible spectrum. Points located on this line represent nonspectral colors, which will be more clearly defined later.

2. Color Mixing

The general shape of the chromaticity diagram, according to Wright, is due in part to the choice of reference stimuli but primarily to the shape of the spectral sensitivity curve. An important characteristic of the color system is that the boundaries of the diagram are either concave or straight when viewed from within. This statement means that the color resulting from the additive mixture of any two colors is represented by a point either within the diagram or on the boundary. The additive mixing can be described by equations involving the chromaticity coordinates of the colors. The coordinates are weighted by the corresponding tristimulus values.[39] Let the tristimulus values of two colors, represented by the chromaticity coordinates, (x_0, y_0) and (x_1, y_1), be X_0, Y_0, Z_0 and X_1, Y_1, Z_1, respectively. The additive mixture of the two has the coordinates, (x, y), and the corresponding tristimulus values are

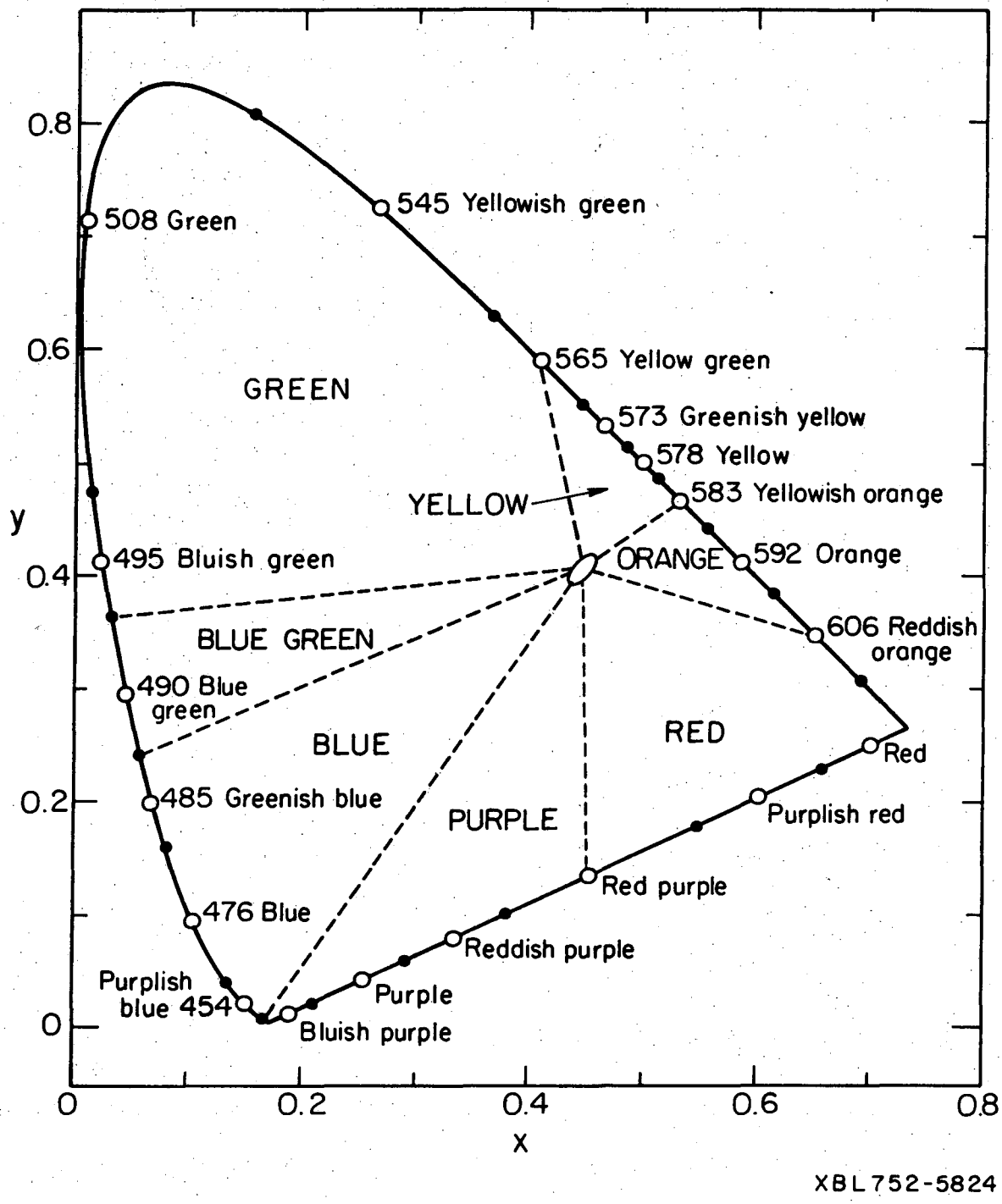

Fig. 11. 1931 C.I.E. chromaticity diagram with achromatic region five times actual size around coordinates of standard source A (tungsten lamp). Hue regions bounded by solid circles and dominant wavelengths (nm) at open circles are those given by Kelley.[40] Dashed lines divide the diagram into a condensed list of hue names.

$$X = X_0 + X_1 \tag{43a}$$

$$Y = Y_0 + Y_1 \tag{43b}$$

$$Z = Z_0 + Z_1 \tag{43c}$$

The sum of the tristimulus values of the two component colors are

$$S_0 = X_0 + Y_0 + Z_0 \tag{44a}$$

$$S_1 = X_1 + Y_1 + Z_1 \tag{44b}$$

The chromaticity coordinates (x, y) of the additive mixture can now be derived. They are

$$x = \frac{X_0 + X_1}{S_0 + S_1} = \frac{S_0 x_0 + S_1 x_1}{S_0 + S_1} \tag{45a}$$

$$y = \frac{Y_0 + Y_1}{S_0 + S_1} = \frac{S_0 y_0 + S_1 y_1}{S_0 + S_1} \tag{45b}$$

The point, (x, y), lies on a straight line between the two points, ($x_0 = X_0/S_0$, $y_0 = Y_0/S_0$) and ($x_1 = X_1/S_1$, $y_1 = Y_1/S_1$). This fact can be readily proved by calculating the slopes and distances between each pair of points.

3. Hue and Purity

Segments of the spectrum locus represent hue regions in the spectrum. Areas of the chromaticity diagram are also defined by hue names. Kelley[40] has presented such a diagram (1931 C.I.E.) for the standard illuminant C. The intersections of dividing lines between hue regions and the boundaries of the diagram are shown in his article along with a list of the dominant wavelengths corresponding to these regions. The dominant wavelength of a region is the one whose hue is believed to most closely represent the hue name. A 1931 C.I.E. diagram

for 2° foveal vision that includes the standard tungsten source A for use in the present study has been shown in Fig. 11. As closely as possible, it retains the intersections of the dividing lines with the boundaries of the diagram and the dominant wavelengths as given by Kelley. His curved dividing lines are replaced by straight ones that converge on the white point A. The dashed lines divide the diagram into a condensed number of hue regions for photographic applications.

An achromatic point (white) in the chromaticity diagram represents a color that elicits no sensation of hue. The achromatic stimulus will vary depending upon the conditions under which colors are viewed. A straight line between this point and one on the spectrum locus is referred to as a line of constant dominant wavelength. Any point along the line represents what is called a spectral color and the intersection with the spectrum locus naturally represents a spectrum color. The wavelength of the spectrum color is called the dominant wavelength. Points that lie on the straight line boundary in the lower part of the diagram represent a mixture of wavelengths from both ends of the spectrum. They are called nonspectral colors. Points between this boundary and the achromatic point are included in this classification. These colors cannot be assigned a dominant wavelength, since no single wavelength has the same hue, but for convenience it can be specified by a complementary wavelength. If a line is drawn through the points that represent the nonspectral color and the achromatic source, the complementary wavelength is represented by the point at which this line intersects the spectrum locus. No further distinction will be made between lines of dominant and complementary wavelength.

Points along the boundary of the chromaticity diagram represent the purest colors. The achromatic point has a purity of zero, since its intensity distribution has no wavelength that is dominant. Points on a line between the achromatic point and the boundary have a purity which is proportional to their distance from the achromatic point. The maximum value is 1. Color purity is clearly defined in Fig. 12. However, purity is only an operational definition, as is dominant wavelength. The actual visual response related to purity is saturation of color, which is a sensation of the difference in a chromatic color sensation and an achromatic color sensation of the same brightness. If purity increases, though, saturation increases. It should be noted that a line of constant dominant wavelength is seldom a line of constant hue. In addition, equal purities along lines of different dominant wavelength do not signify equal saturations.[39]

Color discrimination and an associated purity discrimination vary throughout the chromaticity diagram. The change in chromaticity coordinates required to detect a just noticeable difference in color is not constant.[41] A purity threshold, defined by the least perceptible purity, exists at the achromatic point and varies for different lines of constant dominant wavelength. As a consequence, the achromatic point should actually be regarded as a small region. Figure 11 shows this region as five times the actual size. It is based on the just noticeable difference in color and is taken to be an ellipse.

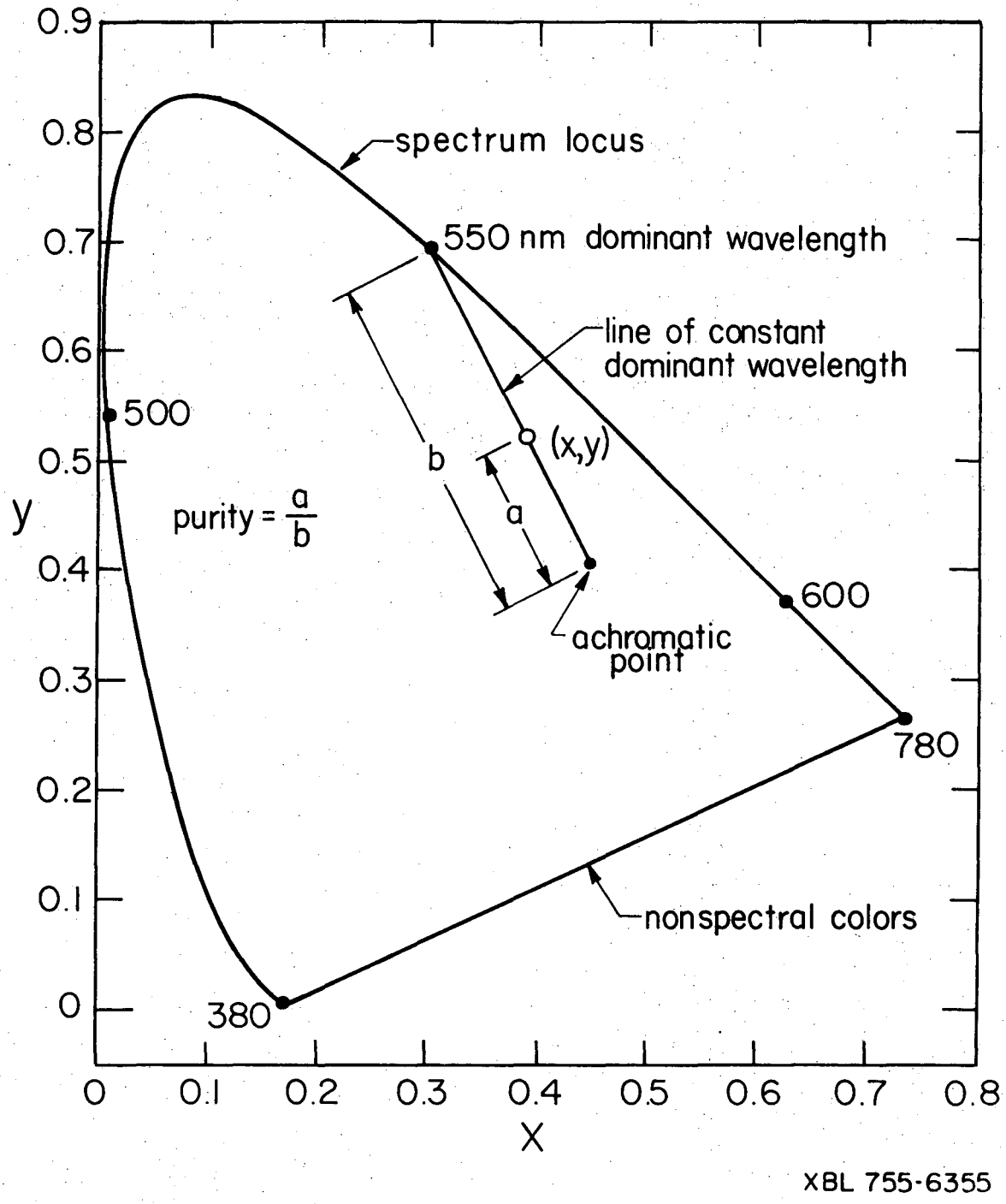

Fig. 12. Definition of color purity in C.I.E. chromaticity diagram.

III. ANALYSIS OF WHITE-LIGHT INTERFERENCE

An analysis of the phenomenon of white-light interference in thin films requires extensive use of a computer due to the complexity of the equations and the immense quantity of repetitive calculations. A computer program "HUE" for determining film thicknesses from white-light interference fringes is given in the Appendix. With this program, one can determine the angle of incidence at which fringes are most easily distinguished and also calculate the color of light reflected from a specific film and substrate combination at each film thickness. Extensive calculations are presented in graphical form in this section. Thus, close approximations for specific cases can be found without the use of lengthy computations.

A. Optimum Angle of Incidence

The ability of an observer to distinguish color fringes in white-light interference depends highly on the saturation of the colors. The angle of incidence at which the colors of the reflected light from a thin film are most saturated is the optimum angle to observe them. The operational definition that gives a measure of the saturation is the color purity, which is the fractional distance of a point within the chromaticity diagram from the achromatic point to the boundary of the diagram.

A detailed treatment of the problem is not available in the literature. Kubota[42] recognized the change in saturation with angle of incidence. He stated that in order for the purity of the interference color of thin dielectric films on metallic surfaces to be sufficiently high, the reflection coefficients at both interfaces must be nearly equal. For

this condition to hold, the angle of incidence must be greater than Brewster's angle. Muller[31] used the criterion of complete destructive interference at some angle of incidence to calculate the optimum angle to observe monochromatic interference fringes for some dielectric films on specific metal substrates. He found this procedure useful in the study of thin electrolyte films on polished metal surfaces. Turney[27] studied the problem further in comparing the optimum angles to observe monochromatic and white-light interference fringes from the same film-covered surface. He calculated the Michelson fringe visibility for many angles in order to determine the optimum angle. For the same film and substrate in white-light interference, he plotted the chromaticity coordinates as a function of optical path difference. The phase change due to reflection, $\delta_3 - \delta_1$, in Eq. (31) was taken equal to zero. When he compared such curves for many angles of incidence, he established the optimum angle on the basis of which curve was closest to the spectrum locus. He found agreement to within 1° between the two methods for a film of refractive index, 1.50, on platinum. With silver as the substrate, colors were most saturated at angles less than the optimum angle based on maximum Michelson fringe visibility. The reason for this discrepancy was not resolved. He concluded that a criterion other than a maximum Michelson fringe visibility might have to be used to determine the optimum angle to view white-light interference fringes for a highly reflective substrate.

The present study endeavors to clarify the relationship between the optimum angles to observe monochromatic and white-light interference fringes. A brief analysis of the problem is sufficient to demonstrate

that they are related. The intensity of monochromatic light, which is a periodic function of film thickness, and the spectral intensity distribution at each film thickness for white-light interference are both determined by Eq. (31). They fall on the same curve with δ in Eq. (22) as the abscissa, although the latter curve is limited in extent by the range of the visible spectrum. The effect of the wavelength dependence of the optical constants is assumed to be minor. The range of δ is the same at all angles of incidence, if the optical path difference is constant. Since the quantity, $\delta_3 - \delta_1$, varies relatively little from an angle of incidence of 0 to 90°, similar spectral energy distributions can be compared at any angle. If the spectral energy distributions at these angles are plotted on the same graph, the maxima or minima would occur at the same value of δ except for the small variation of δ_1 over the range of the angle of refraction in the film. The value of δ_3 differs by 180° above Brewster's angle from that below for p-polarized light. However, this abrupt difference does not make the analysis more difficult. Complete destructive interference at some angle of incidence has been shown in Section II-C-3 to be the criterion for maximum fringe visibility in monochromatic interference. This same condition in white-light interference yields a spectral energy distribution that appears to be most different from that of the source.

1. Color Purity

The variation of color purity with angle of incidence in the C.I.E. chromaticity diagram is analyzed on the basis of constant optical path difference. A method of representing the mixture of colors in the chromaticity diagram by the addition of terms in an equation for the

spectral energy distribution is employed.[29] The problem is discussed first for the relatively simple double-beam equation, Eq. (33). As explained earlier, this equation has a mathematical similarity to the multiple-beam equation, Eq. (31). The intensity derived by use of the multiple-beam equation approaches that of the double-beam equation in the limit of very small reflection coefficients. Conditions for the interference maxima or minima are the same in the two equations and complete destructive interference can occur only when r_3 and r_1 are equal.

The double-beam intensity equation is of the form

$$I_\lambda = c_0 + c_1 f_\lambda \quad . \tag{46}$$

For this analysis, c_0 and c_1 are assumed to be independent of wavelength, and f_λ is a function of wavelength only. If P_λ is the spectral energy distribution of the white-light source, the tristimulus values that correspond to Eq. (46) are

$$X = \Sigma P_\lambda [c_0 + c_1 f_\lambda] \bar{x}_\lambda = c_0 \Sigma P_\lambda \cdot \bar{x}_\lambda + c_1 \Sigma P_\lambda \cdot f_\lambda \cdot \bar{x}_\lambda \tag{47a}$$

$$Y = \Sigma P_\lambda [c_0 + c_1 f_\lambda] \bar{y}_\lambda = c_0 \Sigma P_\lambda \cdot \bar{y}_\lambda + c_1 \Sigma P_\lambda \cdot f_\lambda \cdot \bar{y}_\lambda \tag{47b}$$

$$Z = \Sigma P_\lambda [c_0 + c_1 f_\lambda] \bar{z}_\lambda = c_0 \Sigma P_\lambda \cdot \bar{z}_\lambda + c_1 \Sigma P_\lambda \cdot f_\lambda \cdot \bar{z}_\lambda \tag{47c}$$

As in Section II-D-2, expressions that represent the addition of two points in the plane of chromaticity coordinates are to be derived. The tristimulus value of the two points, (x_0,y_0) and (x_1,y_1), are

$$X_0 = \Sigma P_\lambda \cdot \bar{x}_\lambda \tag{48a}$$

$$Y_0 = \Sigma P_\lambda \cdot \bar{y}_\lambda \tag{48b}$$

$$Z_0 = \Sigma P_\lambda \cdot \bar{z}_\lambda \tag{48c}$$

and

$$X_1 = \Sigma P_\lambda \cdot f_\lambda \cdot \bar{x}_\lambda \tag{49a}$$

$$Y_1 = \Sigma P_\lambda \cdot f_\lambda \cdot \bar{y}_\lambda \tag{49b}$$

$$Z_1 = \Sigma P_\lambda \cdot f_\lambda \cdot \bar{z}_\lambda \tag{49c}$$

These last two sets of tristimulus values can be substituted into Eqs. (47a) through (47c) to obtain another expression for the tristimulus values of the mixture.

$$X = c_0 X_0 + c_1 X_1 \tag{50a}$$

$$Y = c_0 Y_0 + c_1 Y_1 \tag{50b}$$

$$Z = c_0 Z_0 + c_1 Z_1 \tag{50c}$$

No longer are the tristimulus values of the two component colors simply additive. Their addition is weighted by the values of c_0 and c_1. The chromaticity coordinates (x,y) of the mixture can be derived with the use of the definitions in Eqs. (44a) and (44b).

$$x = \frac{c_0 X_0 + c_1 X_1}{c_0 S_0 + c_1 S_1} = \frac{c_0 S_0 x_0 + c_1 S_1 x_1}{c_0 S_0 + c_1 S_1} \tag{51a}$$

$$y = \frac{c_0 Y_0 + c_1 Y_1}{c_0 S_0 + c_1 S_1} = \frac{c_0 S_0 y_0 + c_1 S_1 y_1}{c_0 S_0 + c_1 S_1} \tag{51b}$$

The point (x_0,y_0) has the coordinates of the white-light source, while (x_1,y_1) may represent a point that is outside the boundaries of the chromaticity diagram because of negative contributions to the tristimulus

values. The chromaticity coordinates of the mixture are weighted averages of the coordinates of the component colors. They are weighted by the corresponding tristimulus values and the relative values of c_0 and c_1. The point (x,y) always represents a color within the boundaries of the chromaticity diagram and lies on a straight line extending from the achromatic point (x_0,y_0).

The line segment defined by Eqs. (51a) and (51b) is one of constant dominant wavelength. Since purity increases with distance from the achromatic point, the condition for maximum purity is the highest ratio of c_1 to c_0. It can be seen from Eq. (33) that

$$c_0 = r_3^2 + r_1^2$$

and

$$c_1 = 2r_1r_3 \quad .$$

The ratio of c_1 to c_0 is

$$\frac{c_1}{c_0} = \frac{2r_1r_3}{r_3^2 + r_1^2} \quad .$$

This ratio has a maximum value of one when r_3 and r_1 are equal.

$$r_3 = r_1 \tag{52}$$

The result given by Eq. (52) is identical to that given by Eq. (39). A practical conclusion would be that when the reflection coefficients are low, the condition for the optimum angle in white-light interference is the same when determined on the basis of maximum color purity or maximum Michelson fringe visibility.

For high reflection coefficients, the multiple-beam intensity equation has to be considered. It is an extension of the arguments just presented that the color corresponding to the spectral energy distribution given by the multiple-beam intensity equation, Eq. (35), can be regarded as the addition of an infinite number of colors. This addition can be accomplished by adding the tristimulus values of all the component colors weighted by the coefficients of each term in the equation. Alternatively, the chromaticity coordinates of the mixture are averages of the coordinates of the component colors weighted by both the corresponding tristimulus values and the coefficients of each term in the equation. With the addition of more than two colors in the plane of chromaticity coordinates, the angles of incidence at which maximum monochromatic (Michelson) fringe visibility and maximum color purity occur do not coincide. An optimum angle based on maximum color purity cannot be calculated owing to the number of terms in Eq. (35). It is interesting to note that the optimum angle varies with film thickness. Although the coefficients do not, the colors represented by each term in the series do vary with film thickness. At small film thicknesses, the optimum angle based on color purity should be noticeably different from that at large thicknesses, except when the reflection coefficients are low.

2. Optimum Angle Based on Monochromatic (Michelson) Fringe Visibility

An approach to characterizing the optimum angle to view white-light interference fringes is to use the monochromatic optimum angle as a basis for comparison. The monochromatic optimum angle can be determined exactly. For p or s-polarized light, it varies only with the

optical constants of the film and substrate. Since this optimum angle is a function of three variables, the amount of information that can be contained in one figure is limited. The most convenient way of expressing the variation is demonstrated in Fig. 13. The optimum angle is plotted as a function of the real part of the substrate refractive index for curves of constant substrate extinction index. The film refractive index and the light polarization have to be specified. Values for this figure and others were determined to the nearest tenth of a degree. To establish curves of constant extinction index would require a significant amount of calculations, if program "VIS" in the Appendix were used. The amount was substantially reduced by using the method of matching reflection coefficients at the two interfaces in determining the optimum angle. A total of six figures was produced in this manner for s and p-polarized light and films of refractive index 1.35 (Figs. 13 and 14), 1.50 (Figs. 17 and 18) and 2.00 (Figs. 21 and 22). The value 1.35 was taken to represent the refractive index of dilute aqueous solutions with 1.50 representing an upper limit. Curves for a film refractive index of 2.0 were made for comparison.

Some aspects of these figures should be noted. In all of them are included some substrate refractive indices that are not physically realizable. Segments of curves with low values of both n and k were excluded when they crossed other curves. The figures clearly indicate which curves were not completely drawn. For p-polarized light, an optimum angle always exists, because the reflection coefficient at the air-film interface varies between 0 and 1. However, an optimum angle defined by matched reflection coefficients at the two interfaces does not always

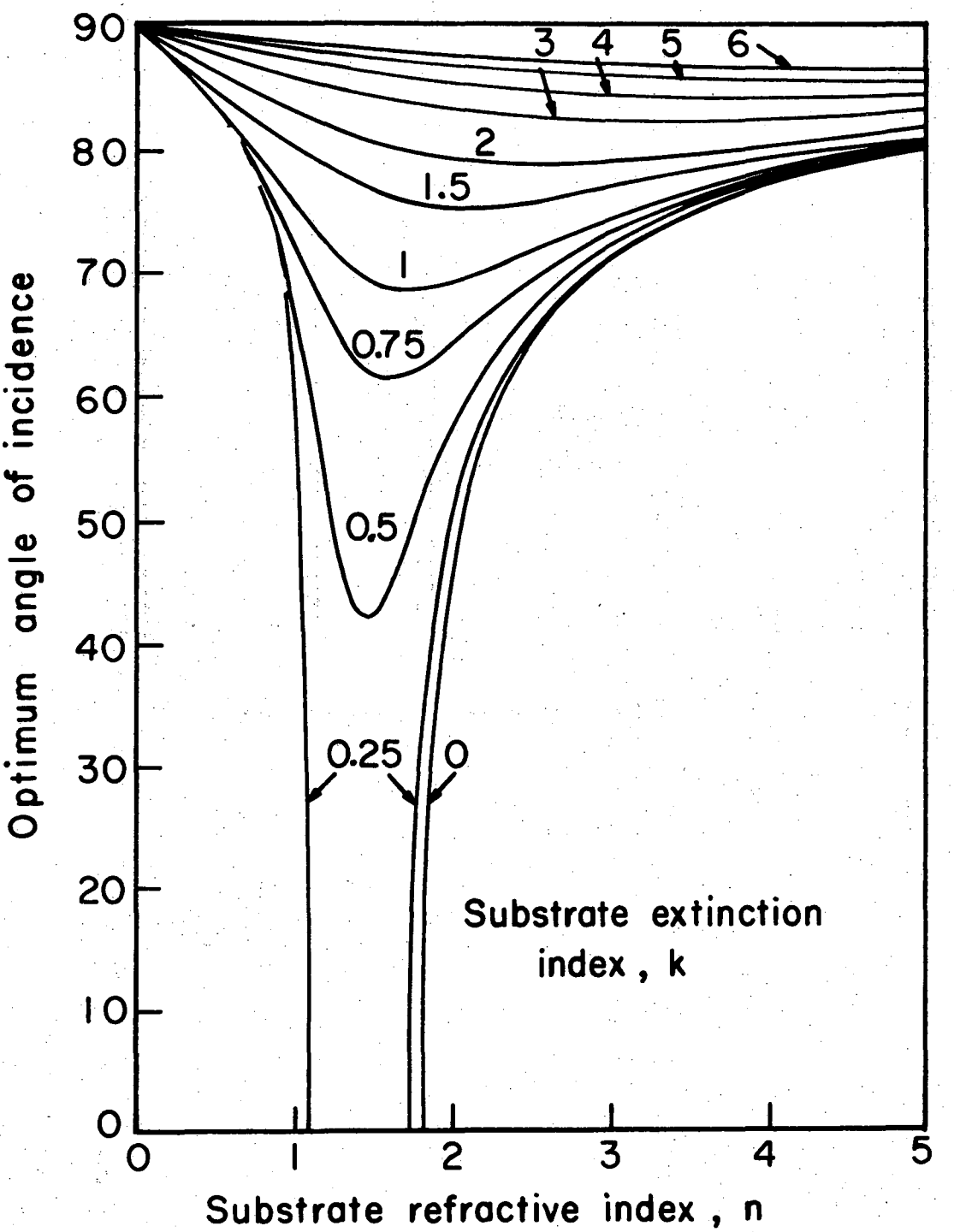

XBL751-2093

Fig. 13. Monochromatic optimum angle of incidence (Michelson fringe visibility = 1) for the observation of film interference. Dielectric film (refractive index = 1.35) on absorbing substrates (complex refractive index = n - ik), s-polarized light, incident medium air.

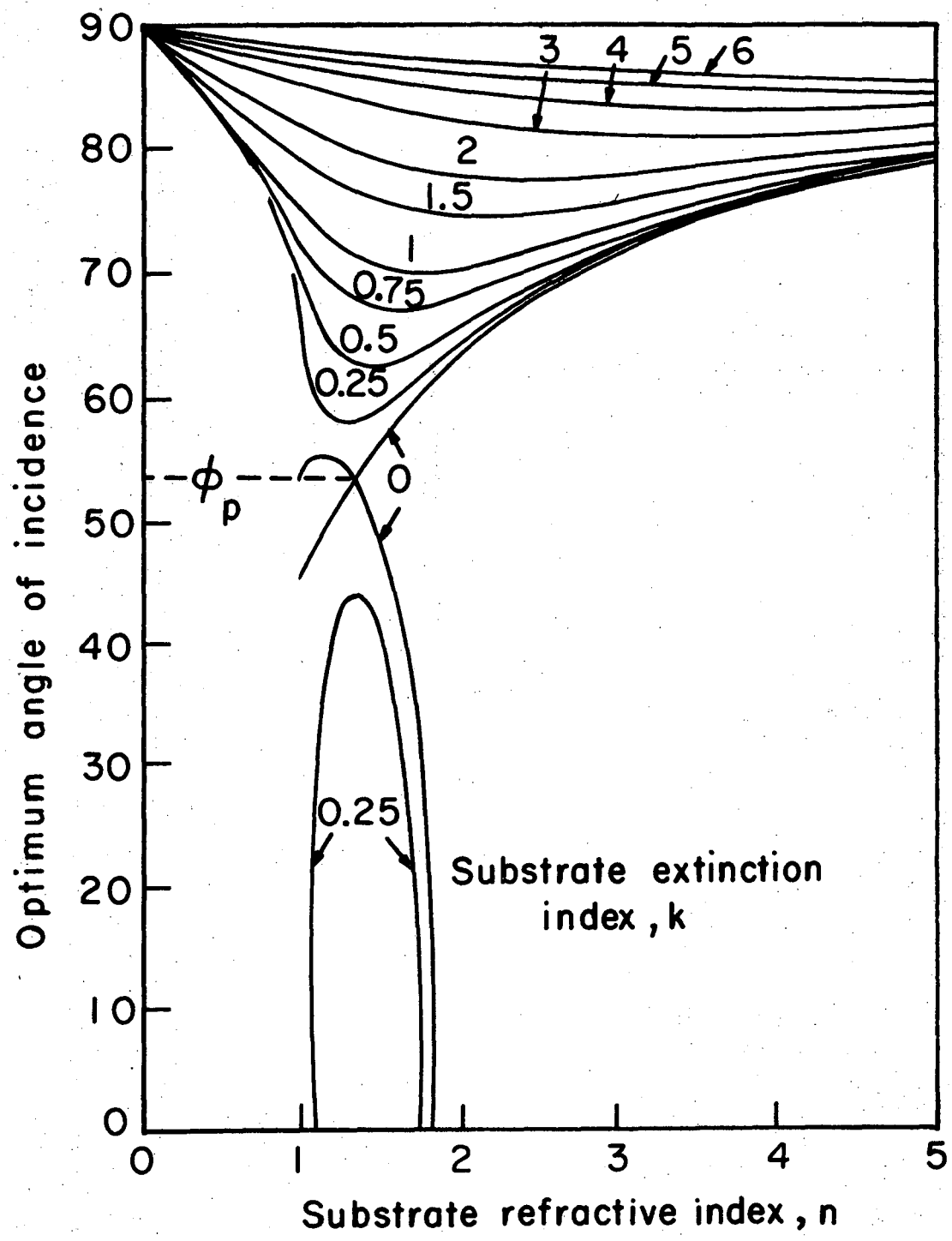

XBL751-2092

Fig. 14. See Fig. 13. p-polarized light. Brewster's angle, $\phi_p = 53.5°$.

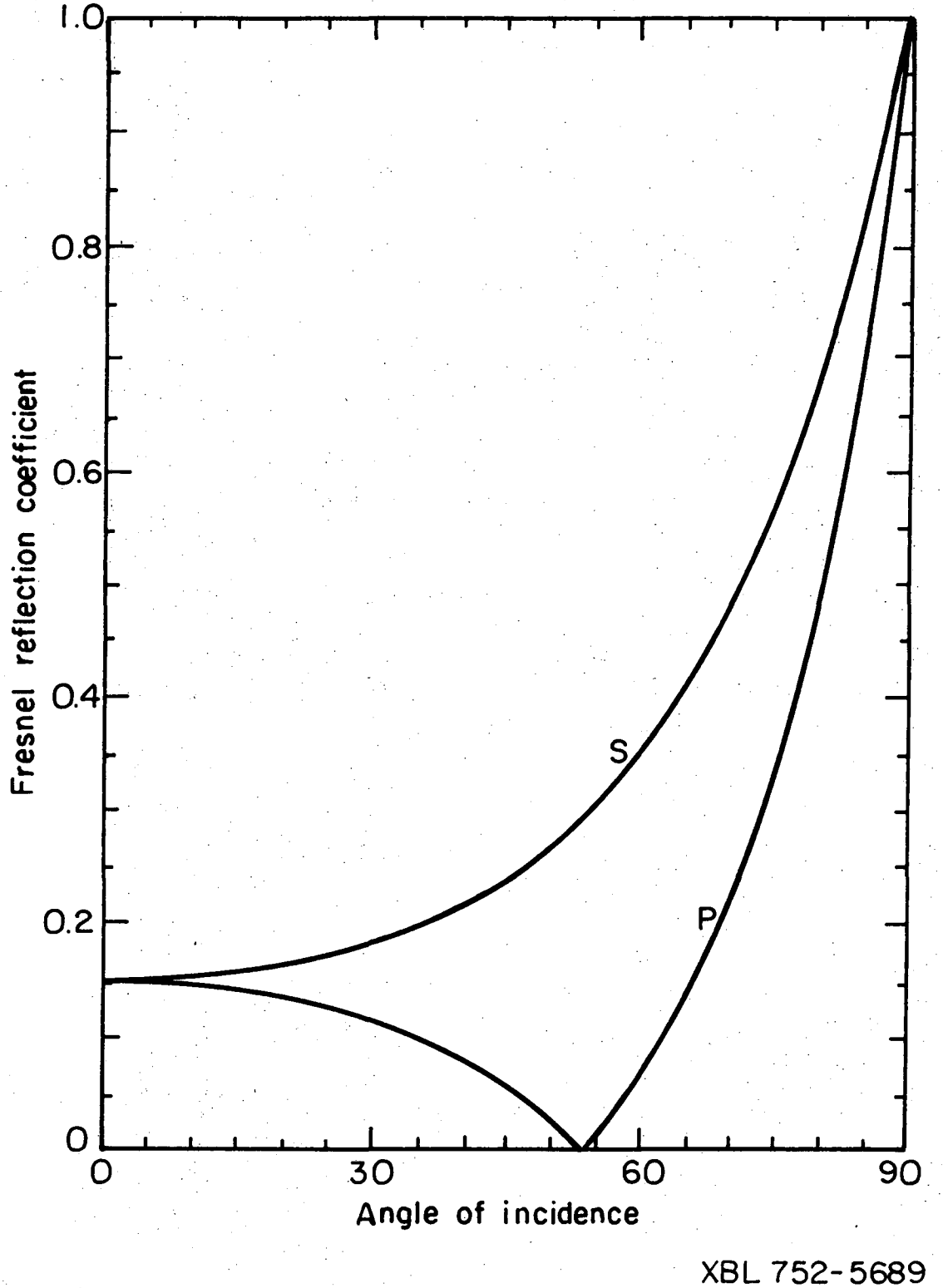

Fig. 15. Fresnel reflection coefficient for dielectric medium of refractive index = 1.35 for s and p-polarized light. Incident medium air. Brewster's angle, $\phi_p = 53.5°$.

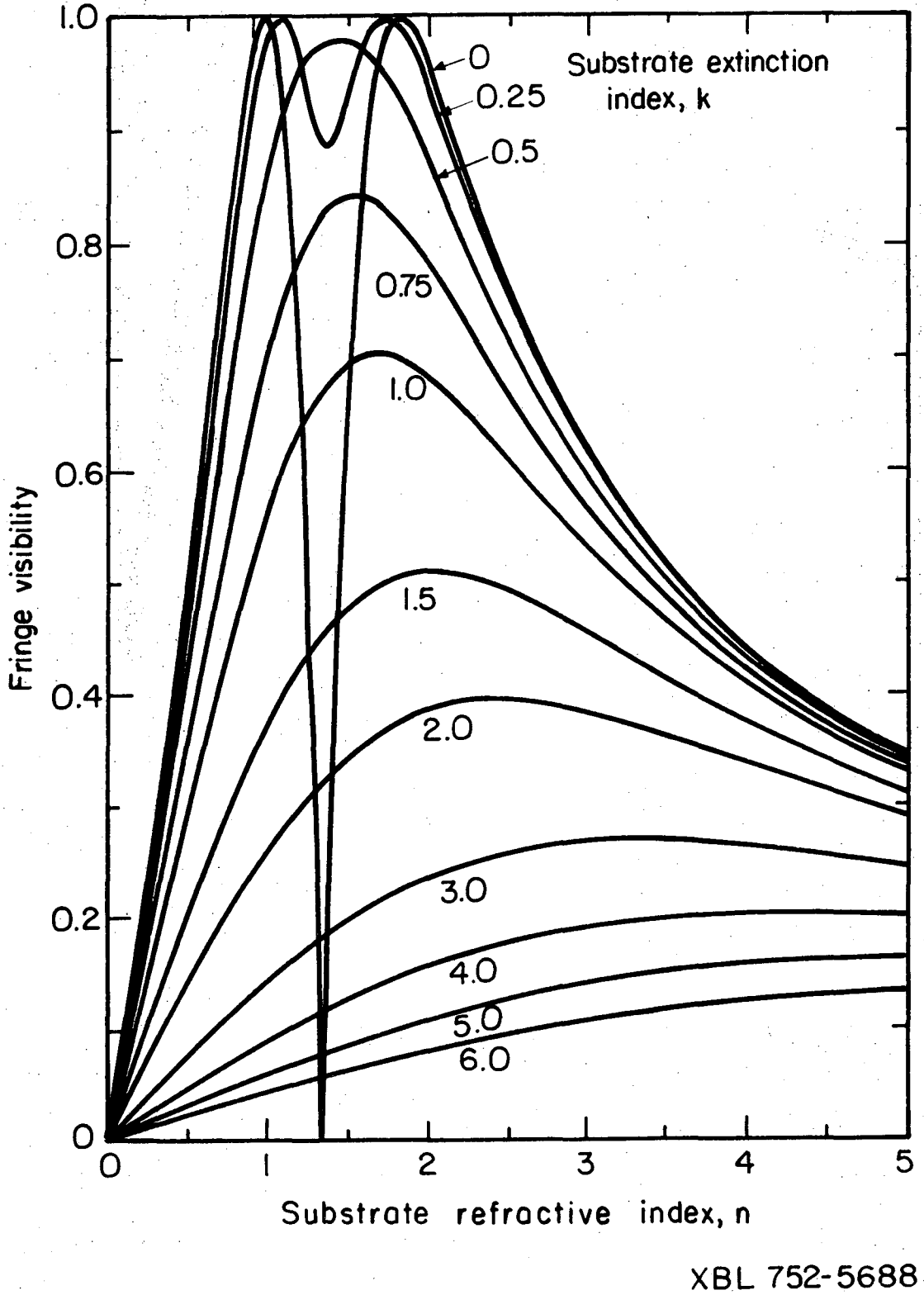

XBL 752-5688

Fig. 16. Michelson fringe visibility of monochromatic interference fringes from a dielectric film (refractive index = 1.35) on absorbing substrates (complex refractive index = n - ik). Normal incidence. Incident medium air.

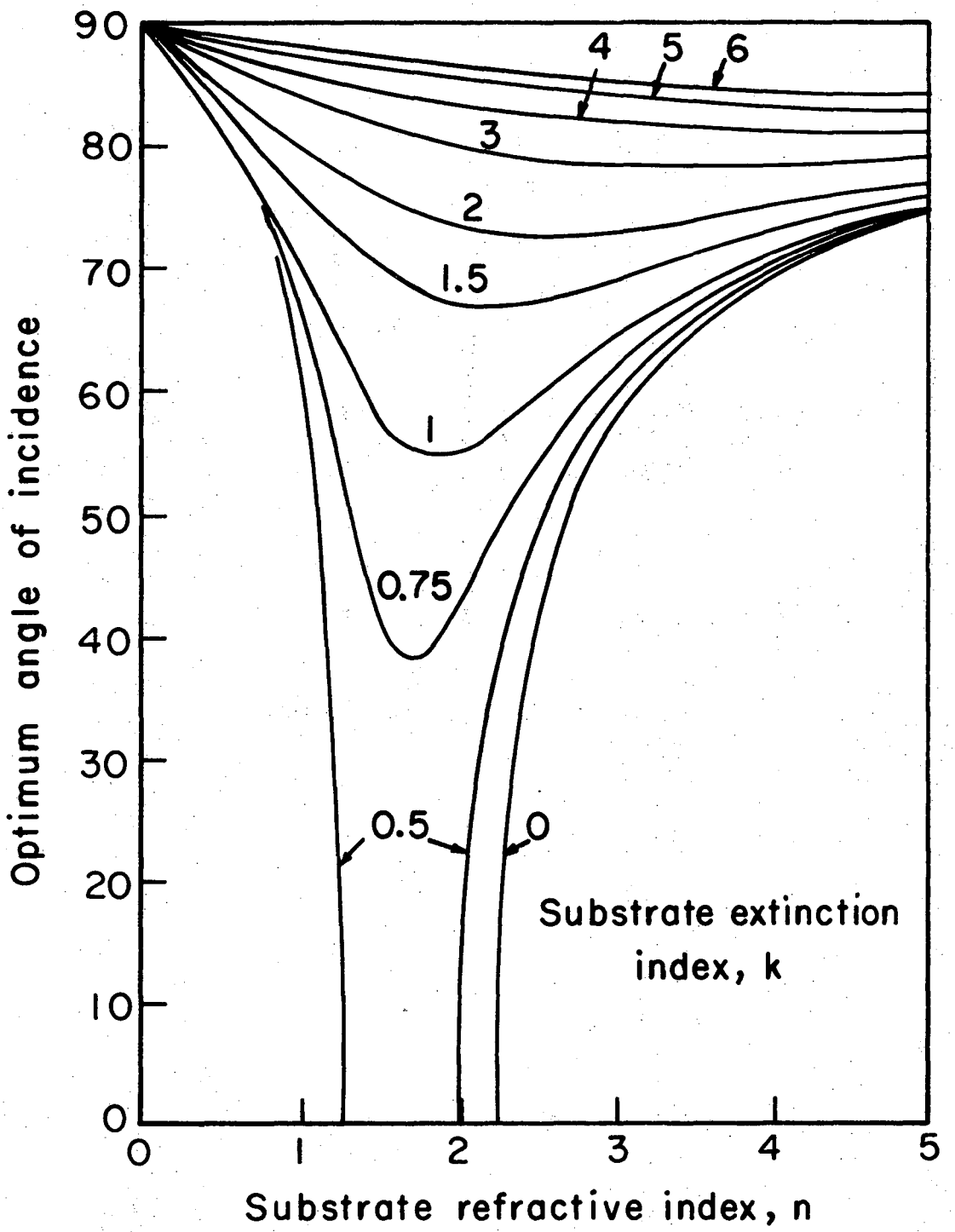

XBL751-2091

Fig. 17. See Fig. 13. Film refractive index = 1.50.

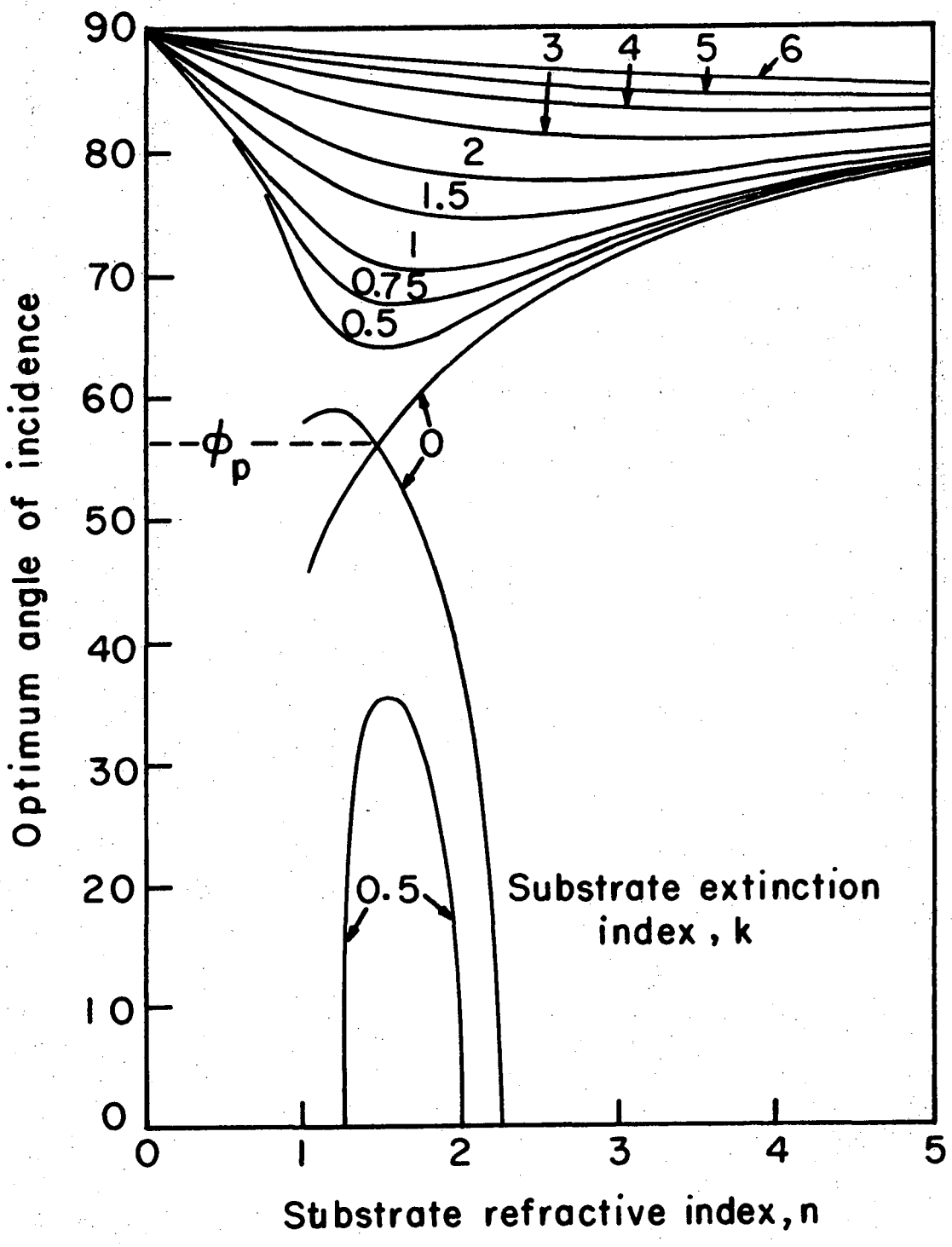

XBL751-2094

Fig. 18. See Fig. 13. p-polarized light. Film refractive index = 1.50. Brewster's angle, $\phi_p = 56.3°$.

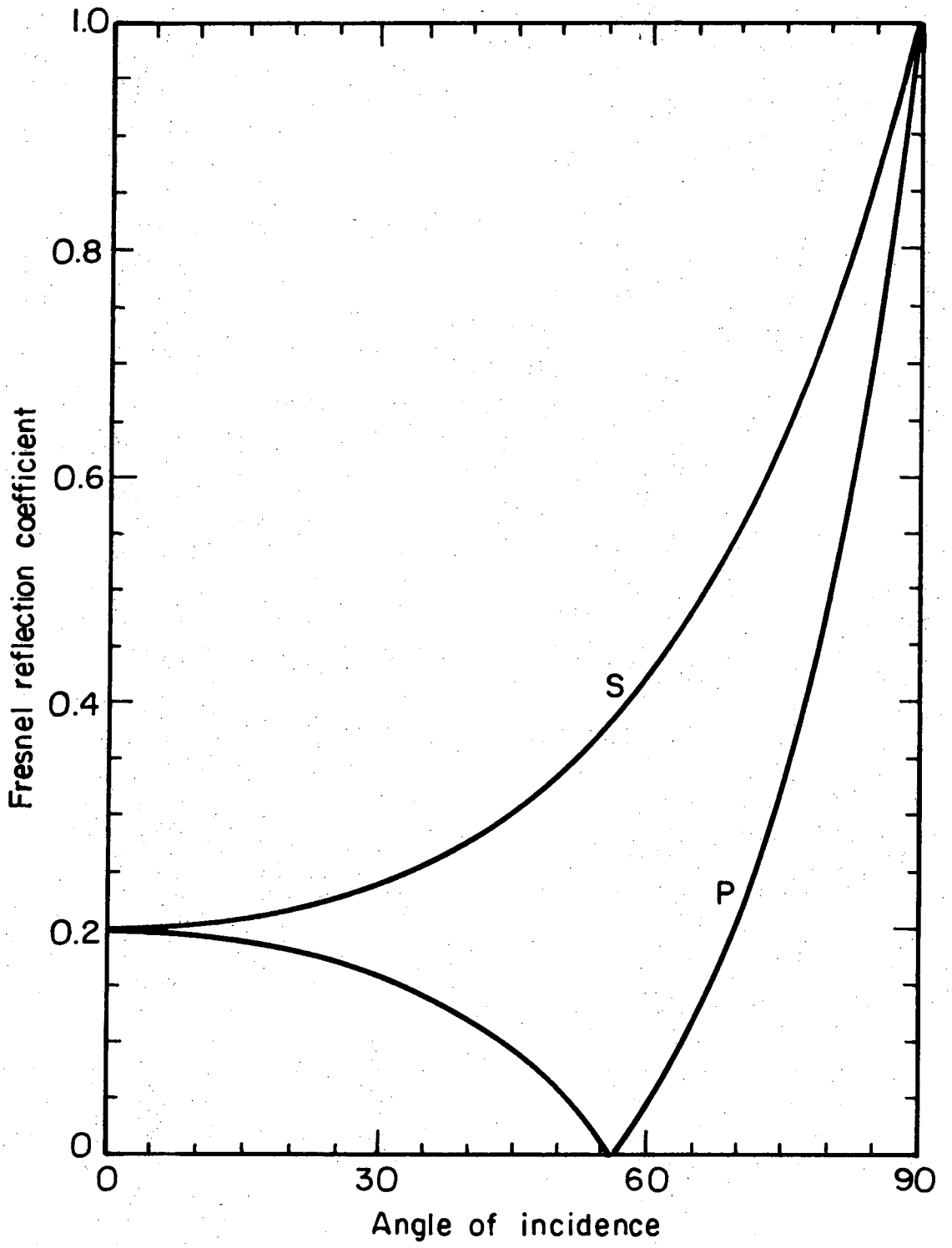

XBL752-5691

Fig. 19. Fresnel reflection coefficient for dielectric medium of refractive index = 1.50 for s and p-polarized light. Incident medium air. Brewster's angle, $\phi_p = 56.3°$.

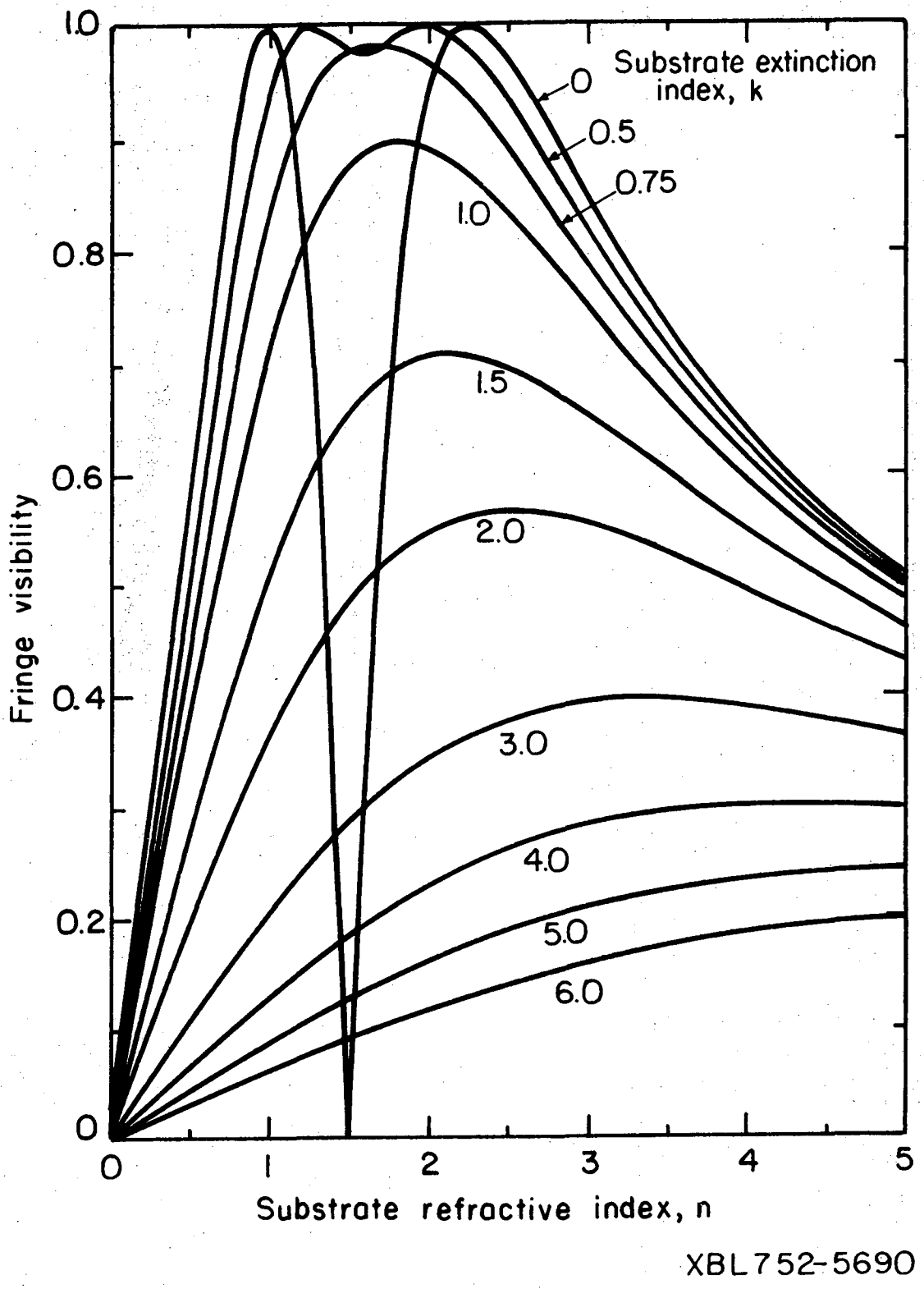

Fig. 20. See Fig. 16. Film refractive index = 1.50.

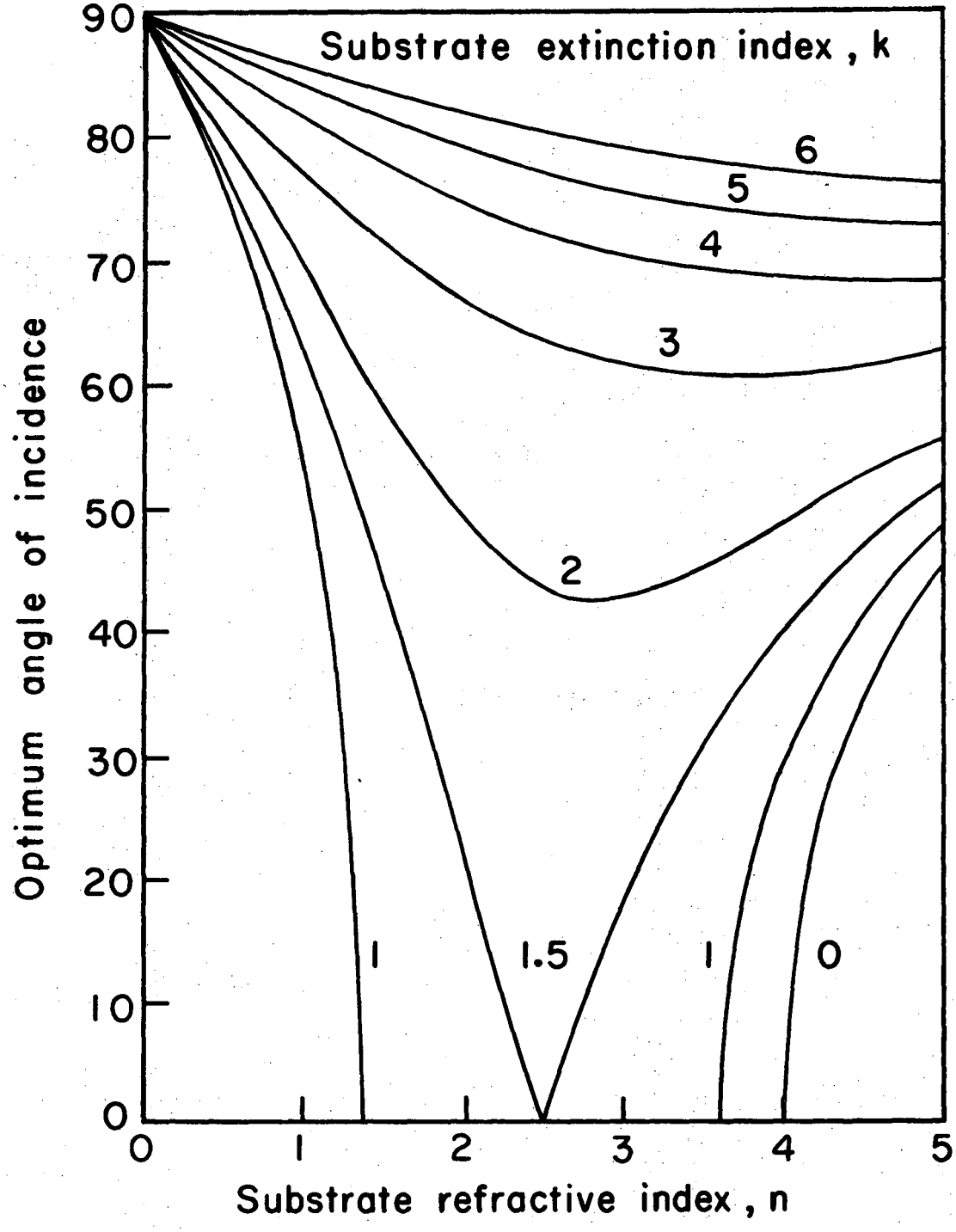

XBL751-2090

Fig. 21. See Fig. 13. Film refractive index = 2.0.

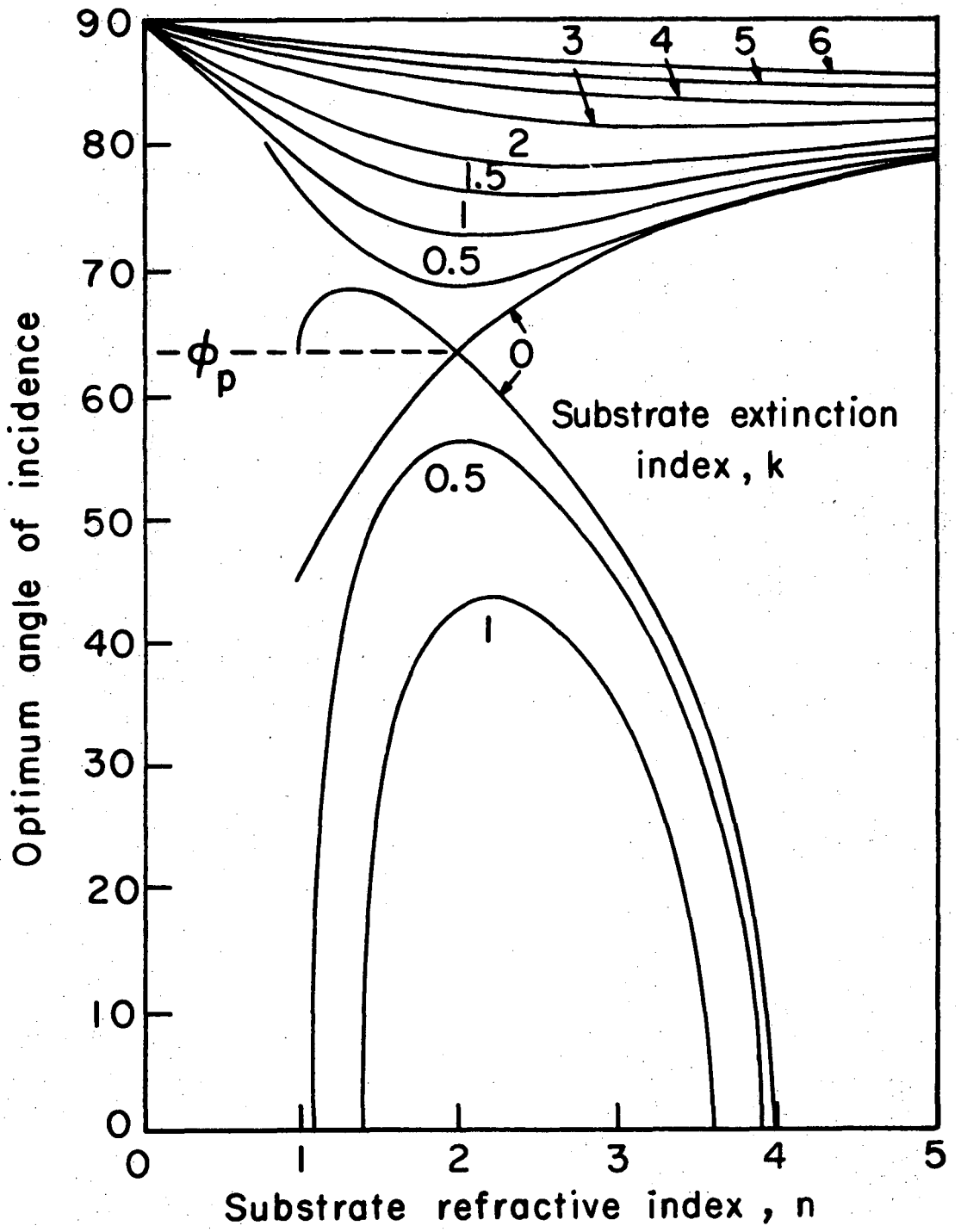

XBL751 - 2089

Fig. 22. See Fig. 13. p-polarized light. Film refractive index = 2.0. Brewster's angle, $\phi_p = 63.5°$.

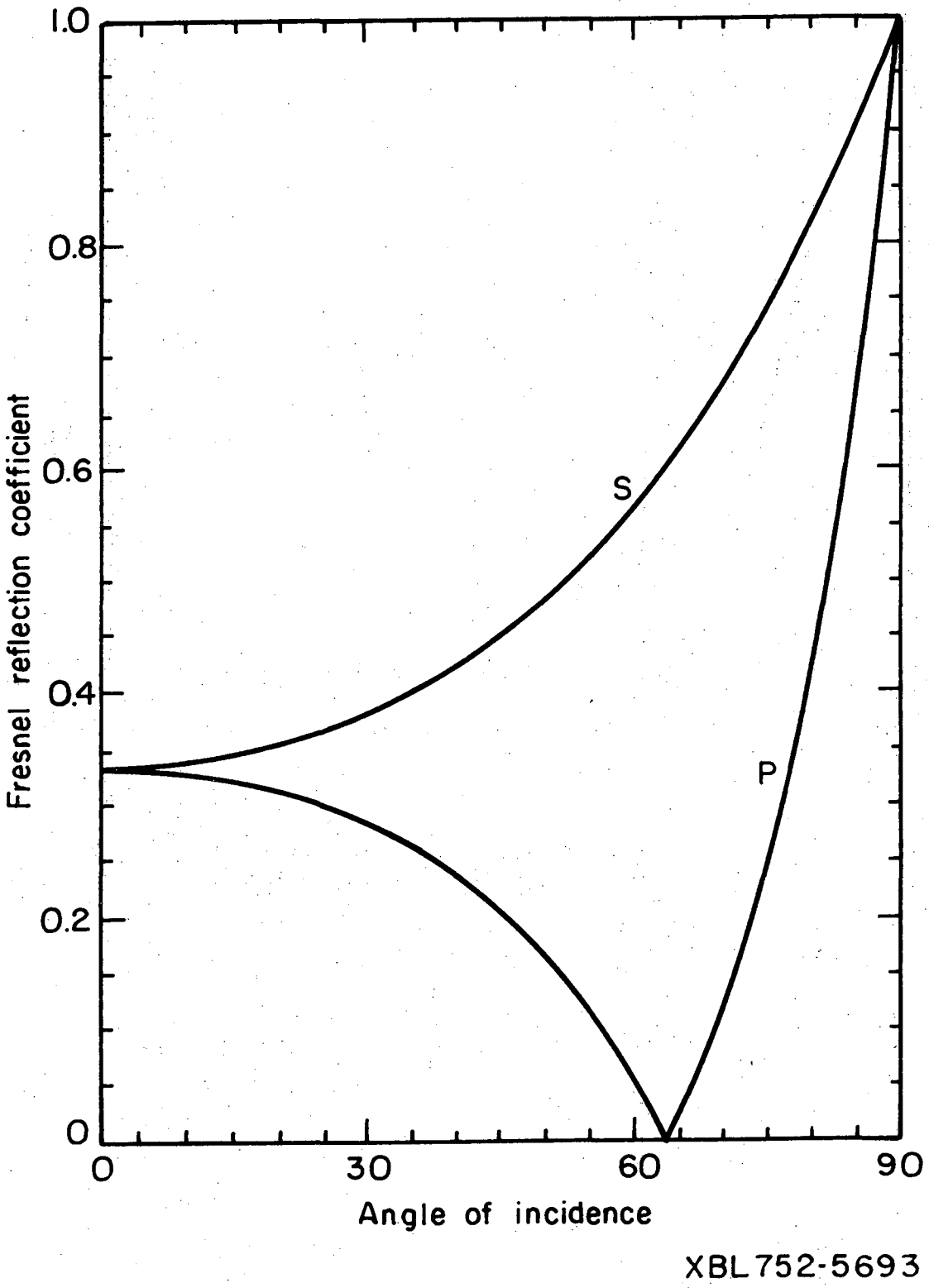

Fig. 23. Fresnel reflection coefficient for dielectric medium of refractive index = 2.0 for s and p-polarized light. Incident medium air. Brewster's angle, $\phi_p = 63.5°$.

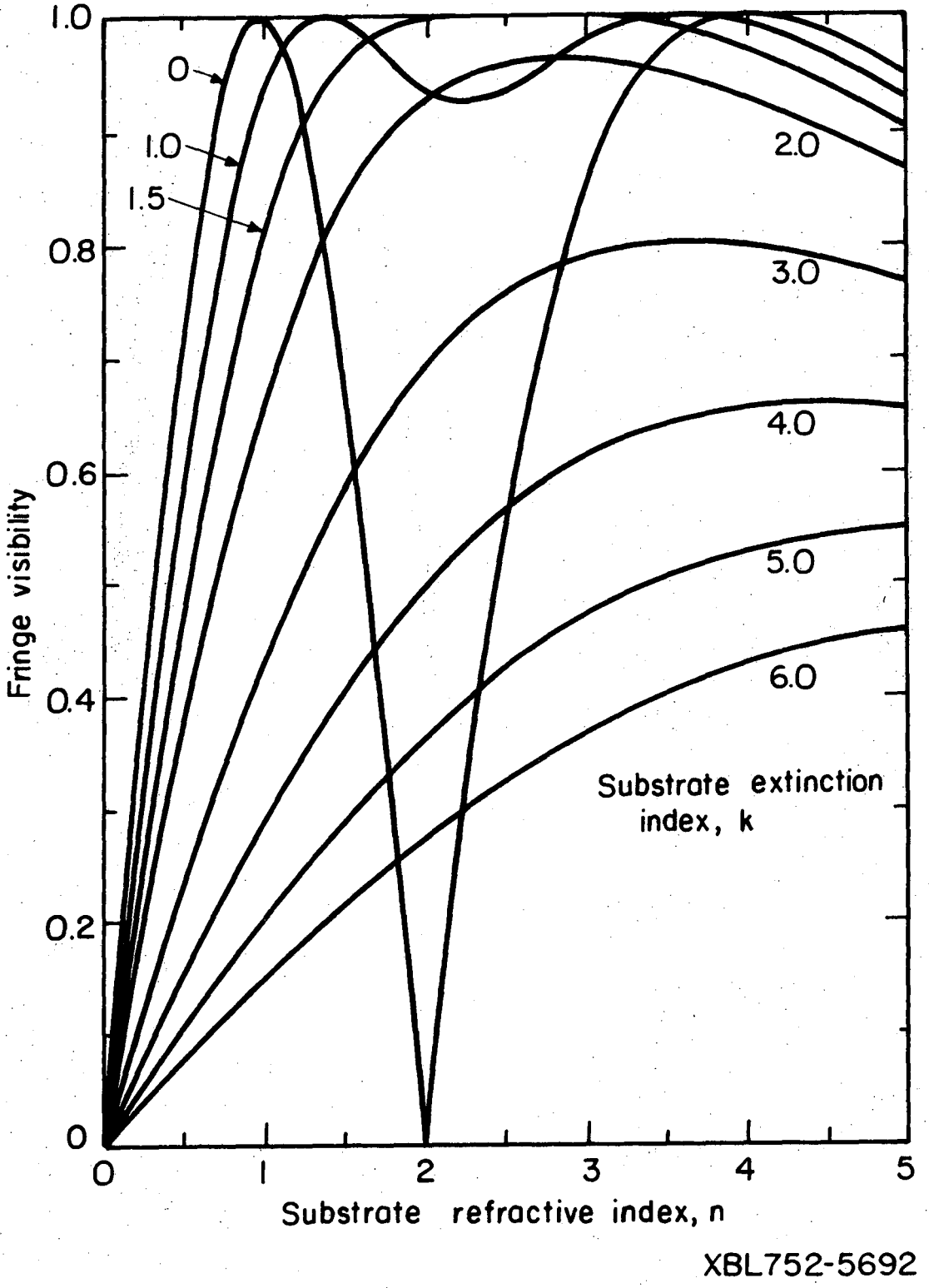

Fig. 24. See Fig. 16. Film refractive index = 2.0.

exist for s-polarized light. Zero degrees would then be considered the best angle of incidence, since it is at this angle that the monochromatic fringe visibility would be highest (although not equal to one).

Two other types of curves associated with the optimum angle curves are included. They, too, are for specified film refractive indices of 1.35, 1.50 and 2.0. Figures 15, 19 and 23 give Fresnel reflection coefficients as a function of angle of incidence for both s and p-polarized light. These give the reflection coefficient at the air-film interface and thus contribute the reflection coefficients at both interfaces at the optimum angle of incidence. At the optimum angle, the monochromatic (Michelson) fringe visibility equals one. Figures 16, 20 and 24 show the dependence of the fringe visibility at normal incidence on the optical constants of the substrate. They enable one to accurately sketch the variation of the fringe visibility with angle of incidence for a particular film and substrate. Also, they clearly demonstrate the advantage of observing interference fringes at angles other than normal incidence. This concept is most important for films of low refractive index and an associated low reflectivity.

3. Optimum Angle Based on Color Purity

The initial attempt at examining the optimum angle of incidence based on maximum color purity was through Figs. 13, 14, 17 and 18. Points along the curves in these figures were selected for a comparison. For several widely different values of the optical path difference, chromaticity coordinates were calculated as the angle of incidence varied. The angle at which the coordinates were furthest from the achromatic point was

considered to be the optimum angle. From this comparison, it was concluded that the optimum angle varied with the optical path difference. No exact curves could be constructed, but some definite conclusions were drawn. The trend in the variation of the optimum angle for white-light interference was the same as that for monochromatic interference. The curves, however, were not quantitatively the same. The monochromatic optimum angle was always higher than that based on a maximum color purity. The difference was more marked the higher the optimum angle (higher reflection coefficients). Also, the difference was greater for s-polarized light than for p-polarized light. Higher reflection coefficients were again the cause. When the reflection coefficients were low, the two methods yielded nearly the same optimum angle at several values of the optical path difference.

The next step was to examine the optimum angle in greater detail for a limited number of substrates. Three substrate refractive indices were selected to obtain a wide range of reflection coefficients at the optimum angle. These optical constants were intended to represent silver,[43,44] platinum[43,44] and silicon.[45] Curves of chromaticity coordinates as a function of film thickness were plotted in 100Å increments for film thicknesses between 0 and 1.5 microns. Several curves were drawn in one degree increments around the monochromatic optimum angle in order that the optimum angle based on maximum color purity could be estimated to the nearest degree. The angle at which the curves appeared to be closest to the spectrum locus was chosen as the optimum angle. The results are displayed in Table I. Since the curves were visually compared by superimposing them, the optimum angle was often difficult to pinpoint.

Table I. Optimum angle of incidence (deg).

Dielectric Film Refractive Index -		1.35		1.50		2.0	
Light Polarization -		s	p	s	p	s	p
Substrate Complex Refractive Index	Criteria*						
0.18-i(3.71) (Silver)	a	89.4	89.3	89.2	89.3	88.2	89.3
	b	88	89	88	88	86	89
	c	88	88	85	87	82	88
2.63-i(3.55) (Platinum)†	a	84	83	80.5	83	68	83
	b	83	82	80	82	66	83
	c	79	81	75	81	59	82
4.14-i(0.03) (Silicon)	a	77.5	76.5	70	76.5	19.5	76.5
	b	76.5	76	69	76	**	76
	c	74	76	65	76	**	76

*Criteria a Michelson fringe visibility = 1

b Maximum color purity, first color order

c Maximum color purity, higher color orders

**Not sensitive to angle of incidence.

†Value for platinum used elsewhere in this section was 2.07 - i(4.40).

At small film thicknesses, the curves were not smooth. With silver as the substrate, they were rather compact and harder to compare. Nevertheless, Table I presents a valid picture. The variation of the curves with angle of incidence in the first color order was significantly different from that in the higher orders. It follows that the optimum angle for the first order and that for the higher orders should be estimated separately.

Agreement between results based on Michelson fringe visibility and color purity is rather close. As stated earlier, the monochromatic optimum angle is used as the basis for comparison. It serves as an upper limit. The optimum angle for the first color order differs from it by no more than about 2°. This result appears to hold for p-polarized light independent of the color order. In the case of s-polarized light, the agreement worsens for the higher color orders and the optimum angle is seen to be generally several degrees lower. The change in color purity with angle of incidence was observed to be much more gradual in the higher color orders, though, than in the first order. An overall view of the table shows that for p-polarized light the optimum angle is nearly independent of the film refractive index. A comparison of Figs. 14, 18 and 22 confirms this observation. As in Figs. 13, 17 and 21, the optimum angle for s-polarized light decreases with an increase in the film refractive index.

The description of the optimum angle has been accurate but lacks sufficient detail. A much closer look at both the variation of the color purity with angle of incidence and the dependence of the optimum angle on the optical path difference would be very instructive. Figures were devised that would display these dependencies. They were constructed

for a film of refractive index 1.35 on substrates with widely varying optical constants. In all the figures, the film refractive index was assumed to be independent of wavelength. With platinum or silver as the substrate, the substrate refractive index varied with wavelength as shown in Fig. 25 or was taken to be that at an intermediate wavelength of 5892Å. Straight lines in Fig. 25 were fitted to the data given in the International Critical Tables.

Figures discussed in the previous paragraph are shown next starting with Fig. 26. Most importantly, they contain curves of chromaticity coordinates as a function of angle of incidence for constant values of the optical path difference. Curves of constant angle of incidence are also drawn. The outer curve is taken to represent the optimum angle of incidence, since its chromaticity coordinates are furthest from the achromatic point throughout most of the color order. Points that represent constant intervals of the optical path difference are indicated by dots along this curve. It appears that curves such as these do not occur in the literature. However, Kubota[29] has presented a figure that is outwardly similar. It included curves of constant optical thickness and curves of constant angle of incidence for a film and substrate refractive index of 2.20 and 1.50, respectively, and p-polarized light. Angles of incidence included those below Brewster's angle. The purpose of this figure was to follow the change in chromaticity coordinates with angle of incidence for this type of layer and to demonstrate the changes of hue and purity. He contrasted the relative change of hue and purity with that for a layer whose refractive index was less than that of the substrate.

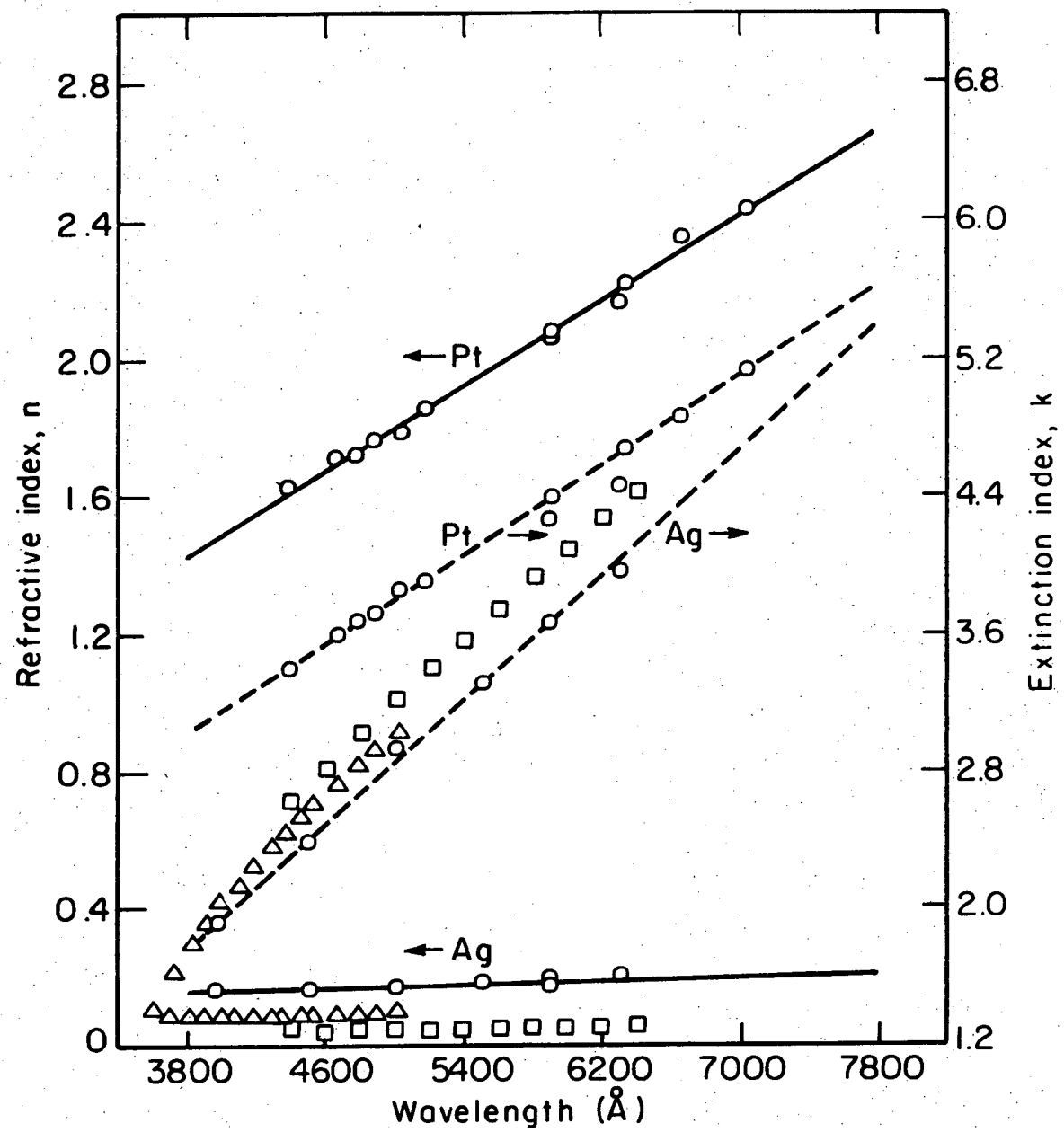

Fig. 25. Complex refractive index of platinum and silver in the visible spectrum. Straight line fit to data given in the International Critical Tables.
O International Critical Tables[43]
Δ Reference[46]
□ Reference[47]

Figure 26 presents results for a dielectric film on a dielectric substrate. This situation contrasts with interference in dielectric films on metal surfaces, which is described in later figures. Since the reflection coefficients are low, curves of constant optical path difference should be nearly straight. The optimum angle should be low and invariant with optical path difference. It agrees very closely to the monochromatic optimum angle given in Fig. 13. General characteristics of interference in thin films on dielectric substrates are that color purity is high and changes slowly with angle of incidence. The fact that interference fringes can be viewed satisfactorally at normal incidence is demonstrated in Fig. 26 by the considerable color purity obtainable at 0°.

Figures 27 and 28 were constructed for substrates of medium and high reflectivity. Curves of constant optical path difference are not straight to the extent they are in Fig. 26. Nevertheless, changes in purity dominate over any change in hue. The significance of the concept of an optimum angle becomes evident for substrates of higher reflectivity. With silver as the substrate, it would be impossible to observe interference colors at normal incidence. In the progression from Fig. 26 through 28, the fractional change in the color purity with angle of incidence becomes sharper about the optimum angle. Since away from the optimum angle the color purity is extremely low for a highly reflective substrate, the concept of an optimum angle gains in importance. However, the best obtainable color purity is still quite low. These three figures contain curves for just the first color order. Throughout this order, the optimum angle shows little variation with optical path difference. When the variation of the optical constants of the substrate with wavelength (Fig. 25) is included in the calculations, the curves undergo

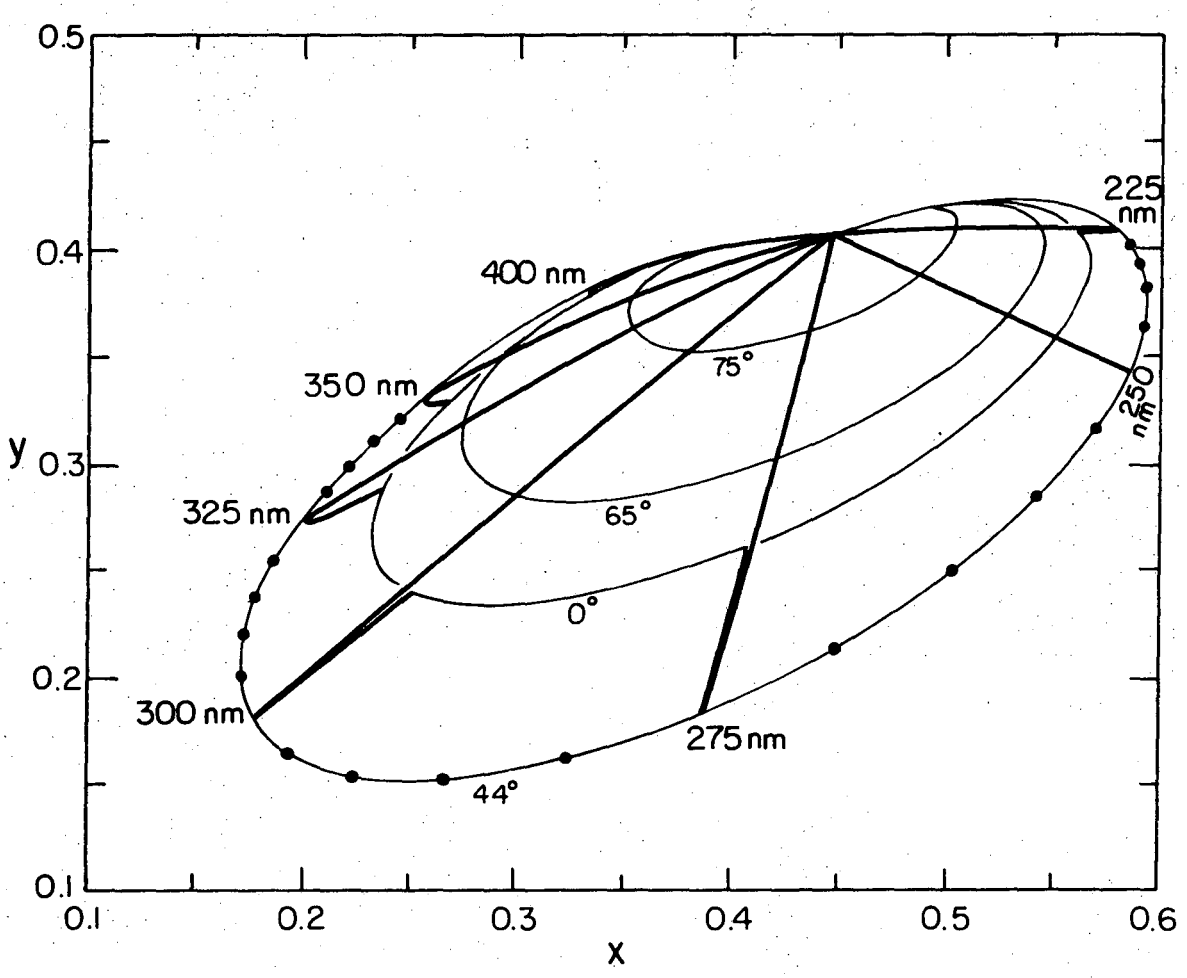

XBL752-5694

Fig. 26. Optimum angle of incidence for white-light interference. Chromaticity coordinates as a function of angle of incidence and optical path difference. Dielectric film (refractive index = 1.35) on dielectric substrate (refractive index = 2.0), s-polarized light, first color order (optimum angle, 44°).

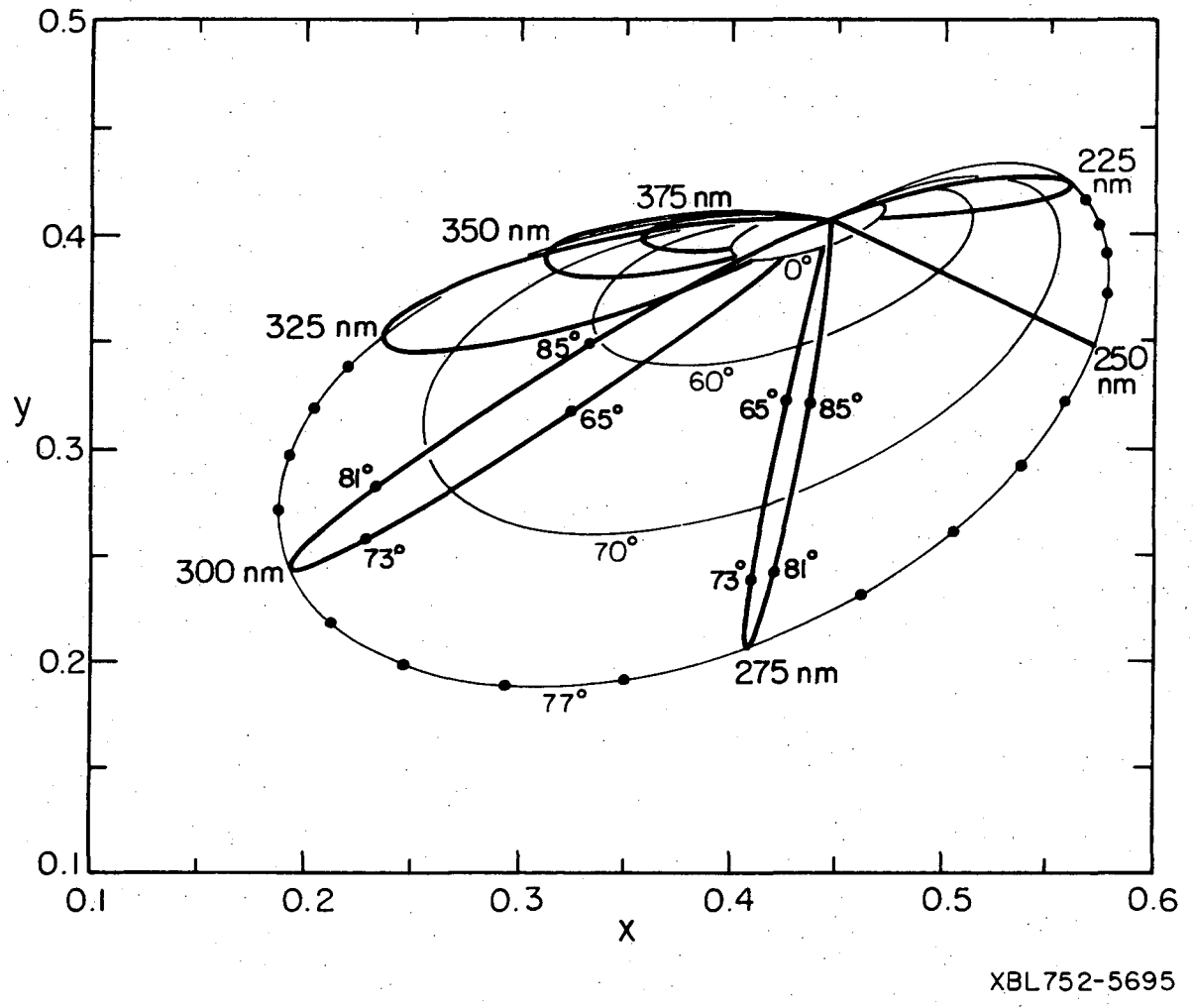

Fig. 27. See Fig. 26. Dielectric film (refractive index = 1.35) on substrate (silicon, refractive index = 4.14 - i(0.03)) of medium reflectance, s-polarized light, first color order (optimum angle, 77°).

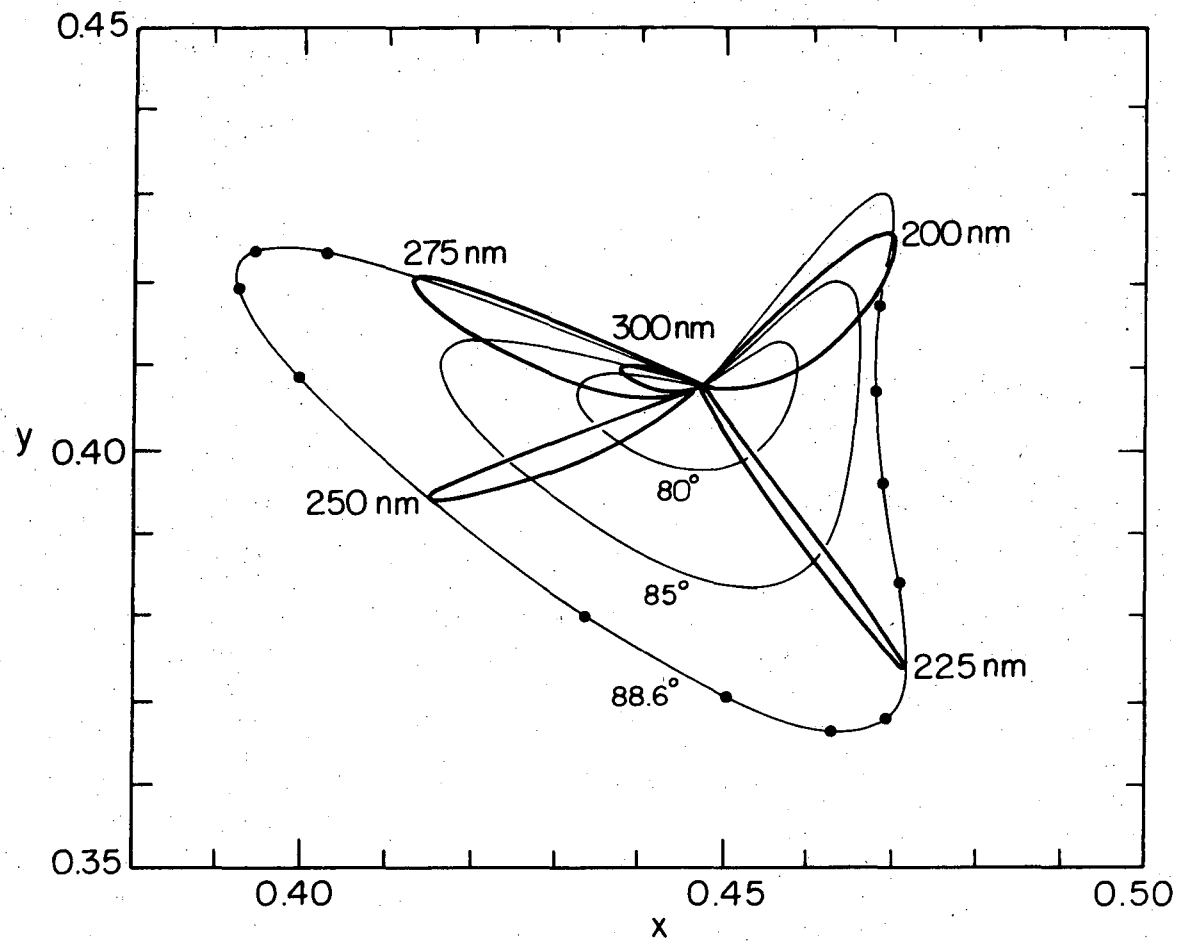

XBL752-5698

Fig. 28. See Fig. 26. Dielectric film (refractive index = 1.35) on substrate (silver, refractive index = 0.18 - i(3.71)) of high reflectance, s-polarized light, first color order (optimum angle, 88.6°).

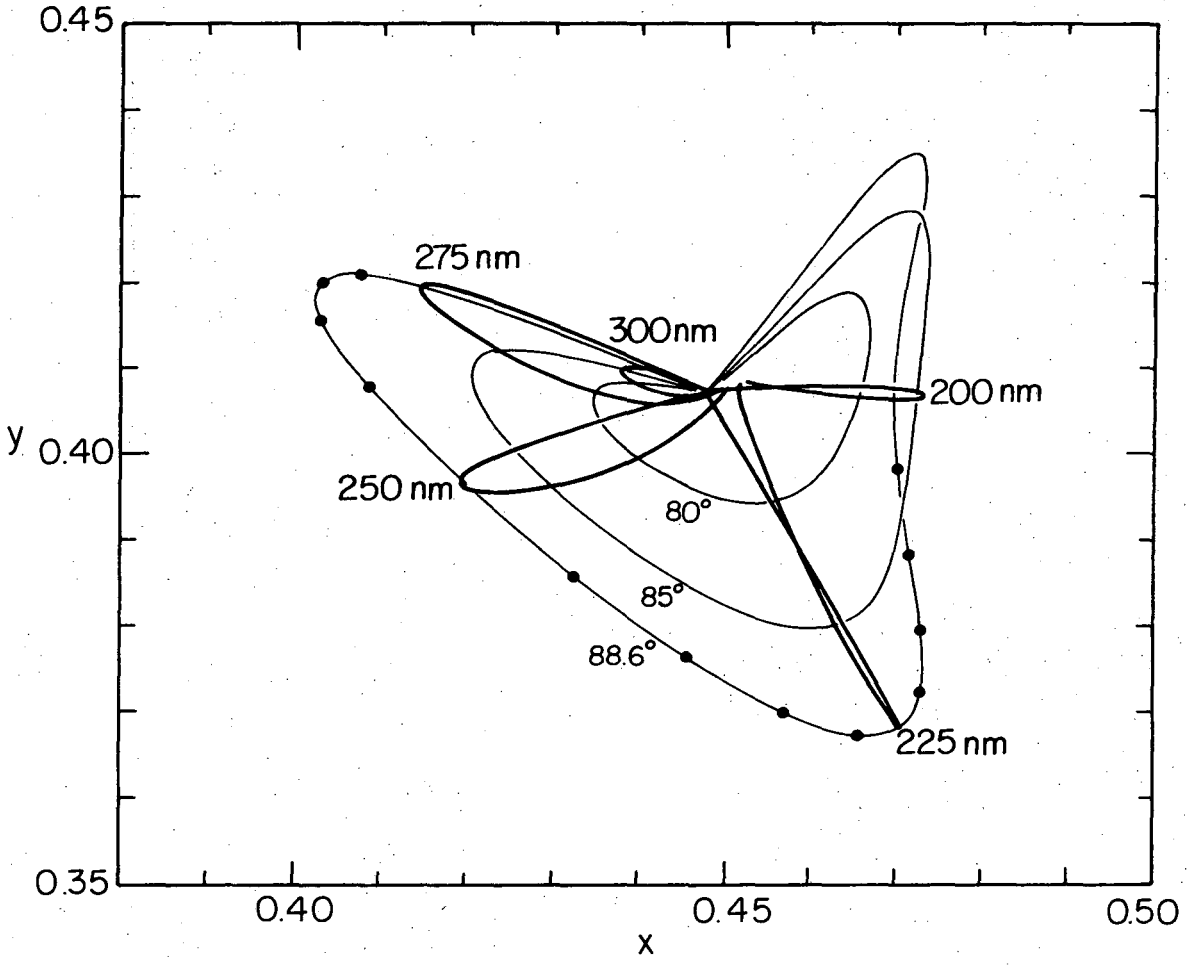

Fig. 29. See Fig. 26. Wavelength dependence of optical constants of substrate (silver) considered for comparison with Fig. 28. Dielectric film (refractive index = 1.35) on substrate of refractive index n - ik, where n = 0.155 + 0.0000125 (λ - 3800) and k = 1.76 + 0.000905 (λ - 3800).

slight changes. Compare Figs. 28 and 29 for differences. The optimum angles are still nearly equal.

The next six figures, Figs. 30 through 35, are for a platinum substrate. For both s and p-polarized light, curves were constructed for the first and second color orders. Curves that include the variation of the substrate refractive index with wavelength are also presented for the first color order. A comparison of Figs. 30 and 31 shows the difference between the first and second color orders. The colors in the second order are much less pure. The optimum angle is lower but still remains nearly constant throughout the order. It is broader in the sense that the fractional change in purity with angle of incidence is less. One can reach the same conclusions by comparing Figs. 33 and 34 for p-polarized light. For the sake of clarity, only angles of incidence above Brewster's angle are shown.

In addition to the second order in Figs. 31 and 34, some higher orders will now be considered. Figures 36 and 37 for s and p-polarized light and a specified film and substrate show the purity of red interference fringes as a function of the angle of incidence. The particular red hue is defined by a line of constant dominant wavelength. Compare these curves with the fringe visibility curves in Figs. 8 and 9, which give the monochromatic optimum angles. The curves have the same general shape, but their maxima occur at different angles. The optimum angle based on maximum color purity is lower and decreases from the first to the third order. Also, the maxima in color purity become broader in the higher orders.

Some general observations concerning the optimum angle can be explained graphically. For this purpose, the curves in Figs. 38

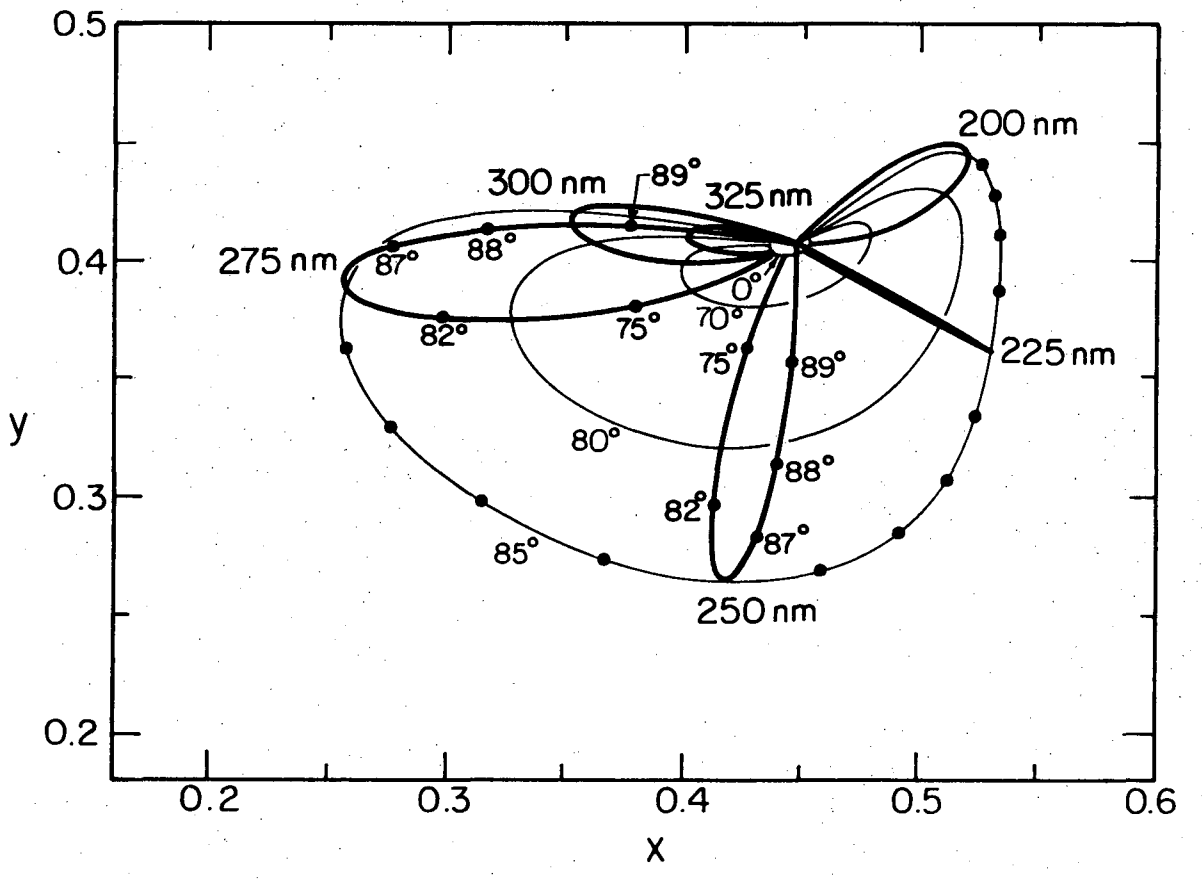

XBL752-5696

Fig. 30. Optimum angle of incidence for white-light interference. Chromaticity coordinates as a function of angle of incidence and optical path difference. Dielectric film (refractive index = 1.35) on platinum substrate (refractive index = 2.07 - i(4.40)), s-polarized light, first color order (optimum angle, 85°).

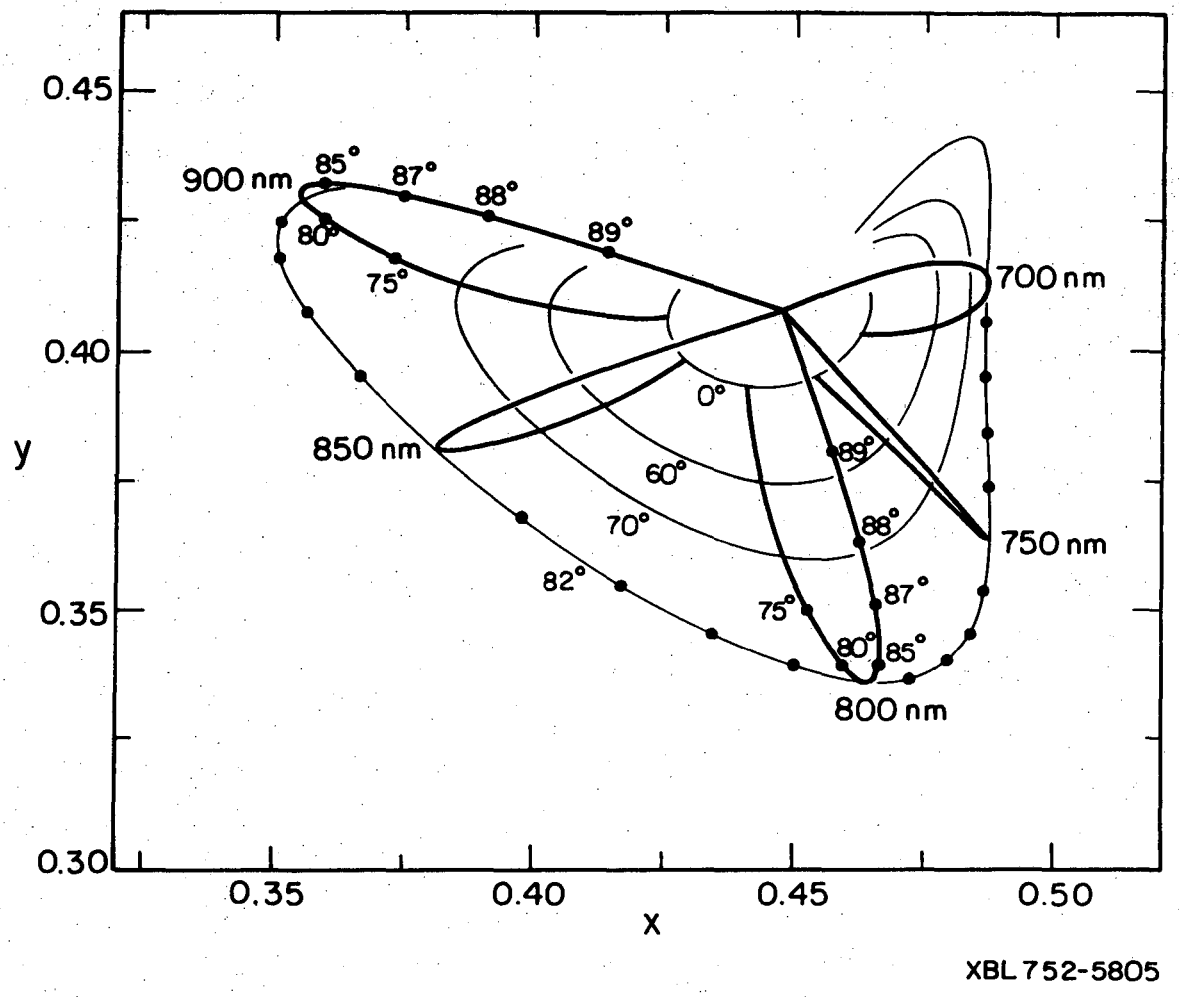

XBL 752-5805

Fig. 31. See Fig. 30. Dielectric film (refractive index = 1.35) on platinum substrate (refractive index = 2.07 - i(4.40)), s-polarized light, second color order (optimum angle, 82°).

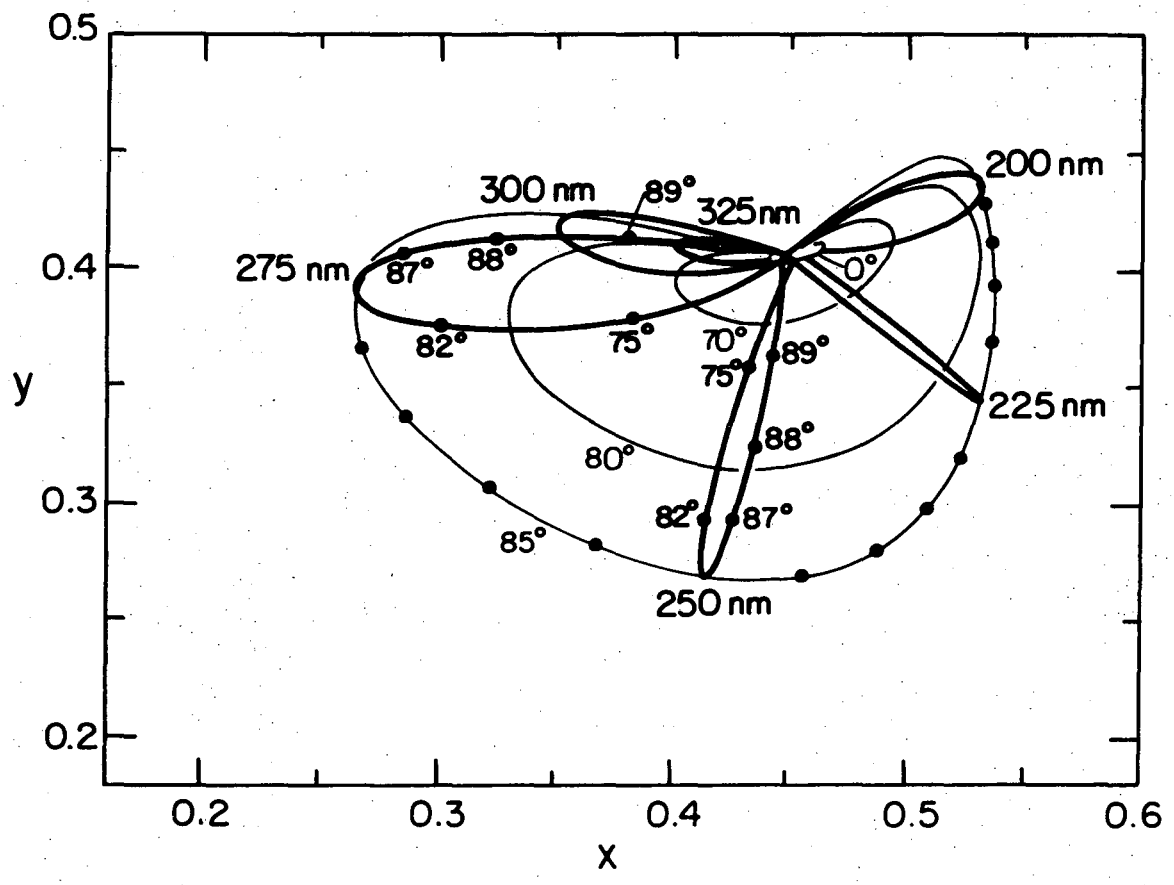

Fig. 32. See Fig. 30. Wavelength dependence of optical constants of substrate (platinum) considered for comparison with Fig. 30. Dielectric film (refractive index = 1.35) on substrate of refractive index $n - ik$, where $n = 1.43 + 0.000308\ (\lambda - 3800)$ and $k = 3.03 + 0.000605\ (\lambda - 3800)$.

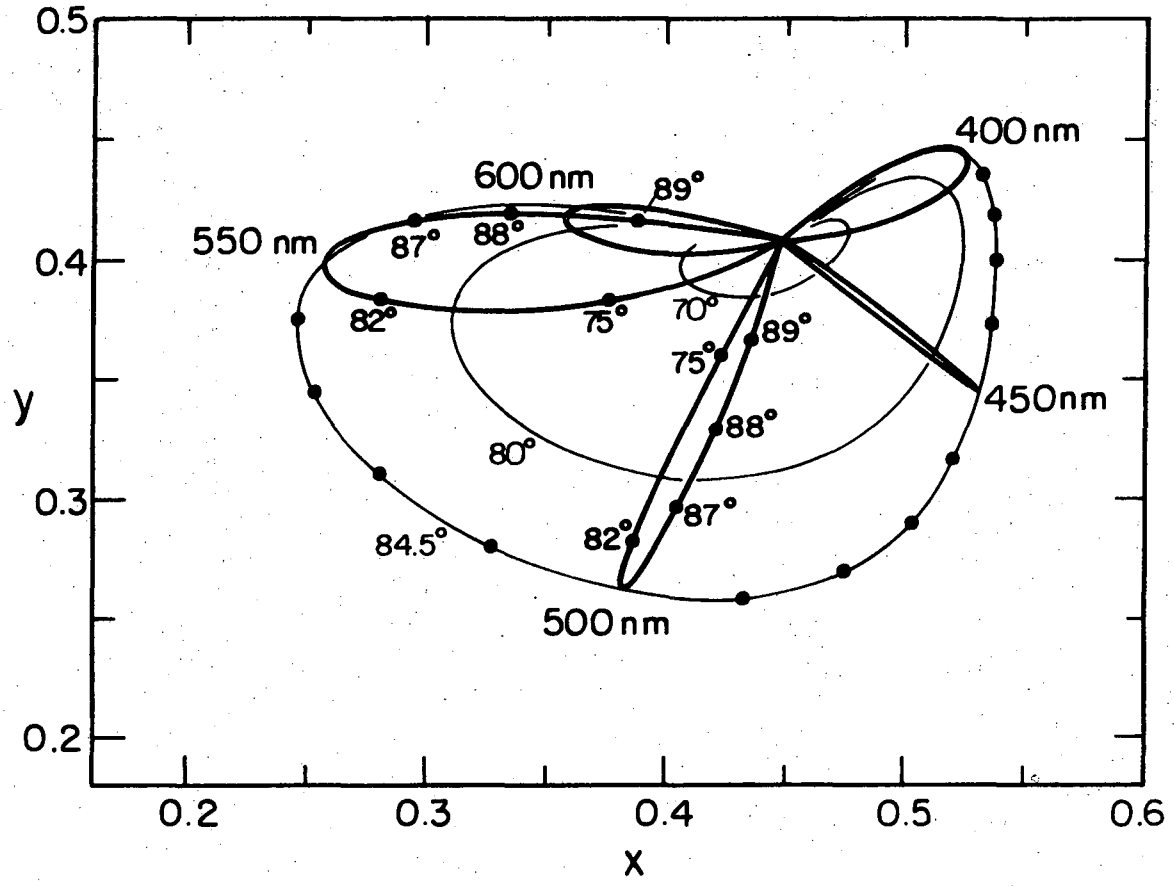

XBL 752-5807

Fig. 33. Optimum angle of incidence for white-light interference. Chromaticity coordinates as a function of angle of incidence and optical path difference. Dielectric film (refractive index = 1.35) on platinum substrate (refractive index = 2.07 - i(4.40)), p-polarized light, first color order (optimum angle, 84.5°). Angles of incidence above Brewster's angle.

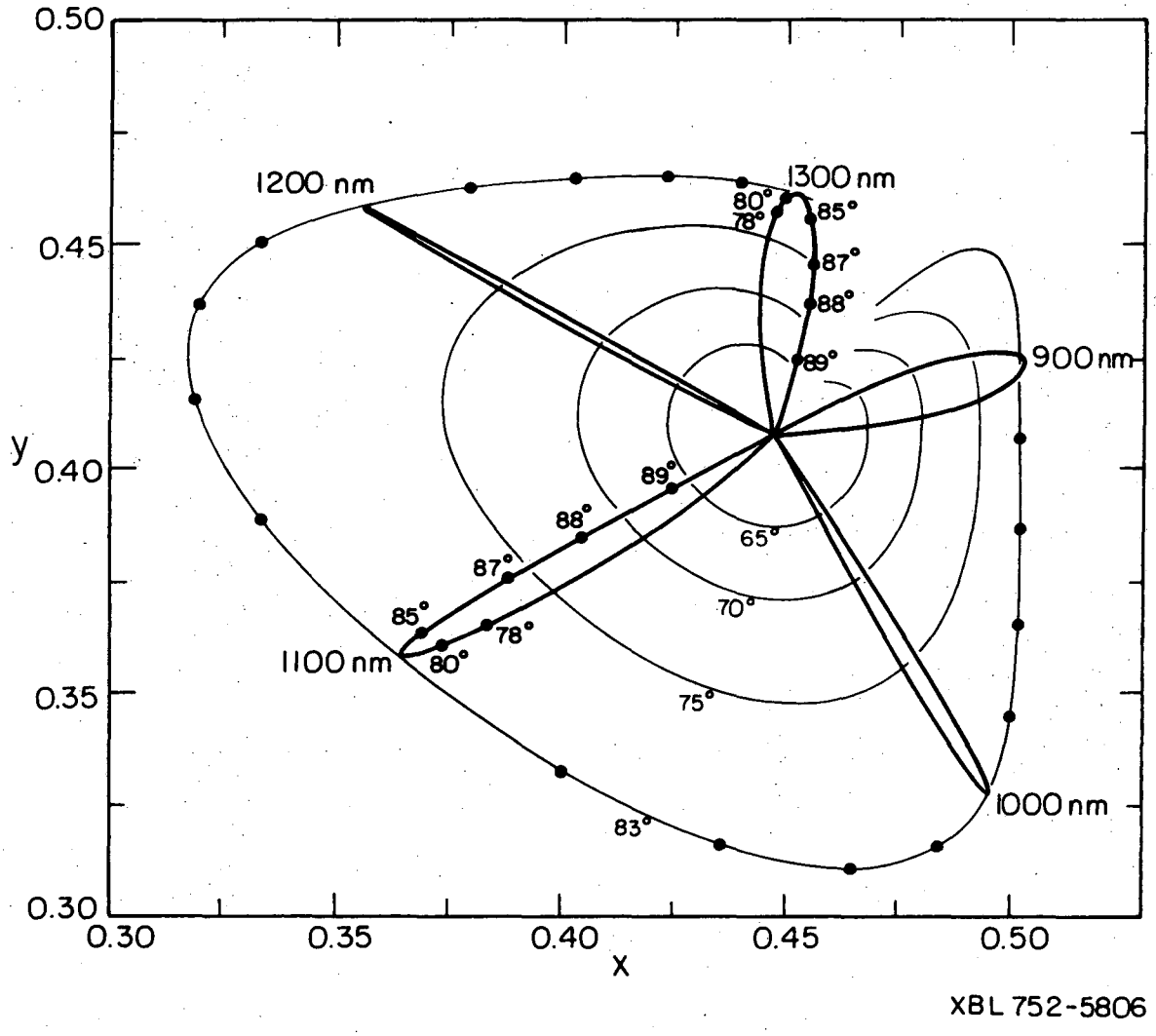

Fig. 34. See Fig. 33. Dielectric film (refractive index = 1.35) on platinum substrate (refractive index = 2.07 - i(4.40)), p-polarized light, second color order (optimum angle, 83°). Angles of incidence above Brewster's angle.

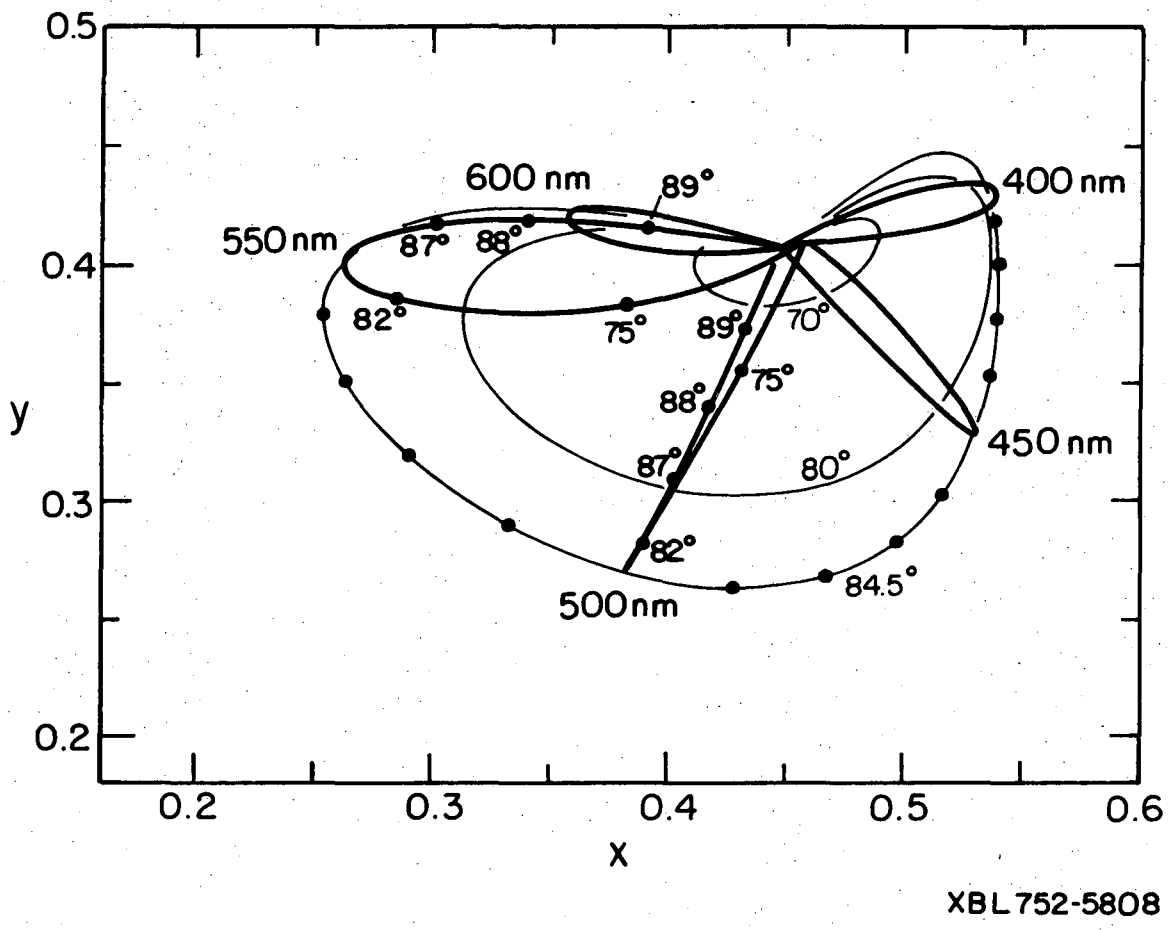

Fig. 35. See Fig. 33. Wavelength dependence of optical constants of substrate (platinum) considered for comparison with Fig. 33. Dielectric film (refractive index = 1.35) on substrate of refractive index n - ik, where $n = 1.43 + 0.000308\ (\lambda - 3800)$ and $k = 3.03 + 0.000605\ (\lambda - 3800)$.

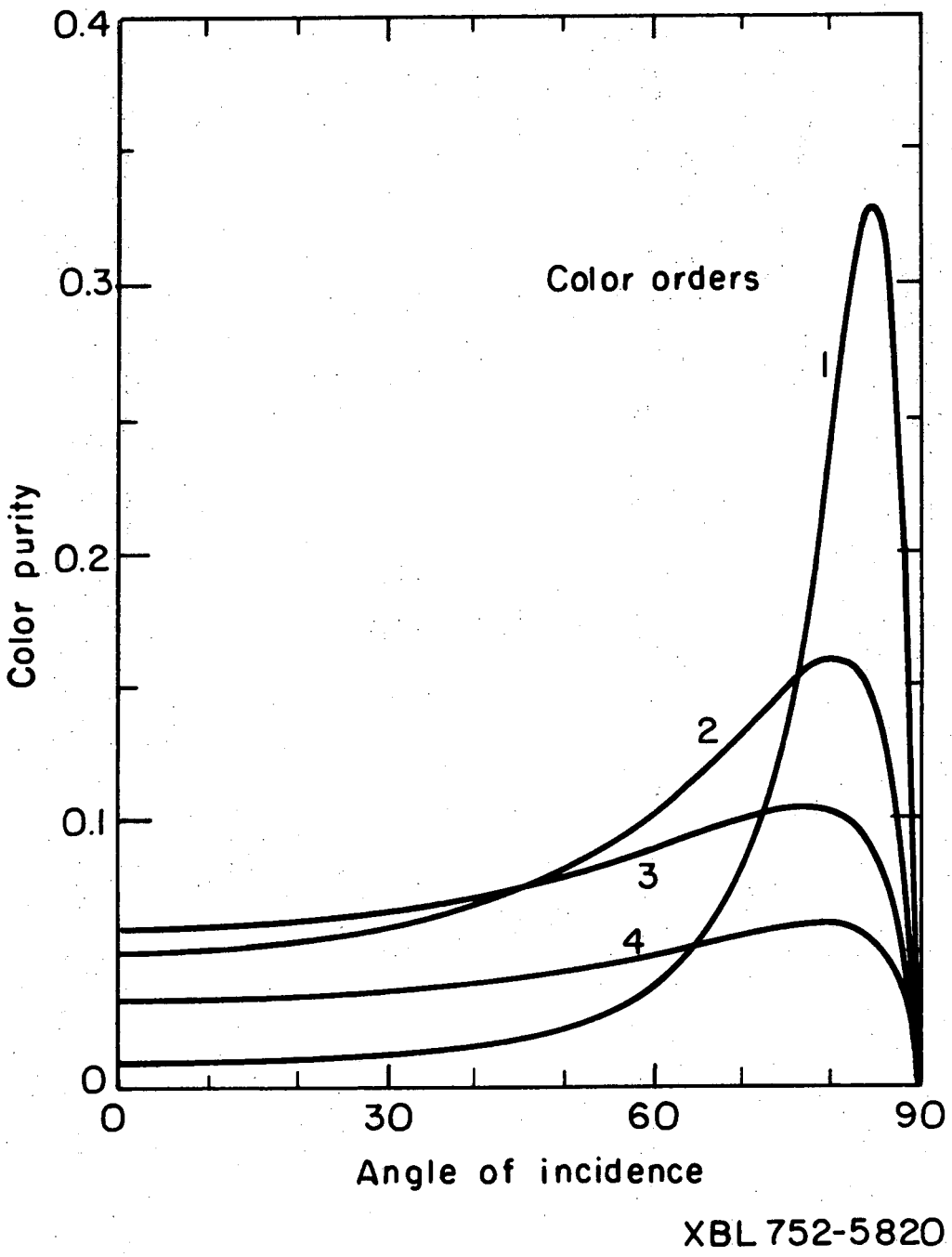

Fig. 36. Dependence of the optimum angle in white-light interference on the color order. Variation of color purity with angle of incidence. Dielectric film (refractive index = 1.35) on platinum substrate (refractive index = 2.07 - i(4.40)). Red interference color, complementary wavelength 506.4 nm, s-polarized light.

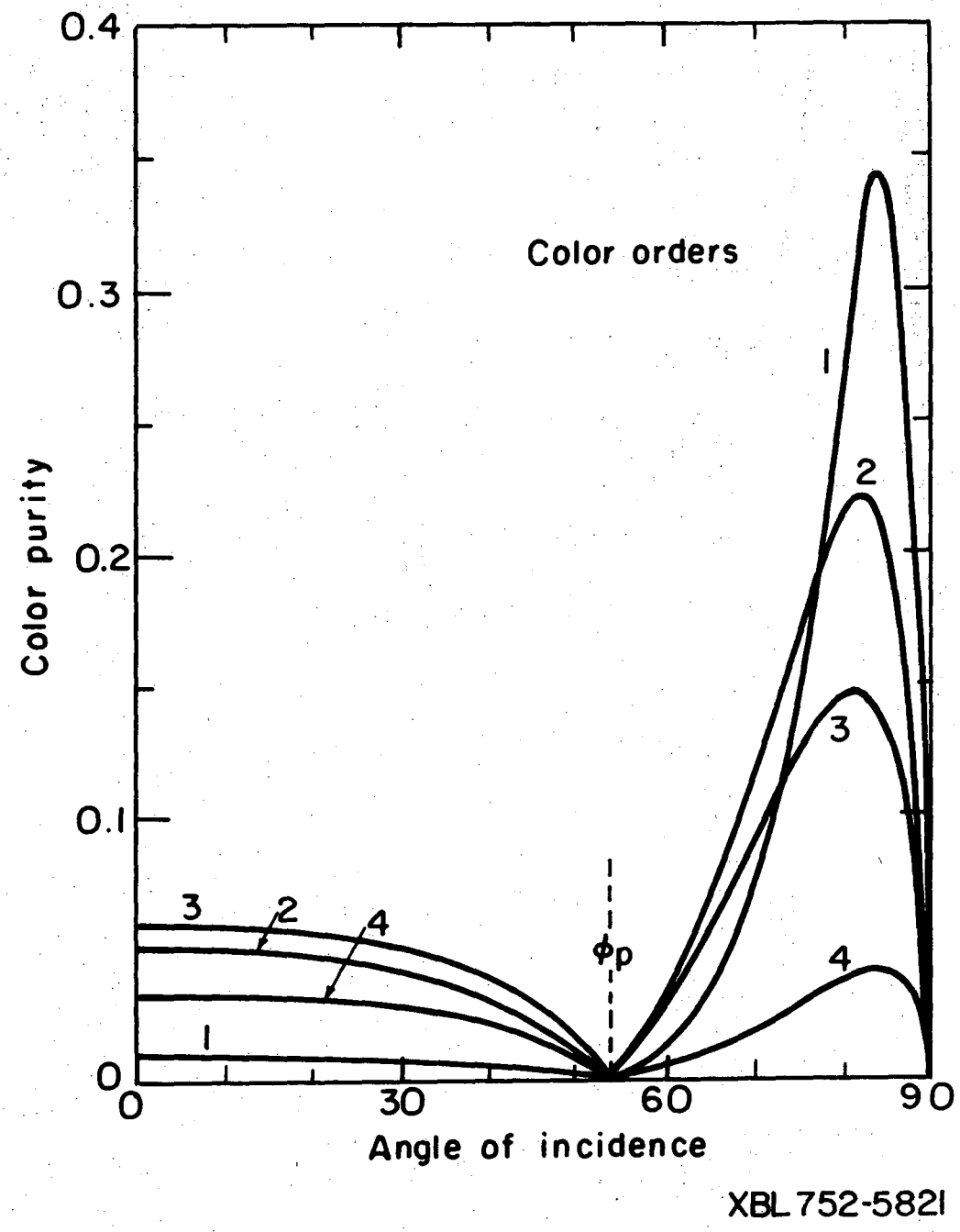

Fig. 37. See Fig. 36. p-polarized light. Brewster's angle, ϕ_p.

through 40 were calculated. They all follow the change in purity of an interference color (red) as a function of the reflection coefficient, r_3. In Figs. 38 and 39, the phase change due to reflection, $\delta_3 - \delta_1$, is zero and the reflection coefficient, r_1, is specified to equal 0.6 and 0.8, respectively. In Fig. 40, r_1 and r_3 are equal. The independent variable is taken to be the reflection coefficient at the air-film interface, since the primary effect of changing the angle of incidence is to change this reflection coefficient. It is the nonlinear relationship between these variables (Fig. 15) that makes the optimum angle sharper for more reflective substrates. This trend was clearly demonstrated by Figs. 26 through 28. Other factors that affect the optimum angle can be better understood by contrasting the multiple-beam equation with the double-beam equation in Figs. 38 through 40. As predicted by Eq. (52), the double-beam curves have their maxima at a value of r_3 equal to the specified value of r_1. Maxima in the curves for the multiple-beam equation occur at lower values of r_3. The relative shifts of these maxima are qualitatively the same as in Figs. 36 and 37. The reason for the shift to lower reflection coefficients is contained in Fig. 40. As the matched reflection coefficients increase in value, the color purity decreases. This trend in the color purity is superimposed on the increase in purity shown by the double-beam curves in Figs. 38 and 39 as the condition of matched reflection coefficients is approached. A decreased purity and a broadening of the optimum angle in the higher orders is exhibited by both the double-beam and multiple-beam curves. Thus, these characteristics are simply a result of the increase in the optical path difference.

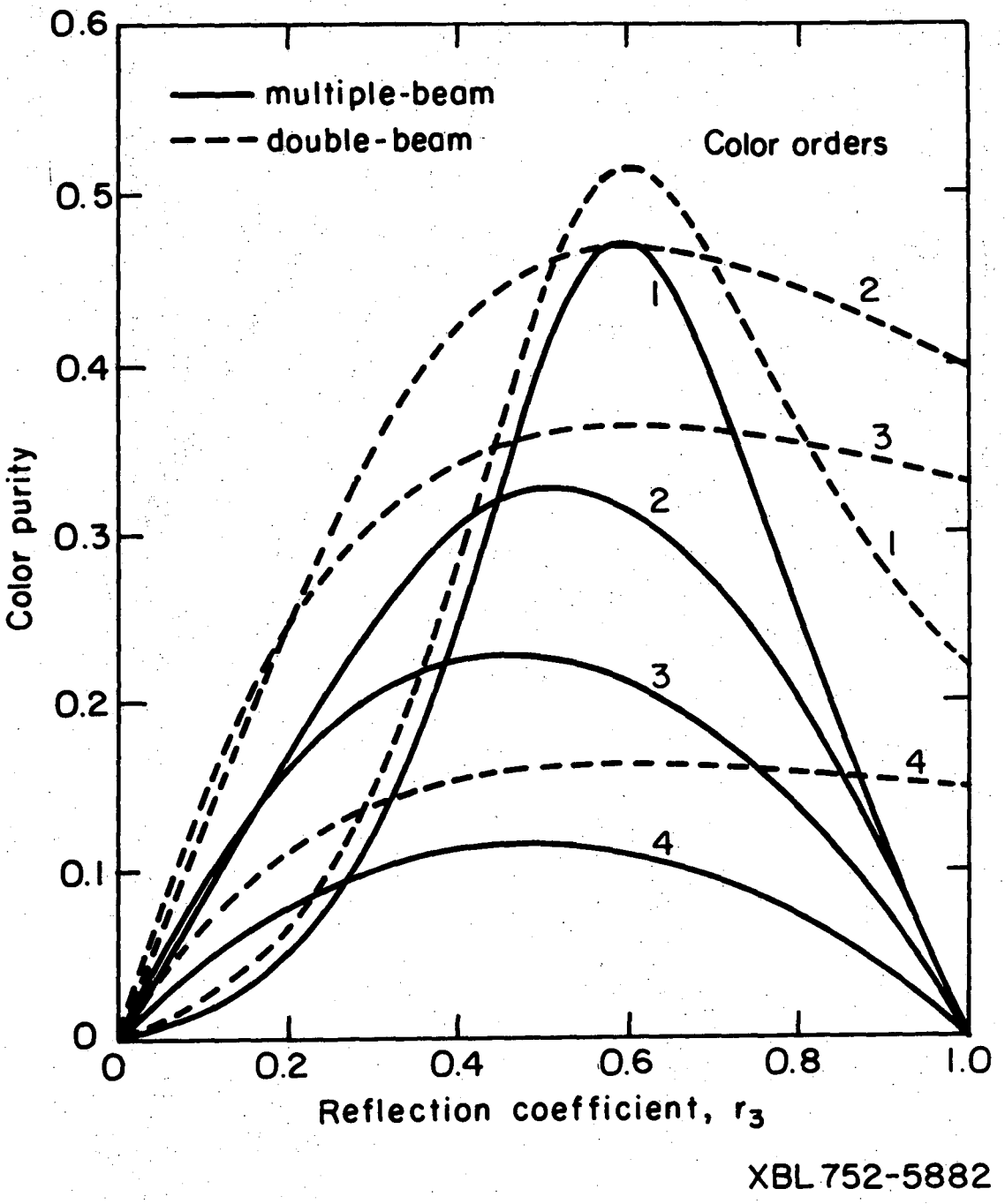

Fig. 38. Variation of color purity with the amplitude reflection coefficient, r_3, at the air-film interface. Amplitude reflection coefficient, r_1, at the film-substrate interface equals 0.6. Phase change due to reflection, $\delta_3 - \delta_1$, equals zero. Red interference color, complementary wavelength 506.4 nm.

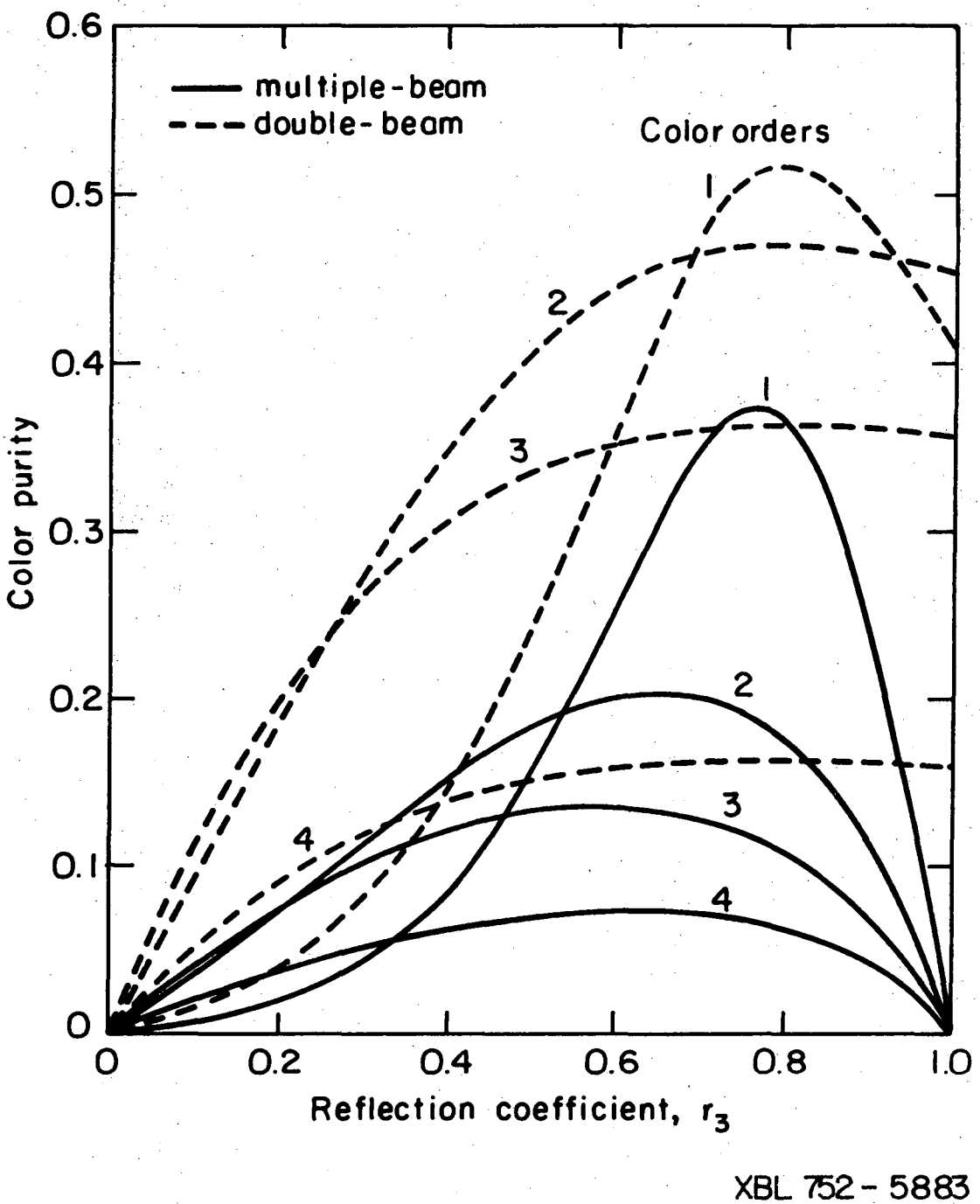

Fig. 39. See Fig. 38. $r_1 = 0.8$.

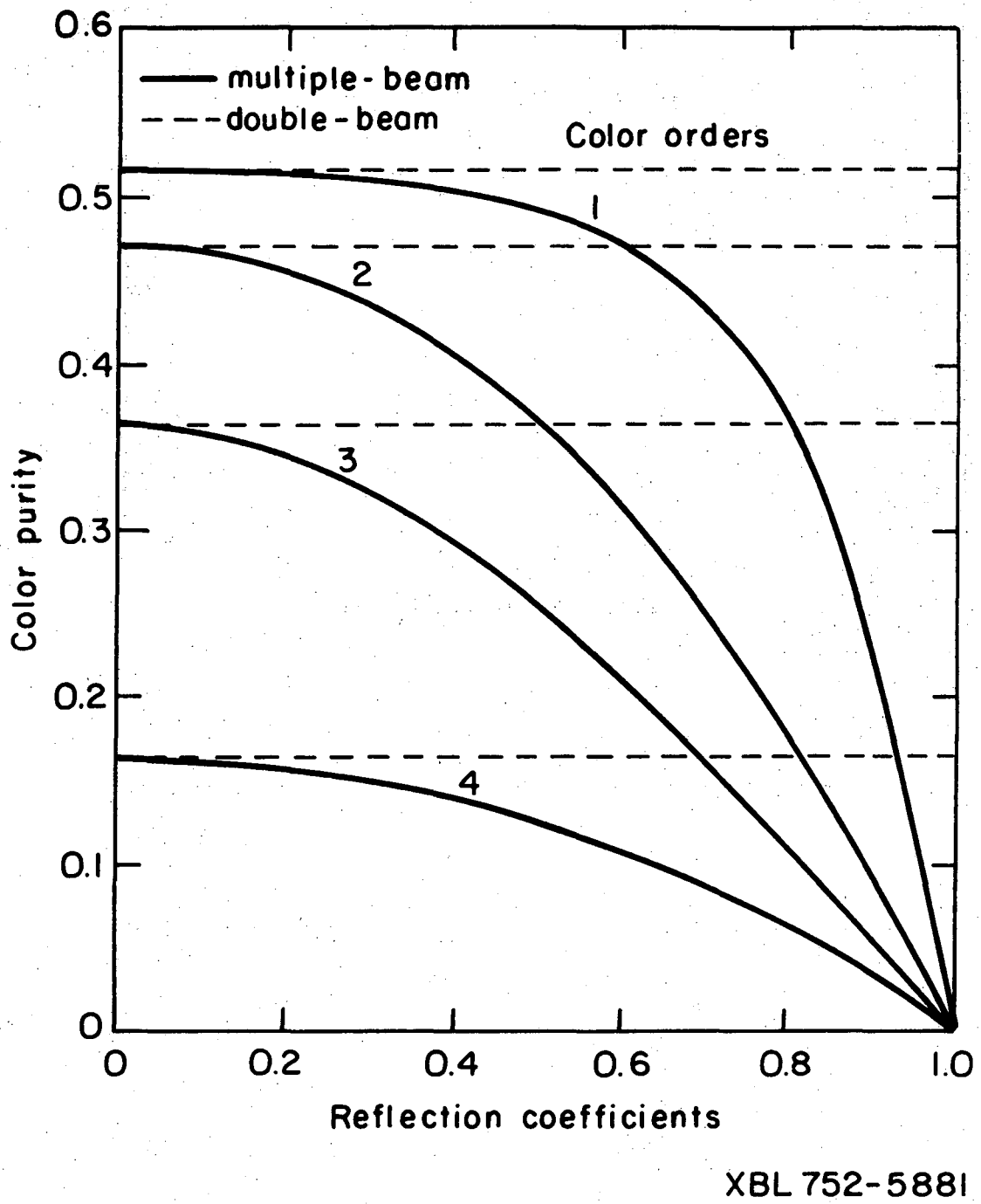

Fig. 40. Variation of color purity with amplitude reflection coefficients at both interfaces. Phase change due to reflection, $\delta_3 - \delta_1$, equals zero. Red interference color, complementary wavelength 506.4 nm.

4. Optimum Angle Based on Polychromatic Fringe Visibility

Figure 41 contributes a final note to the present discussion of the optimum angle. A fringe visibility defined by the maximum and minimum tristimulus value Y varies with the reflection coefficient, r_3 (or with angle of incidence for a specific film and substrate). Its definition is similar to the monochromatic (Michelson) fringe visibility in Eq. (36). The tristimulus value Y (relative luminance) varies with the optical path difference.

$$\text{Polychromatic fringe visibility} = \frac{Y_{max} - Y_{min}}{Y_{max} + Y_{min}} \tag{53}$$

However, successive maxima or minima are not identical. A maximum succeeded by a minimum at a higher value of the optical path difference was used in the definition of the polychromatic fringe visibility and defined a color order. Figure 41 shows a shift in the maxima to lower reflection coefficients that is remarkably similar to that in Fig. 39. This result indicates that a fringe visibility defined for white-light interference predicts the optimum angle in each color order more closely than the monochromatic fringe visibility.

B. Color Series

Accurately determined color series are required for accurate thickness measurements. The spectral energy distribution of light reflected from a film-covered substrate is calculated through the use of Eq. (31). By coupling it with the tristimulus color system, one can predict the color of reflected light at any film thickness.

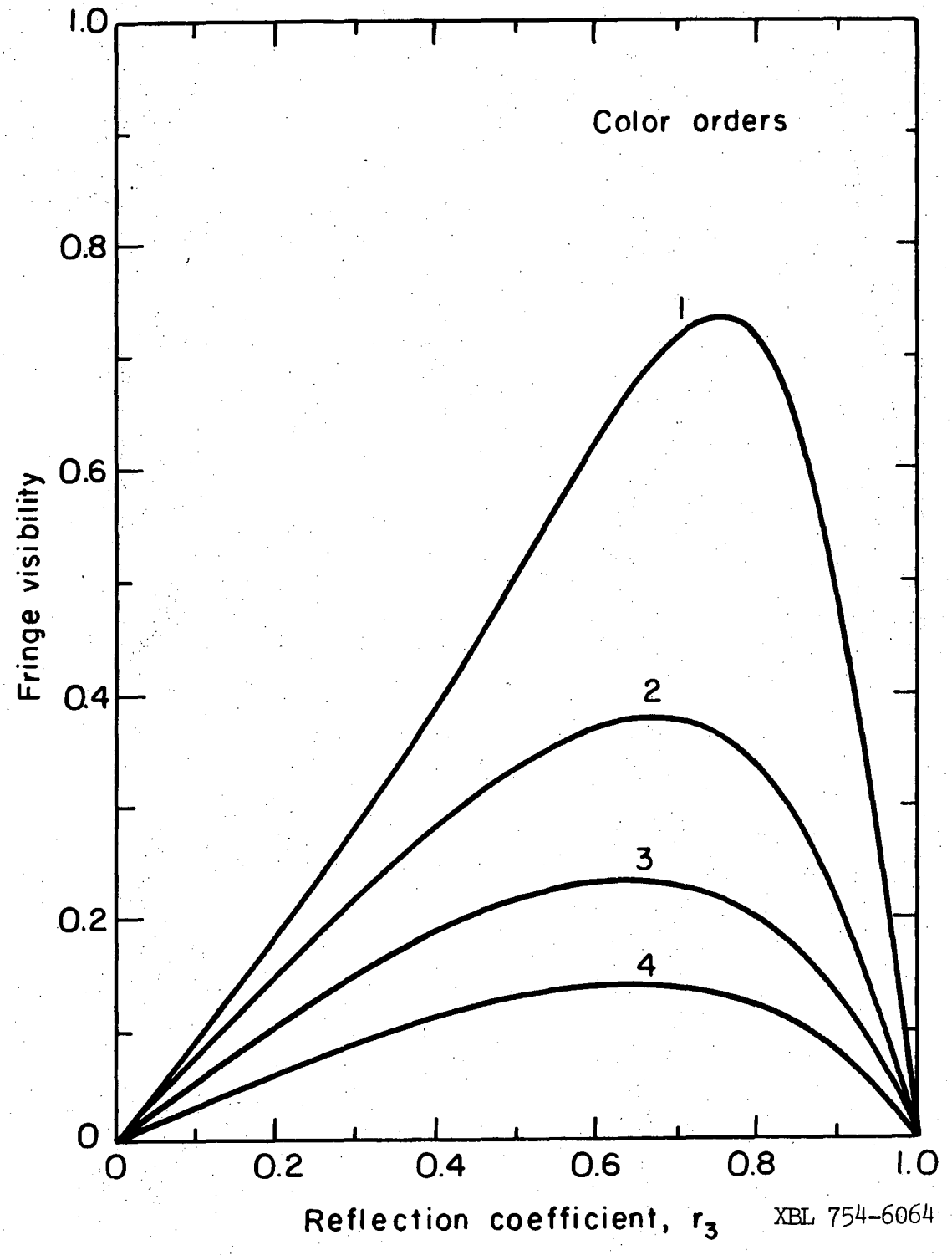

Fig. 41. Variation of polychromatic fringe visibility (based on minimum and maximum tristimulus values Y) with amplitude reflection coefficient, r_3, at the air-film interface. Amplitude reflection coefficient, r_1, at the film-substrate interface equals 0.8. Phase change due to reflection, $\delta_3 - \delta_1$, equals zero. Red interference color, complementary wavelength 506.4 nm.

1. Dispersion of Optical Constants

Exact calculations include the variation of the optical constants of both the film and substrate with wavelength. They can be substantially reduced, if the dispersion of the optical constants has a minimal effect on the color series. If the refractive index of a dielectric film is high, the dispersion might have a noticeable effect on the maximum in the spectral energy distribution.[48] For dielectric films on metal surfaces, Kubota[29] considered the effect on the color to be small. In the study of aqueous solutions on metal surfaces, the effect should be negligible. Figure 42 shows the refractive index of aqueous potassium hydroxide solutions throughout most of the visible spectrum. The variation is within 1%. Dispersion of the refractive index of a metal, though, may be significant. Figure 25 has shown the variation to be nearly linear for platinum and silver. An average value of the refractive index at an intermediate wavelength of 5892Å has already been used in determining the optimum angle of incidence. Refer to Figs. 28 and 29 at small optical path differences for the most noticeable change. It would be instructive to substitute an average value in the calculation of a color series. Figures 43 and 44 are curves of chromaticity coordinates as a function of the optical path difference for a dielectric film on platinum for s and p-polarized light, respectively. The angle of incidence, 85°, is near the optimum angle. The solid curve was calculated assuming a constant value for the refractive index of the platinum. Calculation of the dashed curve included the dispersion of the refractive index. They exhibit only slight differences at low values of the optical path difference.

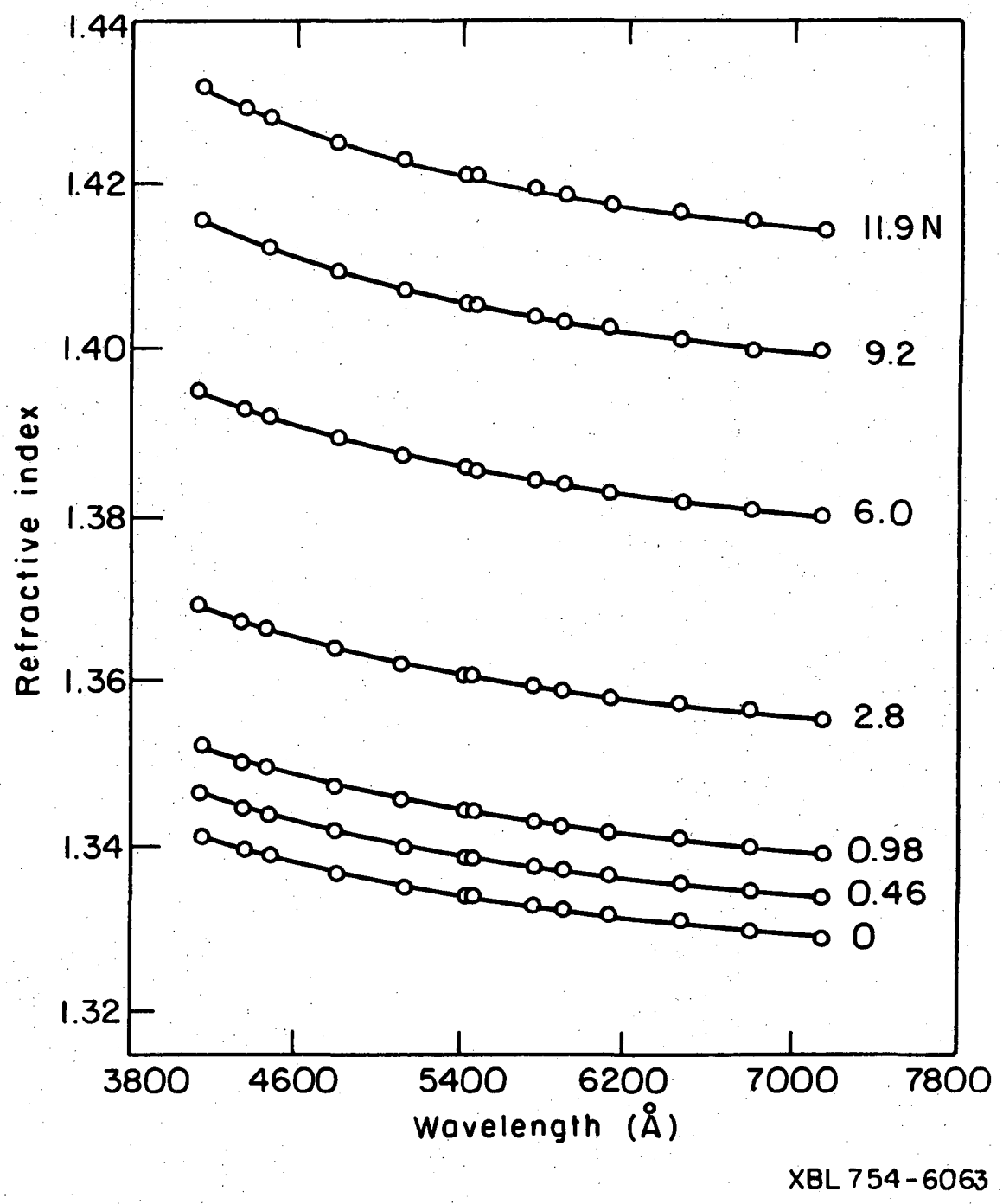

Fig. 42. Refractive index of aqueous potassium hydroxide solutions in the visible spectrum. Measurements made with Bausch and Lomb precision refractometer,[49] 25°C.

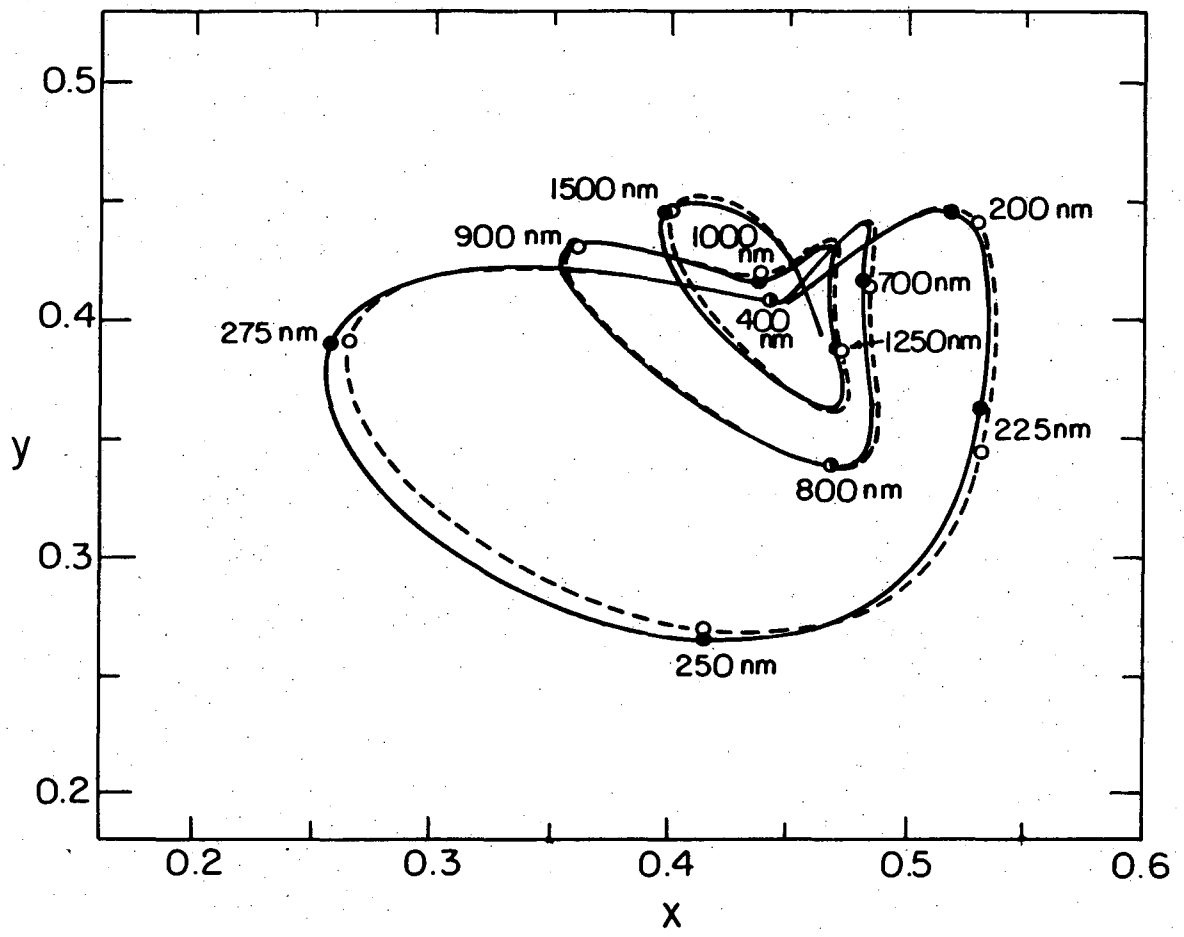

Fig. 43. Effect of wavelength dependence of substrate optical constants. Chromaticity coordinates as a function of the optical path difference. Angle of incidence equals 85°. Film of refractive index 1.35. Solid curve for substrate of refractive index 2.07 - i(4.40). Dotted curve for substrate of refractive index n - ik, where $n = 1.43 + 0.000308\ (\lambda - 3800)$ and $k = 3.03 + 0.000605\ (\lambda - 3800)$. s-polarized light.

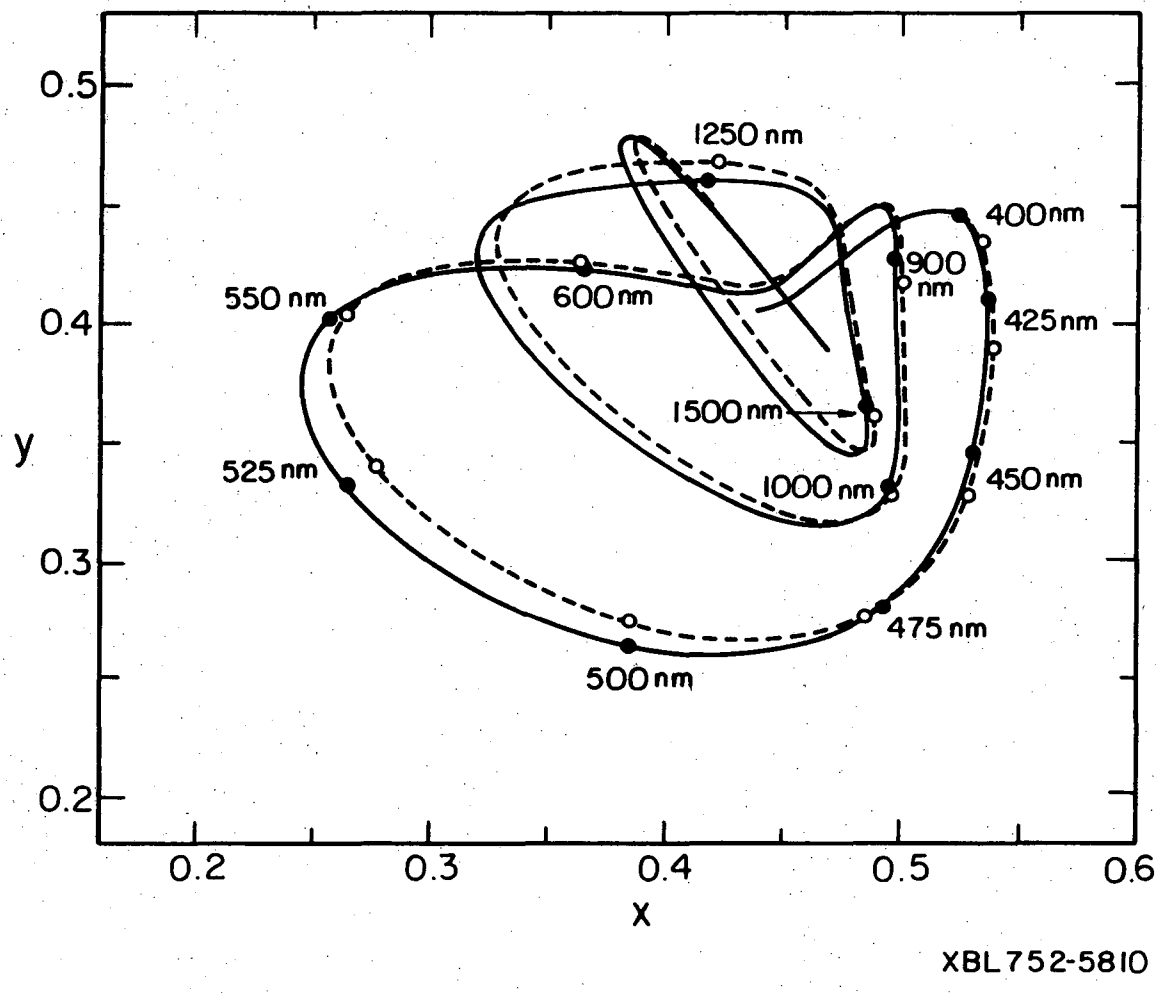

Fig. 44. See Fig. 43. p-polarized light.

Color series corresponding to the dashed and solid curves in Figs. 43 and 44 are presented in Figs. 45 and 46. For a comparison, color series for angles of incidence of 80 and 75° are also given. The hue names correspond to the seven names in the chromaticity diagram in Fig. 11. The region considered white is 1/5 the size shown in Fig. 11. The color series in Figs. 45 and 46 do not show a significant difference from each other. Variations at low optical path differences are misleading, since the colors are very low in saturation. Color series are actually limited in the detail they provide. A large range of the optical path difference is assigned one hue name. The continuous variation of the hue within this range is not indicated but must be inferred. Information concerning the variation of brightness and saturation is absent throughout the series.

2. Color Charts

When dispersion of the optical constants is ignored, more generally valid color series can be determined. According to Eq. (31), the spectral energy distribution varies with the reflection coefficients (r_3 and r_1), the phase change due to reflection ($\delta_3 - \delta_1$) and the optical path difference, ΔS in Eq. (21). If the reflection coefficients are specified, the variation of hue with the optical path difference for values of $\delta_3 - \delta_1$ can be expressed in a two-dimensional diagram. Turney [27] constructed such diagrams, which he termed "generalized color charts." He made a chart for low amplitude reflection coefficients (0.2) at both interfaces and one for medium amplitude reflection coefficients (0.6). A chart for high reflection coefficients was not made, because it fell entirely within the white region of the chromaticity diagram which he

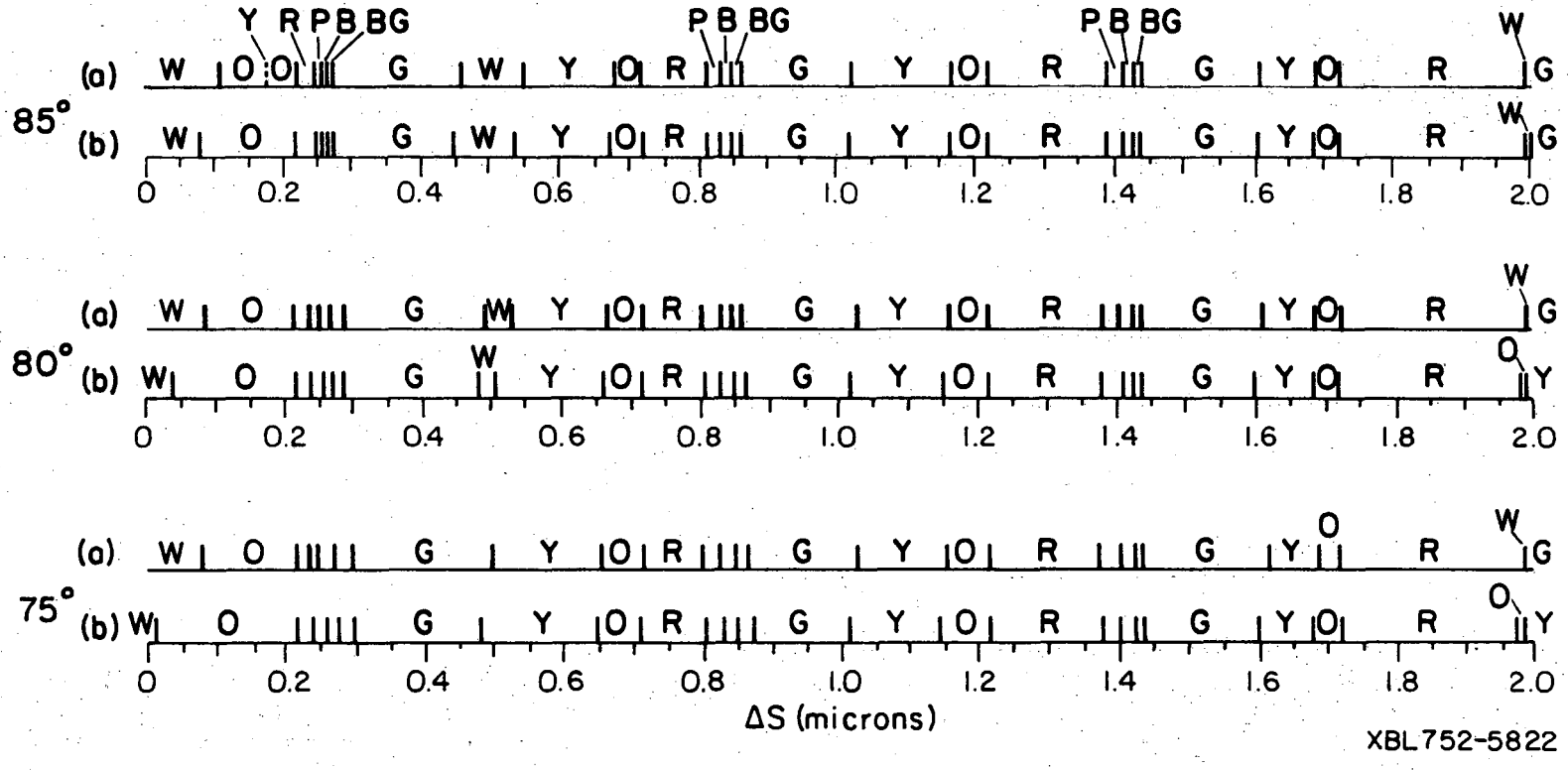

Fig. 45. Color series for film of refractive index, 1.35, on platinum substrate with complex refractive index (a) 2.07 - i(4.40), (b) that varies with wavelength as in Fig. 25. s-polarized light. Reflection coefficients and phase changes due to reflection for part (a) are

$\phi = 85°$	$r_1 = 0.862$	$r_3 = 0.825$	$\delta_3 - \delta_1 = 19.23°$
$\phi = 80°$	$r_1 = 0.861$	$r_3 = 0.683$	$\delta_3 - \delta_1 = 19.49°$
$\phi = 75°$	$r_1 = 0.858$	$r_3 = 0.569$	$\delta_3 - \delta_1 = 19.91°$

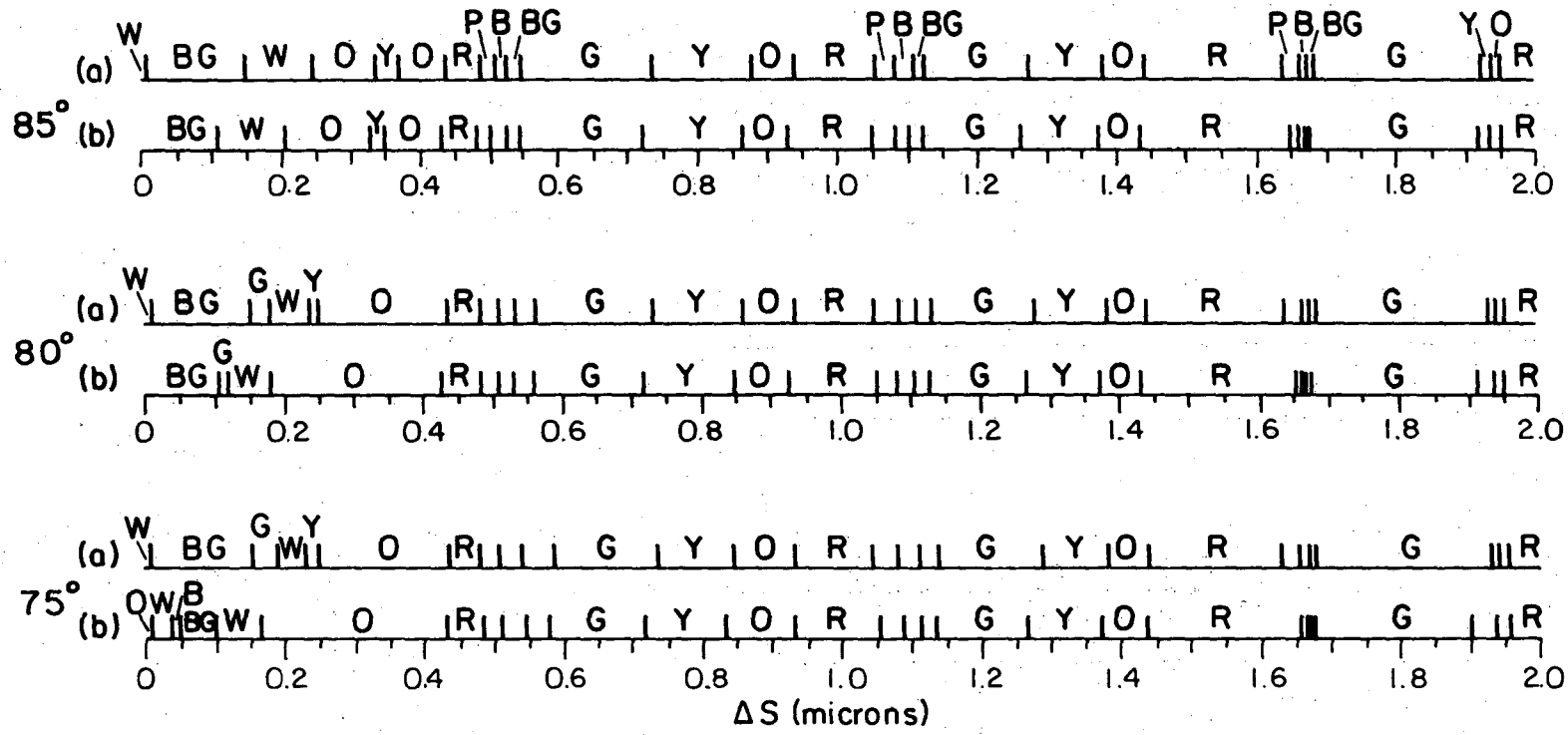

Fig. 46. See Fig. 45. p-polarized light.

$\phi = 85°$	$r_1 = 0.724$	$r_3 = 0.703$	$\delta_3 - \delta_1 = 222.19°$
$\phi = 80°$	$r_1 = 0.726$	$r_3 = 0.490$	$\delta_3 - \delta_1 = 221.64°$
$\phi = 75°$	$r_1 = 0.730$	$r_3 = 0.333$	$\delta_3 - \delta_1 = 220.79°$

chose to be ten times the size of the region given by Wright[41] to represent the ability of an observer to perceive a difference in color. In order to determine the color distribution within the charts, he changed the quantity, $\delta_3 - \delta_1$, in increments of 10° from 0 to 360° and the film thickness in increments of 100Å. The range of the optical path difference extended from 0 to 3 microns. It is at approximately an optical film thickness of 1.5 microns that the transition from a "thin" to a "thick" film has been said to occur.[36] The reflection coefficients were not assumed but were calculated for a film of refractive index, 1.50, on specific substrates. The angle of incidence was the optimum angle for each of the film-substrate combinations based on a maximum Michelson fringe visibility. For substrates of refractive index, 2.25 and 2.63 - i(3.55) (platinum), the amplitude reflection coefficients at both interfaces were 0.2 (s and p-polarized light) and 0.61 (p-polarized light), respectively.

Brown[30] made independent thickness measurements of thin films in order to establish the accuracy of the generalized color charts. He found that some colors assumed by Turney to fall within the achromatic region could indeed be observed in practice. Upon comparing color series from the generalized color charts with photographically observed fringes, he found this technique to be in satisfactory agreement with several other methods of film thickness measurement. Gu[28] used the color charts and ellipsometry to determine the thickness of aqueous potassium hydroxide films on a platinum electrode and found excellent agreement between the two measurements.

Even though Turney's color charts were shown to be useful, they still lacked sufficient detail. Colors with a very low tristimulus

value Y were designated as "black", but the values of Y represented by this designation were not given. It appears, though, from calculations made in the present study that he used values of 5 and 10% of the maximum Y value at each $\delta_3 - \delta_1$ as the criterion for the designation "black" in the charts for low and medium reflection coefficients, respectively. The achromatic region was much too large. For this reason, a chart for highly reflective surfaces could not be constructed. An overall view of the charts indicated that some color transitions might not be represented correctly. Thus, a recalculation of the color charts was undertaken.

A set of seven color charts is presented in Fig. 47 through 53. Matched reflection coefficients with values between 0.2 and 0.95 at the air-film and film-substrate interfaces were specified for each chart. Essentially, the charts were constructed for use at the monochromatic optimum angle. Since several charts were made, interpolations between successive charts should be sufficiently accurate for thickness determinations. The phase change due to reflection is the quantity, $\delta_3 - \delta_1$ in Eq. (31). The optical path in the film is equivalent to the optical path difference, ΔS, which can be converted to film thickness through the relationship in Eq. (21). The seven hue names are those given in Fig. 11. The designation, "white", was assigned to chromaticity coordinates that fell within a region 1/5 the size shown in Fig. 11 around the achromatic point.

These color charts were generated with the aid of a computer program. The reflection coefficients were input data for the calculations. The optical path difference was varied by increments of 100Å from 0 to 3 microns for values of $\delta_3 - \delta_1$ that were varied by 10° increments from

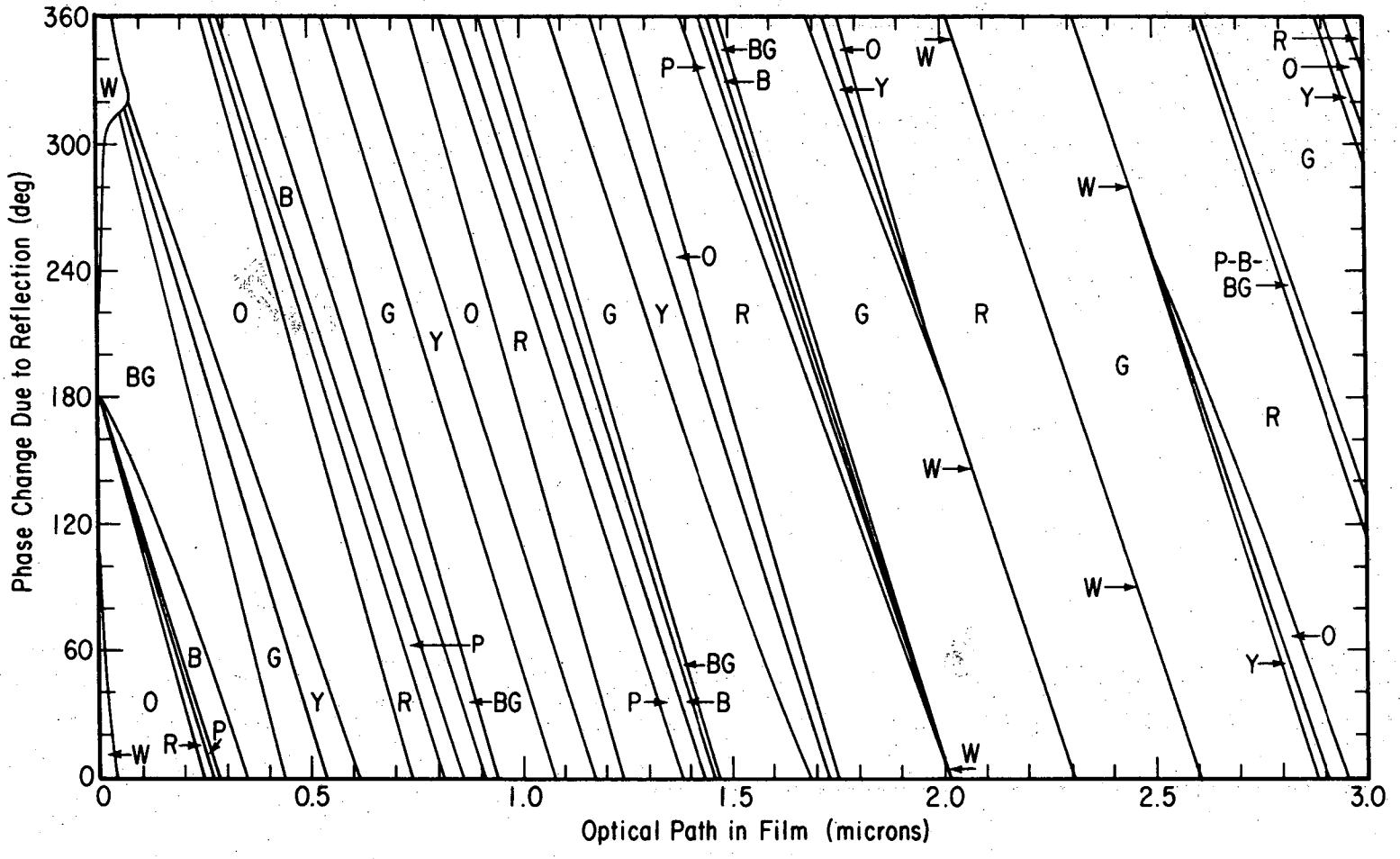

XBL 751-5589

Fig. 47. Color chart for multiple-beam interference. B=blue, BG=blue green, G=green, O=orange, P=purple, R=red, W=white, Y=yellow. Amplitude reflection coefficient at both interfaces = 0.20.

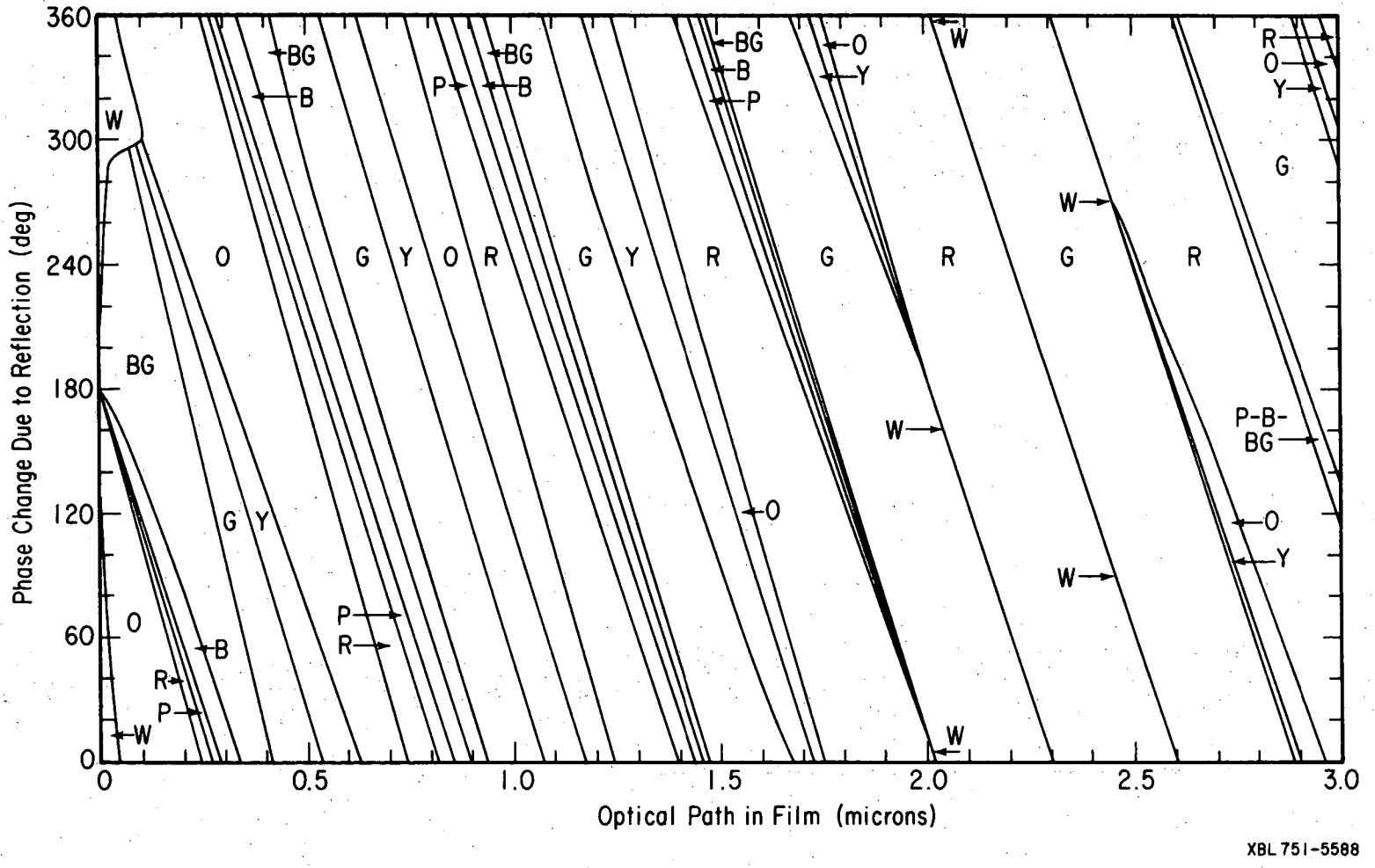

Fig. 48. See Fig. 47. Amplitude reflection coefficient at both interfaces = 0.40.

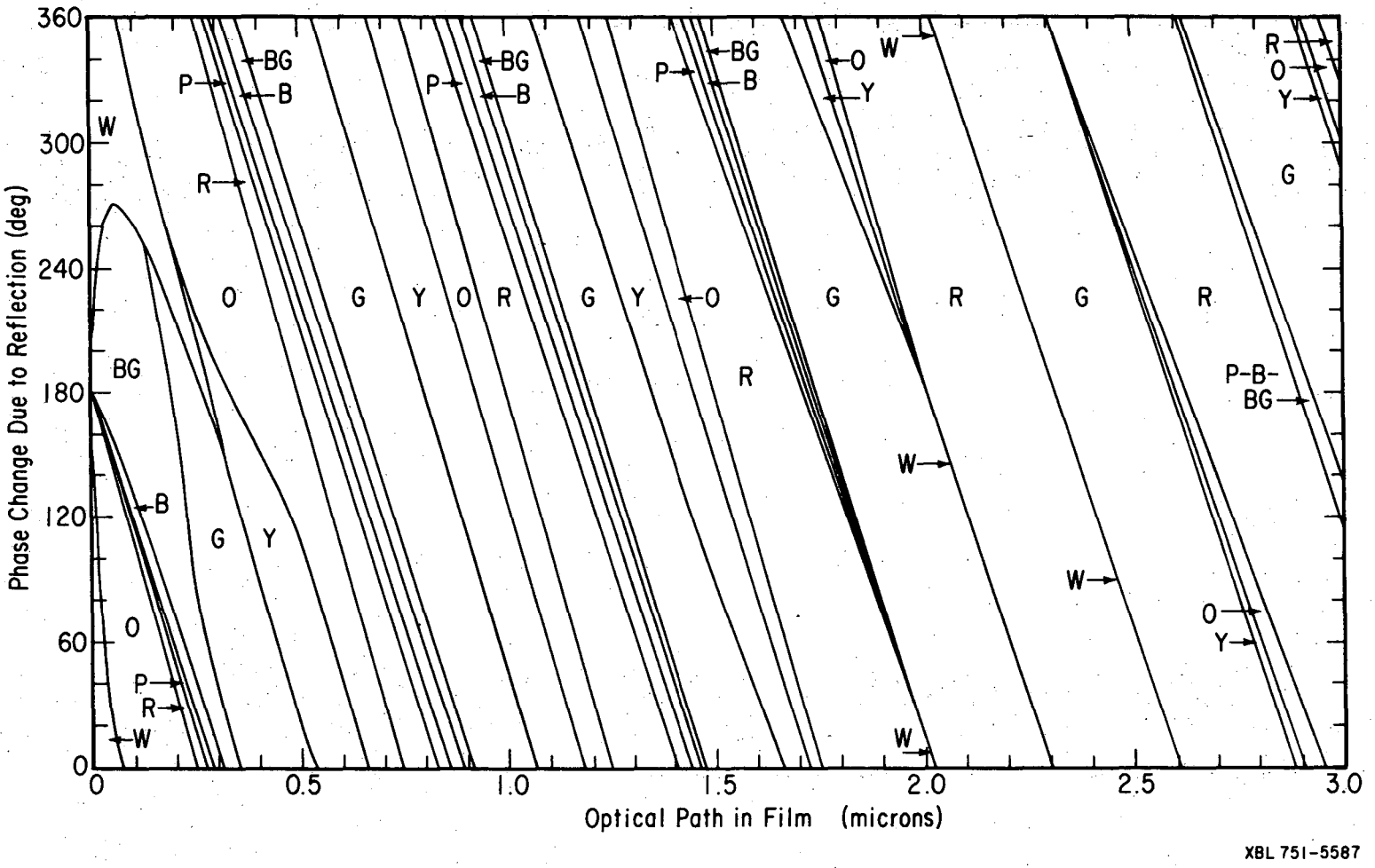

Fig. 49. See Fig. 47. Amplitude reflection coefficient at both interfaces = 0.60.

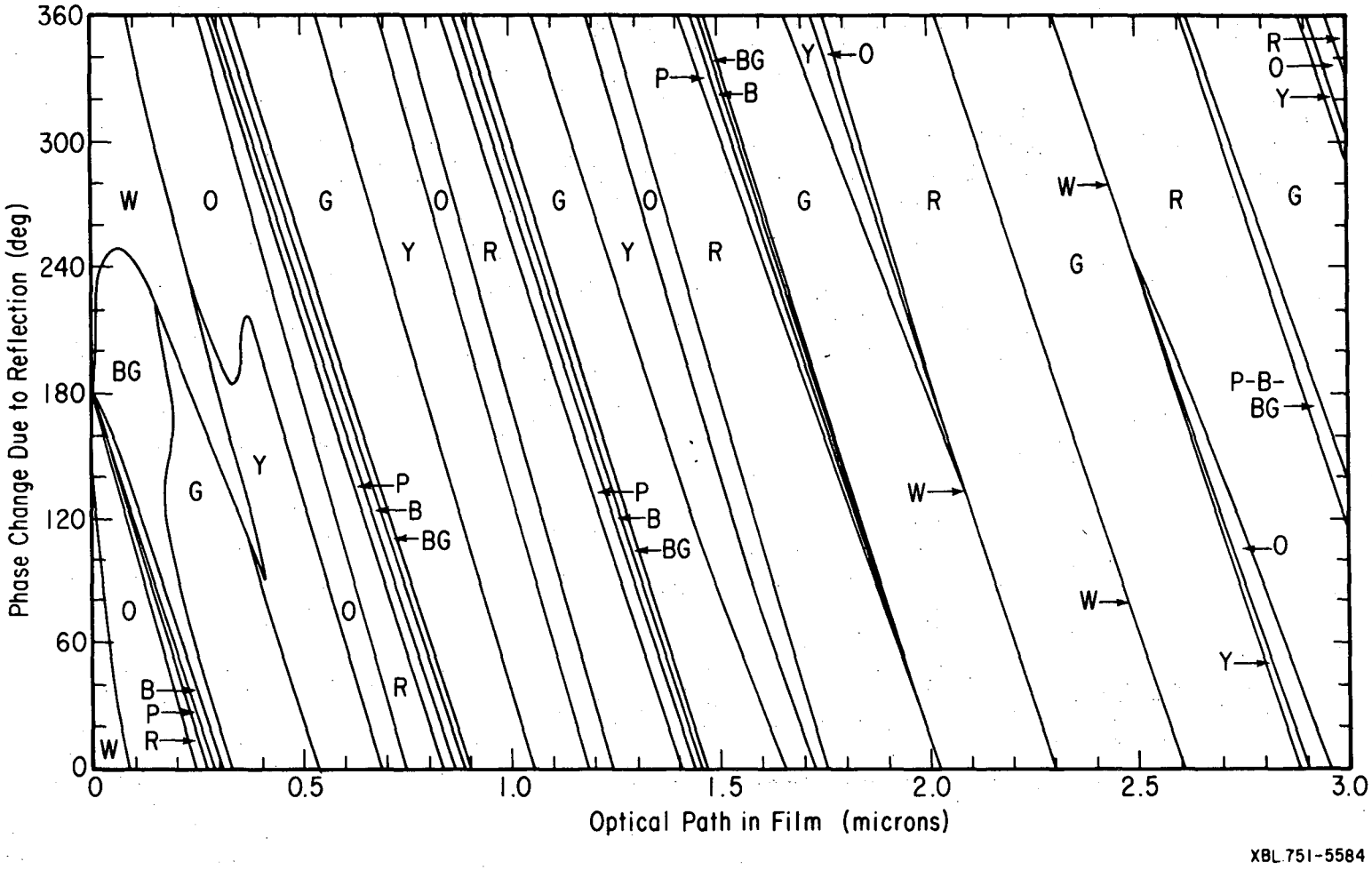

Fig. 50. See Fig. 47. Amplitude reflection coefficient at both interfaces = 0.70.

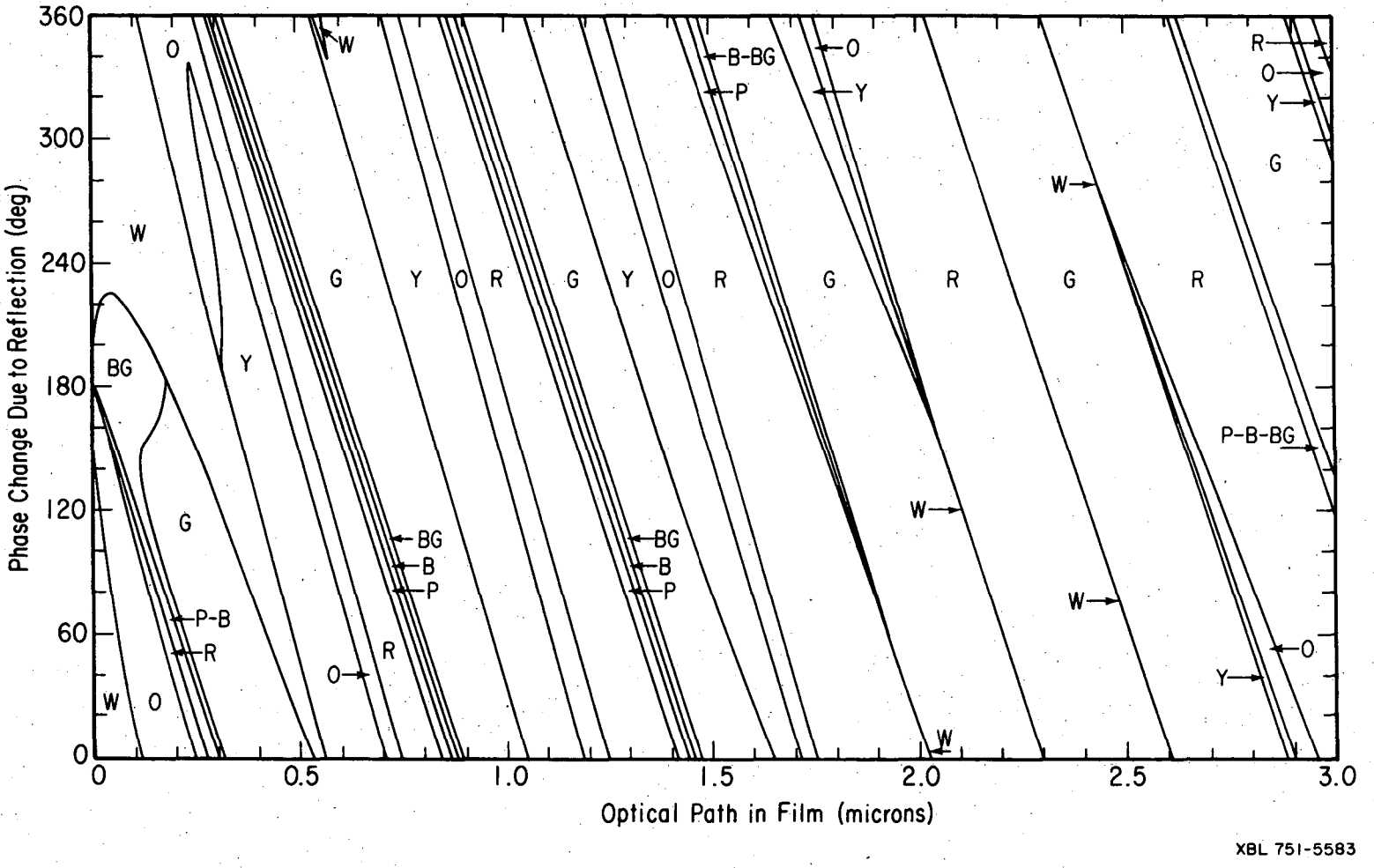

Fig. 51. See Fig. 47. Amplitude reflection coefficient at both interfaces = 0.80.

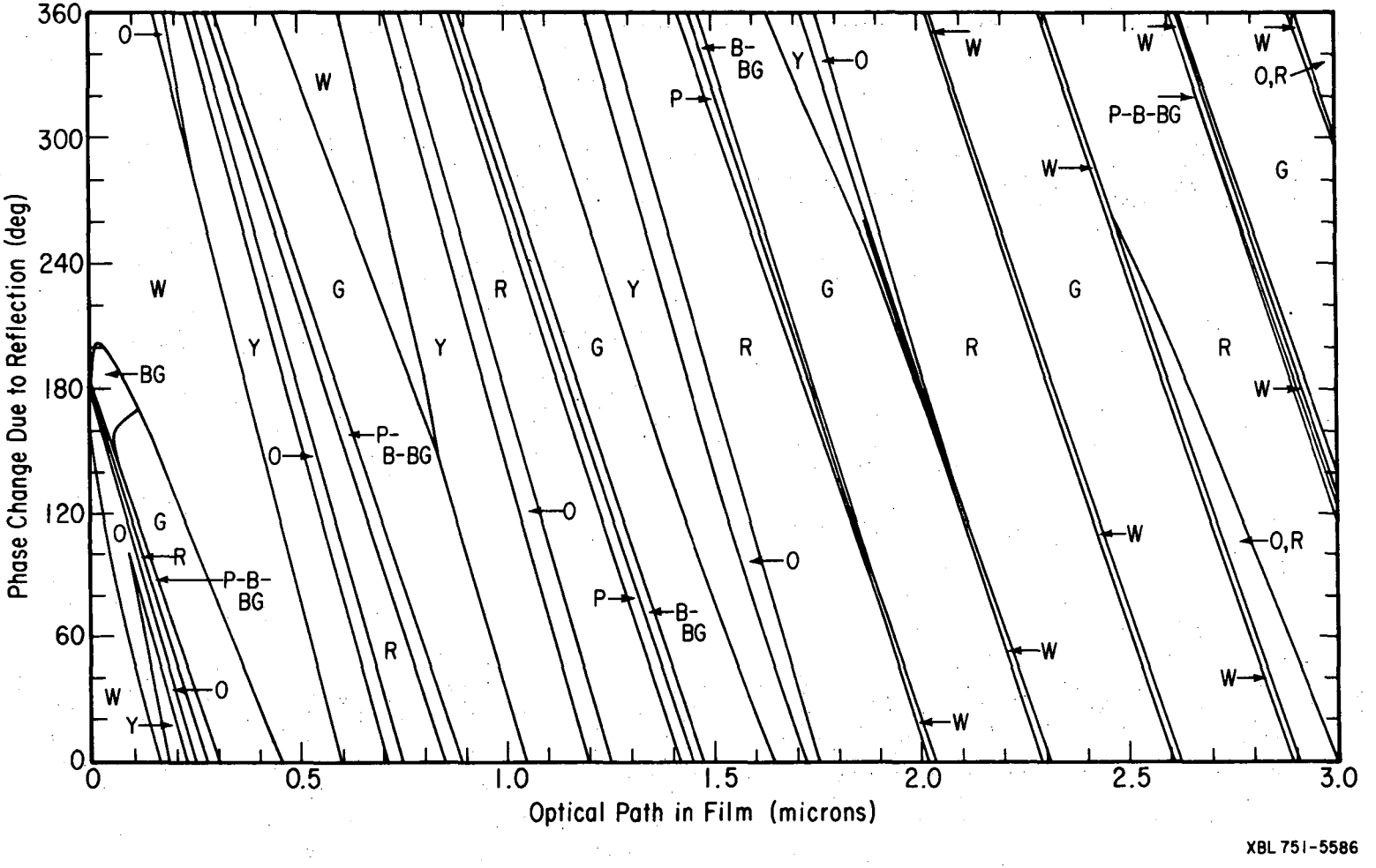

Fig. 52. See Fig. 47. Amplitude reflection coefficient at both interfaces = 0.90.

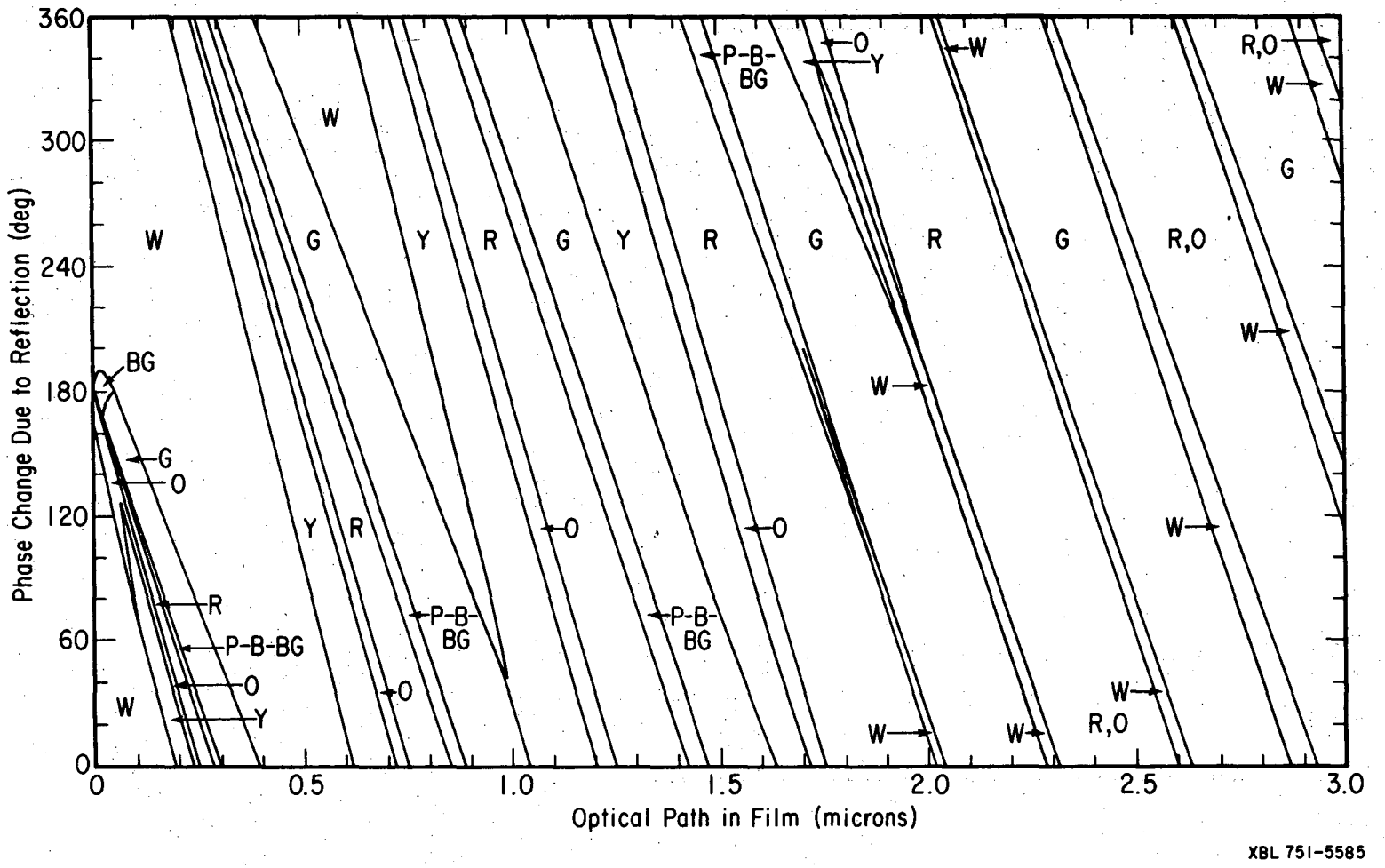

XBL 751-5585

Fig. 53. See Fig. 47. Amplitude reflection coefficient at both interfaces = 0.95.

0 to 360°. Chromaticity coordinates were assigned a hue name in a manner identical to that in program "HUE" in the Appendix. Assigning the designation, "white", to areas of the charts was done separately. The label, "W", designates white areas which may be extended or narrow (red-green transitions). For the narrow regions, the letter "W" was positioned where the chromaticity coordinates were closest to the achromatic point. If the hue changed sharply with the optical path difference, individually labelled areas of the charts could not be drawn clearly. Under these conditions, the hue designations were written in the order the hues occurred and were separated by dashes. When two hues occurred in a seemingly random fashion in the same area of the charts, the area was labelled with the designations of the two hues separated by a comma. The hue that appeared to be dominant was listed first. Two aspects of the labelling may still be unclear. In Fig. 52 toward the right side of the chart, a narrow area with the designation, "P-B-BG", also has the designation, "W", associated with it. The "W" refers to a narrow band extending through the larger area. In Fig. 53, one large area contains both the designations, "R" and "R,O". Along this area, the amount of "orange" gradually decreases to none.

3. Intensity and Purity Changes in Color Charts

Various aspects of the color charts should be considered carefully. The designations for areas of the charts strictly adhere to the definitions of the hues given in Fig. 11. Gradual transitions between hues have been replaced by sharp boundaries. Besides not fully representing the change in hue, the charts neglect the changes in purity and intensity. Some areas of the chart not designated as "white" may represent colors of

very low purity. Their locations can be inferred from the charts for high reflection coefficients. The "white" areas become much more expanded and cover areas of very low purity. Intensity variations within the charts have not been indicated at all. Areas of low intensity relative to the maximum intensity across a chart should not be identified in a manner that obscures the changes in hue.

Changes in intensity are shown in Fig. 54 by the variation of the tristimulus value Y. Curves are presented for $\delta_3 - \delta_1$ of 0 (or 360) and 180°. The reflection coefficients at both interfaces correspond to those used in the color charts. Positions of minimum and maximum intensity were located throughout the charts and were found to be nearly independent of the reflection coefficient. Dotted and dashed lines connect positions of the minima and maxima, respectively. These lines were verified to be correct at a $\delta_3 - \delta_1$ of 20° for all combinations of the reflection coefficients. Low intensity areas of the chart are associated with purples and blues. The hue changes rapidly with optical path difference in these areas as demonstrated in Figs. 26 through 35. Kubota[29] referred to this phenomenon as the "sensitive color". High intensity areas in the charts are associated with yellows.

A similar chart is presented in Fig. 55 for monochromatic interference. The reflectance in Eq. (31) was calculated for light of wavelength 5700Å, because the lines connecting positions of minima or maxima for this wavelength were nearly identical throughout most of the chart to those in Fig. 54. Note the increased sharpness of the minima in the curves for higher reflection coefficients. This effect is easily attributed to the denominator in the multiple-beam intensity equation.

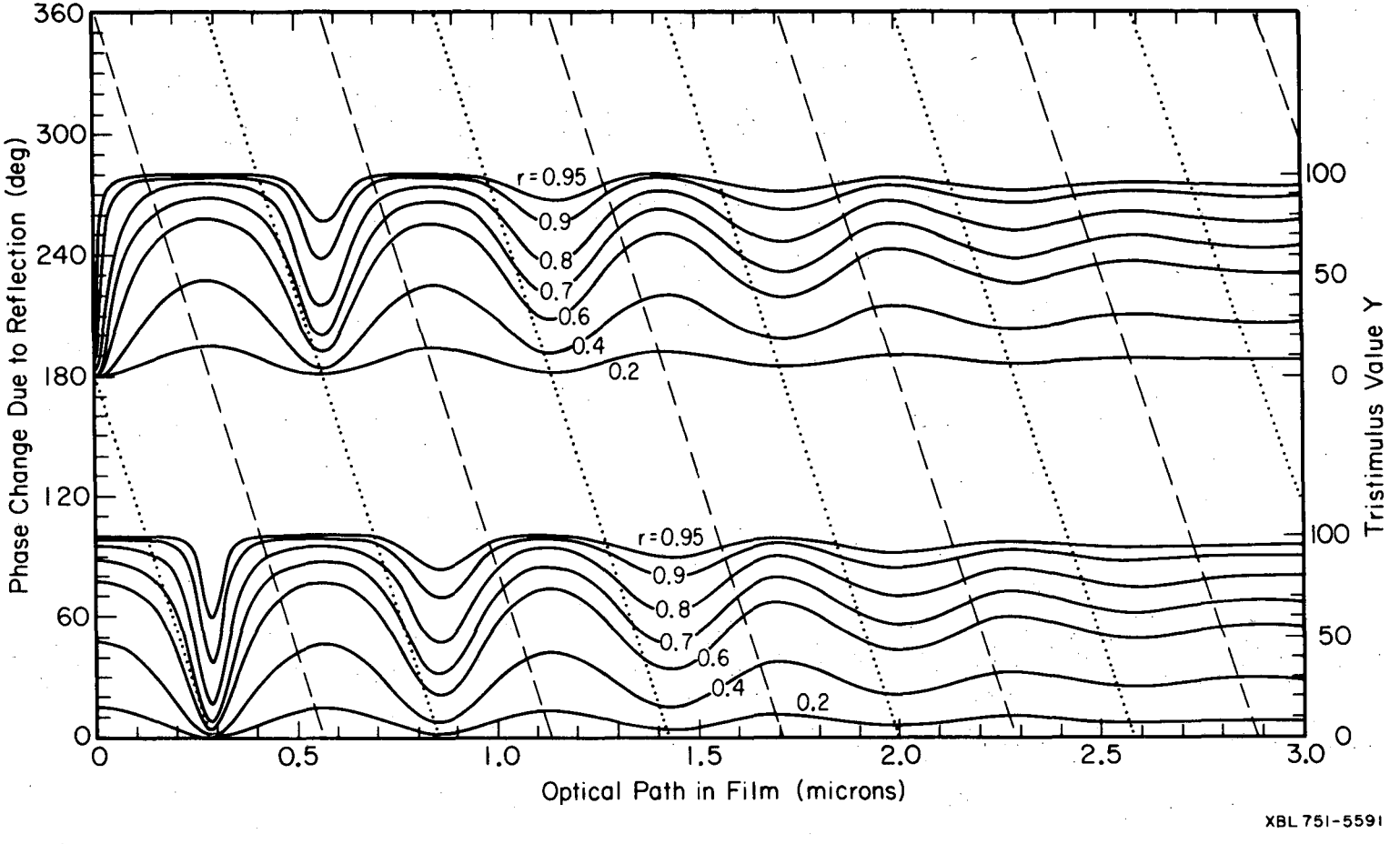

Fig. 54. Relative luminance of white light reflected from a film-covered substrate as given by the tristimulus value Y. Curves for selected values of the amplitude reflection coefficient (r) at both interfaces. Phase change due to reflection, of 0° for one set of curves and 180° for other set. Dotted lines connect positions of minimum luminance in the diagram and dashed lines connect positions of maximum luminance.

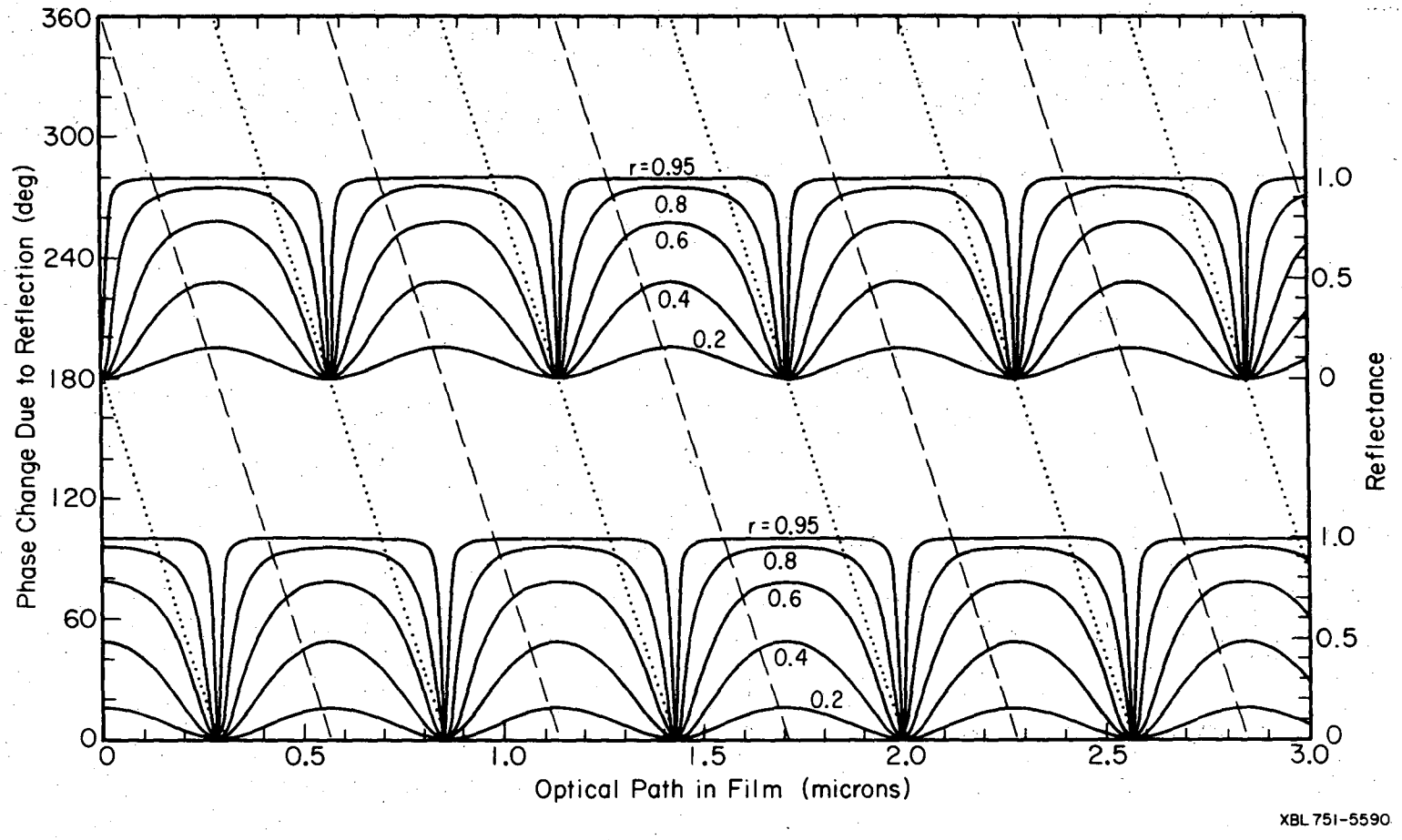

Fig. 55. Reflectance of monochromatic light of wavelength 5700Å incident onto a film-covered substrate as given by the multiple-beam intensity equation. Curves for selected values of the amplitude reflection coefficient (r) at both interfaces. Phase change due to reflection of 0° for one set of curves and 180° for other set. Dotted lines connect positions of minimum intensity in the diagram and dashed lines connect positions of maximum intensity.

It is responsible for the decrease in color purity at high reflection coefficients and the resultant shift of the optimum angle to angles lower than the monochromatic optimum angle.

The general difference between intensity variations in white-light and monochromatic interference can be perceived at a glance. In monochromatic interference, the intensity repeats at equal intervals of the optical path difference (one wavelength) corresponding to a phase shift of 360°. In white-light interference, the magnitude of the variations of intensity lessens with higher values of the optical path difference. The underlying reason for the difference is the fact that in white-light interference the optical path difference does not uniquely determine the phase in Eq. (22). The resulting spectral energy distribution becomes more uniform at higher values of the optical path difference. Thus, the intensity variation shows a general decrease across the color charts. Variations of the tristimulus values X, Y and Z in each of the charts reflect a corresponding general decrease in the color purity with higher values of the optical path difference. Figures 56 and 57 show the trend toward averaged values across the charts. Curves in these figures were drawn by the plotting facility associated with the computer. Unevenness in the curves for the highest reflection coefficients appears to be the result of calculations and not stray pen movement.

4. Use of Color Charts

Interpolations between color charts in Figs. 47 through 53 and between intensity variations in them as shown in Fig. 54 can be done accurately, if the reflection coefficients at the two interfaces are equal. If the reflection coefficients are not equal but are also not

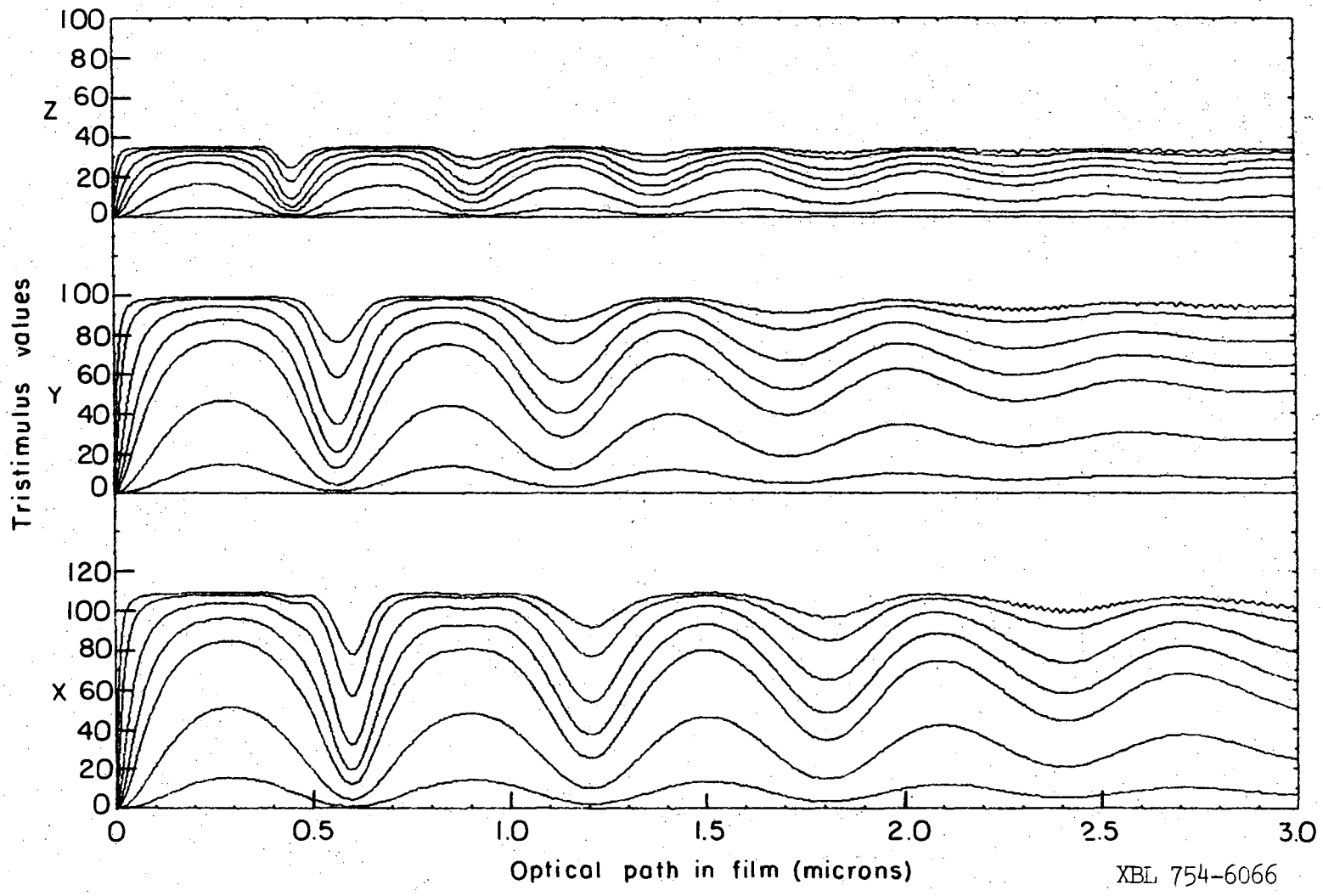

Fig. 56. Variation of the tristimulus values with optical path difference for phase change due to reflection, $\delta_3 - \delta_1$, of 180°. Reflection coefficients at both interfaces of 0.2, 0.4, 0.6, 0.7, 0.8, 0.9 and 0.95.

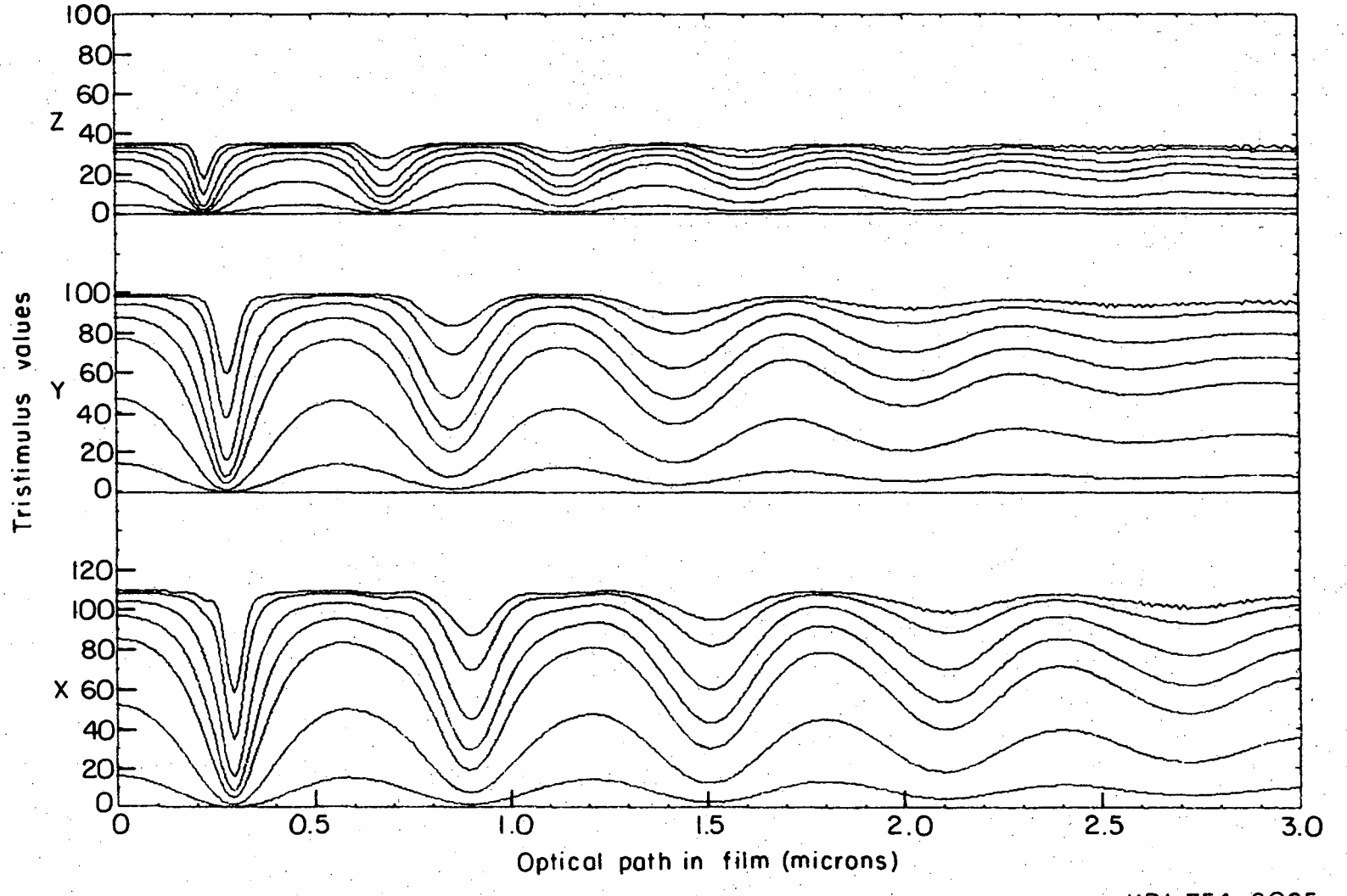

Fig. 57. See Fig. 56. Phase change due to reflection of 0°.

XBL754-6065

widely different, a color series can again be determined fairly accurately, but interpolations involving the size of the white areas cannot be made. Color series were investigated for a $\delta_3 - \delta_1$ of 20° and many combinations of unequal reflection coefficients and were found to be intermediate between series for the corresponding equal reflection coefficients. Interpolations were not merely averages, though, of the values of the optical path difference at which transitions between hues occurred. The dependence of the hue on the reflection coefficients could be expressed more clearly in figures similar to Figs. 26 through 35. Curves of constant optical path difference and curves of constant reflection coefficient, r_3, could be drawn for specified values of $\delta_3 - \delta_1$ and r_1.

The color charts were designed to provide accurate color series with a minimal amount of computation. A method will be discussed next to compute both the reflection coefficients and the phase changes at the interfaces for a selected angle of incidence and the conversion of the optical path difference to film thickness. Calculations to determine the reflection coefficient and phase change at the film-metal interface can be almost eliminated by using graphs such as Figs. 58 and 59. The angle of incidence onto the substrate is specified to be 45°, which corresponds to approximately a 75° angle of incidence onto a film of refractive index, 1.35. As demonstrated in Fig. 4, the reflection coefficient and phase change for metal substrates in contact with aqueous solutions are nearly constant above this angle.

The calculations can be further reduced, if the experimental angle of incidence is also the monochromatic optimum angle. Curves such as those in Figs. 13 and 14 yield the monochromatic optimum angle for a specific film and substrate. The reflection coefficients at the two interfaces

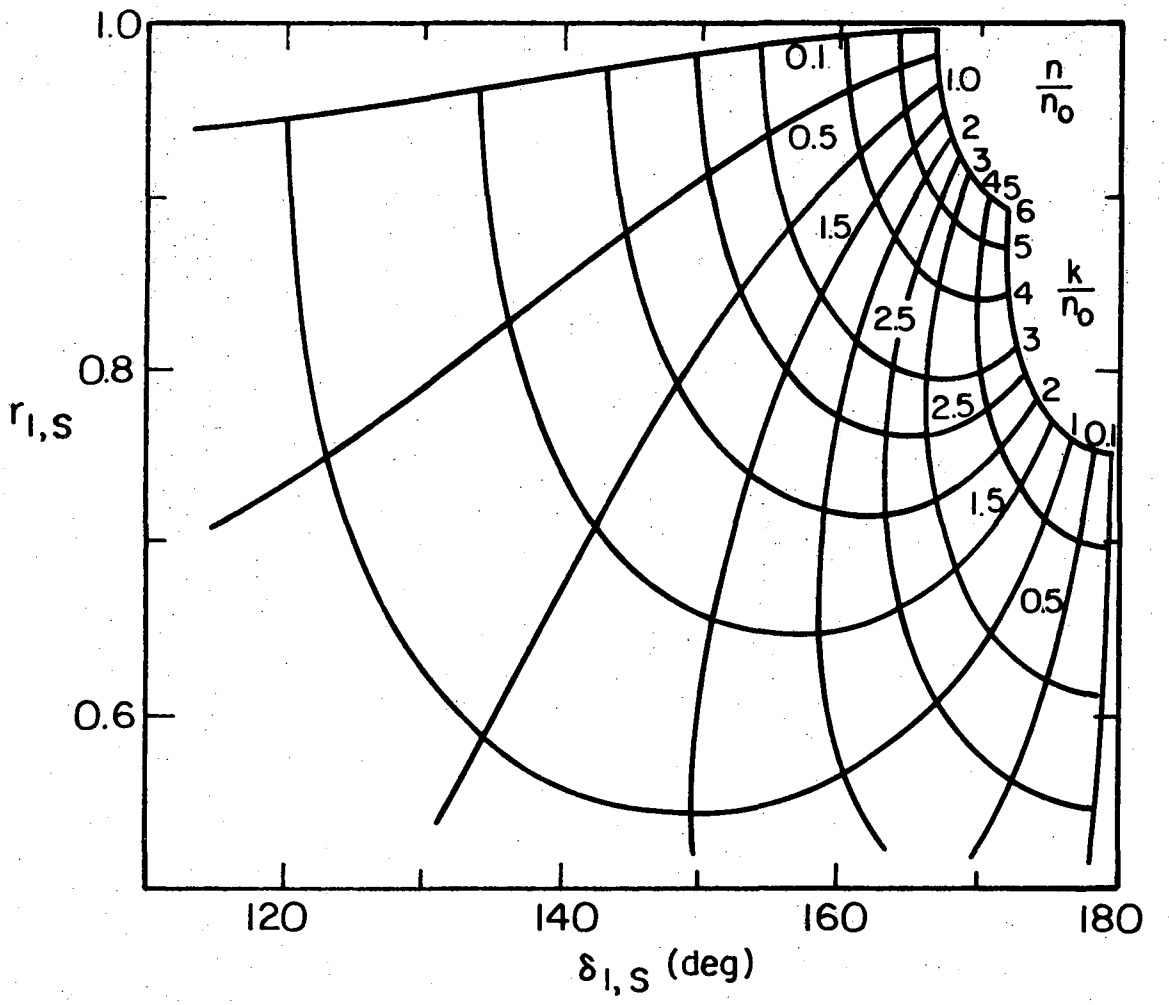

Fig. 58. Amplitude reflection coefficient and phase change for reflection from absorbing medium at 45° angle of incidence. Absorbing medium and dielectric incident medium in contact with it have refractive indices of n - ik and n_o, respectively. s-polarized light.

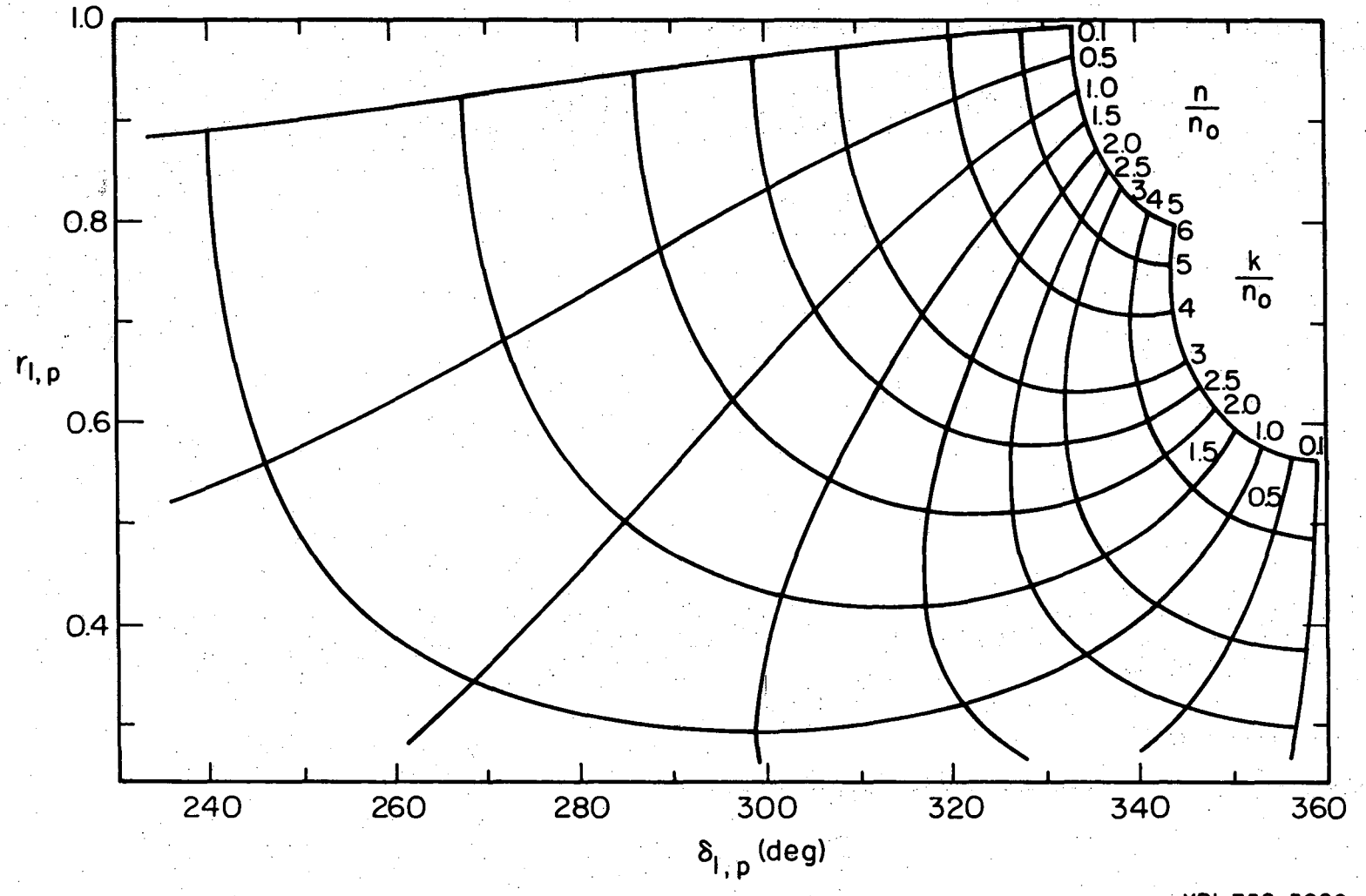

XBL 752-5826

Fig. 59. See Fig. 58. p-polarized light.

are specified to be equal and can be determined from curves such as those in Fig. 15. As before, the phase change, δ_1, at the film-metal interface is given closely by Figs. 58 and 59. The value of the reflection coefficient, r_1, should be the same as that found earlier for both reflection coefficients.

The phase change at the air-film interface above Brewster's angle is equal to 180° for both polarizations. If the angle of incidence is above Brewster's angle for a film-covered metal surface, the phase change due to reflection, $\delta_3 - \delta_1$, is greater than 0 and 180°, respectively, for s and p-polarized light. The value of $\delta_3 - \delta_1$ for p-polarized light has been adjusted by 360° to make it positive. If the reflection coefficients at the two interfaces are equal, the color series can be determined accurately from one of the charts or by interpolation between two charts. The conversion factor from optical path difference to film thickness is a readily calculated quantity, which is the reciprocal of $2n_1\cos\phi'$ in Eq. (21).

IV. EXPERIMENTAL: PROCEDURES AND RESULTS

A. Thin Film Interference Optical Bench

A diagram of the optical bench is shown schematically in Fig. 60 along with a numbered list of components. Figure 61 is a photograph of this same apparatus. The optical components on the left side of the figures produce two collimated and polarized beams of light incident onto a film-covered surface. Those on the right side focus images of captions and the surface and adjust their positions in the plane of a photographic film. The left side can be moved along a track about a vertical axis. The film-covered surface, which is oriented in the vertical position, can be rotated about this same axis so that the reflected images pass through the mirror system. The beams have an angular separation of 6°. The angles of incidence are equal to half the reading (in degrees) on the semicircular track plus or minus 3°.

The light sources are two tungsten microscope lamps, which are focused on ground glass diffusing screens. Irises behind the screens approximate point sources. The beams are collimated and polarized with lenses and polaroid filters. Light reflected from the film-covered surface is focused at a point beyond the mirror system, in which it undergoes reflection from two mirrors. The focusing is achieved with a field lens placed just behind the film-covered surface and a lens placed in front of the camera. If the camera lens has a diaphragm, it should be positioned such that the diameter of the beams is smallest at the diaphragm in order to avoid vignetting of the images.

A set of lenses focuses the image of captions, and mirrors adjust the image position in the plane of the photographic film. When necessary,

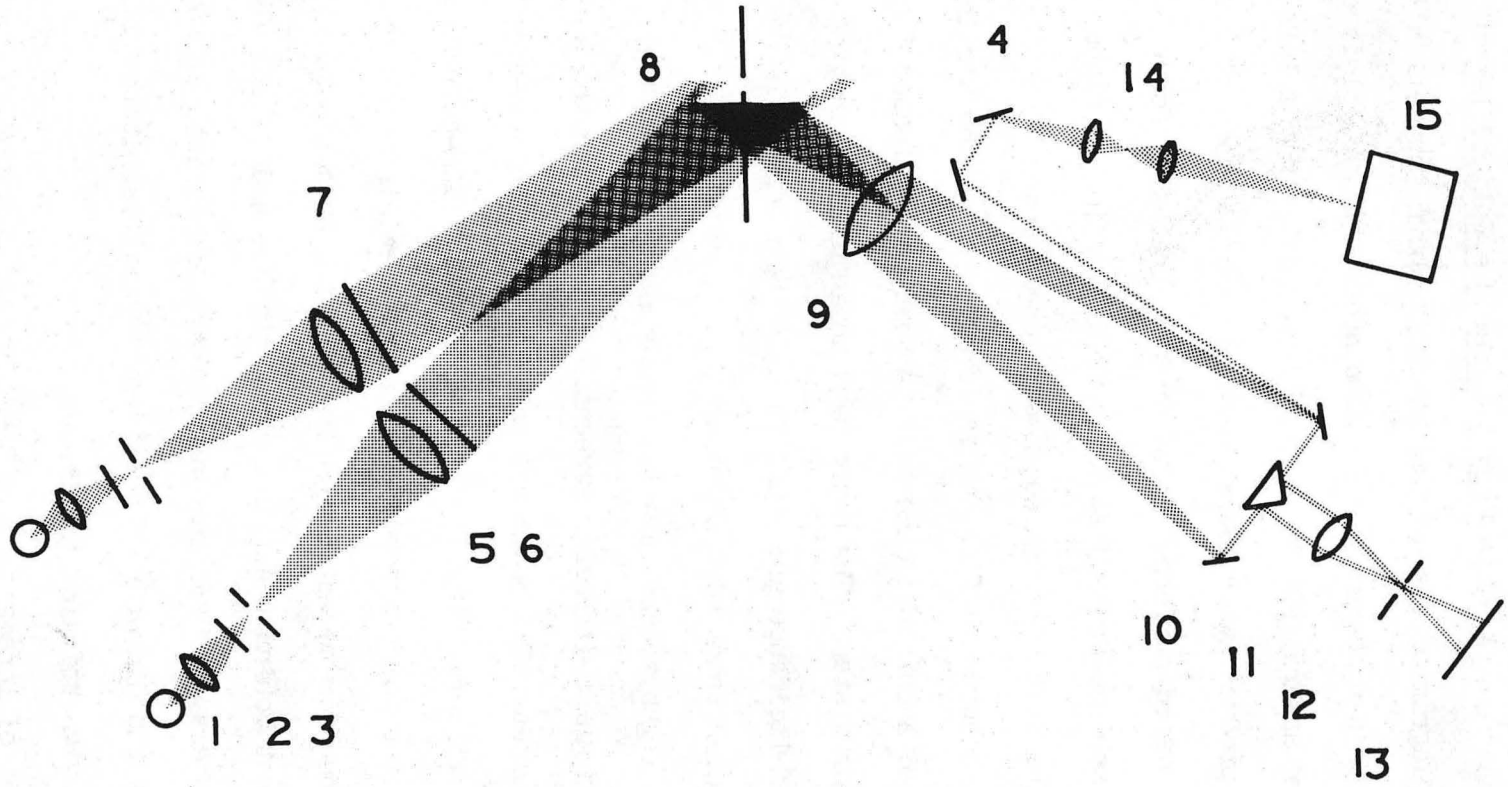

XBL 7012-7482

Fig. 60. Schematic diagram of thin film interference optical bench.[27] 1. Microscope lamps, 2. Neutral density filters, 3. Source irises with diffusing screens, 4. Front surface mirrors, 5. Collimating lenses, 6. Polarizing filter, s-polarization, 7. Polarizing filter, p-polarization, 8. Thin film-covered surface, 9. Field lens, 10. Mirror system for reflected images, 11. Camera objective, 12. Camera diaphragm, 13. Photographic film plane, 14. Focusing lenses for captions, 15. Captions.

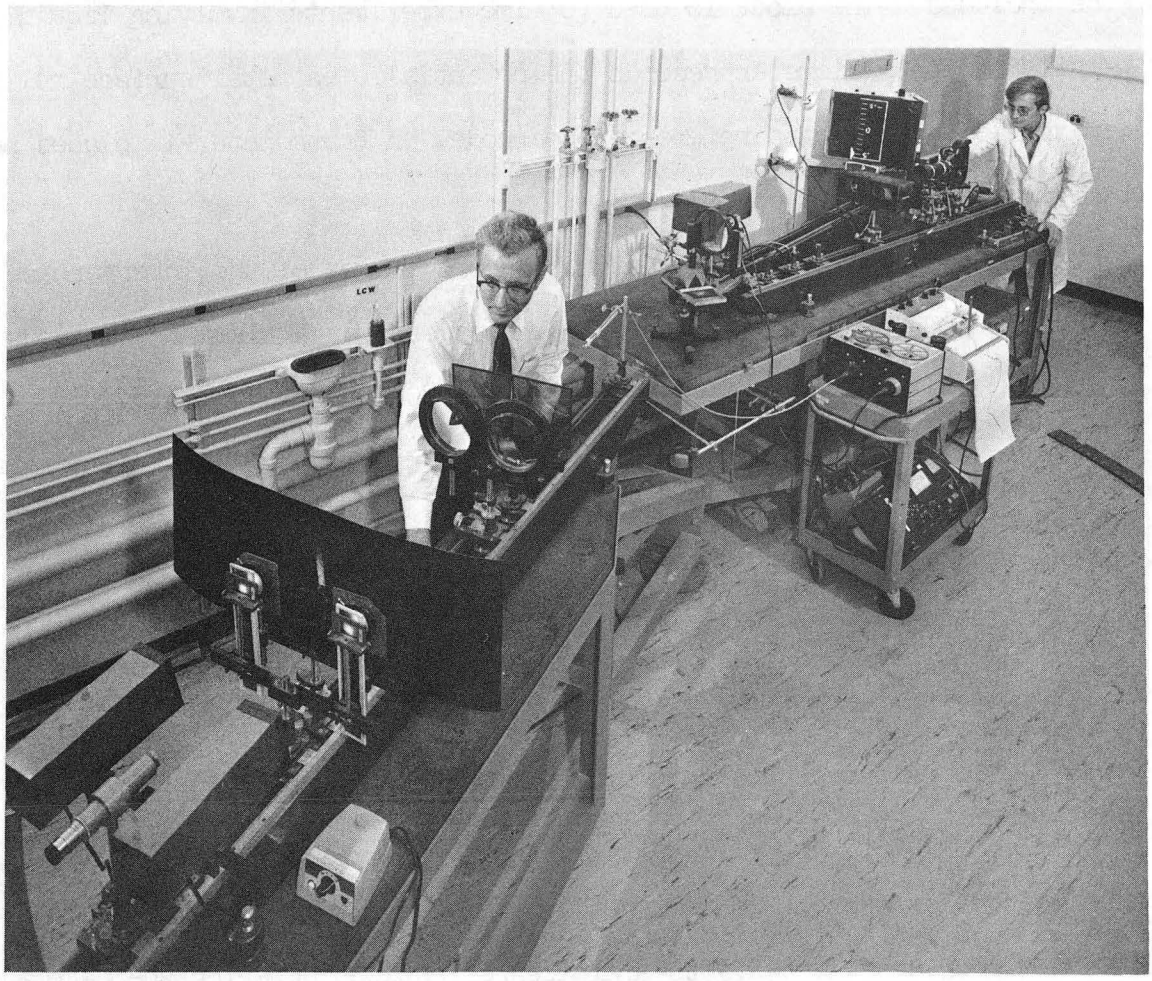

CBB 755-3842

Fig. 61. Thin film interference optical bench. See Fig. 60 for list of components. Light from tungsten lamps (left) reflects from film-covered surface (center) into camera (right). Fiber optic probes sample light in incident and reflected beams.

images of a clock and a potentiometer (illuminated with flood lights) can be included. The clock is used to time experiments involving liquid films, while the potentiometer records the potential of a metal surface relative to the potential of a reference electrode. A thermometer is placed next to the experimental cell.

One of two cameras was used to record images of the interference patterns. For single photographs, the camera was a Nikon F 35mm body used with a 400mm objective made from two 800mm achromatic lenses. A timer on the camera ensured a gentle shutter release. For sequences of photographs in which the time of drainage of a liquid film was recorded by the image of a clock, a Bolex H-16 16mm movie camera was used with a Vario-Switar 18-86mm zoom objective. Frames were exposed at constant intervals that were set by a timer in a movie control box. The shutter was gently released by a motor with a crank and a connecting rod to the camera. Lights that illuminated the captions turned on about 2 sec before the exposure. The source lights, though, were on continuously. Room lights were kept off to minimize reflections entering the camera from optical components. The photographic film for either slides or movies was Kodak Ektachrome type EF balanced for 3200°K tungsten light. Intensities of the reflected images relative to each other could be adjusted with neutral density filters in front of the source irises.

An alignment procedure for the optical bench has been described in detail by Turney.[27] He has also presented a complete description of the spectrophotometer, which measures the intensity of light reflected from the film-covered surface relative to the incident intensity. One fiber optic probe (1/8 in. diameter) is placed in the incident beam and

one in the reflected beam. The probe that samples the reflected light is held in a rack and pinion mount, with which the vertical position can be scanned.

B. Ellipsometry

A compensating automatic ellipsometer[50] was used to determine film thicknesses of cryolite films on chromium and aluminum. Principles of ellipsometry have been explained elsewhere.[51] However, a brief description and a summary of equations will be presented for the sake of clarity.

Overall complex amplitude reflection coefficients of a film-covered surface for s- and p-polarized light have been given by the Drude equation, Eq. (30). These complex quantities are designated by $\hat{r}_s$ and $\hat{r}_p$ and the real amplitudes by r_s and r_p, respectively. Overall phase changes are designated by δ_s and δ_p. They must not be confused with the individual phase changes at an interface, which are contained in the complex reflection coefficients $\hat{r}_1$ and $\hat{r}_3$ at the two interfaces. δ is the phase shift due to the presence of the film.

$$\hat{r}_s = \frac{\hat{r}_{3,s} + \hat{r}_{1,s}e^{-i\delta}}{1 + \hat{r}_{1,s}\hat{r}_{3,s}e^{-i\delta}} = r_s e^{i\delta_s}$$

$$\hat{r}_p = \frac{\hat{r}_{3,p} + \hat{r}_{1,p}e^{-i\delta}}{1 + \hat{r}_{1,p}\hat{r}_{3,p}e^{-i\delta}} = r_p e^{i\delta_p}$$

An essential definition in ellipsometry is that of ρ, which is the ratio of the complex reflection coefficient of the p-polarization to that of the s-polarization. In the definition of ρ, both the phases and the amplitudes of the two orthogonal polarizations are taken to be equal in the incident beam.

$$\rho = \frac{\hat{r}_p}{\hat{r}_s} = \frac{r_p}{r_s} e^{i(\delta_p - \delta_s)} = (\tan\psi)\, e^{i\Delta}$$

$$= \frac{\left(\hat{r}_{3,p} + \hat{r}_{1,p} e^{-i\delta}\right)\left(1 + \hat{r}_{1,s}\hat{r}_{3,s} e^{-i\delta}\right)}{\left(\hat{r}_{3,s} + \hat{r}_{1,s} e^{-i\delta}\right)\left(1 + \hat{r}_{1,p}\hat{r}_{3,p} e^{-i\delta}\right)}$$

The quantity, $\tan\psi$, is thus the relative amplitude attenuation, and Δ is the relative phase shift between the two polarizations upon reflection by the film-covered substrate.

Monochromatic light with a vacuum wavelength of 5461Å is used. Two components of the apparatus are adjusted in order that elliptically polarized light incident onto the film-covered substrate is reflected and then extinguished as linearly polarized light. Elliptic polarization is achieved by passing the light through a polarizer and a quarter-wave plate. The s and p polarizations of the incident light must be equal but shifted in phase. Extinction of the polarized light by the analyzer has been reached upon rotation of the polarizer and analyzer to the proper azimuth angles. The azimuth angle of the quarter-wave plate is fixed during the rotations of the other two components.

The values of ψ and Δ can be derived from the azimuth readings of the analyzer and polarizer, respectively. Two combinations of these readings can yield the same values of ψ and Δ for a given azimuth angle of the quarter-wave plate. This result occurs, because linear polarization of the reflected light can be achieved if the difference in phase between two orthogonal components equals 180° or 360° (or 0°). Different combinations of the azimuth readings correspond to what are called "zones". Another azimuth angle of the quarter-wave plate

contributes two more zones. Experimentally determined values of ψ and Δ are four zone averages. An average value minimizes the error caused by a misalignment of the equipment and nonideality of the quarter-wave plate.

C. Solid Films

1. Deposition

Deposition of metal substrates and dielectric films was accomplished by way of vacuum vapor deposition. The apparatus used for this purpose was a Mikros Automatic Valving Vacuum Evaporator (Model VE-10). A mechanical pump and a diffusion pump performed the pumping. Pressure was monitored with a Pirani transducer system and with a vacuum discharge gauge at successively lower pressure ranges. Even with the aid of a liquid nitrogen cold trap, pressures were generally $2\text{-}5\times10^{-5}$ Torr.

Depositing was confined to a bell jar with a 10 in. outside diameter and a height of 12 in. The base plate had several feedthroughs. A rotary feedthrough allowed rotation of the substrate in a horizontal plane. Sources could be connected to one of two pairs of electrodes, which passed a current of up to 100 amperes. Thermocouple feedthroughs were constructed to monitor source temperatures. The platinum/platinum-rhodium thermocouples were connected to a digital temperature indicator. Unfortunately, its use was not developed to the point that it became well-suited to rapid deposition.

Three by one in. microscope slides were used as supports for the deposited films. In order for the metal films to adhere properly, the slides had to be thoroughly cleaned. After a detergent cleaning, they were soaked in a warm solution of sulfuric acid and potassium dichromate for about 5 hr. At the end of this time, the slides were rinsed with

distilled water and soaked in warm distilled water for an hour.[30] They were dried by passing dry nitrogen over them.

Either aluminum or chromium was deposited onto the glass slides as the metal substrate. The aluminum was in the form of wire 60 mil in diameter. Chromium (99.9% pure), manufactured by United Mineral and Chemical Corp., was used as 325 mesh powder. The film material that was deposited onto the metal substrates was cryolite (Na_3AlF_6), which is distributed by Ventron Corp.--Alfa Products. It has a purity of 98.5% and a 325 mesh size.

Sources were composed of either tungsten or tantalum.[52] These metals are generally used because of their high melting points. Aluminum was deposited from two 25-30 mil tungsten wires. Pieces of aluminum were hung onto a u-shaped bend in these wires. Two wires of tungsten had to be used, because the aluminum alloyed with the tungsten and caused rapid destruction of a source made from one segment.[52] Tantalum foil was the source material for the deposition of both chromium and cryolite. The design of the sources was such as to obtain the highest possible temperatures. Two pieces of 10 mil thick tantalum sheet were connected to electrodes with screws. They extended horizontally from the electrodes and had a gap between them. This gap was bridged by 2 mil thick tantalum foil with a reduced width in the center. The piece of foil was bent at two opposing sides in order to connect it by crimping to the 10 mil tantalum sheet that had similarly bent edges. For the deposition of chromium, the narrow section of the foil was flat. Chromium was spread out evenly over this area. For the deposition of cryolite, the narrow section consisted of a boat.

Glass slides were mounted horizontally on a stand whose motion was controlled by a rotary feedthrough in the center of the vacuum chamber. Two pairs of electrodes were situated on opposite sides. The source for the aluminum or chromium was connected to one pair of electrodes, while the boat for the cryolite was connected to the other pair. For the deposition of cryolite, the slide was oriented so that its long axis was parallel to and directly above a horizontal line extending radially from the source. Vertical displacement of the slide from the source was about 4 in., and the horizontal displacement of the front edge of the 3 in. slide was about 2 in. Within the physical constraints of the chamber, this geometry appeared to be the optimum to obtain good quality films with a reasonably large gradient of thickness. When aluminum or chromium was deposited, the slide remained the same vertical distance from the source but was rotated back and forth over it. The glass was masked in the lengthwise direction near the edges with metal strips during the deposition of the metal substrate material. Similarly, the metal substrate was partially masked, while the cryolite was deposited. This procedure was followed in case step-height measurements were to be made. Figure 62 is a representation of a film deposited onto a metal substrate, which is supported by a glass slide. Specimen coordinates for use in film profiles are indicated.

The minimum quantity of material to be evaporated was calculated from the required film thicknesses and the geometry of the deposition. Metal layers of about 1000Å thickness were desired in order to insure that they would be opaque. The slide was assumed to be part of either a hemispherical (chromium or cryolite deposition) or a spherical

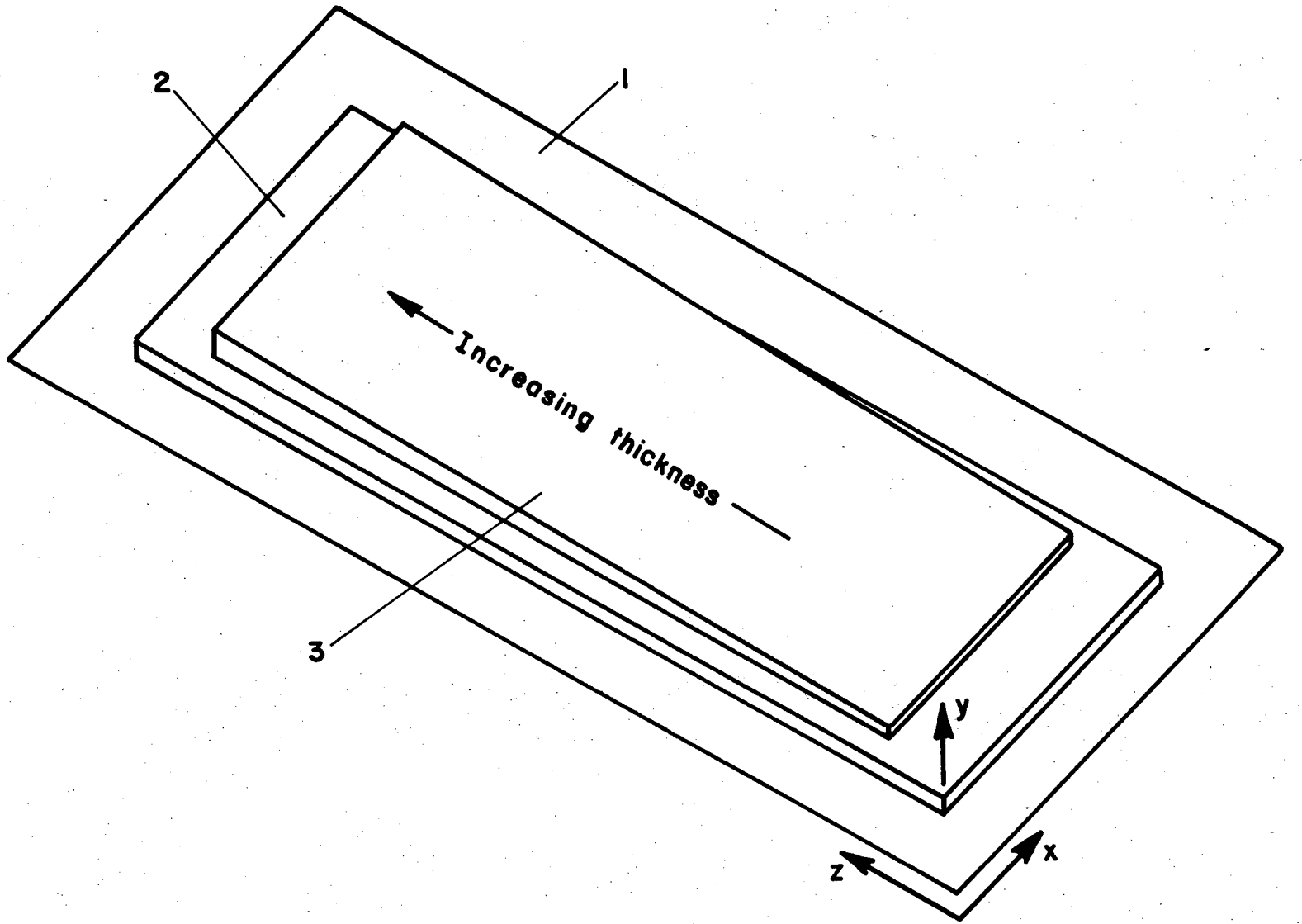

XBL7310-1988

Fig. 62. Coordinate system for deposited solid films.[30] 1. Glass slide. 2. Metal substrate layer. 3. Dielectric film.

(aluminum deposition) surface, whose radius was the average distance from the source to the slide. An amount in excess of this calculated quantity was used, though, because some material would evaporate as the source was heated to the melting temperature. During this time, the slide was shielded from the source on the other side of the chamber. Also, it was assumed that not all of the atoms or molecules impinging on the slide wound be adsorbed.

Monitoring the evaporation was done visually. When current was passed at a slowly increasing rate through the tungsten wires, which held the pieces of aluminum, the aluminum initially formed a liquid drop. It then spread upward in both directions and evaporated rapidly as it progressed along the wire. As current was passed through the source containing the chromium, the tantalum foil heated until it glowed red and the chromium then began to disappear.. Deposition of the entire amount of aluminum and chromium occurred within a period of 20 and 45 sec, respectively. During the time when the current was high, the pressure in the chamber rose significantly. After the deposition of the metal was complete, the slide was removed from the chamber in order to mask part of the metal. The slide was again mounted in the stand and aligned for the deposition of cryolite. The orientation of the slide was noted before rotating it to the other side of the evacuated chamber. Upon the gradual increase of current, the tantalum boat heated until it glowed red and the cryolite began to melt. At this point, the slide was quickly rotated back to its original position and the current was raised. Again, the pressure in the chamber rose significantly. The period of deposition varied with the quantity of cryolite that was evaporated but was on

the order of 10 sec.

The metal layers were opaque to ordinary lighting. However, they did show pinholes when the room lights were turned off and they were held in front of a high intensity lamp. Both the metal and the cryolite layers appeared to be adhering very well. Interference fringes were only slightly curved and were symmetrical about the axis of the slide. Since the thicknesses of the films on the numerous slides varied over a wide range, the films appeared to be satisfactory for use in a study of the colorimetry of interference colors of dielectric films on metals.

2. Ellipsometric Measurements

Azimuth readings of the analyzer and polarizer were recorded for different locations along the vertical axis of the glass slides, which supported the cryolite film-covered chromium and aluminum layers. The ψ and Δ values derived from the azimuth readings are four zone averages.[51] Positions along each slide were measured at the center of the circular light beam, which was about 3 mm in. diameter. The angle of incidence was 75°. Thus, the measured thickness was an average over an ellipsoidal area (3×12 mm).

Experimental ψ and Δ values are shown in Figs. 63 and 64. Calculated curves were drawn for metal refractive indices that vary about the average value determined in this study of 2.23-i(1.23) for chromium (measured value for bare chromium) and 0.8-i(5.4) for aluminum. Agreement of the experimental with the calculated curves was best for a cryolite refractive index of 1.34.[53] A range of 1.30-1.33 has been given elsewhere[54] for cryolite films. The computer program LAYER[55] was modified to plot the curves in Figs. 63 and 64. The curves repeat themselves at thickness

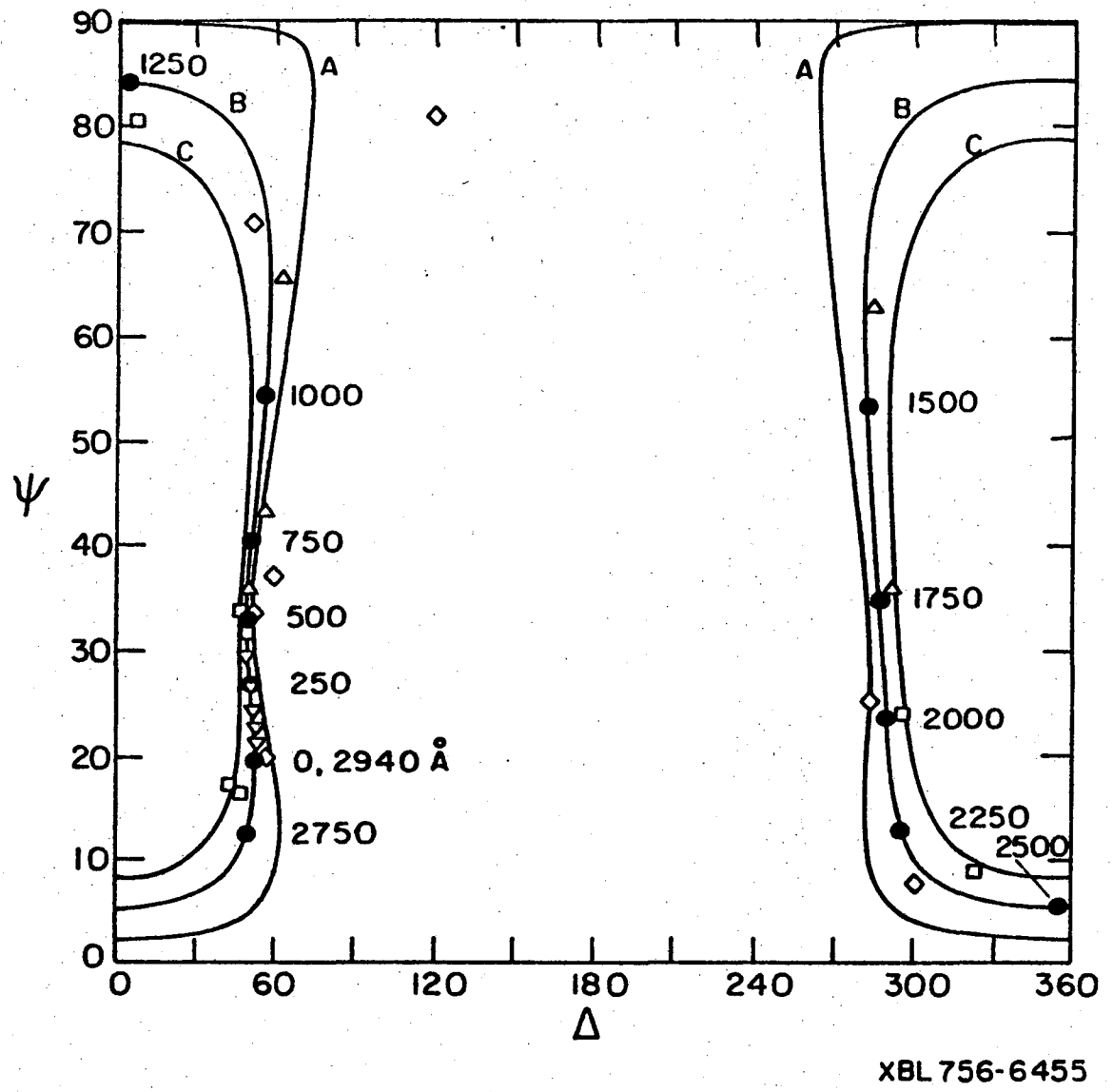

XBL 756-6455

Fig. 63. Experimental values of ellipsometric parameters ψ and Δ. Calculated curves for cryolite film of refractive index 1.34 on chromium substrate of refractive index A. 2.2-i(1.4), B. 2.2-i(1.2), C. 2.2-i(1.0).
▽ Film 1
△ Film 2
□ Film 3
◇ Film 4

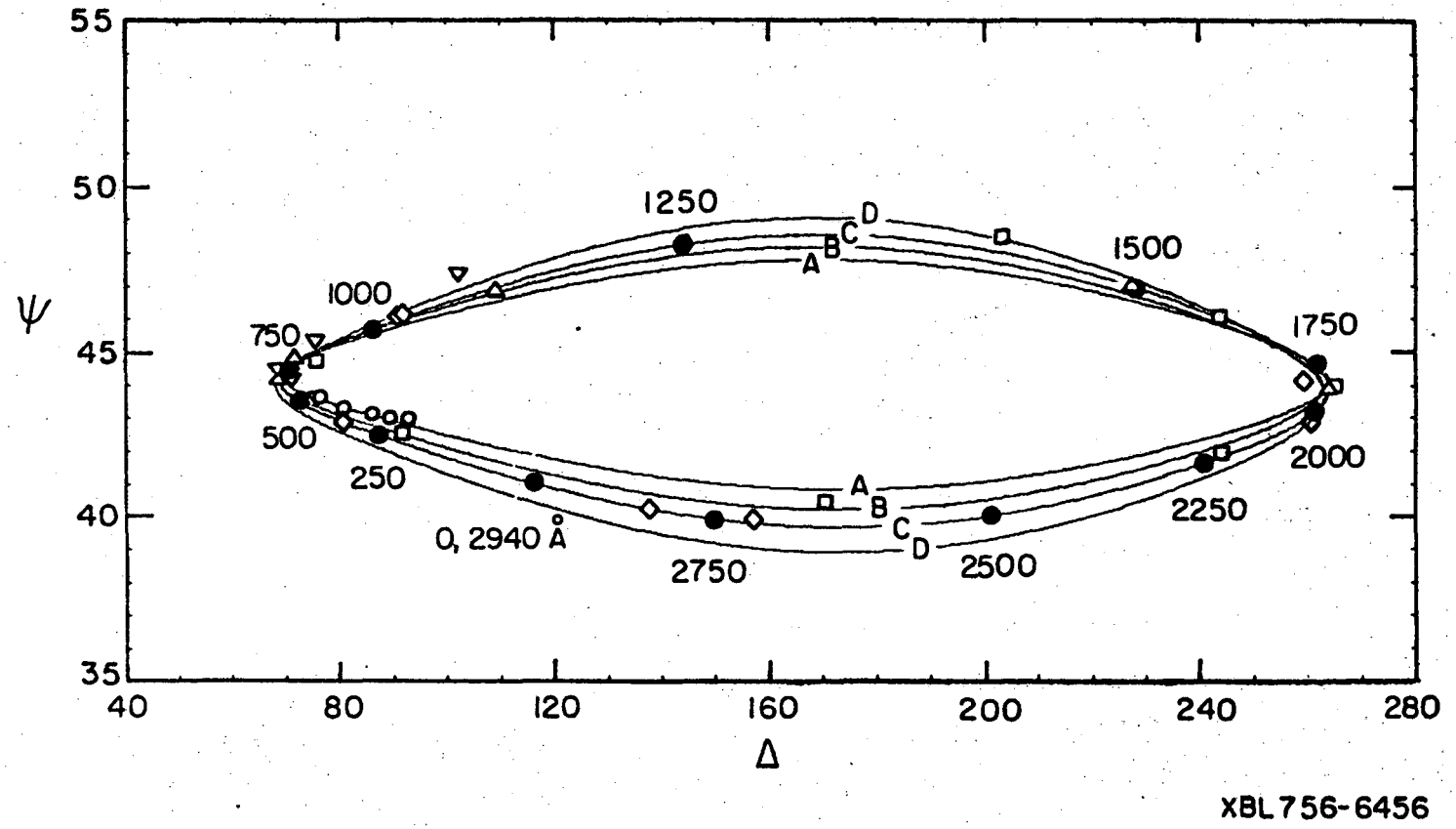

Fig. 64. Experimental values of ellipsometric parameters ψ and Δ. Calculated curves for cryolite film of refractive index 1.34 on aluminum substrate of refractive index, A. 0.7-i(5.6), B. 0.7-i(5.2), C. 0.9-i(5.6), D. 0.9-i(5.2).
○ Film 5
▽ Film 6
△ Film 7
□ Film 8
◇ Film 9

intervals (2940Å) which correspond to wavelength intervals (5461Å) in the optical path difference.

3. Interference Measurements

Interference colors of the deposited films were recorded photographically on positive slide film. The experimental angles of incidence were slightly less than the calculated monochromatic optimum angles. Observation of the colors as a function of distance along the supporting glass slides was accomplished by projecting the photographic images onto a white background. The light source for the projector was a tungsten lamp. Figures 65 through 68 show the observed color series and the calculated series, which are drawn as a function of the optical path difference.

For each film, the correspondence between an observed and calculated color is indicated by an arrow. Difficultly was encountered in matching the white areas. In Fig. 66 (film 2), the center of the white area (W) is matched with a part of the calculated series that is very close to the white region in the chromaticity diagram. A similar matching occurs in Fig. 68 (Films 8 and 9) but is not indicated by arrows. Slight overexposure of the photographic film could cause very unsaturated colors to appear white. The transition between white (W) and yellow (Y) or orange (O) at the beginning of an observed series is assumed to correspond to the same transition in the calculated series.

4. Film Profiles

A comparison between colorimetrically and ellipsometrically determined film profiles is given in Figs. 69 and 70 for cryolite films on chromium and aluminum substrates, respectively. The agreement is very good, when

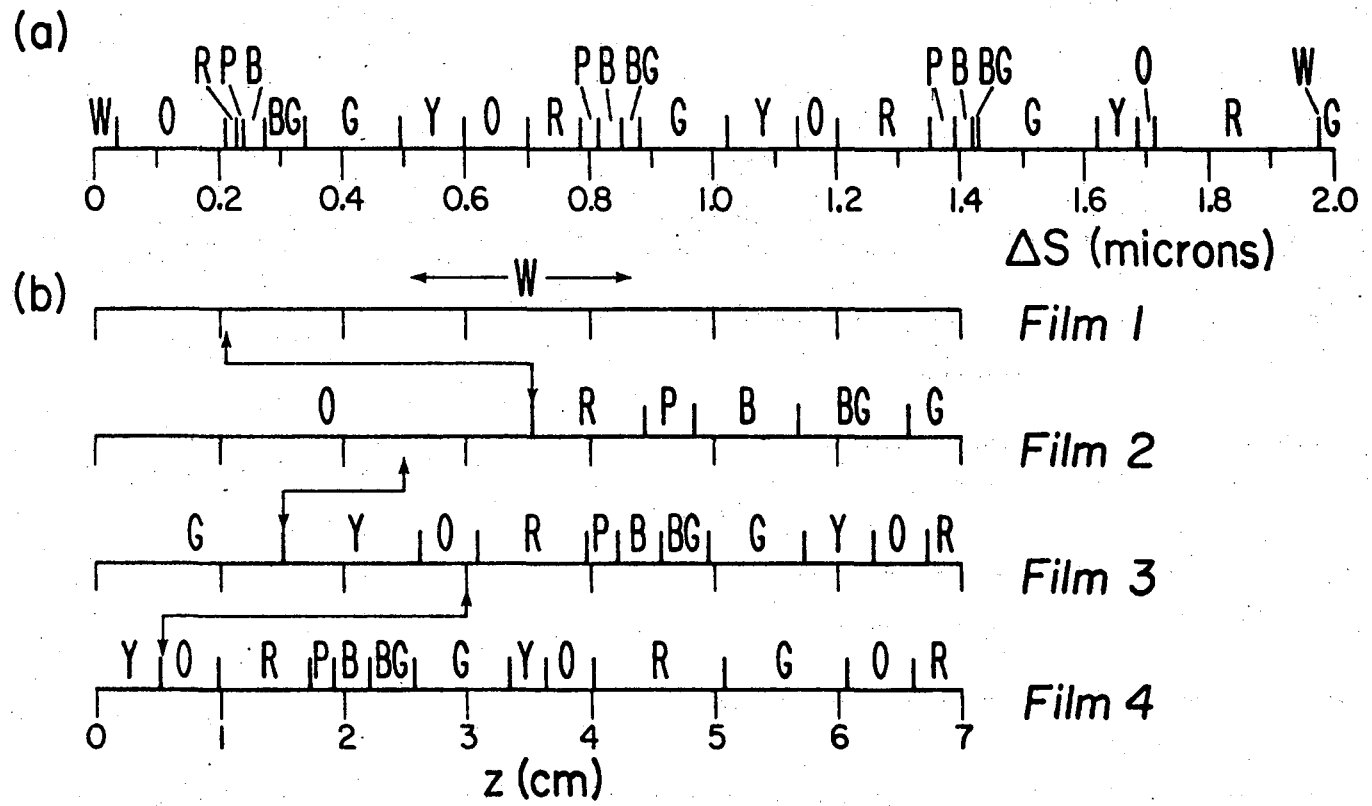

XBL 756-3142

Fig. 65. Cryolite film (refractive index = 1.34) on chromium substrate (refractive index = 2.23-i(1.23)), angle of incidence 72°, s-polarized light. (a) Calculated color series as a function of the optical path difference, ΔS. Film thickness, $d = 0.530 \cdot \Delta S$. $\delta_3 - \delta_1 = 25.8°$, $r_1 = 0.528$, $r_3 = 0.507$. (b) Observed color series as a function of distance, z, along slide.

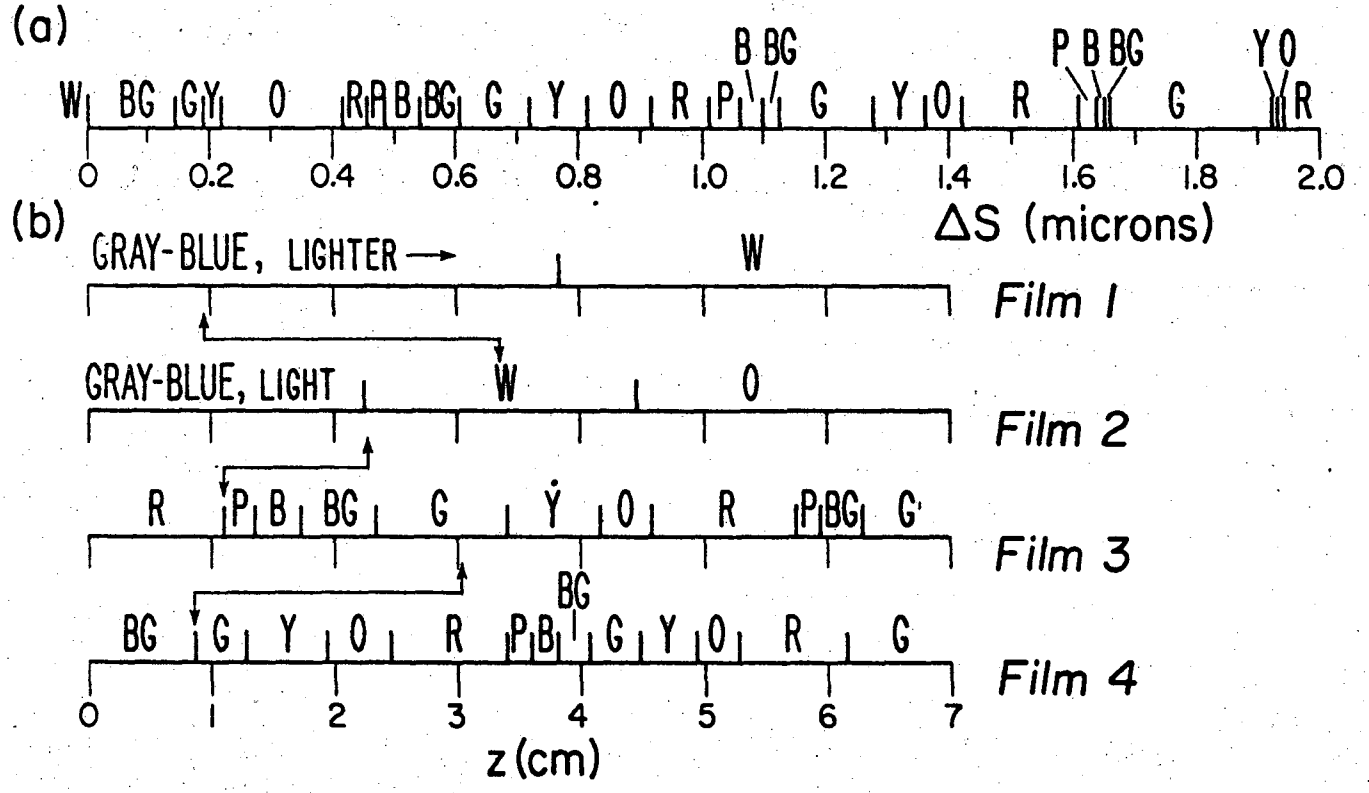

XBL 756-3143

Fig. 66. Cryolite film (refractive index = 1.34) on chromium substrate (refractive index = 2.23-i(1.23)), angle of incidence 72°, p-polarized light. (a) Calculated color series as a function of the optical path difference, ΔS. Film thickness, $d = 0.530 \cdot \Delta S$. $\delta_3 - \delta_1 = 232.1°$, $r_1 = 0.276$, $r_3 = 0.260$. (b) Observed color series as a function of distance, z, along slide.

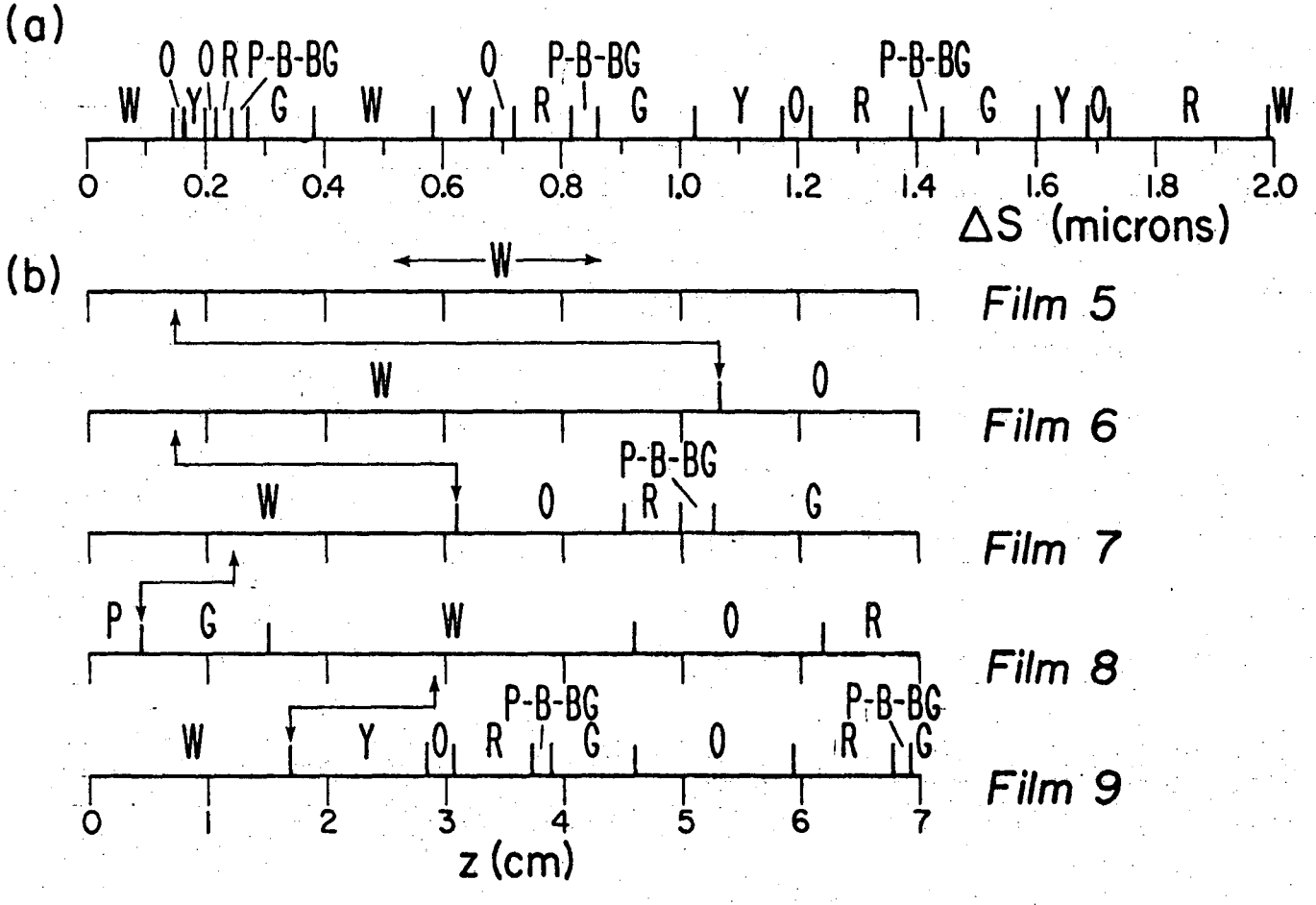

XBL 756-3140

Fig. 67. Cryolite film (refractive index = 1.34) on aluminum substrate (refractive index = 0.80-i(5.40)), angle of incidence 86°, s-polarized light.
(a) Calculated color series as a function of the optical path difference, ΔS. Film thickness, d = 0.559·ΔS. $\delta_3-\delta_1 = 18.2°$, $r_1 = 0.956$, $r_3 = 0.855$.
(b) Observed color series as a function of distance, z, along slide.

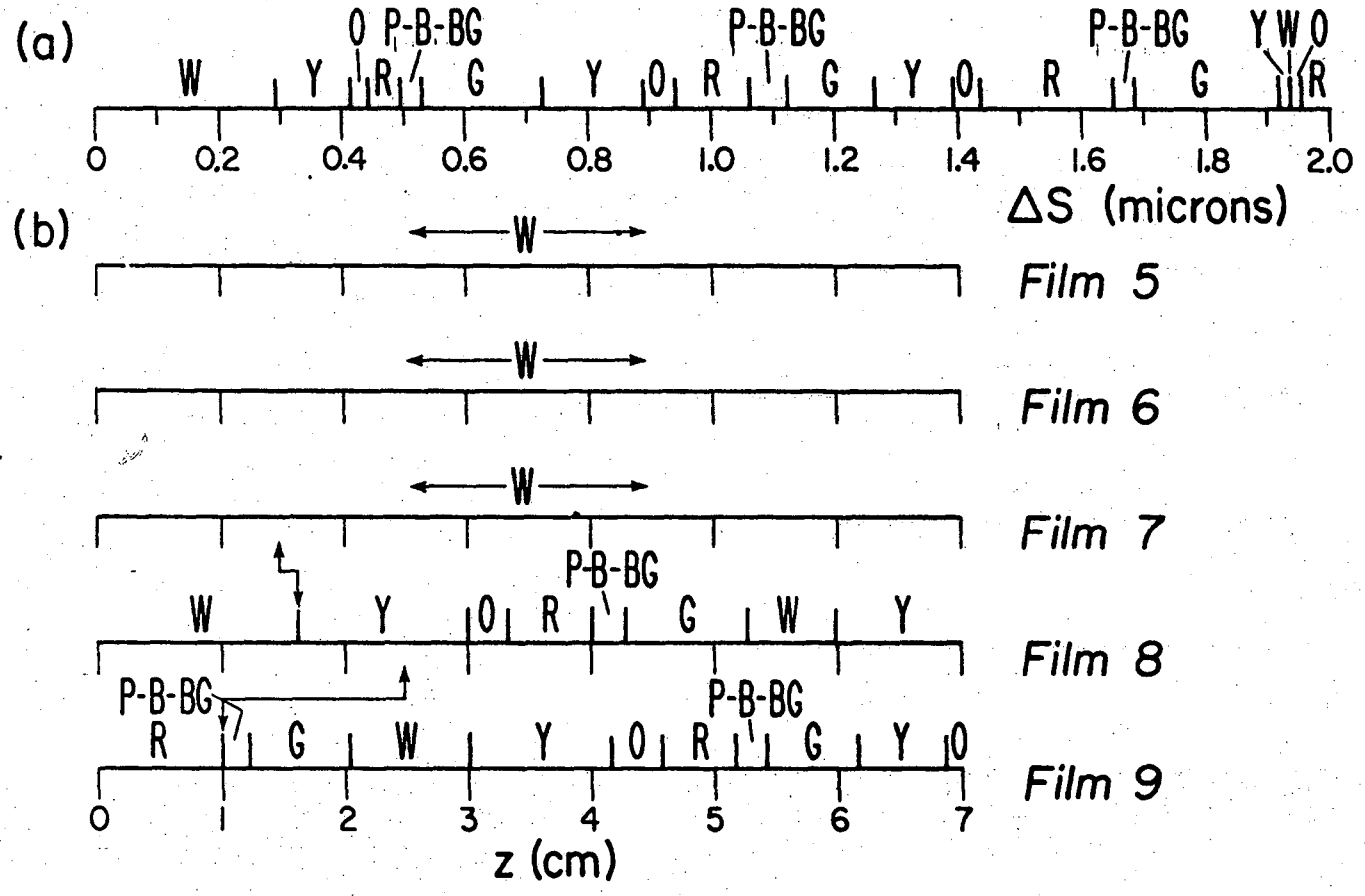

XBL 756-3141

Fig. 68. Cryolite film (refractive index = 1.34) on aluminum substrate (refractive index = 0.80-i(5.40)), angle of incidence 86°, p-polarized light. (a) Calculated color series as a function of the optical path difference, ΔS. Film thickness, $d = 0.559 \cdot \Delta S$, $\delta_3 - \delta_1 = 220.6°$, $r_1 = 0.905$, $r_3 = 0.754$. (b) Observed color series as a function of distance, z, along slide.

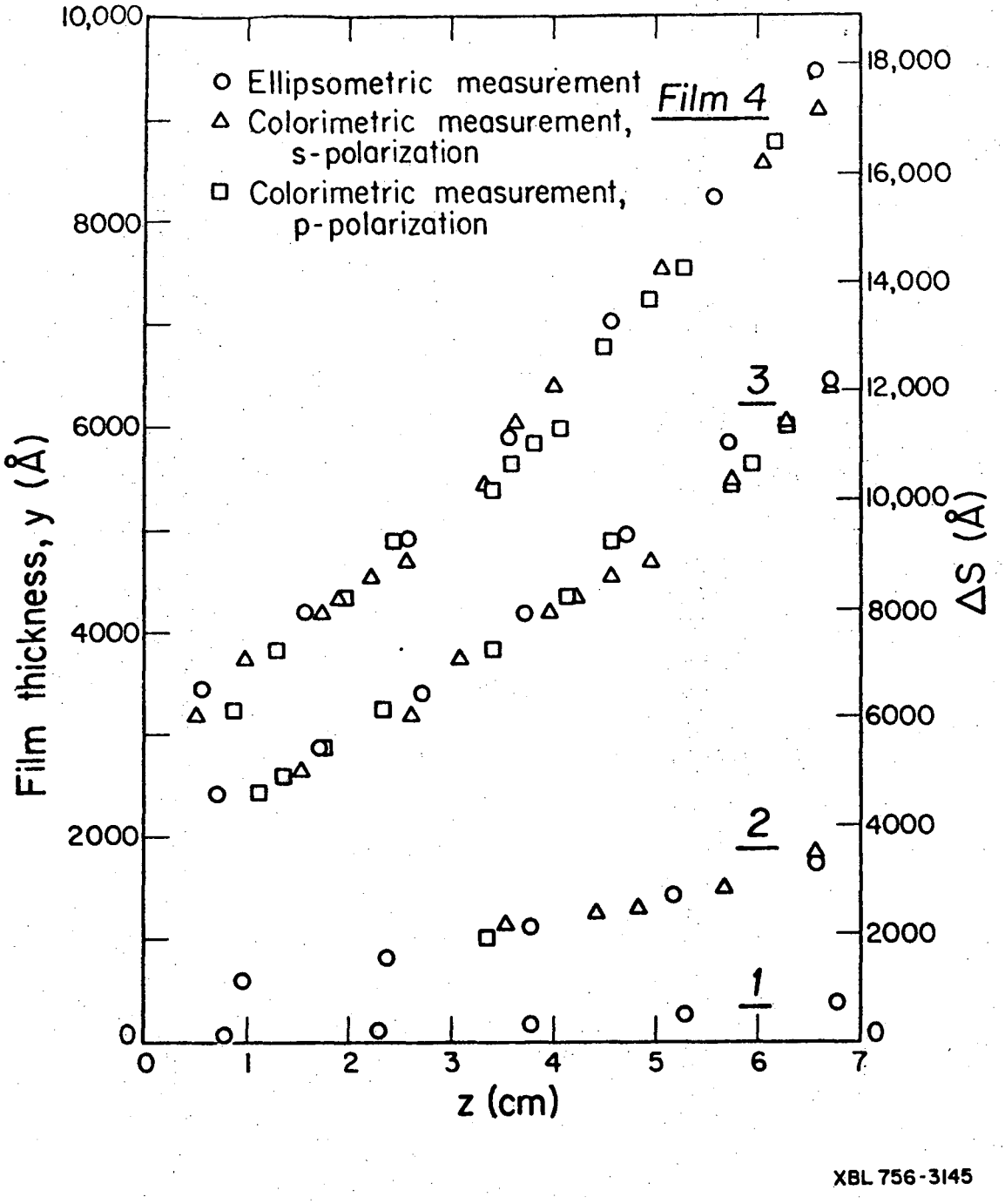

Fig. 69. Comparison between colorimetric and ellipsometric thickness measurements. Cryolite film on chromium substrate.

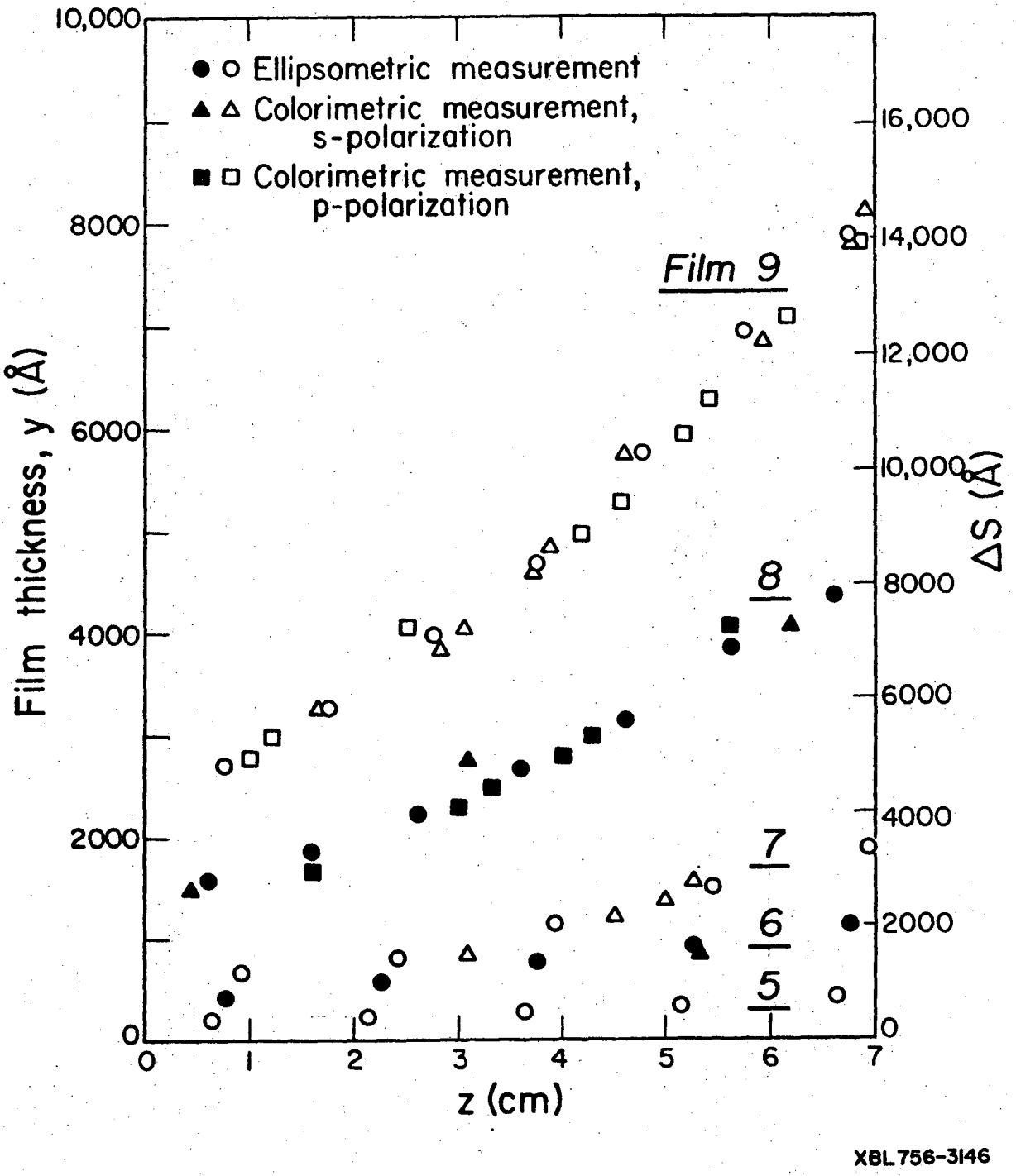

Fig. 70. Comparison between colorimetric and ellipsometric thickness measurements. Cryolite film on aluminum substrate.

one considers the physiological dependence of the colorimetric measurements. Both figures demonstrate that a lower thickness limit exists for colorimetric measurements. This limit is somewhat less than 0.1 micron for films of low refractive index.

Brown[30] made comparisons similar to those in Figs. 69 and 70. He included spectroscopic measurements and also measurements independent of the optical constants of the film and substrate (optical step-height with interference microscope and profilometer step-height). Some of his colorimetrically determined profiles were noticeably different from those determined with ellipsometry. The discrepancy has been resolved in the present study. Refer to Section V for further discussion.

5. Optimum Angle of Incidence

The concept of an optimum angle of incidence has been verified experimentally. The monochromatic optimum angle will be discussed first as an introduction. Early in this study, intensity measurements (relative to unit incident intensity) were made of the light reflected from a cryolite film-covered silicon substrate.[30] The maximum and minimum intensities along the film were found in order to calculate the Michelson fringe visibility in Eq. (36). The readings were calibrated with neutral density filters. Refer to Figs. 71 and 72 for a comparison of experimental values of the fringe visibility with the theoretical curves. At the higher angles, the measurements were limited by the width of the reflected image. For both p and s polarized light, the optimum angles were closely predicted.

Films 3 and 8 (Figs. 69 and 70) were used to observe the optimum angle of incidence in white-light interference. The observers were the

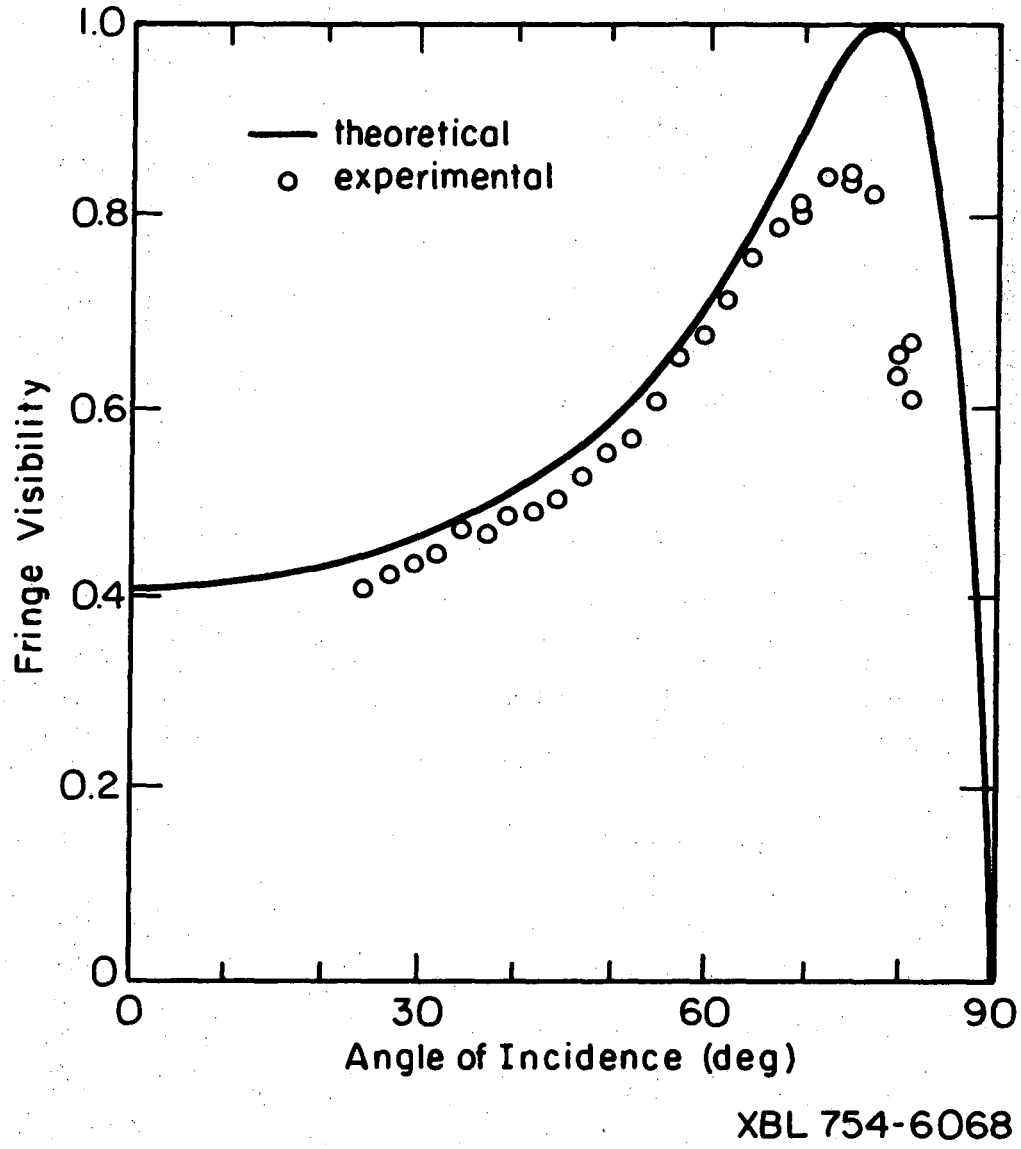

Fig. 71. Monochromatic (Michelson) fringe visibility as a function of angle of incidence for light reflected from a cryolite film (refractive index = 1.34) on a silicon substrate (refractive index = 4.14-i(0.03)). s-polarization.

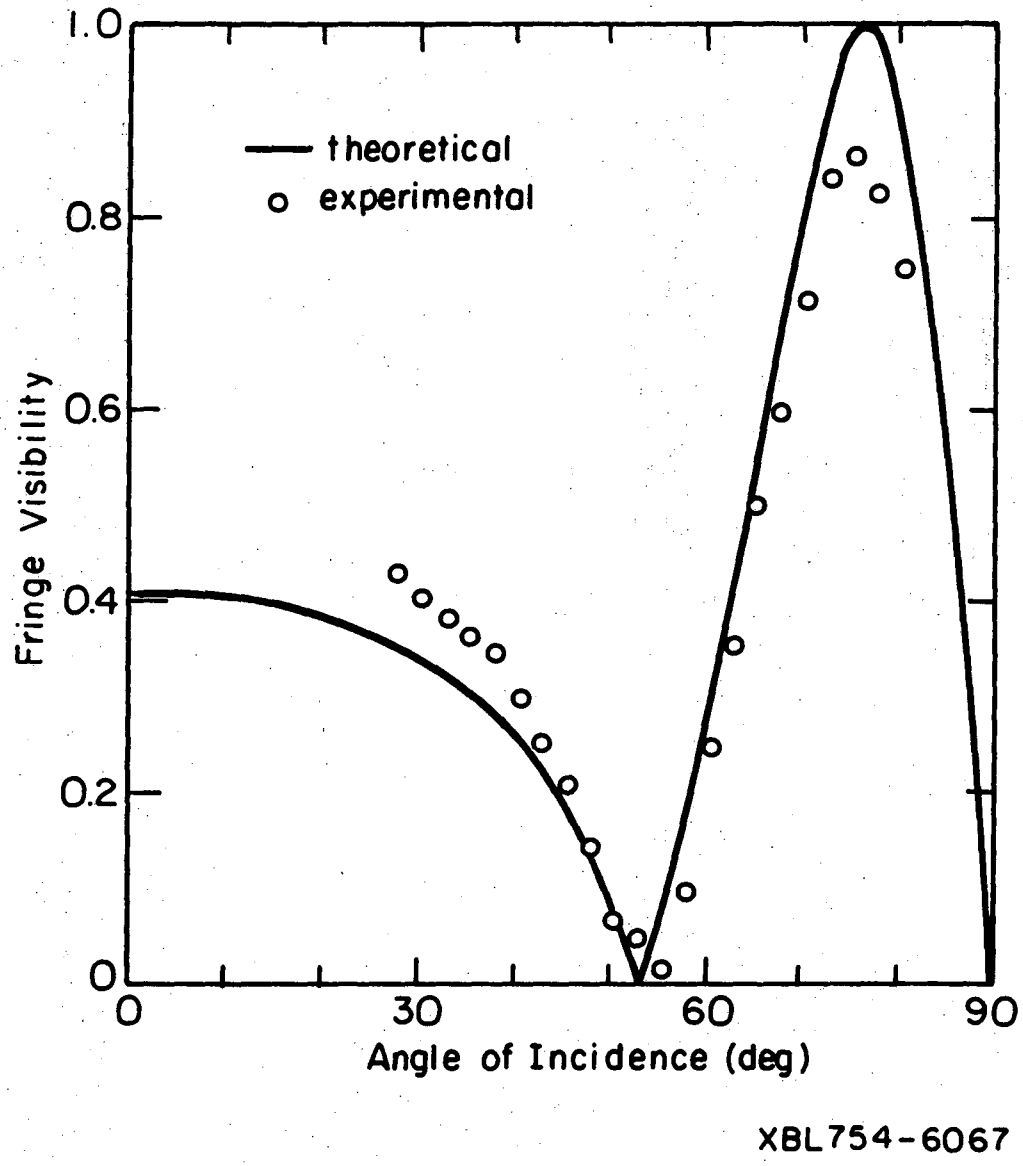

Fig. 72. See Fig. 71. p-polarization.

author and a second unbiased observer, who will be designated by his initials, CGS. The interference colors were judged either by direct viewing through a 35 mm camera on the optical bench or by examination of color photographs. Photographic color slides were viewed on a light table illuminated by a fluorescent lamp or projected onto a white surface with a tungsten lamp. Calculated values of the monochromatic optimum angle to the nearest degree for both polarizations were 73° and 88° for films 3 and 8, respectively. The author observed the optimum angle for film 3 to be 70° (s) and 74° (p) on the light table and 70° (s) and 72°, 74° (p) from the projected images on the white background. Optimum angles observed by CGS on the light table were 70° (s) and 74° (p) and on the optical bench were 67-1/2° (s) and 72-1/2° (p). All three sets of observations by the author showed that the optimum angle for film 8 was 87°. Observer CGS determined the optimum angles to be 87° (s and p) on the light table and 83° (s) and 84° (p) on the optical bench.

Observation of the optimum angle was not a simple matter. The interference colors of each film did not belong entirely to one interference order. Difficulty was encountered in distinguishing between the effects of color saturation and brightness both in direct visual observation on the optical bench and in exposures of the photographic slide film. The optimum angle was easiest to determine when the photographic slides were side by side on the light table. Two additional points should be mentioned. Daylight film was accidently used instead of film balanced for 3200°K tungsten light. Thus, the interference colors became more yellowish in the photographic exposures. The light

table employs a fluorescent lamp whose spectral composition is different from other white-light sources. These factors, which could affect the interpretation of colors, have been found to have little effect in determining the optimum angle.

Color purity and the change of color purity with angle of incidence is at least qualitatively the same as that determined through calculations. The interference colors of cryolite on aluminum were low in saturation even at the optimum angle, while those for cryolite on chromium were very much higher in saturation. Below Brewster's angle, the colors (film 3) were similar for the s and p polarizations. At Brewster's angle, interference colors were absent for the p polarization. As the angle of incidence increased further, the color saturation increased up to the optimum angle at which point the saturation began to decrease. Observer CGS commented that for film 3 the optimum angle was more difficult to judge on the optical bench for the s-polarization than for the p-polarization. Low values of the optimum angles observed on the optical bench by CGS (film 8) are left unexplained.

Overall, agreement between observed and calculated optimum angles was very good for both films 3 and 8. The monochromatic optimum angle was given as an upper limit to the optimum angle in white-light interference. The observed optimum angle was expected to be no more than 2° less than the calculated for the p-polarization. Nearly the same result was expected for the s-polarization, because the reflection coefficients for film 3 were fairly low and colors important in determining the optimum angle for film 8 were in the first color order.

D. Liquid Films

1. Experimental Cell

The experimental cell in which liquid films were formed on vertical metal surfaces was that used by Turney.[27] Side and top views are shown in Figs. 73a and 73b. The cell body was made of chemically inert polypropylene. Plate glass was used for cell windows even though it would be gradually etched by potassium hydroxide solutions. The cell consisted of a main chamber and a counter-electrode chamber. In the main chamber, the platinum electrode on which the film was to be observed was mounted in the vertical position. Light entering through one window could reflect from the electrode surface and propagate out through the other window. The platinum counter-electrode was located in a chamber connected to the main chamber by a narrow passage.

The gas phase in the cell consisted of nitrogen that had been saturated with water vapor by sparging through a solution with the same concentration as that used in the cell. Filling and draining the cell was accomplished by gravitational flow of the solution. For film formation, the liquid level in the cell was lowered until only the bottom 0.5 cm of the electrode remained immersed. Connections of the liquid and gas phases to the surrounding atmosphere were made with dust and carbon dioxide filters.

The electrode, which was 10.5 cm high by 4.0 cm wide, was constructed of 0.02 in. thick platinum sheet bonded to a 1/4 in. stainless steel backing. The platinum was optically polished. Except for a small area on top for electrical connection to a stainless steel pin (also used to clamp electrode in place), the stainless steel backing was coated with

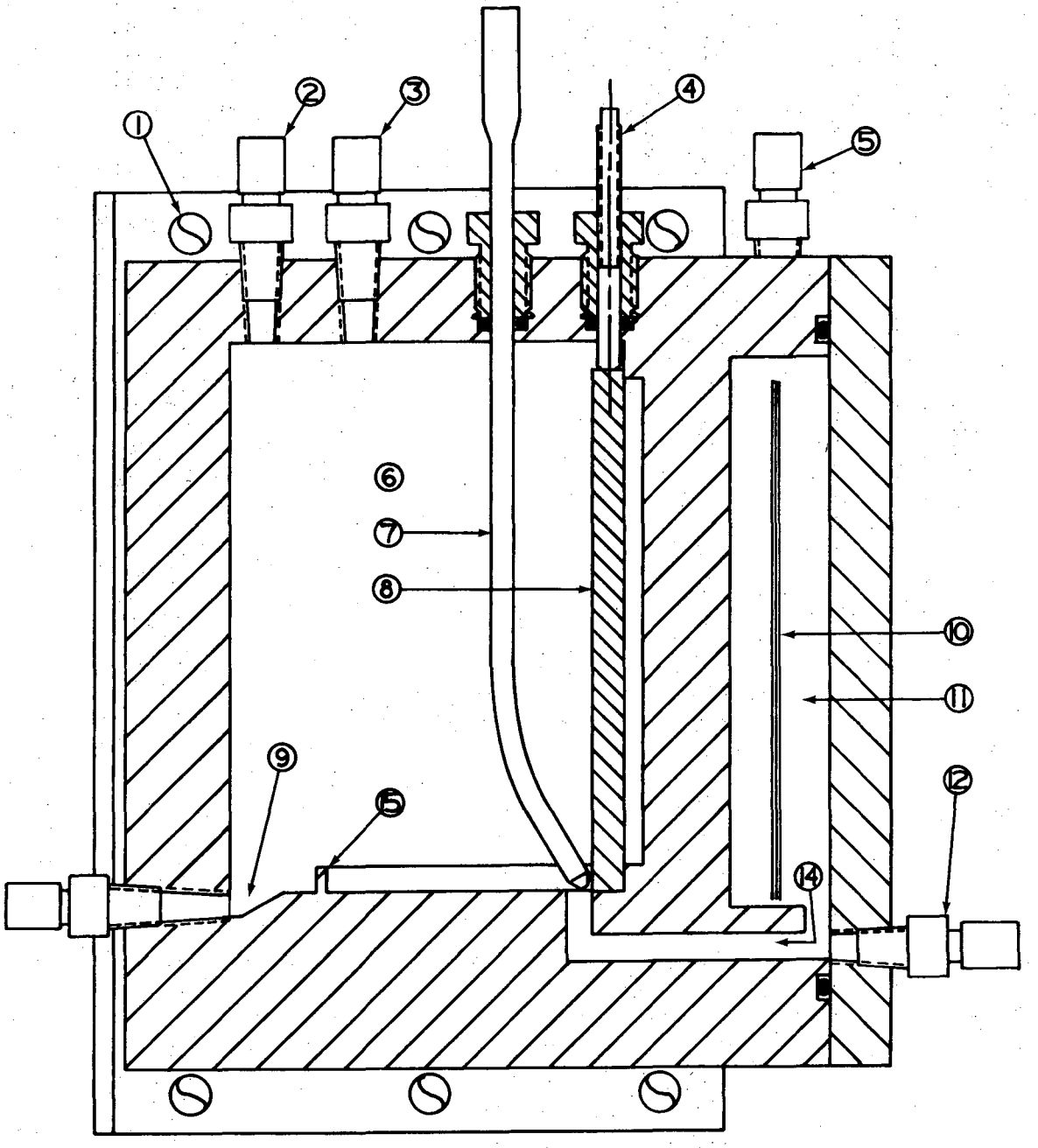

Fig. 73a. Side sectional view of liquid film cell.[27]

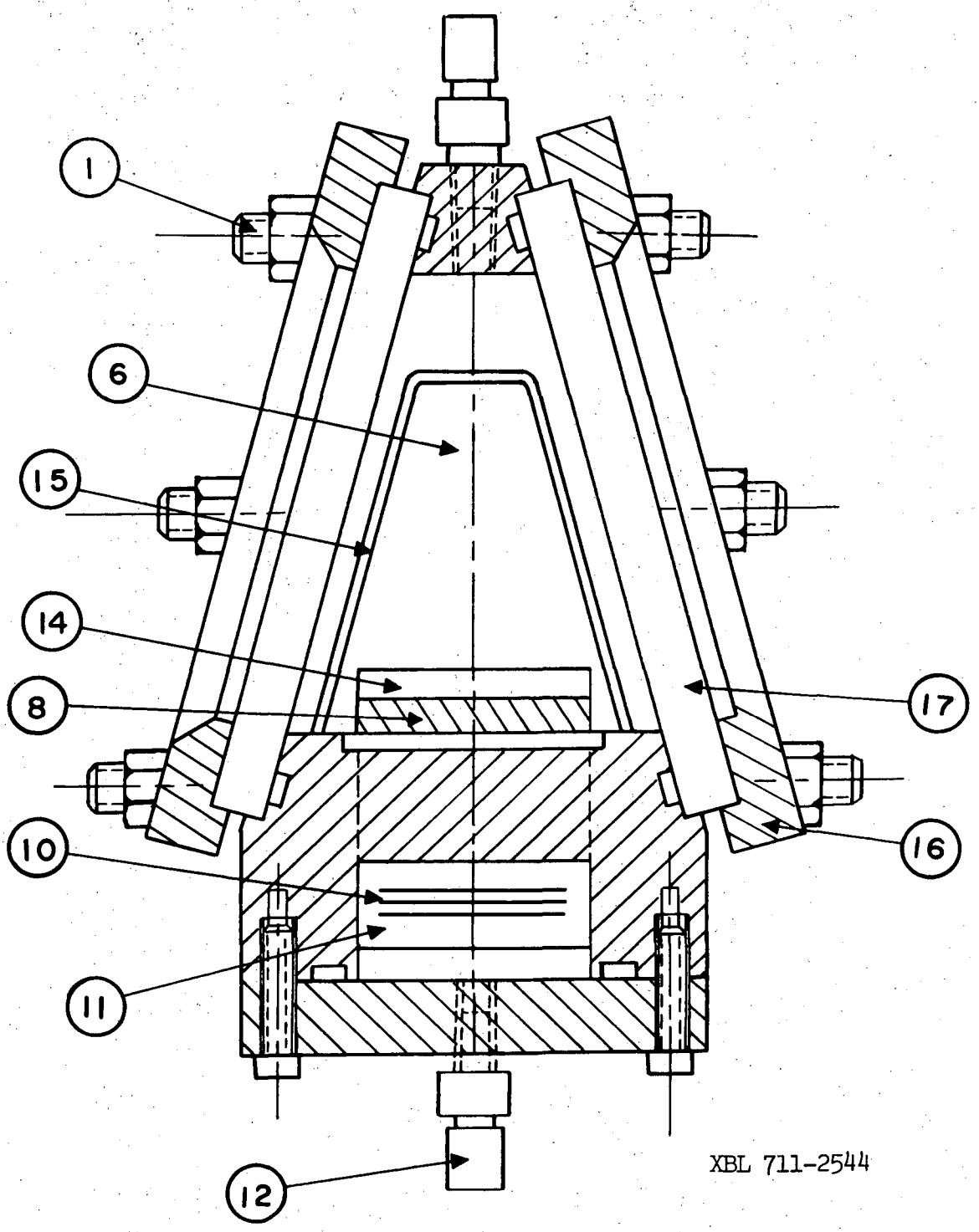

Fig. 73b. Top sectional view.[27] 1. Studs for clamping windows to cell body, 2. Gas inlet, 3. Gas outlet, 4. Clamp and electrical contact, 5. Gas outlet for counter-electrode chamber, 6. Main chamber, 7. Teflon capillary for reference electrode, 8. Optically polished platinum electrode, 9. Liquid drain, 10. Platinum counter-electrode, 11. Counter-electrode chamber, 12. Liquid inlet, 14. Passage between chambers, 15. Weir to establish liquid level, 16. Frame to hold windows, 17. Plate glass windows.

Kynar, a material that is highly resistant to most acid or base environments.

2. Chemical

The electrode surface had to be reasonably free of contamination for the formation of a smooth and continuous film. A preliminary cleaning removed dirt and oils from the cell interior and the electrode surface. Oxide layers, particles and remaining oils on the electrode were removed in the final cleaning by evolution of hydrogen until a continuous film could form on the surface.

Solutions were made form analytical reagent grade potassium hydroxide (Mallinckrodt) and distilled water. They were vacuum filtered through a succession of three Teflon filter membranes (Chemplast, Inc.), the finest of which had a mean pore size of 2-5 micron. A standard hydrochloric acid solution and phenolphthalein (indicator) were used in the titration to determine the concentration.

3. Film Drainage

Drainage of a Newtonian liquid from a vertical surface is governed by gravitational and viscous forces. The equation that gives the film thickness as a function of time and distance from the top of the electrode is[56]

$$y = \left(\frac{\mu}{\rho g}\right)^{1/2} \left(\frac{z}{t}\right)^{1/2} , \qquad (54)$$

where y = film thickness

z = distance from top of electrode

t = time

μ = viscosity

ρ = density

g = acceleration of gravity

Film profiles were determined by interpretation of interference colors resulting from the reflection of polarized light. The angles of incidence of the s and p components were 74° and 80°, respectively. These values are somewhat lower than the optimum angles of incidence. Interference color series used in this study for the thickness measurement of 0.46N and 9.2N aqueous potassium hydroxide films on platinum are closely represented by the series in Fig. 74, which are intermediate between the series calculated for each concentration.

At times, an observed series was difficult to judge. Observations would have been improved with higher angles of incidence and a different exposure of the photographic film. The overriding difficulty, though, was the unevenness of the color fringes both on a small scale and on a large scale. In the upper part of the electrode during drainage of the 9.2N film, the colors observed at the vertical center line of the surface were displaced downward from those on either side.

Measured and calculated thickness profiles are shown in Figs. 75 and 76. For the theoretical curves, viscosities for the 0.46N and 9.2N solutions were taken to be 1.0 cp and 3.3 cp, respectively.[57] The measured profiles are markedly different from the curves calculated through Eq. 54. Good agreement can be obtained, if one assumes a value for the

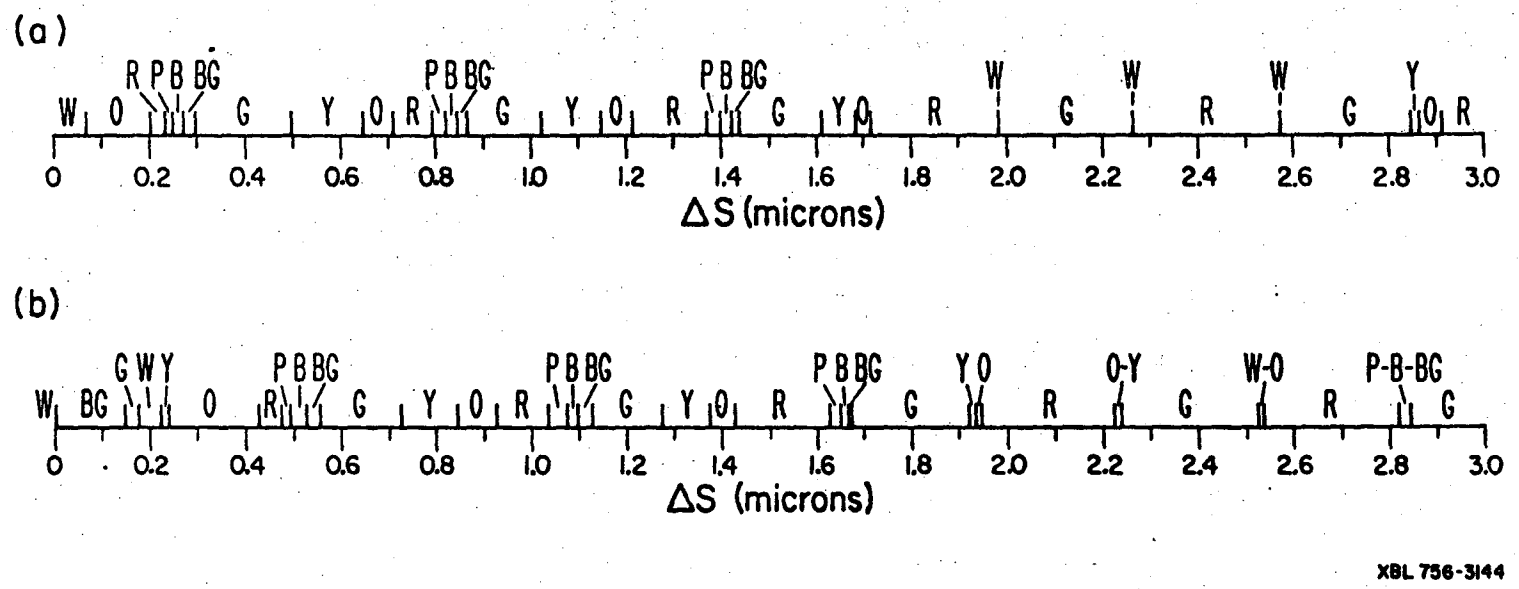

Fig. 74. Interference color series for aqueous potassium hydroxide solution on platinum substrate (refractive index = 1.93-i(3.75)).[28] (a) s-polarized light, $\delta_3-\delta_1 = 23°$, $r_1 = 0.82$, $r_3 = 0.56$. (b) p-polarized light, $\delta_3-\delta_1 = 227°$, $r_1 = 0.68$, $r_3 = 0.49$.

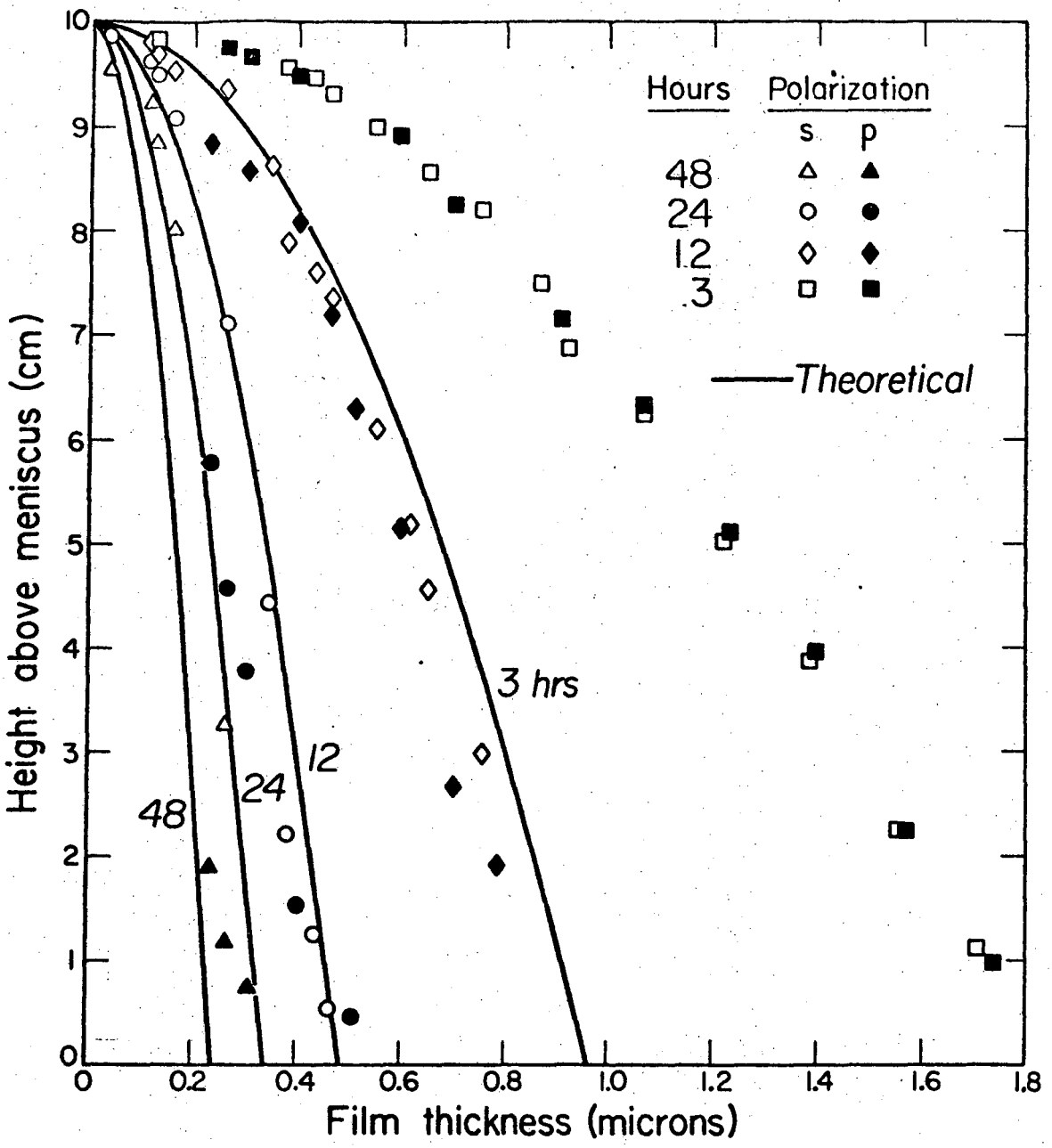

XBL 756-3147

Fig. 75. Film thickness profiles of 0.46N aqueous potassium hydroxide during drainage from a vertical platinum electrode. Colorimetric measurements.

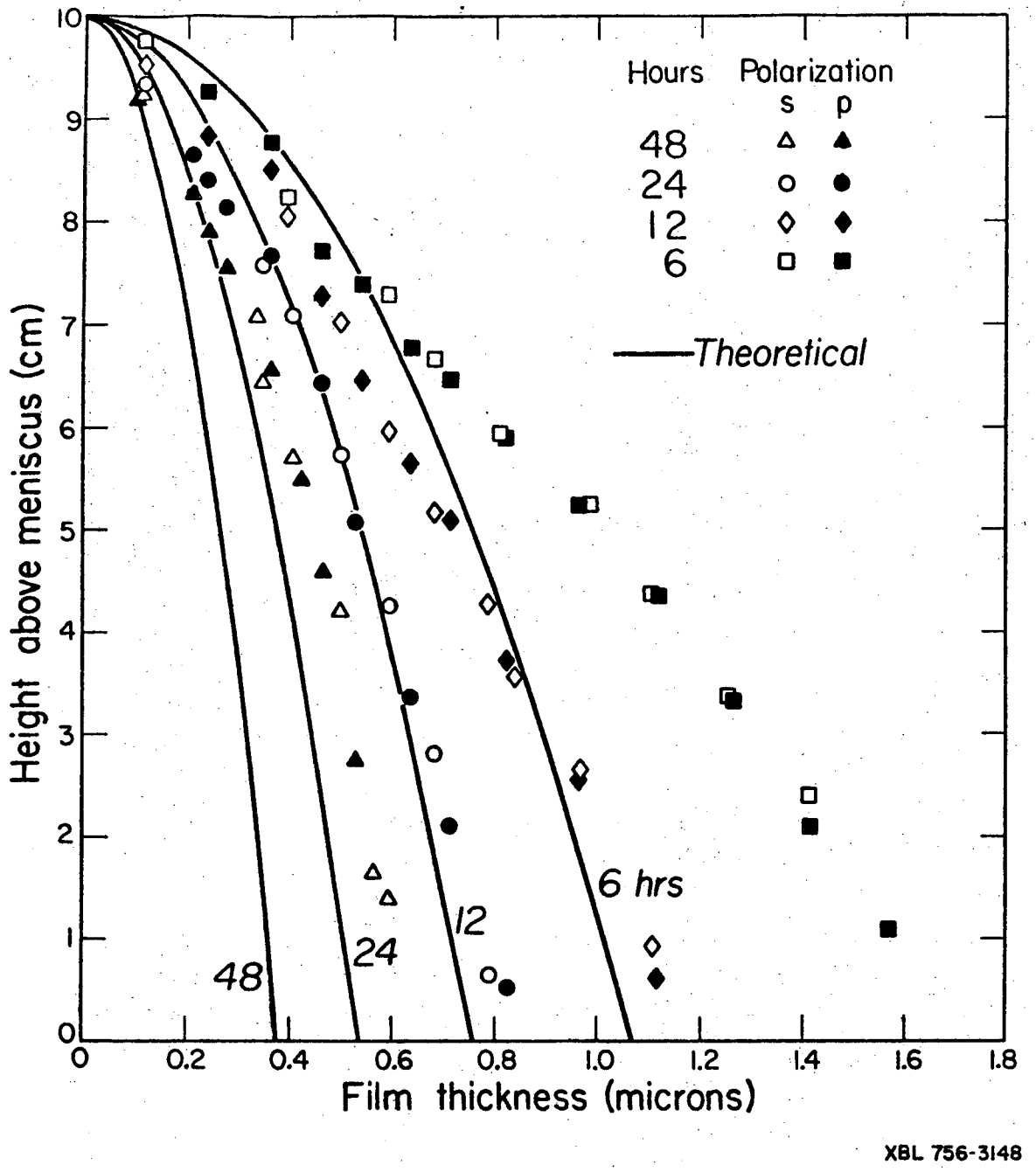

Fig. 76. Film thickness profiles of 9.2N aqueous potassium hydroxide during drainage from a vertical platinum electrode. Colorimetric measurements.

viscosity about twice that of the bulk solution. As opposed to previous studies,[20,27] film drainage continued at times much longer than 1 day.

V. DISCUSSION

The present work is an extension of studies conducted by Turney [27] and Brown.[30] The multiple-beam intensity equation employed by Turney in the computer programs CHROM and MBINF has been found to contain an error in the sign of the phase change, $\delta_3 - \delta_1$. As a result, film thicknesses derived from visual observations and spectroscopy of interference colors were incorrect. Because the phase change, $\delta_3 - \delta_1$, was defined differently in the program CHROM and in the color charts, Turney's color charts essentially agree with the present ones. Brown eliminated one of the compensating errors in using program CHROM and possibly introduced an additional error. The first error is mainly responsible for the difference in Brown's calculated color series from those of Turney.

Brown compared film thickness profiles derived from observations of interference colors with those determined by other measurement techniques. Close agreement, which would be expected at least among those measurements that depend on the optical constants of the film and substrate, was not always obtained. The error now found in the programs accounts for this disagreement. This interpretation agrees with the statement by Brown that the use of Turney's color charts leads to better agreement with independent thickness measurements than the use of his series.

Thickness profile measurements of an electrolyte film on a polished metal substrate have been hindered by local variations of thickness probably caused by particulate impurities. Preparations for future work with thin films should include efforts to obtain smooth films.

ACKNOWLEDGEMENTS

The author is especially grateful to Dr. Rolf H. Muller for giving me the opportunity to work and learn.

Walter Giba and other members of the Inorganic Materials Research Division have always been very helpful with their technical assistance.

Craig G. Smith gave his time in assisting with ellipsometric measurements and some observations of interference colors.

The excellent appearance of this manuscript has been contributed by Jean Wolslegel, who has done the typing, and Gloria Pelatowski, who has drawn most of the figures.

The author appreciates the time spent by Professor Scott Lynn and Professor Sumner P. Davis in reading the manuscript.

This work was performed under the auspices of the U. S. Energy Research and Development Administration.

APPENDICES. COMPUTER PROGRAMS FOR THIN DIELECTRIC FILMS ON METAL SURFACES

The appendices contain three computer programs written in Fortran IV language for use in thickness measurements with light interference in thin dielectric films on metal surfaces. The program "HUE" is used to interpret white-light interference fringes. "MBINT" (Multiple-Beam Intensity) is used to interpret either the spectral energy distribution of a sample of reflected light in white-light interference or monochromatic interference fringes. "VIS" calculates the variation of the Michelson fringe visibility with angle of incidence in order that one can determine the monochromatic optimum angle of incidence. Appendix I contains equations that are used in the programs. The three programs are presented in Appendices II through IV along with a description of program variables, inputs and samples of output. Two functions, REFRXC(SCALE, WAVLTH) and RIC(WAVLTH), that are common to the three programs are shown at the end of program "HUE". Standard Fortran functions and library subroutines are not described here. The programs were originally based on those written by Turney.[27] However, some corrections, revisions and additions have been made.

APPENDIX I. EQUATIONS IN PROGRAMS "HUE", "MBINT" AND "VIS"

Equations in all three programs are expressed in terms of real arithmetic. These equations have been explained in the text. Some of them have been modified, though, for a particular physical situation. The incident medium is taken to be a gas with a refractive index of one. Light incident onto the dielectric film at an angle, ϕ, is refracted in the film at an angle, ϕ'. The angle at which light is incident onto the metal substrate is ϕ'. Refractive indices of the metal substrate and the film in contact with the metal are $n_c = n - ik$ and n_1, respectively. Subscripts on variables refer either to an interface or to the two orthogonal polarizations of light, s and p. As in the text, the film-metal and gas-film interfaces are represented by the subscripts, 1 and 3, respectively.

The numbering system for equations in the appendix includes an "A" for "Appendix" in order to avoid confusion with the numbering system in the text. These numbers preceded by an "A" are used both in explanations of variables and in comment cards within the programs.

Refer to Eq. (8) in the text. The angle of refraction in the film is

$$\phi' = \sin^{-1}\left(\frac{1}{n_1}\sin\phi\right) \quad . \tag{A-1}$$

Refer to Eqs. (3) and (4) in the text. The amplitude reflection coefficients at the gas-film interface are

$$r_{3,s} = \left|\frac{\cos\phi - n_1\cos\phi'}{\cos\phi + n_1\cos\phi'}\right| \tag{A-2}$$

$$r_{3,p} = \left| \frac{n_1 \cos\phi - \cos\phi'}{n_1 \cos\phi + \cos\phi'} \right| \quad . \tag{A-3}$$

Refer to Eqs. (15) and (16) in the text. Intermediate variables in the equations for reflection at the film-metal interface are

$$A = \sqrt{\frac{1}{2n_1^2} \left[\sqrt{(n^2 - k^2 - n_1^2 \sin^2\phi')^2 + 4n^2k^2} + (n^2 - k^2 - n_1^2 \sin^2\phi') \right]} \tag{A-4}$$

$$B = \sqrt{\frac{1}{2n_1^2} \left[\sqrt{(n^2 - k^2 - n_1^2 \sin^2\phi')^2 + 4n^2k^2} - (n^2 - k^2 - n_1^2 \sin^2\phi') \right]} \quad . \tag{A-5}$$

Refer to Eqs. (13), (14) and (17) through (19) in the text. Reflection of light at the film-metal interface is described by the amplitude reflection coefficients and the phase changes.

$$r_{1,s} = \sqrt{\frac{A^2 + B^2 - 2A\cos\phi' + \cos^2\phi'}{A^2 + B^2 + 2A\cos\phi' + \cos^2\phi'}} \tag{A-6}$$

$$r_{1,p} = r_{1,s} \sqrt{\frac{A^2 + B^2 - 2A\sin\phi'\tan\phi' + \sin^2\phi'\tan^2\phi'}{A^2 + B^2 + 2A\sin\phi'\tan\phi' + \sin^2\phi'\tan^2\phi'}} \tag{A-7}$$

$$\delta_{1,s} = \tan^{-1}\left[\frac{-2B\cos\phi'}{A^2 + B^2 - \cos^2\phi'} \right] \tag{A-8}$$

$0 \leq \delta_{1,s} \leq \pi$ radians

$$\Delta = \tan^{-1}\left[\frac{-2B\sin\phi'\tan\phi'}{A^2 + B^2 - \sin^2\phi'\tan^2\phi'} \right] \tag{A-9}$$

$0 \leq \Delta \leq \pi$ radians

$$\delta_{1,p} = \Delta + \delta_{1,s} \tag{A-10}$$

Refer to Eqs. (21) and (22) in the text. The symbol for film thickness is "d". The optical path difference in the film is

$$\Delta S = 2n_1 d\cos\phi' \quad , \tag{A-11}$$

and the corresponding phase shift is

$$\delta = \frac{2\pi}{\lambda} \cdot \Delta S = \frac{4\pi n_1 d\cos\phi'}{\lambda} \quad . \tag{A-12}$$

Refer to Eq. (31) in the text. The multiple-beam intensity equation for light reflected from a dielectric film-covered metal surface is

$$I = \frac{r_3^2 + r_1^2 + 2r_3 r_1 \cos(\delta + \delta_3 - \delta_1)}{1 + r_3^2 r_1^2 + 2r_3 r_1 \cos(\delta + \delta_3 - \delta_1)} \quad . \tag{A-13}$$

Refer to Eq. (41a) through (41c) in the text. P_λ is the product of the spectral composition, P_A, of source A and I_λ in Eq. (A-13). The products, $P_A \cdot \bar{x}_\lambda$, $P_A \cdot \bar{y}_\lambda$ and $P_A \cdot \bar{z}_\lambda$ are called the distribution coefficients weighted by energy values of illuminant A.[38] X, Y and Z are the tristimulus values of light reflected from a film-covered metal surface.

$$X = \Sigma P_\lambda \cdot \bar{x}_\lambda = \Sigma I_\lambda \cdot P_A \cdot \bar{x}_\lambda \tag{A-14}$$

$$Y = \Sigma P_\lambda \cdot \bar{y}_\lambda = \Sigma I_\lambda \cdot P_A \cdot \bar{y}_\lambda \tag{A-15}$$

$$Z = \Sigma P_\lambda \cdot \bar{z}_\lambda = \Sigma I_\lambda \cdot P_A \cdot \bar{z}_\lambda \tag{A-16}$$

Refer to Eqs. (42a) through (42c) in the text. The chromaticity values of a sample of light are

$$x = \frac{X}{X + Y + Z} \tag{A-17}$$

$$y = \frac{Y}{X + Y + Z} \tag{A-18}$$

$$z = \frac{Z}{X + Y + Z} \tag{A-19}$$

Refer to Eqs. (36) through (38) in the text. The monochromatic interference minima and maxima and Michelson fringe visibility are

$$I_{min} = \left(\frac{r_1 - r_3}{1 - r_1 r_3}\right)^2 \tag{A-20}$$

$$I_{max} = \left(\frac{r_1 + r_3}{1 + r_1 r_3}\right)^2 \tag{A-21}$$

$$V = \frac{I_{max} - I_{min}}{I_{max} + I_{min}} \tag{A-22}$$

APPENDIX II. PROGRAM "HUE"

This program calculates the tristimulus values of light reflected from a dielectric film on a metal substrate for thicknesses that are varied by increments. The angles of incidence of the p and s polarizations can be the same or different and can be varied by any increment. In this program, the entire spectrum is involved at once and one can choose to include the variation of the optical constants with wavelength or use the values at an intermediate wavelength. A wavelength of 5892Å is a practical choice, because it is near the middle of the visible spectrum and data are generally available. The input for a variable refractive index of the film material is either the refractometer scale reading, from which the refractive index can be calculated (function REFRXC(SCALE,WAVLTH)), or the refractive index at several wavelengths through the visible spectrum. The film refractive index is fitted to a polynomial expression that is a function of wavelength. The library subroutine, LSQPOL, for a least squares polynomial fit is not shown. The variation of the film refractive index with wavelength is plotted by the Calcomp plotting facility. Coefficients calculated by LSQPOL are used in the function RIC(WAVLTH) to calculate the film refractive index at any wavelength in the visible spectrum. Optical constants of the substrate are fitted to a linear function of wavelength. Coefficients for the linear approximation are input parameters.

Equations that are employed in this program are Eqs. (A-1) through (A-19). Important features of the printed output are the chromaticity coordinates x and y, the tristimulus value Y and the name of the hue of the film as a function of film thickness. For the prediction of the

hue, the chromaticity diagram is divided into four quadrants with the achromatic point as the origin. The quadrant in which a point in the diagram lies and the slope of the line between this point and the achromatic point, together, locate the chromaticity coordinates, x and y, of the reflected light within a defined hue region. The graphical output is in the form of chromaticity coordinates as a function of film thickness contained within a chromaticity diagram with labeled hue regions on the boundaries. The labels are at the dominant wavelengths corresponding to the hue names of the regions.

The intersections of the straight dividing lines between hue regions with the boundaries of the diagram are those given by Kelley[40] for the 1931 C.I.E. chromaticity diagram. His dividing lines are curved and converge on the coordinates of source C. Straight lines that converge on the coordinates of source A are used in this program. A series of cards that assigns one of among seven hue names to a particular set of chromaticity coordinates is included in the program. These can be replaced by cards that assign one of among nineteen hue names to the chromaticity coordinates. The correspondence between these two sets of hue names is demonstrated in Table II. A set of cards could be included to define a white region, but was not. Colors of low purity can be found by inspecting the chromaticity coordinates. Also, colors of very low intensity are identified by a low tristimulus value Y.

Appendix II contains several parts. Program variables are listed first after Table II along with the corresponding symbols and descriptions. A description of the input is presented next with a list of the cards for the 1931 C.I.E. chromaticity diagram and source A that do not change

Table II. Correspondence between two sets of hue names.*
1931 C.I.E. Chromaticity Diagram

Hue Name	Dominant Wavelength (nm)	Chromaticity Coordinates x	y	Presently Used Photographic Hue Name
bluish purple	566c	0.189	0.012	
		0.167	0.008**	----------
purplish blue	454	0.1521	0.0217	
		0.136	0.041	
blue	476	0.1059	0.0960	blue
		0.082	0.163	
greenish blue	485	0.0687	0.2007	
		0.057	0.242**	----------
blue green	490	0.0454	0.2950	blue green
		0.031	0.364**	----------
bluish green	495	0.0235	0.4127	
		0.015	0.474	
green	508	0.0099	0.7120	green
		0.155	0.806	
yellowish green	545	0.2658	0.7243	
		0.367	0.630	
yellow green	565	0.4087	0.5896**	----------
		0.446	0.551	
greenish yellow	573	0.4649	0.5340	
		0.485	0.516	
yellow	578	0.4990	0.5000	yellow
		0.512	0.486	
yellowish orange	583	0.5319	0.4673**	----------
		0.557	0.443	
orange	592	0.5863	0.4131	orange
		0.615	0.385	
reddish orange	606	0.6517	0.3479**	----------
		0.692	0.308	
red	493c	0.700	0.250	red
		0.656	0.229	
purplish red	496c	0.602	0.203	
		0.548	0.179	
red purple	506c	0.457	0.136**	----------
		0.380	0.102	
reddish purple	545c	0.334	0.079	
		0.291	0.060	
purple	560c	0.253	0.042	purple
		0.209	0.022	
bluish purple	566c	0.189	0.012	
		0.167	0.008**	----------
purplish blue	454	0.1521	0.0217	

*The nineteen hue names and dominant wavelengths are those suggested by Kelley.[40] The 1931 C.I.E. chromaticity coordinates represent either the dominant wavelength or the intersection of dividing lines between hue regions with the boundary of the diagram. Wavelengths followed by a "c" are complementary wavelengths based on source C. The condensed list of hue names is for use in photographic work.

**Intersections of dividing lines between hue regions (condensed list) with the boundary of the diagram.

from program to program. The alternate set of cards that assigns one of among nineteen hue names to chromaticity coordinates appears just before the program. Table III, which appears after the program, differs from Table II in that the chromaticity coordinates are associated with the 1964 C.I.E. chromaticity diagram. Two sets of cards, each of which assigns a hue name to chromaticity coordinates, are also shown. One assigns one of among seven hue names and the other assigns one of among nineteen. They must be used along with the data cards for the 1964 C.I.E. diagram and source A that do not vary from program to program. These cards are listed next. The distribution coefficients, XBAR(I), YBAR(I) and ZBAR(I), were calculated from two tables in The Measurement of Colour[38] of the energy distribution of source A and the distribution coefficients for an equal-energy stimulus in 50Å wavelength increments. Values of XBAR(I), YBAR(I) and ZBAR(I) were adjusted in order that the tristimulus value Y for source A equalled 100.0. The cards and the data for the 1964 C.I.E. chromaticity diagram have not been used to obtain color series in this study. A sample of the printed output and the graphical output for the 1931 C.I.E. chromaticity diagram is given last.

Variables in Program "HUE"

Variable	Symbol	Description
A,ASQ B,BSQ	A, A^2 B, B^2	Intermediate variables to calculate amplitude reflection coefficients and phase changes (interface 1), Eqs. (A-4) and (A-5).
AMN	ϕ(deg)	Initial angle of incidence.

Variable	Symbol	Description
BOUNDX(N),BOUNDY(N)	x,y	Chromaticity coordinates on boundary of chromaticity diagram that are the dividing points between hue regions for graphical output. Refer to Tables II and III and data cards for list.
BORDX(N),BORDY(N)	x,y	Chromaticity coordinates of dominant wavelengths corresponding to hue names. Hue names are written at these points in the graphical output. Refer to Tables II and III and data cards for list.
CAPX	X	Tristimulus value, Eq. (A-14).
CAPY	Y	Tristimulus value, Eq. (A-15).
CAPZ	Z	Tristimulus value, Eq. (A-16).
CK1,CK2 CN1,CN2		$k = CK1 + CK2(\lambda - 3800)$. $n = CN1 + CN2(\lambda - 3800)$. Coefficients for a linear approximation of the complex refractive index of the substrate, $n_c = n - ik$.
COLOR1(N),COLOR2(N)		Hue names for regions of the chromaticity diagram. Refer to Tables II and III and data cards for list.
CROPOX(N),CROPOY(N)	x,y	Chromaticity coordinates of spectrum locus to draw boundary of diagram for graphical output. Refer to data cards for list.
CX	$\cos\phi'$	COS(PHIPR(J,M))
DDEL	Δ	Relative phase change, $\delta_{1,p} - \delta_{1,s}$ (interface 1), Eq. (A-9).
DEL(J,1),DEL(J,2)	$\delta_{1,s}, \delta_{1,p}$ (rad)	Phase change for s and p polarizations (interface 1), Eqs. (A-8) and (A-10).
DELD(J,1),DELD(J,2)	$\delta_{3,s}, \delta_{3,p}$ (rad)	Phase change for s and p polarizations (interface 3).

Variable	Symbol	Description
DELT	δ(rad)	Phase change associated with an optical path difference in the film, Eq. (A-12).
FILM1,FILM2 FILM3,FILM4		Name of film to appear in output.
INT	I	Relative intensity of reflected light in multiple-beam interference, Eq. (A-13).
LAMBDA	λ(Å)	Wavelength that is varied in 50Å increments.
LOWX(L)	x	Chromaticity value, Eq. (A-17).
LOWY(L)	y	Chromaticity value, Eq. (A-18).
LOWZ	z	Chromaticity value, Eq. (A-19).
NTOT		Number of angles of incidence (one more than the number of increments added to initial angle of incidence).
PHI(1),PHI(2)	ϕ(rad)	Angle of incidence for s and p polarizations (interface 3).
PHID(1),PHID(2)	ϕ(deg)	Angle of incidence for s and p polarizations (interface 3).
PHIPR(J,1) PHIPR(J,2)	ϕ'(rad)	Angle of refraction for s and p polarizations (interface 3), Eq. (A-1). Also, angle of incidence (interface 1).
R(J,1),R(J,2)	$r_{1,s}$,$r_{1,p}$	Amplitude reflection coefficient for s and p polarizations (interface 1), Eqs. (A-6) and (A-7).
RSQ(J,1),RSQ(J,2)	$r^2_{1,s}$,$r^2_{1,p}$	Refer to R(J,1) and R(J,2).
RI(N)	n_1	Refractive index of dielectric film at a specified wavelength in the input.

Variable	Symbol	Description
RL(J,1),RL(J,2)	$r_{3,s}, r_{3,p}$	Amplitude reflection coefficient for s and p polarizations (interface 3), Eqs. (A-2) and (A-3).
RSQL(J,1),RSQL(J,2)	$r^2_{3,s}, r^2_{3,p}$	Refer to RL(J,1) and RL(J,2).
SBSTRA1,SBSTRA2		Name of substrate to appear in output.
SCALE(N)		Refractometer scale reading of liquid film material (Bausch and Lomb precision refractometer with prism, 749-1).
SEP	$\Delta\phi$(deg)	Separation between angles of incidence for s and p polarizations.
SLOPE		Slope of line from achromatic point to chromaticity coordinates of light reflected from a film-covered substrate.
SOURCE1,SOURCE2		Name of light source to be printed in output.
STEPS	$\Delta\phi$(deg)	Increment of change of angle of incidence.
SX	$\sin\phi'$	SIN(PHIPR(J,M))
THK	d(Å)	Film thickness.
THKINC	d(Å)	Increment of change of film thickness.
TMN	d(Å)	Initial film thickness.
TMX	d(Å)	Final film thickness.
TNA(J),TN TKA(J),TK	n k	Real and imaginary parts of the complex refractive index of the metal substrate, $n_c = n - ik$.
TX	$\tan\phi'$	SX/CX

Variable	Symbol	Description
WAVLTH(N)	$\lambda(\text{Å})$	Wavelength associated with the variation of the refractive index of the film material with wavelength in the input.
XBAR(I),YBAR(I), ZBAR(I)	$P_A \cdot \bar{x}_\lambda, P_A \cdot \bar{y}_\lambda, P_A \cdot \bar{z}_\lambda$	Distribution coefficients weighted by energy values of source A. Refer to data cards for list.

Input for Program "HUE"

Explanations of these input variables have been given in the list of variables. Data cards 8 through 211 do not vary from program to program. These cards for the 1931 C.I.E. chromaticity diagram and source A are presented on the pages immediately following.

Card	Variable	Units	Column and Format
1	SBSTRA1,SBSTRA2		1-20,2A10
2	FILM1,FILM2, FILM3,FILM4		1-40,4A10
3	CN1	Dimensionless	1-10,F10.7
	CN2	1/Å	11-20,F10.7
	CK1	Dimensionless	21-30,F10.7
	CK2	1/Å	31-40,F10.7
4	AMN	Degrees	1-10,F10.2
	STEPS	Degrees	11-20,F10.2
	NTOT		21-23,I3*
5	SOURCE1,SOURCE2		1-20,2A10
6	TMN	Å	1-10,F10.1
	TMX	Å	11-20,F10.1

*Integers must be written at the far right of the field.

Card	Variable	Units	Column and Format
	THKINC	Å	21-30,F10.1
7	SEP	Degrees	1-10,F10.6
8	XBAR(I)	Dimensionless	1-10,F10.4
	YBAR(I)	Dimensionless	11-20,F10.4
	ZBAR(I)	Dimensionless	21-30,F10.4
9-88	Same as Card 8		
89	COLOR1(N),COLOR2(N)		1-20,2A10
90-107	Same as card 89		
108	BORDX(N)	Dimensionless	1-10,F10.4
	BORDY(N)	Dimensionless	11-20,F10.4
109-126	Same as Card 108		
127	CROPOX(N)	Dimensionless	1-10,F10.4
	CROPOY(N)	Dimensionless	11-20,F10.4
128-192	Same as Card 127		
193	BOUNDX(N)	Dimensionless	1-10,F10.4
	BOUNDY(N)	Dimensionless	11-20,F10.4
194-211	Same as card 193		
212*	WAVLTH(N)	Å	1-5,F5.0
	RI(N)	Dimensionless	6-15,F10.5
	SCALE(N)	Dimensionless	16-25,F10.5
213-225	Same as card 212		

*From one to fourteen of these cards may be used. If one is used, then the value of RI(1) is an average value to be used with every wavelength in the program. If more than one card is used, it is recommended that as many as possible over the visible range from 3800 to 7800Å be in the input for the fit of the refractive index of the film to a polynomial expression. If the refractive index is to be calculated from the refractometer scale reading with the function, REFRXC(SCALE,WAVLTH), then RI(N) = 0.0. If fewer than fourteen cards are used, then the last one should have WAVLTH(N) = 0000.

THESE ARE THE DATA CARDS FOR THE 1931 C.I.E. CHROMATICITY DIAGRAM THAT DO NOT VARY FROM PROGRAM TO PROGRAM. (CARDS 8-211)

	COLUMNS 1-10	11-20	21-30
CARD 8	0.0006	0.0000	0.0029
	0.0011	0.0000	0.0053
XBAR(I), YBAR(I)	0.0024	0.0000	0.0113
AND ZBAR(I)	0.0047	0.0001	0.0224
	0.0097	0.0003	0.0463
	0.0174	0.0004	0.0825
	0.0356	0.0010	0.1699
	0.0694	0.0020	0.3319
	0.1308	0.0039	0.6283
	0.2269	0.0077	1.0974
	0.3246	0.0133	1.5840
	0.4055	0.0207	2.0036
	0.4632	0.0306	2.3236
	0.4976	0.0426	2.5484
	0.5155	0.0583	2.7173
	0.5230	0.0788	2.8621
	0.5097	0.1052	2.9254
	0.4690	0.1380	2.8539
	0.3882	0.1808	2.5581
	0.2958	0.2375	2.1979
	0.2128	0.3108	1.8179
	0.1372	0.4004	1.4575
	0.0799	0.5196	1.1622
	0.0387	0.6813	0.9308
	0.0136	0.8960	0.7545
	0.0070	1.1876	0.6191
	0.0285	1.5398	0.4843
	0.0934	1.9518	0.3585
	0.2127	2.3855	0.2627
	0.3849	2.7859	0.2012
	0.6069	3.1509	0.1547
	0.8631	3.4987	0.1140
	1.1567	3.7999	0.0809
	1.4904	4.0618	0.0555
	1.8660	4.2841	0.0375
	2.2887	4.4701	0.0255
	2.7550	4.6110	0.0181
	3.2564	4.6974	0.0130
	3.7853	4.7285	0.0104
	4.3259	4.7002	0.0092
	4.8594	4.6139	0.0090
	5.3549	4.4668	0.0077
	5.7896	4.2704	0.0062
	6.1403	4.0379	0.0058
	6.3518	3.7733	0.0048
	6.4299	3.4855	0.0037
	6.3346	3.1780	0.0019
	6.0877	2.8622	0.0013
	5.6365	2.5358	0.0013
	5.1267	2.1901	0.0007
	4.4902	1.8523	0.0000
	3.8779	1.5529	0.0000
	3.2791	1.2812	0.0000

		COLUMNS		
		1-10	11-20	21-30
		2.7004	1.0344	0.0000
		2.1681	0.8183	0.0000
		1.7078	0.6372	0.0000
		1.3141	0.4861	0.0000
		0.9850	0.3625	0.0000
		0.7241	0.2651	0.0000
		0.5368	0.1958	0.0000
		0.4022	0.1461	0.0000
		0.2877	0.1041	0.0000
		0.2019	0.0729	0.0000
		0.1429	0.0515	0.0000
		0.1047	0.0377	0.0000
		0.0756	0.0271	0.0000
		0.0549	0.0199	0.0000
		0.0394	0.0144	0.0000
		0.0283	0.0097	0.0000
		0.0198	0.0069	0.0000
		0.0140	0.0050	0.0000
		0.0101	0.0041	0.0000
		0.0072	0.0031	0.0000
		0.0052	0.0021	0.0000
		0.0032	0.0010	0.0000
		0.0021	0.0010	0.0000
		0.0021	0.0010	0.0000
		0.0011	0.0000	0.0000
		0.0011	0.0000	0.0000
		0.0000	0.0000	0.0000
		0.0000	0.0000	0.0000
CARD 89		RED		
		REDDISH ORANGE		
COLOR1(N), COLOR2(N)		ORANGE		
		YELLOWISH ORANGE		
		YELLOW		
		GREENISH YELLOW		
		YELLOW GREEN		
		YELLOWISH GREEN		
		GREEN		
		BLUISH GREEN		
		BLUE GREEN		
		GREENISH BLUE		
		BLUE		
		PURPLISH BLUE		
		BLUISH PURPLE		
		PURPLE		
		REDDISH PURPLE		
		RED PURPLE		
		PURPLISH RED		
CARD 108		0.700	0.250	
		0.6917	0.3479	
BORDX(N), BORDY(N)		0.5863	0.4131	
		0.5319	0.4673	
		0.4990	0.5000	
		0.4649	0.5340	
		0.4087	0.5896	
		0.2658	0.7243	
		0.0099	0.7120	

CARD 127

CROPOX(N), CROPCY(N)

COLUMNS 1-10	COLUMNS 11-20
0.0235	0.4127
0.0454	0.2950
0.0687	0.2007
0.1059	0.0960
0.1521	0.0217
0.189	0.012
0.253	0.042
0.334	0.079
0.457	0.136
0.602	0.203
0.1741	0.0050
0.1740	0.0050
0.1738	0.0049
0.1736	0.0049
0.1733	0.0048
0.1730	0.0048
0.1726	0.0048
0.1721	0.0048
0.1714	0.0051
0.1703	0.0058
0.1689	0.0069
0.1669	0.0086
0.1644	0.0109
0.1611	0.0138
0.1566	0.0177
0.1510	0.0227
0.1440	0.0297
0.1355	0.0399
0.1241	0.0578
0.1096	0.0868
0.0913	0.1327
0.0687	0.2007
0.0454	0.2950
0.0235	0.4127
0.0082	0.5384
0.0039	0.6548
0.0139	0.7502
0.0389	0.8120
0.0743	0.8338
0.1142	0.8262
0.1547	0.8059
0.1929	0.7816
0.2296	0.7543
0.2658	0.7243
0.3016	0.6923
0.3373	0.6589
0.3731	0.6245
0.4087	0.5896
0.4441	0.5547
0.4788	0.5202
0.5125	0.4866
0.5448	0.4544
0.5752	0.4242
0.6029	0.3965
0.6270	0.3725
0.6482	0.3514

	COLUMNS 1-10	11-20
	0.6658	0.3340
	0.6801	0.3197
	0.6915	0.3083
	0.7006	0.2993
	0.7079	0.2920
	0.7140	0.2859
	0.7190	0.2809
	0.7230	0.2770
	0.7260	0.2740
	0.7283	0.2717
	0.7300	0.2700
	0.7311	0.2689
	0.7320	0.2680
	0.7327	0.2673
	0.7334	0.2666
	0.7340	0.2660
	0.7344	0.2656
	0.7346	0.2654
	0.7347	0.2653
	0.1741	0.0050
CARD 193	0.015	0.474
	0.155	0.806
BOUNDX(N), BOUNDY(N)	0.367	0.630
	0.446	0.551
	0.485	0.516
	0.512	0.486
	0.557	0.443
	0.615	0.385
	0.692	0.308
	0.656	0.229
	0.548	0.179
	0.380	0.102
	0.291	0.060
	0.209	0.022
	0.167	0.008
	0.136	0.041
	0.082	0.163
	0.057	0.242
	0.031	0.364

```
C  THESE ARE CARDS FOR THE 1931 C.I.E. CHROMATICITY DIAGRAM TO DETER-
C  MINE THE HUE OF LIGHT FROM THE CHROMATICITY COORDINATES.  THEY
C  MUST BE USED ALONG WITH THE DATA CARDS FOR THE 1931 C.I.E. CHROMA-
C  TICITY DIAGRAM AND SOURCE A.  THEY REPLACE THE SECTION PRECEDING
C  THE CARD WITH REFERENCE NUMBER 211 IN THE PROGRAM.  THE DIAGRAM IS
C  DIVIDED INTO 19 HUE REGIONS.

      SLOPE=(LOWY(L)-0.40745)/(LOWX(L)-0.44757)
      IF((LOWX(L).LT.0.44757).OR.(LOWY(L).LT.0.40745)) GO TO 1200
      IF(SLOPE.LE.0.325) PRINT 919,THK,CAPX,CAPY,CAPZ,LOWX(L),LOWY(L),LO
     XWZ,O
      IF((SLOPE.GE.0.325).AND.(SLOPE.LE.1.220)) PRINT 919,THK,CAPX,CAPY,
     XCAPZ,LOWX(L),LOWY(L),LOWZ,YHO
      IF((SLOPE.GE.1.220).AND.(SLOPE.LE.2.904)) PRINT 919,THK,CAPX,CAPY,
     XCAPZ,LOWX(L),LOWY(L),LOWZ,YELLOW
      IF(SLOPE.GE.2.904) PRINT 919,THK,CAPX,CAPY,CAPZ,LOWX(L),LOWY(L),LO
     XWZ,GHY
      GO TO 211
1200  IF((LOWX(L).GT.0.44757).OR.(LOWY(L).LT.0.40745)) GO TO 1300
      IF(SLOPE.LE.-89.75) PRINT 919,THK,CAPX,CAPY,CAPZ,LOWX(L),LOWY(L),L
     XOWZ,GHY
      IF((SLOPE.GE.-89.75).AND.(SLOPE.LE.-2.762)) PRINT 919,THK,CAPX,CAP
     XXY,CAPZ,LOWX(L),LOWY(L),LOWZ,YG
      IF((SLOPE.GE.-2.762).AND.(SLOPE.LE.-1.362)) PRINT 919,THK,CAPX,CAP
     XXY,CAPZ,LOWX(L),LOWY(L),LOWZ,YHG
      IF((SLOPE.GE.-1.362).AND.(SLOPE.LE.-0.154)) PRINT 919,THK,CAPX,CAP
     XXY,CAPZ,LOWX(L),LOWY(L),LOWZ,G
      IF(SLOPE.GE.-0.154) PRINT 919,THK,CAPX,CAPY,CAPZ,LOWX(L),LOWY(L),L
     XOWZ,BHG
      GO TO 211
1300  IF((LOWX(L).GT.0.44757).OR.(LOWY(L).GT.0.40745)) GO TO 1400
      IF(SLOPE.LE.0.104) PRINT 919,THK,CAPX,CAPY,CAPZ,LOWX(L),LOWY(L),LO
     XWZ,BHG
      IF((SLOPE.GE.0.104).AND.(SLOPE.LE.0.423)) PRINT 919,THK,CAPX,CAPY,
     XCAPZ,LOWX(L),LOWY(L),LOWZ,BG
      IF((SLOPE.GE.0.423).AND.(SLOPE.LE.0.668)) PRINT 919,THK,CAPX,CAPY,
     XCAPZ,LOWX(L),LOWY(L),LOWZ,GHB
      IF((SLOPE.GE.0.668).AND.(SLOPE.LE.1.176)) PRINT 919,THK,CAPX,CAPY,
     XCAPZ,LOWX(L),LOWY(L),LOWZ,BLUE
      IF((SLOPE.GE.1.176).AND.(SLOPE.LE.1.423)) PRINT 919,THK,CAPX,CAPY,
     XCAPZ,LOWX(L),LOWY(L),LOWZ,PHB
      IF((SLOPE.GE.1.423).AND.(SLOPE.LE.1.615)) PRINT 919,THK,CAPX,CAPY,
     XCAPZ,LOWX(L),LOWY(L),LOWZ,BHP
      IF((SLOPE.GE.1.615).AND.(SLOPE.LE.2.218)) PRINT 919,THK,CAPX,CAPY,
     XCAPZ,LOWX(L),LOWY(L),LOWZ,P
      IF((SLOPE.GE.2.218).AND.(SLOPE.LE.4.518)) PRINT 919,THK,CAPX,CAPY,
     XCAPZ,LOWX(L),LOWY(L),LOWZ,RHP
      IF(SLOPE.GE.4.518) PRINT 919,THK,CAPX,CAPY,CAPZ,LOWX(L),LOWY(L),LO
     XWZ,RP
      GO TO 211
1400  IF(SLOPE.LE.-2.275) PRINT 919,THK,CAPX,CAPY,CAPZ,LOWX(L),LOWY(L),L
     XOWZ,RP
      IF((SLOPE.GE.-2.275).AND.(SLOPE.LE.-0.856)) PRINT 919,THK,CAPX,CAP
     XXY,CAPZ,LOWX(L),LOWY(L),LOWZ,PHR
      IF((SLOPE.GE.-0.856).AND.(SLOPE.LE.-0.407)) PRINT 919,THK,CAPX,CAP
     XXY,CAPZ,LOWX(L),LOWY(L),LOWZ,RED
      IF((SLOPE.GE.-0.407).AND.(SLOPE.LE.-0.134)) PRINT 919,THK,CAPX,CAP
     XXY,CAPZ,LOWX(L),LOWY(L),LOWZ,RHO
      IF(SLOPE.GE.-0.134) PRINT 919,THK,CAPX,CAPY,CAPZ,LOWX(L),LOWY(L),L
     XOWZ,O
```

```
      PROGRAM HUE (INPUT,OUTPUT,TAPE 98, PLOT, TAPE 99=PLOT)
C
C
C     THIS PROGRAM CALCULATES THE INTENSITY OF LIGHT REFLECTED FROM A
C     DIELECTRIC FILM(NON-ABSORBING) COVERING A METAL(ABSORBING) SUR-
C     FACE.  THE INTENSITY OF REFLECTED LIGHT IS A PERIODIC FUNCTION OF
C     FILM THICKNESS AT EACH WAVELENGTH AND ANGLE OF INCIDENCE.  FOR A
C     SPECIFIED ANGLE OF INCIDENCE AND A WHITE-LIGHT SOURCE, THE SPECT-
C     RAL INTENSITY DISTRIBUTION AT EACH FILM THICKNESS IS COUPLED WITH
C     THE C.I.E. TRISTIMULUS COLOR SYSTEM TO DETERMINE THE COLOR OF THE
C     REFLECTED LIGHT.  THE VARIATION OF OPTICAL CONSTANTS OF BOTH THE
C     FILM AND SUBSTRATE WITH WAVELENGTH IS INCLUDED IN THE CALCULATIONS.
C
C
      REAL PHID(2),PHI(2),PHIPR(81,2),TNA(81),TKA(81),RSQ(81,2),R(81,2),
     XDEL(81,2),RL(81,2),INT,RSQL(81,2),DELD(81,2),LAMBDA,XBAR(81),
     XYBAR(81),ZBAR(81),LOWX(1000),LOWY(1000),LOWZ
      INTEGER BHP(2),PHB(2),BLUE(1),GHB(2),BG(1),BHG(2),G(1),YHG(2),YG(2
     X),GHY(2),YELLOW(1),YHO(2),O(1),RHO(2),RED(1),PHR(2),RP(1),RHP(2),
     XP(1)
      DIMENSION WAVLTH(50),RI(50),W(50),RESID(50),S(1),AI(20,6),BI(20),
     XTWVLTH(52),TRI(52),SCALE(50)
      DIMENSION CROPOX(66),CROPOY(66),BOUNDX(19),BOUNDY(19),COLOR1(19),
     XCOLOR2(19),BORDX(19),BORDY(19)
      COMMON/RICOM/ BI, NO
      COMMON/CCPOOL/XMIN,XMAX,YMIN,YMAX,CCXMIN,CCXMAX,CCYMIN,CCYMAX
      COMMON/CCFACT/FACTOR
      DATA BHP(1),BHP(2)/13HBLUISH PURPLE/
      DATA PHB(1),PHB(2)/13HPURPLISH BLUE/
      DATA BLUE(1)/4HBLUE/
      DATA GHB(1),GHB(2)/13HGREENISH BLUE/
      DATA BG(1)/10HBLUE GREEN/
      DATA BHG(1),BHG(2)/12HBLUISH GREEN/
      DATA G(1)/5HGREEN/
      DATA YHG(1),YHG(2)/15HYELLOWISH GREEN/
      DATA YG(1),YG(2)/12HYELLOW GREEN/
      DATA GHY(1),GHY(2)/15HGREENISH YELLOW/
      DATA YELLOW(1)/6HYELLOW/
      DATA YHO(1),YHO(2)/16HYELLOWISH ORANGE/
      DATA O(1)/6HORANGE/
      DATA RHO(1),RHO(2)/14HREDDISH ORANGE/
      DATA RED(1)/3HRED/
      DATA PHR(1),PHR(2)/12HPURPLISH RED/
      DATA RP(1)/10HRED PURPLE/
      DATA RHP(1),RHP(2)/14HREDDISH PURPLE/
      DATA P(1)/6HPURPLE/
    1 FORMAT(2A10)
    2 FORMAT(4A10)
    3 FORMAT(4F10.7)
    4 FORMAT(F10.6)
    5 FORMAT(2A10)
    6 FORMAT(3F10.4)
   12 FORMAT(10X,2A10,//)
   19 FORMAT(2F10.2,I3)
   22 FORMAT(3F10.1)
    8 FORMAT(10X,*S POLARIZATION*,5X,*ANGLE OF INCIDENCE IS*,2X,F4.1,//)
    9 FORMAT(10X,*P POLARIZATION*,5X,*ANGLE OF INCIDENCE IS*,2X,F4.1,//)
   18 FORMAT(F5.0,2F10.5)
   31 FORMAT(10X,4A10,*FILM ON A SMOOTH, FLAT*,2A10,*ELECTRODE*)
   46 FORMAT(10X,*COMPLEX REFRACTIVE INDEX OF SUBSTRATE IS  NC=N-I(K).
     XN=CN1+CN2(LAMBDA-3800.)  K=CK1+CK2(LAMBDA-3800.)*)
```

```
   45 FORMAT(10X,*LAMBDA IS THE WAVELENGTH BETWEEN 3800. AND 7800. A.
     XCN1=*,F10.7,*  CN2=*,F10.7,*  CK1=*,F10.7,*  CK2=*,F10.7,//)
   47 FORMAT(10X,*REFRACTIVE INDEX OF FILM AT 5892. A IS*,F7.4,//)
   48 FORMAT(20X,*TRISTIMULUS AND CHROMATICITY VALUES AND HUE OF FILM
     XAS A FUNCTION OF FILM THICKNESS*,////)
   75 FORMAT(1H1,//)
  919 FORMAT(4X,F7.0,4X,6F12.4,10X,2A10)
  914 FORMAT(*FILM THICKNESS*,8X,*CAPX*,8X,*CAPY*,8X,*CAPZ*,9X,*LOWX*,8X
     X,*LOWY*,8X,*LOWZ*,10X,*HUE*,//)
C
C
C      INPUTS ARE  (1) THE METAL SUBSTRATE, (2) THE FILM, (3) FOUR COEFF-
C      ICIENTS FOR A LINEAR APPROXIMATION OF THE COMPLEX INDEX OF RE-
C      FRACTION OF THE METAL SUBSTRATE, (4) THE INITIAL ANGLE OF INCI-
C      DENCE, THE STEP CHANGE AND THE NUMBER OF ANGLES, (5) THE LIGHT
C      SOURCE, (6) THE INITIAL AND FINAL VALUES OF THE FILM THICKNESS AND
C      THE INCREMENT, (7) THE ANGULAR SEPARATION BETWEEN THE INCIDENT P
C      AND S-POLARIZED LIGHT, (8) THE DISTRIBUTION COEFFICIENTS WEIGHTED
C      FOR THE LIGHT SOURCE, (9) THE REFRACTIVE INDEX OR REFRACTOMETER
C      SCALE READING FOR THE FILM AT UP TO 14 WAVELENGTHS, (10) BOUNDAR-
C      IES AND COLOR REGIONS FOR THE GRAPHICAL RESULT.
C
C
       READ 1,SBSTRA1,SBSTRA2
       READ 2,FILM1,FILM2,FILM3,FILM4
       READ 3,CN1,CN2,CK1,CK2
       READ 19,AMN,STEPS,NTOT
       READ 5,SOURCE1,SOURCE2
       READ 22,TMN,TMX,THKINC
       READ 4,SEP
       DO 310 I=1,81
       READ 6,XBAR(I),YBAR(I),ZBAR(I)
  310  CONTINUE
       DO 320 N=1,19
       READ 623,COLOR1(N),COLOR2(N)
  320  CONTINUE
       DO 386 N=1,19
       READ 67,BORDX(N),BORDY(N)
  386  CONTINUE
       DO 777 N=1,66
       READ 67,CROPOX(N),CROPOY(N)
  777  CONTINUE
       DO 888 N=1,19
       READ 67,BOUNDX(N),BOUNDY(N)
  888  CONTINUE
C      EITHER 1 OR MANY VALUES OF THE REFRACTIVE INDEX OR REFRACTOMETER
C      SCALE READINGS FOR THE FILM OVER THE VISIBLE RANGE OF LIGHT SHOULD
C      BE ON THE INPUT CARDS.
       DO 401 N=1,14
       READ 18,WAVLTH(N),RI(N),SCALE(N)
       IF (WAVLTH(N).EQ.0000.) GO TO 402
  401  CONTINUE
  402  MI=N-1
       NC=6
C      ENTER RI(N) OR HAVE IT CALCULATED FROM THE REFRACTOMETER SCALE
C      READING.
       DO 403 N=1,MI
       IF (RI(N).EQ.C.C) RI(N)=REFRXC(SCALE(N),WAVLTH(N))
       W(N)=1.0
  403  CONTINUE
C      IF THERE IS ONLY ONE INPUT CARD, THEN THAT REFRACTIVE INDEX IS
C      USED IN THE CALCULATIONS AS AN AVERAGE VALUE TO BE USED WITH EVERY
```

```
C     WAVELENGTH IN THE PROGRAM.
      IF (MI.LT.2) GO TO 406
      DO 404 I=1,MI
      WAVLTH(I)=WAVLTH(I)/4000.
  404 CONTINUE
C
C     LEAST SQUARE POLYNOMIAL FIT TO DETERMINE THE COEFFICIENTS FOR THE
C     POLYNOMIAL IN THE FUNCTION RIC(WAVLTH) THAT REPRESENTS THE VARIA-
C     TION OF REFRACTIVE INDEX OF THE FILM WITH WAVELENGTH.  THE RESULT-
C     ING POLYNOMIAL IS PLOTTED ALONG WITH THE SEVERAL INPUT VALUES AS A
C     CHECK ON THE ACCURACY OF THE METHOD OVER THE ENTIRE VISIBLE RANGE.
C
      CALL LSQPOL(WAVLTH,RI,W,RESID,MI,S,1,AI,BI,NO)
      DO 405 I=1,MI
      WAVLTH(I)=WAVLTH(I)*4000.
  405 CONTINUE
      XMIN=3000.
      XMAX=8000.
      YMIN=1.30
      YMAX=1.40
      CALL CCGRID(5,10,6HLABELS,10,10)
      CALL CCPLOT(WAVLTH,RI,MI,6HNOJOIN,6,1)
      TWVLTH(1)=3800.
      DO 30 J=1,41
      TRI(J)=RIC(TWVLTH(J))
      TWVLTH(J+1)=TWVLTH(J)+100.
   30 CONTINUE
      CALL CCPLOT(TWVLTH,TRI,40,4HJOIN,0,1)
      CALL CCNEXT
      GO TO 407
C     COEFFICIENTS FOR POLYNOMIAL IN FUNCTION RIC(WAVLTH) THAT REPRE-
C     SENTS VARIATION OF REFRACTIVE INDEX OF FILM WITH WAVELENGTH-- IN
C     THE CASE THAT JUST ONE REFRACTIVE INDEX OR REFRACTOMETER SCALE
C     READING AND WAVELENGTH IS IN THE INPUT CARDS.
  406 BI(1)=RI(1)
      BI(2)=0.
      BI(3)=0.
      BI(4)=0.
      BI(5)=0.
      BI(6)=0.
  407 CONTINUE
C     K REFERS TO THE ANGLE OF INCIDENCE WHICH CAN BE CHANGED IN INCRE-
C     MENTS.
      DO 500 K=1,NTOT
      PHID(1)=AMN+(K-1)*STEPS-0.5*SEP
      PHID(2)=AMN+(K-1)*STEPS+0.5*SEP
      PI=3.1415926536
C     J REFERS TO THE WAVELENGTH.
      DO 399 J=1,81
      LAMBDA=3800.+50.*(J-1)
      DO 10 I=1,2
C     CONVERSION OF ANGLES FROM DEGREES TO RADIANS.
      PHI(I)=0.0174533*PHID(I)
C     EQUATION (A-1)
      PHIPR(J,I)=ASIN((1./RIC(LAMBDA))*SIN(PHI(I)))
   10 CONTINUE
C
C
C     DIELECTRIC FILM REFLECTION EQUATIONS(WITH THE PRESENT SIGN CONVEN-
C     TION- AT NORMAL INCIDENCE THE POSITIVE P-POLARIZATION ELECTRIC
C     FIELD VECTORS OF THE INCIDENT AND REFLECTED LIGHT DO NOT COUNCIDE)
C
```

```
C
      TEMP1=COS(PHI(1))
      TEMP3=RIC(LAMBDA)*COS(PHIPR(J,1))
C     EQUATION (A-2)
      RL(J,1)=(TEMP1-TEMP3)/(TEMP1+TEMP3)
      RSQL(J,1)=(RL(J,1))**2
      TEMP2=RIC(LAMBDA)*COS(PHI(2))
      TEMP4=COS(PHIPR(J,2))
C     EQUATION (A-3)
      RL(J,2)=(TEMP2-TEMP4)/(TEMP4+TEMP2)
      RSQL(J,2)=(RL(J,2))**2
C
C     SEPARATION OF REFLECTION COEFFICIENT AND PHASE CHANGE AT GAS-FILM
C     INTERFACE.  M=1 FOR S-POLARIZED LIGHT, M=2 FOR P-POLARIZED LIGHT
C
      DO 153 M=1,2
      IF(RL(J,M)) 150,151,152
  150 DELD(J,M)=PI
      RL(J,M)=-RL(J,M)
      GO TO 153
  151 DELD(J,M)=2.*PI
      GO TO 153
  152 DELD(J,M)=2.*PI
  153 CONTINUE
      IF(MI.EQ.1) GO TO 587
  399 CONTINUE
      GO TO 591
  587 CONTINUE
C     ON THE CONDITION THAT ONLY ONE REFRACTIVE INDEX OR REFRACTOMETER
C     SCALE READING IS ON THE INPUT CARDS FOR THE FILM, THE FOLLOWING
C     VALUES ARE CONSTANT AND CAN BE SET EQUAL TO THE FIRST SET OF VAL-
C     UES CALCULATED FOR LAMBDA=3800.  THIS IS DONE TO AVOID UNNECESSARY
C     CALCULATIONS.
      DO 633 M=1,2
      DO 632 J=1,81
      PHIPR(J,M)=PHIPR(1,M)
      DELD(J,M)=DELD(1,M)
      RL(J,M)=RL(1,M)
      RSQL(J,M)=RSQL(1,M)
  632 CONTINUE
  633 CONTINUE
  591 CONTINUE
C
C
C     SECTION TO CALCULATE METALLIC REFLECTION COEFFICIENT FOR S-POLAR-
C     IZED(M=1) AND P-POLARIZED(M=2) LIGHT.  EQUATION FOR THE VARIATION
C     OF THE COMPLEX REFRACTIVE INDEX WITH WAVELENGTH IS INCLUDED.  COM-
C     PLEX REFRACTIVE INDEX=TNA+I(TKA).
C
C
      DO 400 J=1,81
      LAMBDA=3800.+50.*(J-1)
      TNA(J)=CN1+CN2*(LAMBDA-3800.)
      TKA(J)=CK1+CK2*(LAMBDA-3800.)
      TN=TNA(J)
      TK=TKA(J)
      DO 123 M=1,2
      SX=SIN(PHIPR(J,M))
      CX=COS(PHIPR(J,M))
      TX=SX/CX
C     THE FOLLOWING EXPRESSIONS FOR A AND B ARE EQUIVALENT TO EQUATIONS
C     (A-4) AND (A-5).
```

```
      TEMP1=(TN**2-TK**2-RIC(LAMBDA)**2*SX**2)**2+4.*TN**2*TK**2
      TEMP2=TN**2-TK**2-RIC(LAMBDA)**2*SX**2
      TEMP3=2.*RIC(LAMBDA)**2
      ASQ=(SQRT(TEMP1)+TEMP2)/TEMP3
      IF(ASQ) 110,112,112
  110 A=0.
      GO TO 114
  112 A=SQRT(ASQ)
  114 BSQ=(SQRT(TEMP1)-TEMP2)/TEMP3
      IF(BSQ) 116,118,118
  116 B=0.
      GO TO 120
  118 B=SQRT(BSQ)
C
C     EQUATIONS (A-6) AND (A-7)- REFLECTION COEFFICIENTS AT METAL-FILM
C     INTERFACE AND EQUATIONS (A-8), (A-9) AND (A-10)- PHASE CHANGE AT
C     METAL-FILM INTERFACE FOR S AND P LIGHT.
C
  120 IF(M.EQ.1) 121,122
  121 RSQ(J,1)=(ASQ+BSQ-2.0*A*CX+CX*CX)/(ASQ+BSQ+2.0*A*CX+CX*CX)
      IF(RSQ(J,1)) 125,124,124
  125 R(J,1)=0.
      GO TO 126
  124 R(J,1)=SQRT(RSQ(J,1))
  126 CONTINUE
      TEMP1=2.*B*CX
      TEMP2=ASQ+BSQ-CX*CX
      DEL(J,1)=ATAN(-TEMP1/TEMP2)
      IF(DEL(J,1)) 127,127,123
  127 DEL(J,1)=DEL(J,1)+PI
      GO TO 123
  122 TEMP1=(ASQ+BSQ-2.0*A*CX+CX*CX)/(ASQ+BSQ+2.0*A*CX+CX*CX)
      RSQ(J,2)=TEMP1*(ASQ+BSQ-2.0*A*SX*TX+SX*SX*TX*TX)/(ASQ+BSQ+2.0*A*SX
     X*TX+SX*SX*TX*TX)
      IF(RSQ(J,2)) 128,130,130
  128 R(J,2)=0.
      GO TO 132
  130 R(J,2)=SQRT(RSQ(J,2))
  132 CONTINUE
      TEMP1=2.0*B*SX*TX
      TEMP2=ASQ+BSQ-SX*SX*TX*TX
      DDEL=ATAN(-TEMP1/TEMP2)
      IF(DDEL) 135,136,136
  135 DDEL=DDEL+PI
  136 CONTINUE
      TEMP1=2.0*B*CX
      TEMP2=ASQ+BSQ-CX*CX
      TEMP3=ATAN(-TEMP1/TEMP2)
      IF(TEMP3) 145,145,146
  145 TEMP3=TEMP3+PI
  146 DEL(J,2)=TEMP3+DDEL
  123 CONTINUE
      IF((CN2.EQ.0.0).AND.(CK2.EQ.0.0).AND.(MI.EQ.1)) GO TO 595
  400 CONTINUE
      GO TO 596
  595 CONTINUE
C     ON THE CONDITIONS THAT ONLY ONE REFRACTIVE INDEX OR REFRACTOMETER
C     SCALE READING IS ON THE INPUT CARDS AND THE COMPLEX REFRACTIVE
C     INDEX OF THE METAL SUBSTRATE IS CONSTANT, THE FOLLOWING VALUES ARE
C     CONSTANT AND CAN BE SET EQUAL TO THE FIRST SET OF VALUES CALCULA-
C     TED FOR LAMBDA=3800.  THIS IS DONE TO AVOID UNNECESSARY CALCULATIONS.
      DO 597 M=1,2
```

```
      DO 598 J=1,81
      DEL(J,M)=DEL(1,M)
      R(J,M)=R(1,M)
      RSQ(J,M)=RSQ(1,M)
  598 CONTINUE
  597 CONTINUE
  596 CONTINUE
C
C
C     SECTION TO CALCULATE THE RELATIVE AMOUNTS OF THE THREE TRISTIMULUS
C     PRIMARIES IN THE REFLECTED LIGHT AND THE CHROMATICITY COORDINATES.
C     EQUATIONS (A-12) THROUGH (A-19) REPRESENT THE CALCULATIONS IN THIS
C     SECTION.  J REFERS TO THE WAVELENGTH, L TO THE FILM THICKNESS AND
C     M TO S(M=1) AND P(M=2) POLARIZED LIGHT.  THE WAVELENGTHS USED ARE
C     THOSE FOR WHICH THE DISTRIBUTION COEFFICIENTS ARE KNOWN.
C
C
      DO 212 M=1,2
      PRINT 31,FILM1,FILM2,FILM3,FILM4,SBSTRA1,SBSTRA2
      PRINT 46
      PRINT 45,CN1,CN2,CK1,CK2
      RID=RIC(5892.)
      PRINT 47,RID
      PRINT 48
      PRINT 12,SOURCE1,SOURCE2
      IF(M.EQ.1) 311,312
  311 PRINT 8,PHIC(M)
      GO TO 313
  312 CONTINUE
      PRINT 9,PHIC(M)
  313 PRINT 914
      DO 211 L=1,1000
      CAPX=0.
      CAPY=0.
      CAPZ=0.
      THK=THKINC*(L-1)+TMN
      IF(THK.GT.TMX) GO TO 515
      DO 213 J=1,81
      LAMBDA=3800.+50.*(J-1)
      DELT=4.0*PI*RIC(LAMBDA)*THK*COS(PHIPR(J,M))/LAMBDA
      TEMP1=2.0*R(J,M)*RL(J,M)*COS(DELT+DELD(J,M)-DEL(J,M))
      TEMP2=RSQ(J,M)+RSQL(J,M)+TEMP1
      TEMP3=1.0+RSQ(J,M)*RSQL(J,M)+TEMP1
      INT=TEMP2/TEMP3
      X=INT*XBAR(J)
      Y=INT*YBAR(J)
      Z=INT*ZBAR(J)
      CAPX=CAPX+X
      CAPY=CAPY+Y
      CAPZ=CAPZ+Z
  213 CONTINUE
      ZUM=CAPX+CAPY+CAPZ
      LCWX(L)=CAPX/ZUM
      LCWY(L)=CAPY/ZUM
      LCWZ=CAPZ/ZUM
C
C
C     THE PRINTED RESULT IS IN THE FORM OF THE RELATIVE AMOUNTS OF THE
C     TRISTIMULUS PRIMARIES AND THE CHROMATICITY COORDINATES AND THE HUE
C     OF THE REFLECTED LIGHT AS A FUNCTION OF FILM THICKNESS.  PROVISION
C     CAN BE MADE TO PREDICT WHITE POINTS, BUT WAS NOT.  THE SIZE OF THE
C     ACHROMATIC REGION IS IN DOUBT.  THE GRAPHICAL RESULT IS IN THE
```

```
C      FORM OF A CURVE OF CHROMATICITY COORDINATES AS A FUNCTION OF FILM
C      THICKNESS CONTAINED WITHIN A CHROMATICITY DIAGRAM WITH LABELED HUE
C      REGIONS ON THE BOUNDARIES.  THE LABELS ARE AT THE DOMINANT WAVE-
C      LENGTHS CORRESPONDING TO THE HUE NAMES OF THE REGIONS.
C
C
       SLOPE=(LOWY(L)-0.40745)/(LOWX(L)-0.44757)
       IF((LOWX(L).LT.0.44757).OR.(LOWY(L).LT.0.40745)) GO TO 1200
       IF(SLOPE.LE.0.710) PRINT 919,THK,CAPX,CAPY,CAPZ,LOWX(L),LOWY(L),LO
      XWZ,O
       IF(SLOPE.GE.0.710) PRINT 919,THK,CAPX,CAPY,CAPZ,LOWX(L),LOWY(L),LO
      XWZ,YELLOW
       GO TO 211
 1200 IF((LOWX(L).GT.0.44757).OR.(LOWY(L).LT.0.40745)) GO TO 1300
       IF(SLOPE.LE.-4.686) PRINT 919,THK,CAPX,CAPY,CAPZ,LOWX(L),LOWY(L),L
      XOWZ,YELLOW
       IF(SLOPE.GE.-4.686) PRINT 919,THK,CAPX,CAPY,CAPZ,LOWX(L),LOWY(L),L
      XOWZ,G
       GO TO 211
 1300 IF((LOWX(L).GT.0.44757).OR.(LOWY(L).GT.0.40745)) GO TO 1400
       IF(SLOPE.LE.0.104) PRINT 919,THK,CAPX,CAPY,CAPZ,LOWX(L),LOWY(L),LO
      XWZ,G
       IF((SLOPE.GE.0.104).AND.(SLOPE.LE.0.423)) PRINT 919,THK,CAPX,CAPY,
      XCAPZ,LOWX(L),LOWY(L),LOWZ,BG
       IF((SLOPE.GE.0.423).AND.(SLOPE.LE.1.423)) PRINT 919,THK,CAPX,CAPY,
      XCAPZ,LOWX(L),LOWY(L),LOWZ,BLUE
       IF(SLOPE.GE.1.423) PRINT 919,THK,CAPX,CAPY,CAPZ,LOWX(L),LOWY(L),LO
      XWZ,P
       GO TO 211
 1400 IF(SLOPE.LE.-28.79) PRINT 919,THK,CAPX,CAPY,CAPZ,LOWX(L),LOWY(L),L
      XOWZ,P
       IF((SLOPE.GE.-28.79).AND.(SLOPE.LE.-0.292)) PRINT 919,THK,CAPX,CAP
      XY,CAPZ,LOWX(L),LOWY(L),LOWZ,RED
       IF(SLOPE.GE.-0.292) PRINT 919,THK,CAPX,CAPY,CAPZ,LOWX(L),LOWY(L),L
      XOWZ,O
  211 CONTINUE
  515 CONTINUE
       PRINT 75
       L=L-1
       XMIN=0.0
       XMAX=.80
       YMIN=0.0
       YMAX=.90
       FACTOR=100.
       CCXMIN=2.
       CCXMAX=10.
       CCYMIN=1.
       CCYMAX=10.
       CALL CCGRID(1,40,2,6HNCLBLS,1,45,2)
       CALL FIXLBL(8,9,2,-1,-1)
       CALL CCLTR(2.,10.7,0,1,60HCHROMATICITY DIAGRAM.  FILM THICKNESS IS
      X THE ONLY PARAMETER.)
       IF(M.GT.1) GO TO 225
       CALL CCLTR(2.,10.5,0,1,32HS-POLARIZATION OF INCIDENT LIGHT)
       GO TO 226
  225 CALL CCLTR(2.,10.5,0,1,32HP-POLARIZATION OF INCIDENT LIGHT)
  226 CONTINUE
       WRITE(98,100) PHID(M)
       CALL CCLTR(2.,10.3,0,1)
       WRITE(98,101) FILM1,FILM2,FILM3,FILM4,SBSTRA1,SBSTRA2
       CALL CCLTR(2.,10.1,0,1)
       WRITE(98,102) TMA
```

```
      CALL CCLTR(7.2,10.7,0,1)
      WRITE(98,103) TMX
      CALL CCLTR(7.2,10.5,0,1)
      WRITE(98,104) THKINC
      CALL CCLTR(7.2,10.3,0,1)
      CALL CCLTR(5.9,.25,0,5,1HX)
      CALL CCLTR(1.25,5.4,0,5,1HY)
      DO 899 N=1,19
      CCX=2.+BORDX(N)*10.
      CCY=1.+BORDY(N)*10.
      WRITE(98,623) COLOR1(N),COLOR2(N)
      CALL CCLTR(CCX,CCY,0,1)
  899 CONTINUE
      CALL CCPLOT(CROPCX,CROPCY,66,4HJOIN,0,0)
      CALL CCPLOT(BOUNDX,BOUNDY,19,6HNOJOIN,6,1)
      CALL CCPLOT(LOWX,LOWY,L,4HJOIN,1,0)
      CALL CCNEXT
  212 CONTINUE
  500 CONTINUE
      CALL CCEND
   67 FORMAT(2F10.4)
  100 FORMAT(*ANGLE OF INCIDENCE=*F5.1,1X,*DEGREES*)
  101 FORMAT(4A10,*ON A*,2A10,*ELECTRODE*)
  102 FORMAT(*INITIAL THICKNESS=*,F6.0,1X,*ANGSTROMS*)
  103 FORMAT(*FINAL THICKNESS=*,F6.0,1X,*ANGSTROMS*)
  104 FORMAT(*THICKNESS INCREMENT=*,F6.0,1X,*ANGSTROMS*)
  623 FORMAT(2A10)
      STOP
      END
```

```
      FUNCTION RIC(WAVLTH)
C     THIS FUNCTION GIVES THE REFRACTIVE INDEX OF THE SOLUTION AT A
C     SPECIFIED WAVELENGTH USING A POLYNOMIAL OF 6 TERMS.
C
C
      COMMON/RICOM/B,NO
      DIMENSION B(20)
      REAL A
      A=WAVLTH
      C=0.0
      A=A/4000.
      DO 601 K=1,NO
      C=C+(B(K)*(A**(K-1)))
  601 CONTINUE
      RIC=C
      RETURN
      END
C
C
      FUNCTION REFRXC(SCALE,WAVLTH)
C     THIS FUNCTION CALCULATES THE REFRACTIVE INDEX OF THE SOLUTION FROM
C     THE SCALE READINGS OF THE REFRACTOMETER(BAUSCH AND LOMB PRECISION
C     REFRACTOMETER WITH PRISM 749-1).  A DIFFERENT PRISM WOULD REQUIRE
C     DIFFERENT PRISM CONSTANTS, PC(J).
C
C
      REAL NPRIS,PC(8),LAMB
      LAMB=WAVLTH/4000.
      APRIS=0.0174533*68.0
      PC(1)=2.1098525761
      PC(2)=-1.8465725697
      PC(3)=2.4203415165
      PC(4)=-1.6347815115
      PC(5)=0.5602598970
      PC(6)=-0.0773841103
      NPRIS=0.
      DO 701 J=1,6
      NPRIS=NPRIS+PC(J)*(LAMB**(J-1))
  701 CONTINUE
      AMEAS=24.0-(2.0*SCALE)/3.0
      AMEAS=AMEAS*0.0174533
      ACALC=ASIN(SIN(AMEAS)/NPRIS)
      APRIM=APRIS-ACALC
      REFRXC=SIN(APRIM)*NPRIS
      RETURN
      END
```

Table III. Correspondence between two sets of hue names.* 1964 C.I.E. chromaticity diagram.

Hue Name	Dominant Wavelength	x	y	Photographic Hue Name
bluish purple		0.196	0.027	
		0.162	0.022**	----------
purplish blue	454	0.147	0.043	
		0.130	0.077	
blue	476	0.091	0.173	blue
		0.061	0.272	
greenish blue	485	0.045	0.328	
		0.035	0.377**	----------
blue green	490	0.021	0.440	blue green
		0.013	0.511**	----------
bluish green	495	0.007	0.562	
		0.0065	0.616	
green	508	0.038	0.782	green
		0.207	0.766	
yellowish green	545	0.313	0.681	
		0.409	0.591	
yellow green	565	0.447	0.553**	----------
		0.481	0.519	
greenish yellow	573	0.497	0.503	
		0.514	0.486	
yellow	578	0.527	0.473	yellow
		0.539	0.461	
yellowish orange	583	0.555	0.445**	----------
		0.575	0.425	
orange	592	0.599	0.401	orange
		0.621	0.379	
reddish orange	606	0.650	0.350**	----------
		0.683	0.317	
red		0.687	0.264	red
		0.645	0.243	
purplish red		0.593	0.218	
		0.541	0.193	
red purple		0.453	0.151**	----------
		0.379	0.115	
reddish purple		0.335	0.094	
		0.294	0.074	
purple		0.257	0.056	purple
		0.215	0.036	
bluish purple		0.196	0.027	
		0.162	0.022**	----------
purplish blue	454	0.147	0.043	

*The nineteen hue names and dominant wavelengths are those suggested by Kelley.[40] Complementary wavelengths for nonspectral colors are not shown here, since Kelley listed them for the 1931 C.I.E. chromaticity diagram. The 1964 C.I.E. chromaticity coordinates represent either the dominant wavelength or the intersection of dividing lines between hue regions with the boundary of the diagram. The chromaticity coordinates for the nonspectral hues had to be estimated from the 1931 C.I.E. chromaticity diagram in Kelley's article. The condensed list of hue names is for use in photographic work.

**Intersections of dividing lines between hue regions (condensed list) with the boundary of the diagram.

THESE ARE CARDS FOR THE 1964 C.I.E. CHROMATICITY DIAGRAM TO DETERMINE THE HUE OF LIGHT FROM THE CHROMATICITY COORDINATES. THEY MUST BE USED ALONG WITH THE DATA CARDS FOR THE 1964 C.I.E. CHROMATICITY DIAGRAM AND SOURCE A. THEY REPLACE THE SECTION PRECEDING THE CARD WITH REFERENCE NUMBER 211 IN THE PROGRAM. THE DIAGRAM IS DIVIDED INTO 7 HUE REGIONS.

```
      SLOPE=(LOWY(L)-0.40593)/(LOWX(L)-0.45117)
      IF((LOWX(L).LT.0.45117).OR.(LOWY(L).LT.0.40593)) GO TO 1200
      IF(SLOPE.LE.0.376) PRINT 919,THK,CAPX,CAPY,CAPZ,LOWX(L),LOWY(L),LO
     XWZ,O
      IF(SLOPE.GE.0.376) PRINT 919,THK,CAPX,CAPY,CAPZ,LOWX(L),LOWY(L),LO
     XWZ,YELLOW
      GO TO 211
1200  IF((LOWX(L).GT.0.45117).OR.(LOWY(L).LT.0.40593)) GO TO 1300
      IF(SLOPE.LE.-35.27) PRINT 919,THK,CAPX,CAPY,CAPZ,LOWX(L),LOWY(L),L
     XOWZ,YELLOW
      IF((SLOPE.GE.-35.27).AND.(SLOPE.LE.-0.240)) PRINT 919,THK,CAPX,CAP
     XY,CAPZ,LOWX(L),LOWY(L),LOWZ,G
      IF(SLOPE.GE.-0.240) PRINT 919,THK,CAPX,CAPY,CAPZ,LOWX(L),LOWY(L),L
     XOWZ,BG
      GO TO 211
1300  IF((LOWX(L).GT.0.45117).OR.(LOWY(L).GT.0.40593)) GO TO 1400
      IF(SLOPE.LE.0.069) PRINT 919,THK,CAPX,CAPY,CAPZ,LOWX(L),LOWY(L),LO
     XWZ,BG
      IF((SLOPE.GE.0.069).AND.(SLOPE.LE.1.327)) PRINT 919,THK,CAPX,CAPY,
     XCAPZ,LOWX(L),LOWY(L),LOWZ,BLUE
      IF(SLOPE.GE.1.327) PRINT 919,THK,CAPX,CAPY,CAPZ,LOWX(L),LOWY(L),LO
     XWZ,P
      GO TO 211
1400  IF(SLOPE.LE.-139.31) PRINT 919,THK,CAPX,CAPY,CAPZ,LOWX(L),LOWY(L),
     XLOWZ,P
      IF((SLOPE.GE.-139.31).AND.(SLOPE.LE.-0.281)) PRINT 919,THK,CAPX,CA
     XPY,CAPZ,LOWX(L),LOWY(L),LOWZ,RED
      IF(SLOPE.GE.-0.281) PRINT 919,THK,CAPX,CAPY,CAPZ,LOWX(L),LOWY(L),L
     XOWZ,O
```

```
C     THESE ARE CARDS FOR THE 1964 C.I.E. CHROMATICITY DIAGRAM TO DETER-
C     MINE THE HUE OF LIGHT FROM THE CHROMATICITY COORDINATES.  THEY
C     MUST BE USED ALONG WITH THE DATA CARDS FOR THE 1964 C.I.E. CHROMA-
C     TICITY DIAGRAM AND SOURCE A.  THEY REPLACE THE SECTION PRECEDING
C     THE CARD WITH REFERENCE NUMBER 211 IN THE PROGRAM.  THE DIAGRAM IS
C     DIVIDED INTO 19 HUE REGIONS.

      SLOPE=(LOWY(L)-0.40593)/(LOWX(L)-0.45117)
      IF((LOWX(L).LT.0.45117).OR.(LOWY(L).LT.0.40593)) GO TO 1200
      IF(SLOPE.LE.0.154) PRINT 919,THK,CAPX,CAPY,CAPZ,LOWX(L),LOWY(L),LO
     XWZ,O
      IF((SLOPE.GE.0.154).AND.(SLOPE.LE.0.628)) PRINT 919,THK,CAPX,CAPY,
     XCAPZ,LOWX(L),LOWY(L),LOWZ,YHO
      IF((SLOPE.GE.0.628).AND.(SLOPE.LE.1.275)) PRINT 919,THK,CAPX,CAPY,
     XCAPZ,LOWX(L),LOWY(L),LOWZ,YELLOW
      IF((SLOPE.GE.1.275).AND.(SLOPE.LE.3.795)) PRINT 919,THK,CAPX,CAPY,
     XCAPZ,LOWX(L),LOWY(L),LOWZ,GHY
      IF(SLOPE.GE.3.795) PRINT 919,THK,CAPX,CAPY,CAPZ,LOWX(L),LOWY(L),LO
     XWZ,YG
      GO TO 211
1200  IF((LOWX(L).GT.0.45117).OR.(LOWY(L).LT.0.40593)) GO TO 1300
      IF(SLOPE.LE.-4.386) PRINT 919,THK,CAPX,CAPY,CAPZ,LOWX(L),LOWY(L),L
     XOWZ,YG
      IF((SLOPE.GE.-4.386).AND.(SLOPE.LE.-1.475)) PRINT 919,THK,CAPX,CAP
     XY,CAPZ,LOWX(L),LOWY(L),LOWZ,YHG
      IF((SLOPE.GE.-1.475).AND.(SLOPE.LE.-0.472)) PRINT 919,THK,CAPX,CAP
     XY,CAPZ,LOWX(L),LOWY(L),LOWZ,G
      IF((SLOPE.GE.-0.472).AND.(SLOPE.LE.-0.240)) PRINT 919,THK,CAPX,CAP
     XY,CAPZ,LOWX(L),LOWY(L),LOWZ,BHG
      IF(SLOPE.GE.-0.240) PRINT 919,THK,CAPX,CAPY,CAPZ,LOWX(L),LOWY(L),L
     XOWZ,BG
      GO TO 211
1300  IF((LOWX(L).GT.0.45117).OR.(LOWY(L).GT.0.40593)) GO TO 1400
      IF(SLOPE.LE.0.069) PRINT 919,THK,CAPX,CAPY,CAPZ,LOWX(L),LOWY(L),LO
     XWZ,BG
      IF((SLOPE.GE.0.069).AND.(SLOPE.LE.0.343)) PRINT 919,THK,CAPX,CAPY,
     XCAPZ,LOWX(L),LOWY(L),LOWZ,GHB
      IF((SLOPE.GE.0.343).AND.(SLOPE.LE.1.024)) PRINT 919,THK,CAPX,CAPY,
     XCAPZ,LOWX(L),LOWY(L),LOWZ,BLUE
      IF((SLOPE.GE.1.024).AND.(SLOPE.LE.1.327)) PRINT 919,THK,CAPX,CAPY,
     XCAPZ,LOWX(L),LOWY(L),LOWZ,PHB
      IF((SLOPE.GE.1.327).AND.(SLOPE.LE.1.529)) PRINT 919,THK,CAPX,CAPY,
     XCAPZ,LOWX(L),LOWY(L),LOWZ,BHP
      IF((SLOPE.GE.1.529).AND.(SLOPE.LE.2.132)) PRINT 919,THK,CAPX,CAPY,
     XCAPZ,LOWX(L),LOWY(L),LOWZ,P
      IF((SLOPE.GE.2.132).AND.(SLOPE.LE.4.144)) PRINT 919,THK,CAPX,CAPY,
     XCAPZ,LOWX(L),LOWY(L),LOWZ,RHP
      IF(SLOPE.GE.4.144) PRINT 919,THK,CAPX,CAPY,CAPZ,LOWX(L),LOWY(L),LO
     XWZ,RP
      GO TO 211
1400  IF(SLOPE.LE.-2.371) PRINT 919,THK,CAPX,CAPY,CAPZ,LOWX(L),LOWY(L),L
     XOWZ,RP
      IF((SLOPE.GE.-2.371).AND.(SLOPE.LE.-0.835)) PRINT 919,THK,CAPX,CAP
     XY,CAPZ,LOWX(L),LOWY(L),LOWZ,PHR
      IF((SLOPE.GE.-0.835).AND.(SLOPE.LE.-0.384)) PRINT 919,THK,CAPX,CAP
     XY,CAPZ,LOWX(L),LOWY(L),LOWZ,RED
      IF((SLOPE.GE.-0.384).AND.(SLOPE.LE.-0.158)) PRINT 919,THK,CAPX,CAP
     XY,CAPZ,LOWX(L),LOWY(L),LOWZ,RHO
      IF(SLOPE.GE.-0.158) PRINT 919,THK,CAPX,CAPY,CAPZ,LOWX(L),LOWY(L),L
     XOWZ,O
```

THESE ARE THE DATA CARDS FOR THE 1964 C.I.E. CHROMATICITY DIAGRAM THAT DO NOT VARY FROM PROGRAM TO PROGRAM. (CARDS 8-211)

	COLUMNS		
	1-10	11-20	21-30
CARD 8	C.C001	0.0000	0.0003
	0.0003	0.0000	0.0014
XBAR(I), YBAR(I)	C.C013	C.0002	0.CC56
AND ZBAR(I)	0.0042	C.0005	0.C190
	C.0123	0.C013	0.0556
	C.0308	0.0032	0.1359
	C.0658	0.C068	0.3025
	C.1192	0.0123	0.5567
	0.1887	0.0197	0.8974
	0.2651	0.0295	1.2843
	C.3411	0.042C	1.6840
	0.4187	0.0581	2.1053
	0.4839	0.0783	2.4810
	0.5242	0.1013	2.7482
	0.5390	0.1301	2.9004
	0.5337	C.1654	2.9574
	0.5024	0.2130	2.9006
	C.45C0	0.27C6	2.7534
	0.3685	0.3489	2.4820
	0.2646	0.4398	2.0606
	0.17C7	0.5377	1.6370
	C.0922	C.6677	1.2786
	0.0384	0.8033	C.9838
	0.0127	0.9877	0.7554
	0.0100	1.2120	0.5747
	0.0426	1.4694	0.4402
	0.1089	1.7611	0.3251
	0.2173	2.0865	0.2501
	0.3750	2.4269	0.1934
	0.5761	2.7418	0.1435
	0.8223	3.0431	C.1060
	1.1030	3.3497	0.0747
	1.4231	3.6332	0.0517
	1.7742	3.8588	0.0310
	2.1629	4.0491	0.0163
	2.6108	4.2338	0.0047
	3.0987	4.3822	0.0000
	3.6129	4.4713	0.0000
	4.1383	4.5000	0.0000
	4.6311	4.4558	0.0000
	5.1000	4.3693	0.0000
	5.5740	4.2837	0.0000
	5.9828	4.1582	0.0000
	6.2497	3.9692	0.0000
	6.3732	3.7326	0.0000
	6.3505	3.463C	0.0000
	6.1736	3.1632	0.0000
	5.8480	2.8407	0.0000
	5.4039	2.5123	0.0000
	4.8838	2.1970	0.0000
	4.2914	1.8789	0.0000
	3.6308	1.5491	0.0000
	2.9961	1.2481	0.0000

	COLUMNS 1-10	11-20	21-30
	2.4392	0.9950	0.0000
	1.9456	0.7803	0.0000
	1.5127	0.6012	0.0000
	1.1531	0.4556	0.0000
	0.8647	0.3398	0.0000
	0.6386	0.2498	0.0000
	0.4633	0.1809	0.0000
	0.3333	0.1296	0.0000
	0.2371	0.0920	0.0000
	0.1678	0.0649	0.0000
	0.1183	0.0463	0.0000
	0.0836	0.0322	0.0000
	0.0584	0.0230	0.0000
	0.0413	0.0162	0.0000
	0.0283	0.0109	0.0000
	0.0203	0.0074	0.0000
	0.0141	0.0056	0.0000
	0.0095	0.0038	0.0000
	0.0067	0.0029	0.0000
	0.0049	0.0019	0.0000
	0.0039	0.0010	0.0000
	0.0030	0.0010	0.0000
	0.0020	0.0010	0.0000
	0.0010	0.0000	0.0000
	0.0010	0.0000	0.0000
	0.0010	0.0000	0.0000
	0.0000	0.0000	0.0000
	0.0000	0.0000	0.0000
CARD 89	RED		
	REDDISH ORANGE		
COLOR1(N), COLOR2(N)	ORANGE		
	YELLOWISH ORANGE		
	YELLOW		
	GREENISH YELLOW		
	YELLOW GREEN		
	YELLOWISH GREEN		
	GREEN		
	BLUISH GREEN		
	BLUE GREEN		
	GREENISH BLUE		
	BLUE		
	PURPLISH BLUE		
	BLUISH PURPLE		
	PURPLE		
	REDDISH PURPLE		
	RED PURPLE		
	PURPLISH RED		
CARD 108	0.687	0.264	
	0.650	0.350	
BORDX(N), BORDY(N)	0.599	0.401	
	0.555	0.445	
	0.527	0.473	
	0.497	0.503	
	0.447	0.553	
	0.313	0.681	
	0.038	0.782	

CARD 127

CROPOX(N), CROPOY(N)

COLUMNS 1-10	COLUMNS 11-20
0.007	0.562
0.021	0.440
0.045	0.328
0.091	0.173
0.147	0.043
0.196	0.027
0.257	0.056
0.335	0.094
0.453	0.151
0.593	0.218
0.1813	0.0197
0.1809	0.0195
0.1803	0.0194
0.1795	0.0190
0.1784	0.0187
0.1771	0.0184
0.1755	0.0181
0.1732	0.0178
0.1706	0.0179
0.1679	0.0187
0.1650	0.0203
0.1622	0.0225
0.1590	0.0257
0.1554	0.0300
0.1510	0.0364
0.1459	0.0452
0.1389	0.0589
0.1295	0.0779
0.1152	0.1090
0.0957	0.1591
0.0728	0.2292
0.0452	0.3275
0.0210	0.4401
0.0073	0.5625
0.0056	0.6745
0.0219	0.7526
0.0495	0.8023
0.0850	0.8170
0.1252	0.8102
0.1664	0.7922
0.2071	0.7663
0.2436	0.7399
0.2786	0.7113
0.3132	0.6813
0.3473	0.6501
0.3812	0.6182
0.4142	0.5858
0.4469	0.5531
0.4790	0.5210
0.5096	0.4904
0.5386	0.4614
0.5654	0.4346
0.5900	0.4100
0.6116	0.3884
0.6306	0.3694
0.6471	0.3529

CARD 193

BCUNDX(N), BCUNDY(N)

COLUMNS 1-10	COLUMNS 11-20
0.6612	0.3388
0.6731	0.3269
0.6827	0.3173
0.6898	0.3102
0.6955	0.3045
0.7010	0.2990
0.7059	0.2941
0.7103	0.2898
0.7137	0.2863
0.7156	0.2844
0.7168	0.2832
0.7179	0.2821
0.7187	0.2813
0.7193	0.2807
0.7198	0.2802
0.7200	0.2800
0.7202	0.2798
0.7203	0.2797
0.7204	0.2796
0.1813	0.0197
0.0065	0.616
0.207	0.766
0.409	0.591
0.481	0.519
0.514	0.486
0.539	0.461
0.575	0.425
0.621	0.379
0.683	0.317
0.645	0.243
0.541	0.193
0.379	0.115
0.294	0.074
0.215	0.036
0.162	0.022
0.130	0.077
0.061	0.272
0.035	0.377
0.013	0.511

N=1.35 DIELECTRIC FILM ON A SMOOTH, FLAT N=2.07-I(4.40) ELECTRODE
COMPLEX REFRACTIVE INDEX OF SUBSTRATE IS NCNN-I(K). N=CN1+CN2(LAMBDA-3800.) K=CK1+CK2(LAMBCA-3800.)
LAMBDA IS THE WAVELENGTH BETWEEN 3800. AAC 7000. A. CP1= 2.0700000 CN2= 0.0000000 CK1= 4.4000000 CK2= 0.0000000

REFRACTIVE INDEX OF FILM AT 5892. A IS 1.:500

TRISTIMULUS AND CHROMATICITY VALUES AND HUE OF FILM AS A FUNCTION OF FILM THICKNESS

SOURCE A

S POLARIZATION ANGLE OF INCIDENCE IS 75.0

FILM THICKNESS	CAPX	CAPY	CAPZ	LOWX	LOWY	LOWZ	HUE
0	100.7467	91.7153	32.6345	.4476	.4074	.1450	RED
50	100.5839	91.5695	32.5841	.4476	.4075	.1449	ORANGE
100	100.3745	91.3600	32.4885	.4477	.4075	.1448	ORANGE
150	100.1148	91.1099	32.3447	.4478	.4075	.1447	ORANGE
200	99.7998	90.8051	32.1890	.4479	.4076	.1445	ORANGE
250	99.4235	90.4393	31.9962	.4481	.4076	.1442	ORANGE
300	98.9780	90.0046	31.7598	.4484	.4077	.1439	ORANGE
350	98.4560	89.4918	31.4711	.4487	.4079	.1436	ORANGE
400	97.8397	88.8865	31.1189	.4491	.4080	.1428	ORANGE
450	97.1286	88.1757	30.6887	.4497	.4082	.1421	ORANGE
500	96.2787	87.3400	30.1615	.4504	.4086	.1411	ORANGE
550	95.2928	86.3568	29.5127	.4513	.4090	.1398	ORANGE
600	94.1329	85.1949	28.7107	.4525	.4095	.1388	ORANGE
650	92.7678	83.8209	27.7156	.4541	.4103	.1397	ORANGE
700	91.1555	82.1899	26.4792	.4562	.4113	.1325	ORANGE
750	89.2476	80.2485	24.9490	.4590	.4127	.1283	ORANGE
800	86.9869	77.9333	23.0888	.4627	.4145	.1228	ORANGE
850	84.3232	75.1727	20.8680	.4675	.4168	.1157	ORANGE
900	81.2031	71.8929	18.3937	.4735	.4192	.1073	ORANGE
950	77.6047	68.0323	15.8920	.4804	.4212	.0984	ORANGE
1000	73.5326	63.5868	13.7623	.4874	.4214	.0912	ORANGE
1050	69.0223	58.5517	12.4631	.4929	.4181	.0890	ORANGE
1100	64.1233	53.1676	12.3038	.4948	.4103	.0949	ORANGE
1150	58.9226	47.7562	13.2847	.4912	.3981	.1107	ORANGE
1200	53.6047	42.8120	15.1196	.4806	.3838	.1356	RED
1250	48.5141	38.9044	17.4817	.4628	.3712	.1668	RED
1300	44.1933	36.5408	19.7668	.4395	.3637	.1968	PURPLE
1350	41.0878	36.0246	21.9823	.4146	.3635	.2218	BLUE
1400	39.7301	37.3748	23.9261	.3935	.3698	.2367	BLUE
1450	40.4462	40.3394	25.5697	.3803	.3793	.2404	BLUE GREEN
1500	42.9910	44.4849	26.9299	.3757	.3889	.2354	BLUE GREEN
1550	47.0074	49.3159	28.0431	.3780	.3969	.2238	BLUE GREEN
1600	52.0023	54.3769	28.9802	.3843	.4018	.2139	GREEN
1650	57.4161	59.3239	29.6890	.3922	.4051	.2027	GREEN
1700	62.8736	63.9223	30.2918	.4002	.4069	.1928	GREEN
1750	68.0149	68.0543	30.7848	.4076	.4079	.1848	GREEN
1800	72.6906	71.6808	31.1886	.4140	.4083	.1777	GREEN
1850	76.8319	74.8145	31.5204	.4195	.4085	.1721	GREEN
1900	80.4367	77.4963	31.7924	.4240	.4085	.1676	GREEN
1950	83.5406	79.7790	32.0146	.4277	.4084	.1639	GREEN
2000	86.1966	81.7172	32.1949	.4307	.4084	.1609	GREEN
2050	88.4623	83.3619	32.3392	.4333	.4083	.1584	GREEN
2100	90.3932	84.7583	32.4520	.4354	.4083	.1563	GREEN
2150	92.0392	85.9484	32.5367	.4372	.4083	.1546	GREEN
2200	93.4436	86.9855	32.5958	.4387	.4083	.1530	GREEN
2250	94.6433	87.8157	32.6308	.4400	.4083	.1517	GREEN
2300	95.6688	88.5484	32.6426	.4412	.4083	.1505	GREEN
2350	96.5456	89.1716	32.6315	.4422	.4084	.1494	GREEN
2400	97.2946	89.7003	32.5969	.4431	.4085	.1484	GREEN
2450	97.9329	90.1466	32.5376	.4439	.4086	.1478	GREEN
2500	98.4742	90.5201	32.4514	.4447	.4088	.1465	GREEN
2550	98.9299	90.8269	32.3354	.4454	.4090	.1458	GREEN
2600	99.3086	91.0798	32.1884	.4462	.4092	.1446	GREEN
2650	99.6173	91.2753	31.9958	.4469	.4095	.1436	GREEN
2700	99.8608	91.4214	31.7589	.4477	.4099	.1424	YELLOW
2750	100.0426	91.5197	31.4651	.4486	.4104	.1411	YELLOW
2800	100.1642	91.5716	31.1014	.4495	.4109	.1398	YELLOW
2850	100.2258	91.5776	30.6618	.4505	.4117	.1378	YELLOW
2900	100.2268	91.5371	30.0961	.4518	.4126	.1357	YELLOW
2950	100.1618	91.4485	29.4109	.4532	.4138	.1331	YELLOW
3000	100.0296	91.3091	28.5691	.4549	.4152	.1299	YELLOW
3050	99.8252	91.1148	27.5478	.4569	.4170	.1261	YELLOW
3100	99.5461	90.8604	26.3322	.4593	.4192	.1215	YELLOW
3150	99.1938	90.5391	24.9287	.4621	.4218	.1161	YELLOW
3200	98.7757	90.1426	23.3775	.4653	.4246	.1101	YELLOW
3250	98.3065	89.6609	21.7584	.4687	.4275	.1037	YELLOW
3300	97.8044	89.0825	20.1893	.4723	.4302	.0975	YELLOW
3350	97.2959	88.3938	18.7864	.4756	.4323	.0919	YELLOW
3400	96.7911	87.5795	17.6802	.4790	.4335	.0875	YELLOW
3450	96.2986	86.6224	16.9578	.4818	.4334	.0846	YELLOW
3500	95.8136	85.5037	16.6713	.4839	.4319	.0842	ORANGE
3550	95.3186	84.2040	16.8300	.4854	.4288	.0897	ORANGE
3600	94.7844	82.7844	17.3993	.4864	.4244	.0893	ORANGE
3650	94.1719	80.9887	18.3874	.4868	.4186	.0946	ORANGE
3700	93.4356	78.8467	19.4590	.4868	.4118	.1014	ORANGE
3750	92.5277	76.8781	20.7838	.4866	.4043	.1091	ORANGE
3800	91.4829	74.4971	22.1017	.4862	.3963	.1176	ORANGE
3850	90.0212	71.9366	23.4319	.4856	.3880	.1264	RED
3900	88.3516	69.2496	24.6951	.4847	.3799	.1358	RED
3950	86.3752	66.5081	25.8603	.4832	.3721	.1447	RED
4000	84.0881	63.7073	26.9113	.4811	.3690	.1540	RED
4050	81.5033	61.2087	27.8426	.4779	.3589	.1632	RED
4100	78.6524	58.8292	28.6556	.4734	.3541	.1725	RED
4150	75.5859	56.7415	29.3569	.4675	.3509	.1816	RED
4200	72.3731	55.0133	29.9556	.4600	.3496	.1904	RED
4250	69.1015	53.6983	30.4621	.4509	.3504	.1988	RED
4300	65.8753	52.8245	30.9869	.4404	.3532	.2065	PURPLE
4350	62.8124	52.4410	31.2401	.4288	.3588	.2132	PURPLE
4400	60.0384	52.5281	31.5311	.4167	.3645	.2188	BLUE
4450	57.6796	53.0771	31.7681	.4047	.3724	.2229	BLUE
4500	55.8823	54.0815	31.9580	.3937	.3811	.2253	BLUE
4550	54.6540	55.4392	32.1063	.3843	.3899	.2258	BLUE GREEN
4600	54.1593	57.1565	32.2172	.3773	.3982	.2248	BLUE GREEN
4650	54.3697	59.1519	32.2939	.3729	.4057	.2215	GREEN
4700	55.2983	61.3507	32.3381	.3711	.4118	.2170	GREEN
4750	56.8807	63.7087	32.3506	.3719	.4166	.2115	GREEN
4800	59.0259	66.1351	32.3311	.3746	.4199	.2053	GREEN
4850	61.6172	68.5751	32.2780	.3793	.4221	.1987	GREEN
4900	64.5244	70.9732	32.1888	.3848	.4232	.1920	GREEN
4950	67.6161	73.2823	32.0596	.3909	.4237	.1854	GREEN
5000	70.7791	75.4654	31.8852	.3973	.4237	.1790	GREEN

5050	73.8805	77.4957	31.6589	.4036	.4234	.1738	GREEN
5100	76.8625	79.3563	31.3711	.4097	.4230	.1672	GREEN
5150	79.6934	81.7388	31.0130	.4155	.4227	.1610	GREEN
5200	82.2115	83.9420	30.6731	.4209	.4226	.1969	GREEN
5250	84.5139	83.8766	30.0404	.4259	.4227	.1914	GREEN
5300	86.5930	85.0327	29.4062	.4308	.4231	.1463	GREEN
5350	88.3333	86.0394	28.8666	.4351	.4238	.1422	GREEN
5400	89.8587	86.9024	27.8268	.4392	.4247	.1360	GREEN
5450	91.1799	87.6340	26.9801	.4432	.4260	.1308	GREEN
5500	92.2923	88.2457	25.9164	.4470	.4274	.1255	YELLOW
5550	93.2336	88.7481	24.9119	.4506	.4290	.1204	YELLOW
5600	94.0316	89.1507	23.9288	.4540	.4305	.1155	YELLOW
5650	94.7124	89.4612	23.0050	.4572	.4319	.1110	YELLOW
5700	95.2989	89.6861	22.1783	.4600	.4329	.1071	YELLOW
5750	95.8105	89.8302	21.4761	.4626	.4337	.1037	YELLOW
5800	96.2628	89.8970	20.9207	.4649	.4341	.1010	YELLOW
5850	96.6663	89.8885	20.5287	.4666	.4341	.0991	YELLOW
5900	97.0363	89.8053	20.3127	.4684	.4335	.0981	YELLOW
5950	97.3730	89.6471	20.2801	.4697	.4325	.0978	YELLOW
6000	97.6815	89.4122	20.4312	.4707	.4309	.0985	YELLOW
6050	97.9517	89.0980	20.7571	.4714	.4287	.0999	YELLOW
6100	98.2102	88.7810	21.2389	.4718	.4261	.1020	YELLOW
6150	98.4211	88.2168	21.8491	.4721	.4231	.1048	ORANGE
6200	98.5865	87.6406	22.5548	.4722	.4198	.1080	ORANGE
6250	98.6974	86.9689	23.3221	.4723	.4161	.1116	ORANGE
6300	98.7445	86.1938	24.1191	.4723	.4123	.1154	ORANGE
6350	98.7193	85.3145	24.9186	.4724	.4083	.1193	ORANGE
6400	98.6894	84.3283	25.6996	.4726	.4042	.1232	ORANGE
6450	98.4267	83.2363	26.4471	.4729	.4008	.1271	RED
6500	98.1072	82.0431	27.1513	.4733	.3980	.1310	RED
6550	97.6984	80.7583	27.8065	.4737	.3919	.1346	RED
6600	97.1682	79.3958	28.4097	.4741	.3873	.1386	RED
6650	96.5150	77.974"	28.9592	.4744	.3833	.1423	RED
6700	95.7348	76.5145	29.4546	.4746	.3793	.1460	RED
6750	94.8196	75.0411	29.8955	.4747	.3757	.1497	RED
6800	93.7717	73.5778	30.2839	.4745	.3723	.1532	RED
6850	92.5919	72.1478	30.6201	.4743	.3693	.1567	RED
6900	91.2936	70.7725	30.9063	.4731	.3666	.1602	RED
6950	89.8524	69.4712	31.1442	.4717	.3647	.1635	RED
7000	88.3059	68.2610	31.3354	.4708	.3633	.1668	RED
7050	86.6575	67.1570	31.4809	.4677	.3624	.1699	RED
7100	84.9072	66.1721	31.5819	.4648	.3623	.1729	RED
7150	83.0612	65.3179	31.6354	.4615	.3626	.1757	RED
7200	81.1932	64.6040	31.6432	.4576	.3641	.1783	RED
7250	79.2838	64.0385	31.6027	.4532	.3661	.1807	RED
7300	77.3165	63.6278	31.5113	.4483	.3698	.1827	PURPLE
7350	75.3789	63.3759	31.3657	.4431	.3725	.1844	PURPLE
7400	73.4811	63.2850	31.1620	.4376	.3769	.1856	PURPLE
7450	71.6557	63.3547	30.8963	.4319	.3819	.1862	PURPLE
7500	69.9372	63.5820	30.5650	.4262	.3875	.1863	BLUE
7550	68.3511	63.9616	30.1669	.4207	.3936	.1857	BLUE
7600	66.9629	64.4879	29.7013	.4155	.4002	.1843	BLUE GREEN
7650	65.7768	65.1451	29.1746	.4109	.4069	.1822	GREEN
7700	64.8335	65.9277	28.5939	.4069	.4137	.1794	GREEN
7750	64.1618	66.8207	27.9734	.4036	.4204	.1760	GREEN
7800	63.7891	67.8102	27.3306	.4013	.4267	.1720	GREEN
7850	63.7845	68.8813	26.6833	.4000	.4325	.1679	GREEN
7900	63.9307	70.0187	26.0493	.3996	.4376	.1628	GREEN
7950	64.4778	71.2065	25.4443	.4002	.4419	.1579	GREEN
8000	65.3575	72.4285	24.8813	.4016	.4454	.1530	GREEN
8050	66.4043	73.6684	24.3786	.4038	.4480	.1482	GREEN
8100	67.7373	74.9102	23.9197	.4067	.4497	.1436	GREEN

8150	69.2702	76.1379	23.5347	.4100	.4507	.1393	GREEN
8200	70.9834	77.3368	23.2287	.4137	.4509	.1354	GREEN
8250	72.7766	78.4930	22.9827	.4177	.4505	.1319	GREEN
8300	74.6699	79.5941	22.8258	.4216	.4495	.1289	GREEN
8350	76.6256	80.6296	22.7948	.4256	.4480	.1264	GREEN
8400	78.5505	81.5903	22.7737	.4294	.4461	.1248	GREEN
8450	80.4739	82.4688	22.8840	.4331	.4438	.1231	GREEN
8500	82.3695	83.2592	23.0839	.4364	.4412	.1223	GREEN
8550	84.1549	83.9570	23.3673	.4395	.4385	.1220	GREEN
8600	85.8716	84.5592	23.7244	.4423	.4355	.1222	YELLOW
8650	87.4853	85.0637	24.1422	.4448	.4325	.1227	YELLOW
8700	88.9855	85.4696	24.6062	.4470	.4294	.1236	YELLOW
8750	90.3693	85.7765	25.1014	.4490	.4262	.1247	YELLOW
8800	91.6208	85.9849	25.6136	.4508	.4231	.1260	YELLOW
8850	92.7509	86.0955	26.1296	.4525	.4200	.1275	YELLOW
8900	93.7564	86.1092	26.6383	.4540	.4170	.1290	YELLOW
8950	94.6395	86.0275	27.1308	.4554	.4140	.1306	YELLOW
9000	95.4033	85.8521	27.6001	.4566	.4111	.1321	ORANGE
9050	96.0514	85.5854	28.0416	.4581	.4082	.1337	ORANGE
9100	96.5873	85.2305	28.4519	.4593	.4053	.1353	ORANGE
9150	97.0145	84.7916	28.8292	.4606	.4026	.1369	RED
9200	97.3360	84.2741	29.1724	.4618	.3998	.1384	RED
9250	97.5543	83.6847	29.4804	.4628	.3971	.1395	RED
9300	97.6716	83.0314	29.7522	.4641	.3945	.1414	RED
9350	97.6895	82.3234	29.9864	.4652	.3920	.1428	RED
9400	97.6100	81.5709	30.1812	.4662	.3896	.1442	RED
9450	97.4346	80.7847	30.3342	.4672	.3874	.1455	RED
9500	97.1651	79.9756	30.4432	.4681	.3853	.1467	RED
9550	96.8035	79.1541	30.5058	.4689	.3834	.1478	RED
9600	96.3522	78.3300	30.5192	.4695	.3817	.1487	RED
9650	95.8136	77.5121	30.4823	.4701	.3803	.1496	RED
9700	95.1904	76.7086	30.3933	.4706	.3792	.1502	RED
9750	94.4856	75.9263	30.2518	.4709	.3784	.1506	RED
9800	93.7023	75.1714	30.0574	.4710	.3779	.1511	RED
9850	92.8440	74.4501	29.8123	.4710	.3777	.1512	RED
9900	91.9149	73.7666	29.5201	.4709	.3779	.1512	RED
9950	90.9197	73.1256	29.1867	.4705	.3784	.1510	RED
10000	89.8641	72.5312	28.8201	.4700	.3793	.1507	RED

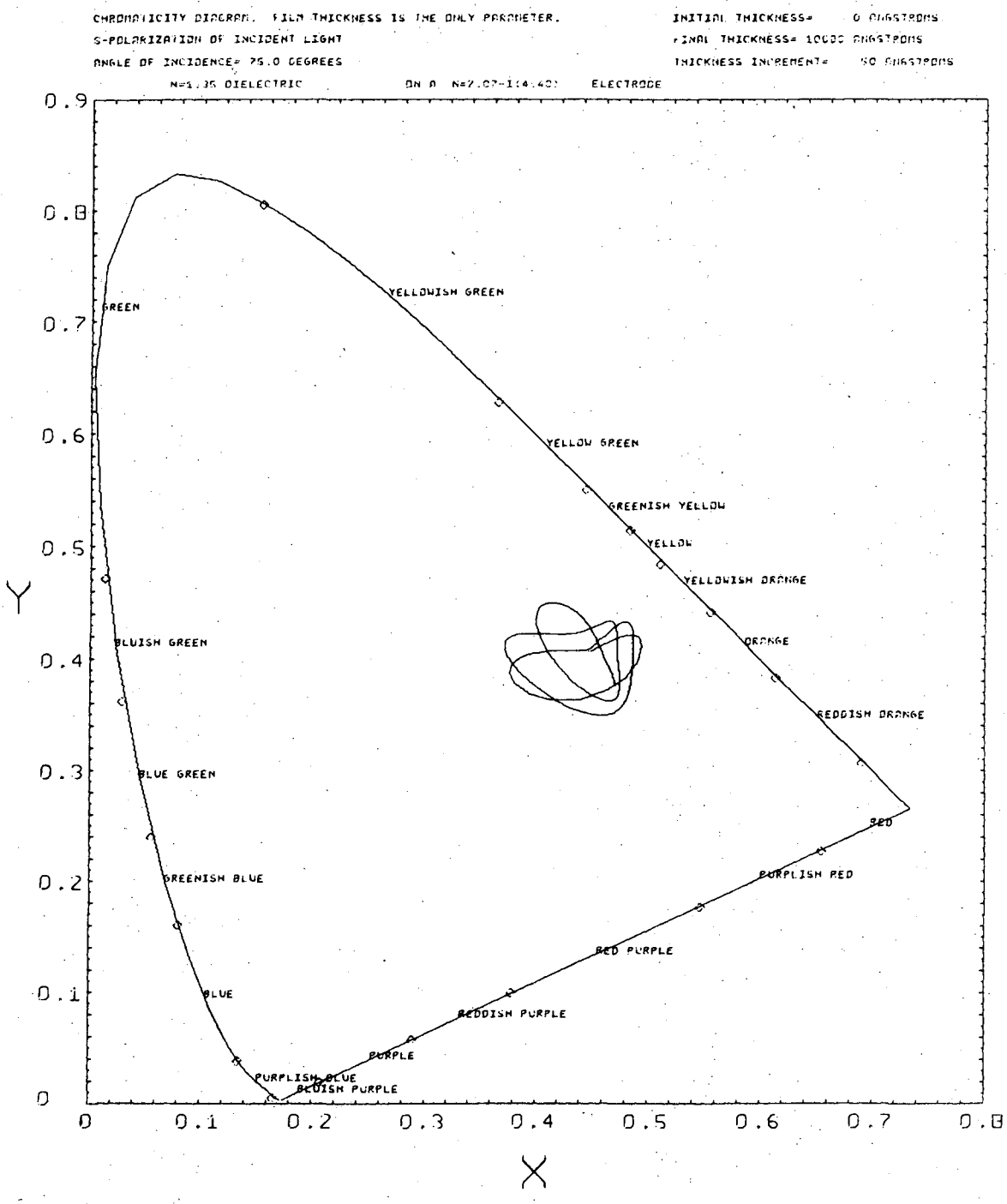
CHROMATICITY DIAGRAM. FILM THICKNESS IS THE ONLY PARAMETER.
S-POLARIZATION OF INCIDENT LIGHT
ANGLE OF INCIDENCE= 75.0 DEGREES
N=1.35 DIELECTRIC
ON A N=2.07-1.14i AG ELECTRODE
INITIAL THICKNESS= 0 ANGSTROMS
FINAL THICKNESS= 10000 ANGSTROMS
THICKNESS INCREMENT= 50 ANGSTROMS
GREEN
YELLOWISH GREEN
YELLOW GREEN
GREENISH YELLOW
YELLOW
YELLOWISH ORANGE
ORANGE
REDDISH ORANGE
RED
PURPLISH RED
RED PURPLE
REDDISH PURPLE
PURPLE
PURPLISH BLUE
BLUISH PURPLE
BLUE
GREENISH BLUE
BLUE GREEN
BLUISH GREEN
Y
X
0
0.1
0.2
0.3
0.4
0.5
0.6
0.7
0.8
0.9

XBL 753-731

APPENDIX III. PROGRAM "MBINT"

This program corresponds to Turney's program "MBINF". It should be noted that corrections and revisions have been made. "MBINT" calculates the multiple-beam intensity of light reflected from a dielectric film on a metal substrate as a function of both wavelength and film thickness. The wavelength is changed in increments of 50Å through the spectrum, while the thickness can be varied in any desired increment. As in the program "HUE", one can include the variation of the optical constants with wavelength or employ a value at an intermediate wavelength. The angles of incidence of the s and p polarizations can be the same or different.

All the film thicknesses at which a minimum or maximum of intensity occurs for each wavelength can be obtained from this program. A thickness difference, Δd, between successive minima or between successive maxima can be derived from Eq. (A-11). The change in the optical path difference is equivalent to a change in phase difference of 2π in Eq. (A-12).

$$2n_1 \cdot \Delta d \cos\phi' = \lambda$$

$$\Delta d = \frac{\lambda}{2n_1 \cos\phi'}$$

For each wavelength, the difference in film thicknesses at which a maximum and a minimum occurs is an odd multiple of $\Delta d/2$. Thus, in order to determine the thicknesses at which the intensity maxima and minima occur for monochromatic light, it is necessary to know only the value of $\Delta d/2$ and the thickness at which the first maximum or minimum occurs.

The output from this program can be used to determine the thickness of a film in white-light interference, if the ratio of reflected light to incident light is measured throughout the visible spectrum (spectral analysis). The wavelengths at which maxima and minima occur in the spectrum are assigned a list of possible film thicknesses based on the program output. One film thickness, corresponding to the spectral composition of the reflected light, is common to all lists. This approach is exact only if the refractive indices of the film and the substrate are constant. When the optical constants vary with wavelength, monochromatic intensity maxima and minima do not coincide with maxima and minima in the spectral intensity distribution. If the output is extensive enough to include the thickness of the film in question, the spectral intensity distribution (with respect to unit incident intensity) is given directly for comparison with the experimentally determined curve. Refer to the sample output, which follows the program.

A list of program variables and a description of the data input immediately follow.

Variables in Program "MBINT"

Variable	Symbol	Description
A,ASQ B,BSQ	A, A^2 B, B^2	Intermediate variables to calculate amplitude reflection coefficients and phase changes (interface 1), Eq. (A-4) and (A-5).
CK1,CK2 CN1,CN2		$k = CK1 + CK2\,(\lambda - 3800)$. $n = CN1 + CN2\,(\lambda - 3800)$. Coefficients for a linear approximation of the complex refractive index of the substrate, $n_c = n - ik$.
CX	$\cos\phi'$	COS(PHIPR(J,M))

Variable	Symbol	Description
DDEL	Δ(rad)	Relative phase change, $\delta_{1,p} - \delta_{1,s}$ (interface 1), Eq. (A-9).
DEL(J,1),DEL(J,2)	$\delta_{1,s}$,$\delta_{1,p}$(rad)	Phase change for s and p polarizations (interface 1), Eqs. (A-8) and (A-10).
DELD(J,1),DELD(J,2)	$\delta_{3,s}$,$\delta_{3,p}$(rad)	Phase change for s and p polarizations (interface 3).
DELT	δ(rad)	Phase change associated with an optical path difference in the film, Eq. (A-12).
DELTA	Δd(Å)	Difference in film thickness at which successive intensity minima or successive intensity maxima occur.
FILM1,FILM2, FILM3,FILM4		Name of film to appear in output.
INT(L)	I	Relative intensity of reflected light in multiple-beam interference, Eq. (A-13).
LAMBDA	λ(Å)	Wavelength that is used in increments of 50Å.
PHI(1),PHI(2)	ϕ(rad)	Angle of incidence for s and p polarizations (interface 3).
PHID(1),PHID(2)	ϕ(deg)	Angle of incidence for s and p polarizations (interface 3).
PHIN	ϕ(deg)	Nominal angle of incidence between s and p polarizations (interface 3).
PHIPR(J,1),PHIPR(J,2)	ϕ'(rad)	Angle of refraction for s and p polarizations (interface 3), Eq. (A-1). Also, angle of incidence (interface 1).
R(J,1),R(J,2)	$r_{1,s}$,$r_{1,p}$	Amplitude reflection coefficient for s and p polarizations (interface 1), Eqs. (A-6) and (A-7).
RSQ(J,1),RSQ(J,2)	$r^2_{1,s}$,$r^2_{1,p}$	Refer to R(J,1) and R(J,2).

Variable	Symbol	Description
RI(N)	n_1	Refractive index of dielectric film at a specified wavelength in the input.
RL(J,1),RL(J,2)	$r_{3,s}$,$r_{3,p}$	Amplitude reflection coefficients for s and p polarizations (interface 3), Eqs. (A-2) and (A-3).
RSQL(J,1),RSQL(J,2)	$r^2_{3,s}$,$r^2_{3,p}$	Refer to RL(J,1) and RL(J,2).
SBSTRA1,SBSTRA2		Name of substrate to appear in output.
SCALE(N)		Refractometer scale reading of liquid film material (Bausch and Lomb precision refractometer with prism 749-1).
SEP	$\Delta\phi$(deg)	Separation between angles of incidence for s and p polarizations.
SX	$\sin\phi'$	SIN(PHIPR(J,M))
THK(L)	d(A)	Film thickness.
THKINC	Δd(A)	Increment of change of film thickness. Not the same as DELTA.
TMN	d(Å)	Initial film thickness.
TMX	d(Å)	final film thickness.
TNA(J),TN TKA(J),TK	n k	Real and imaginary parts of the complex refractive index of the metal substrate, $n_c = n - ik$.
TX	$\tan\phi'$	SX/CX
WAVLTH(N)	λ(Å)	Wavelength associated with the variation of the refractive index of the film material with wavelength in the input.

Input for Program "MBINT"

Explanations of these input variables have been given in the list of variables.

Card	Variable	Units	Column and Format
1	SBSTRA1,SBSTRA2		1-20,2A10
2	FILM1,FILM2 FILM3,FILM4		1-40,4A10
3	CN1	Dimensionless	1-10,F10.7
	CN2	1/Å	11-20,F10.7
	CK1	Dimensionless	21-30,F10.7
	CK2	1/Å	31-40,F10.7
4	PHIN	Degrees	1-10,F10.6
5	SEP	Degrees	1-10,F10.6
6	TMN	Å	1-10,F10.1
	TMX	Å	11-20,F10.1
	THKINC	Å	21-30,F10.1
7*	WAVLTH(N)	Å	1-5,F5.0
	RI(N)	Dimensionless	6-15,F10.5
	SCALE(N)	Dimensionless	16-25,F10.5
8-20	Same as Card 7		

*See footnote for program "HUE".

```
      PROGRAM MBINT (INPUT,OUTPUT,TAPE 98, PLOT, TAPE 99=PLOT)
C
C
C     THIS PROGRAM CALCULATES THE INTENSITY OF REFLECTED LIGHT FROM A
C     DIELECTRIC FILM(NON-ABSORBING) COVERING A METAL(ABSORBING) SUR-
C     FACE.  FOR A SPECIFIED ANGLE OF INCIDENCE, THE INTENSITY OF RE-
C     FLECTED LIGHT IS A PERIODIC FUNCTION OF FILM THICKNESS AT EACH
C     WAVELENGTH, AS WELL AS BEING A PERIODIC FUNCTION OF WAVELENGTH AT
C     EACH FILM THICKNESS.  FROM ONE MAXIMUM OR MINIMUM OF INTENSITY AT
C     EACH WAVELENGTH, ONE CAN CALCULATE ALL THE THICKNESSES FOR WHICH
C     THERE IS A MAXIMUM OR A MINIMUM AT THAT WAVELENGTH.  THE VALUE TO
C     BE USED FOR THIS PURPOSE IS CALCULATED FOR EACH WAVELENGTH.  THE
C     VARIATION OF OPTICAL CONSTANTS OF BOTH THE FILM AND SUBSTRATE WITH
C     WAVELENGTH IS INCLUDED IN THE CALCULATIONS.
C
C
      REAL PHID(2),PHI(2),PHIPR(81,2),TNA(81),TKA(81),RSQ(81,2),R(81,2),
     XDEL(81,2),RL(81,2),RSQL(81,2),DELD(81,2),LAMBDA,INT(10),THK(10)
      DIMENSION WAVLTH(50),RI(50),W(50),RESID(50),S(1),AI(20,6),BI(20),
     XTWVLTH(52),TRI(52),SCALE(50)
      COMMON/RICOM/ BI, NO
      COMMON/CCPOOL/XMIN,XMAX,YMIN,YMAX,CCXMIN,CCXMAX,CCYMIN,CCYMAX
    1 FORMAT(2A10)
    2 FORMAT(4A10)
    3 FORMAT(4F10.7)
    4 FORMAT(F10.6)
   22 FORMAT(3F10.1)
    8 FORMAT(10X,*S POLARIZATION*,5X,*ANGLE OF INCIDENCE IS*,2X,F4.1,//)
    9 FORMAT(10X,*P POLARIZATION*,5X,*ANGLE OF INCIDENCE IS*,2X,F4.1,//)
   18 FORMAT(F5.0,2F10.5)
   31 FORMAT(10X,4A10,*FILM ON A SMOOTH, FLAT*,2A10,*ELECTRODE*)
   41 FORMAT(10X,*INTENSITY AS A FUNCTION OF WAVELENGTH AND FILM THICKNE
     XSS*,///)
   42 FORMAT(10X,*DELTA OR A MULTIPLE THEREOF AT EACH WAVELENGTH IS THE
     XDIFFERENCE IN FILM THICKNESS BETWEEN*)
   43 FORMAT(*TWO MAXIMA OR TWO MINIMA OF INTENSITY.  DELTA/2.0 OR AN OD
     XD MULTIPLE THEREOF IS THE DIFFERENCE IN FILM*)
   44 FORMAT(*THICKNESS BETWEEN A MAXIMUM AND A MINIMUM OF INTENSITY.*,/
     X//)
   46 FORMAT(10X,*COMPLEX REFRACTIVE INDEX OF SUBSTRATE IS  NC=N-I(K).
     XN=CN1+CN2(LAMBDA-3800.)  K=CK1+CK2(LAMBDA-3800.)*)
   45 FORMAT(10X,*LAMBDA IS THE WAVELENGTH BETWEEN 3800. AND 7800. A.
     XCN1=*,F10.7,*  CN2=*,F10.7,*  CK1=*,F10.7,*  CK2=*,F10.7,//)
   47 FORMAT(10X,*REFRACTIVE INDEX OF FILM AT 5892. A IS*,F7.4,//)
   75 FORMAT(1H1,//)
  710 FORMAT(3X,*FILM THICKNESS(A)*,3X,10F10.0,//)
  712 FORMAT(13X,*WAVE-*)
  713 FORMAT(*DELTA(A)*,3X,*LENGTH(A)*,///)
  714 FORMAT(1X,F6.1,6X,F5.0,5X,10F10.4)
C
C
C     INPUTS ARE  (1) THE METAL SUBSTRATE, (2) THE FILM, (3) FOUR COEFF-
C     ICIENTS FOR A LINEAR APPROXIMATION OF THE COMPLEX INDEX OF REFRAC-
C     TION OF THE METAL SUBSTRATE, (4) THE ANGLE OF INCIDENCE, (5) THE
C     ANGULAR SEPARATION BETWEEN THE INCIDENT P AND S-POLARIZED LIGHT,
C     (6) THE INITIAL AND FINAL VALUES OF THE FILM THICKNESS AND THE
C     INCREMENT, (7) THE REFRACTIVE INDEX OR REFRACTOMETER SCALE READING
C     FOR THE FILM AT UP TO 14 WAVELENGTHS.
C
C
      READ 1,SBSTRA1,SBSTRA2
```

```
      READ 2,FILM1,FILM2,FILM3,FILM4
      READ 3,CN1,CN2,CK1,CK2
      READ 4,PHIN
      READ 4,SEP
      READ 22,TMN,TMX,THKINC
C     EITHER 1 OR MANY VALUES OF THE REFRACTIVE INDEX OR REFRACTOMETER
C     SCALE READINGS FOR THE FILM OVER THE VISIBLE RANGE OF LIGHT SHOULD
C     BE ON THE INPUT CARDS.
      DO 401 N=1,14
      READ 18,WAVLTH(N),RI(N),SCALE(N)
      IF (WAVLTH(N).EQ.0000.) GO TO 402
  401 CONTINUE
  402 MI=N-1
      NC=6
C     ENTER RI(N) OR HAVE IT CALCULATED FROM THE REFRACTOMETER SCALE
C     READING.
      DO 403 N=1,MI
      IF (RI(N).EQ.0.0) RI(N)=REFRXC(SCALE(N),WAVLTH(N))
      W(N)=1.0
  403 CONTINUE
C     IF THERE IS ONLY ONE INPUT CARD, THEN THAT REFRACTIVE INDEX IS
C     USED IN THE CALCULATIONS AS AN AVERAGE VALUE TO BE USED WITH EVERY
C     WAVELENGTH IN THE PROGRAM.
      IF (MI.LT.2) GO TO 406
      DO 404 I=1,MI
      WAVLTH(I)=WAVLTH(I)/4000.
  404 CONTINUE
C
C     LEAST SQUARE POLYNOMIAL FIT TO DETERMINE THE COEFFICIENTS FOR THE
C     POLYNOMIAL IN THE FUNCTION RIC(WAVLTH) THAT REPRESENTS THE VARIA-
C     TION OF REFRACTIVE INDEX OF THE FILM WITH WAVELENGTH.  THE RESULT-
C     ING POLYNOMIAL IS PLOTTED ALONG WITH THE SEVERAL INPUT VALUES AS A
C     CHECK ON THE ACCURACY OF THE METHOD OVER THE ENTIRE VISIBLE RANGE.
C
      CALL LSQPOL(WAVLTH,RI,W,RESID,MI,S,1,AI,BI,NO)
      DO 405 I=1,MI
      WAVLTH(I)=WAVLTH(I)*4000.
  405 CONTINUE
      XMIN=3000.
      XMAX=8000.
      YMIN=1.3
      YMAX=1.4
      CALL CCGRID(5,10,6HLABELS,10,10)
      CALL CCPLOT(WAVLTH,RI,MI,6HNOJOIN,6,1)
      TWVLTH(1)=3000.
      DO 30 J=1,51
      TRI(J)=RIC(TWVLTH(J))
      TWVLTH(J+1)=TWVLTH(J)+100.
   30 CONTINUE
      CALL CCPLOT(TWVLTH,TRI,50,4HJOIN,0,1)
      CALL CCEND
      GO TO 407
C     COEFFICIENTS FOR POLYNOMIAL IN FUNCTION RIC(WAVLTH) THAT REPRE-
C     SENTS VARIATION OF REFRACTIVE INDEX OF FILM WITH WAVELENGTH-- IN
C     THE CASE THAT JUST ONE REFRACTIVE INDEX OR REFRACTOMETER SCALE
C     READING AND WAVELENGTH IS IN THE INPUT CARDS.
  406 BI(1)=RI(1)
      BI(2)=0.
      BI(3)=0.
      BI(4)=0.
      BI(5)=0.
      BI(6)=0.
```

```
  407 CONTINUE
      PI=3.1415926536
      PHID(1)=PHIN-0.5*SEP
      PHID(2)=PHIN+0.5*SEP
C     J REFERS TO THE WAVELENGTH.
      DO 399 J=1,81
      LAMBDA=3800.+50.*(J-1)
      DO 10 I=1,2
C     CONVERSION OF ANGLES FROM DEGREES TO RADIANS.
      PHI(I)=0.0174533*PHID(I)
C     EQUATION (A-1)
      PHIPR(J,I)=ASIN((1./RIC(LAMBDA))*SIN(PHI(I)))
   10 CONTINUE
C
C
C     DIELECTRIC FILM REFLECTION EQUATIONS(WITH THE PRESENT SIGN CONVEN-
C     TION- AT NORMAL INCIDENCE THE POSITIVE P-POLARIZATION ELECTRIC
C     FIELD VECTORS OF THE INCIDENT AND REFLECTED LIGHT DO NOT COINCIDE)
C
C
      TEMP1=COS(PHI(1))
      TEMP3=RIC(LAMBDA)*COS(PHIPR(J,1))
C     EQUATION (A-2)
      RL(J,1)=(TEMP1-TEMP3)/(TEMP1+TEMP3)
      RSQL(J,1)=(RL(J,1))**2
      TEMP2=RIC(LAMBDA)*COS(PHI(2))
      TEMP4=COS(PHIPR(J,2))
C     EQUATION (A-3)
      RL(J,2)=(TEMP2-TEMP4)/(TEMP4+TEMP2)
      RSQL(J,2)=(RL(J,2))**2
C
C     SEPARATION OF REFLECTION COEFFICIENT AND PHASE CHANGE AT GAS-FILM
C     INTERFACE.  M=1 FOR S-POLARIZED LIGHT, M=2 FOR P-POLARIZED LIGHT
C
      DO 153 M=1,2
      IF(RL(J,M)) 150,151,152
  150 DELD(J,M)=PI
      RL(J,M)=-RL(J,M)
      GO TO 153
  151 DELD(J,M)=0.
      GO TO 153
  152 DELD(J,M)=0.
  153 CONTINUE
      IF(MI.EQ.1) GO TO 587
  399 CONTINUE
      GO TO 591
  587 CONTINUE
C     ON THE CONDITION THAT ONLY ONE REFRACTIVE INDEX OR REFRACTOMETER
C     SCALE READING IS ON THE INPUT CARDS FOR THE FILM, THE FOLLOWING
C     VALUES ARE CONSTANT AND CAN BE SET EQUAL TO THE FIRST SET OF VAL-
C     UES CALCULATED FOR LAMBDA=3800.  THIS IS DONE TO AVOID UNNECESSARY
C     CALCULATIONS.
      DO 633 M=1,2
      DO 632 J=1,81
      PHIPR(J,M)=PHIPR(1,M)
      DELD(J,M)=DELD(1,M)
      RL(J,M)=RL(1,M)
      RSQL(J,M)=RSQL(1,M)
  632 CONTINUE
  633 CONTINUE
  591 CONTINUE
C
```

```
C
C     SECTION TO CALCULATE METALLIC REFLECTION COEFFICIENT FOR S-POLAR-
C     IZED(M=1) AND P-POLARIZED(M=2) LIGHT.  EQUATION FOR THE VARIATION
C     OF THE COMPLEX REFRACTIVE INDEX WITH WAVELENGTH IS INCLUDED.  COM-
C     PLEX REFRACTIVE INDEX=TNA+I(TKA).
C
C
      DO 400 J=1,81
      LAMBDA=3800.+50.*(J-1)
      TNA(J)=CN1+CN2*(LAMBDA-3800.)
      TKA(J)=CK1+CK2*(LAMBDA-3800.)
      TN=TNA(J)
      TK=TKA(J)
      DO 123 M=1,2
      SX=SIN(PHIPR(J,M))
      CX=COS(PHIPR(J,M))
      TX=SX/CX
C     THE FOLLOWING EXPRESSIONS FOR A AND B ARE EQUIVALENT TO EQUATIONS
C     (A-4) AND (A-5).
      TEMP1=(TN**2-TK**2-RIC(LAMBDA)**2*SX**2)**2+4.*TN**2*TK**2
      TEMP2=TN**2-TK**2-RIC(LAMBDA)**2*SX**2
      TEMP3=2.*RIC(LAMBDA)**2
      ASQ=(SQRT(TEMP1)+TEMP2)/TEMP3
      IF(ASQ) 110,112,112
  110 A=0.
      GO TO 114
  112 A=SQRT(ASQ)
  114 BSQ=(SQRT(TEMP1)-TEMP2)/TEMP3
      IF(BSQ) 116,118,118
  116 B=0.
      GO TO 120
  118 B=SQRT(BSQ)
C
C     EQUATIONS (A-6) AND (A-7)- REFLECTION COEFFICIENTS AT METAL-FILM
C     INTERFACE AND EQUATIONS (A-8), (A-9) AND (A-10)- PHASE CHANGE AT
C     METAL-FILM INTERFACE FOR S AND P LIGHT.
C
  120 IF(M.EQ.1) 121,122
  121 RSQ(J,1)=(ASQ+BSQ-2.0*A*CX+CX*CX)/(ASQ+BSQ+2.0*A*CX+CX*CX)
      IF(RSQ(J,1)) 125,124,124
  125 R(J,1)=0.
      GO TO 126
  124 R(J,1)=SQRT(RSQ(J,1))
  126 CONTINUE
      TEMP1=2.*B*CX
      TEMP2=ASQ+BSQ-CX*CX
      DEL(J,1)=ATAN(-TEMP1/TEMP2)
      IF(DEL(J,1)) 127,127,123
  127 DEL(J,1)=DEL(J,1)+PI
      GO TO 123
  122 TEMP1=(ASQ+BSQ-2.0*A*CX+CX*CX)/(ASQ+BSQ+2.0*A*CX+CX*CX)
      RSQ(J,2)=TEMP1*(ASQ+BSQ-2.0*A*SX*TX+SX*SX*TX*TX)/(ASQ+BSQ+2.0*A*SX
     X*TX+SX*SX*TX*TX)
      IF(RSQ(J,2)) 128,130,130
  128 R(J,2)=0.
      GO TO 132
  130 R(J,2)=SQRT(RSQ(J,2))
  132 CONTINUE
      TEMP1=2.0*B*SX*TX
      TEMP2=ASQ+BSQ-SX*SX*TX*TX
      DDEL=ATAN(-TEMP1/TEMP2)
      IF(DDEL) 135,136,136
```

```
  135 DDEL=DDEL+PI
  136 CONTINUE
      TEMP1=2.0*B*CX
      TEMP2=ASQ+BSQ-CX*CX
      TEMP3=ATAN(-TEMP1/TEMP2)
      IF(TEMP3) 145,145,146
  145 TEMP3=TEMP3+PI
  146 DEL(J,2)=TEMP3+DDEL
  123 CONTINUE
      IF((CN2.EQ.0.0).AND.(CK2.EQ.0.0).AND.(MI.EQ.1)) GO TO 595
  400 CONTINUE
      GO TO 596
  595 CONTINUE
C     ON THE CONDITIONS THAT ONLY ONE REFRACTIVE INDEX OR REFRACTOMETER
C     SCALE READING IS ON THE INPUT CARDS AND THE COMPLEX REFRACTIVE
C     INDEX OF THE METAL SUBSTRATE IS CONSTANT, THE FOLLOWING VALUES ARE
C     CONSTANT AND CAN BE SET EQUAL TO THE FIRST SET OF VALUES CALCULA-
C     TED FOR LAMBDA=3800.  THIS IS DONE TO AVOID UNNECESSARY CALCULATIONS.
      DO 597 M=1,2
      DO 598 J=1,81
      DEL(J,M)=DEL(1,M)
      R(J,M)=R(1,M)
      RSQ(J,M)=RSQ(1,M)
  598 CONTINUE
  597 CONTINUE
  596 CONTINUE
C
C
C     SECTION TO CALCULATE INTENSITY OF LIGHT REFLECTED FROM THE FILM
C     COVERED METAL SURFACE AS A FUNCTION OF WAVELENGTH AT EACH FILM
C     THICKNESS.  L REFERS TO THE FILM THICKNESS, J REFERS TO THE WAVE-
C     LENGTH, AND M REFERS TO THE S-POLARIZED(M=1) OR P-POLARIZED(M=2)
C     LIGHT.
C
C
      DO 212 M=1,2
      PRINT 31,FILM1,FILM2,FILM3,FILM4,SBSTRA1,SBSTRA2
      PRINT 46
      PRINT 45,CN1,CN2,CK1,CK2
      RIC=RIC(5892.)
      PRINT 47,RIC
      PRINT 41
      PRINT 42
      PRINT 43
      PRINT 44
      IF(M.EQ.1) 311,312
  311 PRINT 8,PHID(M)
      GO TO 313
  312 CONTINUE
      PRINT 9,PHIC(M)
  313 CONTINUE
      TADD=TMN
      DO 750 N=1,100
      DO 675 L=1,10
      THK(L)=THKINC*(L-1)+TADD
      IF(THK(L).GT.TMX) GO TO 515
  675 CONTINUE
      TADD=THK(L)+THKINC
      PRINT 710,(THK(L),L=1,10)
      PRINT 712
      PRINT 713
C     DELTA FOR EACH WAVELENGTH IS A THICKNESS INCREMENT DERIVED EITHER
```

```
C      FROM THE RIGHT SIDE OF EQUATION (A-11) BEING SET EQUAL TO THE
C      WAVELENGTH OR FROM THE RIGHT SIDE OF EQUATION (A-12) BEING SET
C      EQUAL TO 2.*PI RADIANS.
       DO 213 J=1,81
       LAMBDA=3800.+50.*(J-1)
       DELTA=LAMBDA/(2.0*RIC(LAMBDA)*COS(PHIPR(J,M)))
       DO 211 L=1,10
       DELT=4.0*PI*RIC(LAMBDA)*THK(L)*COS(PHIPR(J,M))/LAMBDA
       TEMP1=2.0*R(J,M)*PL(J,M)*COS(DELT+DELD(J,M)-DEL(J,M))
       TEMP2=RSQ(J,M)+RSQL(J,M)+TEMP1
       TEMP3=1.0+RSQ(J,M)*RSQL(J,M)+TEMP1
       INT(L)=TEMP2/TEMP3
  211  CONTINUE
       PRINT 714,DELTA,LAMBDA,(INT(L),L=1,10)
  213  CONTINUE
       PRINT 75
  750  CONTINUE
  515  CONTINUE
  212  CONTINUE
       STOP
       END
```

N=1.35 DIELECTRIC FILM ON A SMOOTH, FLAT N=2.07-I(4.40) ELECTRODE
COMPLEX REFRACTIVE INDEX OF SUBSTRATE IS NC=N-I(K). N=CN1+CN2(LAMBDA-3600.) K=CK1+CK2(LAMBDA-3600.)
LAMBDA IS THE WAVELENGTH BETWEEN 3600. AND 7000. A. CN1= 2.0700000 CN2= 0.0000000 CK1= 4.4000000 CK2= 0.0000000

REFRACTIVE INDEX OF FILM AT 5892. A IS 1.3500

INTENSITY AS A FUNCTION OF WAVELENGTH AND FILM THICKNESS

DELTA OR A MULTIPLE THEREOF AT EACH WAVELENGTH IS THE DIFFERENCE IN FILM THICKNESS BETWEEN TWO MAXIMA OR TWO MINIMA OF INTENSITY. DELTA/2.0 OR AN ODD MULTIPLE THEREOF IS THE DIFFERENCE IN FILM THICKNESS BETWEEN A MAXIMUM AND A MINIMUM OF INTENSITY.

S POLARIZATION ANGLE OF INCIDENCE IS 75.0

FILM THICKNESS(A)		0	100	200	300	400	500	600	700	800	900
DELTA(A)	WAVE-LENGTH(A)										
2814.8	3800	.9172	.9111	.9002	.8821	.8529	.8058	.7247	.5925	.4145	.3178
2841.1	3850	.9172	.9112	.9009	.8830	.8548	.8089	.7325	.6078	.4327	.3183
2867.6	3900	.9172	.9113	.9889	.8838	.8566	.8126	.7399	.6207	.4518	.3220
2894.1	3950	.9172	.9114	.9012	.8846	.8583	.8161	.7468	.6335	.4691	.3286
2920.6	4000	.9172	.9115	.9015	.8854	.8599	.8193	.7533	.6456	.4868	.3376
2947.1	4050	.9172	.9116	.9018	.8861	.8615	.8225	.7594	.6578	.5041	.3487
2973.6	4100	.9172	.9117	.9021	.8868	.8630	.8254	.7651	.6677	.5204	.3615
3000.1	4150	.9172	.9118	.9024	.8875	.8644	.8282	.7705	.6778	.5369	.3757
3026.6	4200	.9172	.9119	.9027	.8882	.8657	.8308	.7756	.6872	.5523	.3907
3053.1	4250	.9172	.9120	.9030	.8888	.8670	.8334	.7804	.6962	.5670	.4064
3079.7	4300	.9172	.9120	.9032	.8894	.8682	.8357	.7850	.7045	.5810	.4225
3106.2	4350	.9172	.9121	.9033	.8900	.8694	.8380	.7893	.7125	.5943	.4388
3132.7	4400	.9172	.9122	.9037	.8905	.8706	.8402	.7933	.7199	.6070	.4550
3159.2	4450	.9172	.9123	.9040	.8911	.8716	.8423	.7972	.7270	.6190	.4711
3185.7	4500	.9172	.9123	.9042	.8916	.8727	.8442	.8008	.7336	.6304	.4868
3212.2	4550	.9172	.9124	.9044	.8921	.8737	.8461	.8043	.7399	.6412	.5022
3238.7	4600	.9172	.9125	.9046	.8926	.8747	.8479	.8076	.7458	.6514	.5172
3265.2	4650	.9172	.9126	.9048	.8931	.8756	.8497	.8108	.7515	.6611	.5316
3291.7	4700	.9172	.9126	.9050	.8935	.8765	.8513	.8138	.7568	.6703	.5455
3318.2	4750	.9172	.9127	.9052	.8940	.8773	.8529	.8166	.7619	.6790	.5589
3344.7	4800	.9172	.9127	.9054	.8944	.8782	.8544	.8193	.7667	.6872	.5717
3371.2	4850	.9172	.9128	.9056	.8948	.8790	.8559	.8220	.7713	.6951	.5840
3397.7	4900	.9172	.9129	.9058	.8952	.8797	.8573	.8244	.7756	.7025	.5958
3424.3	4950	.9172	.9129	.9060	.8956	.8805	.8586	.8268	.7797	.7095	.6070
3450.8	5000	.9172	.9130	.9061	.8959	.8812	.8599	.8291	.7837	.7162	.6177
3477.3	5050	.9172	.9130	.9063	.8963	.8819	.8612	.8313	.7874	.7226	.6279
3503.8	5100	.9172	.9131	.9065	.8967	.8825	.8624	.8334	.7910	.7287	.6377
3530.3	5150	.9172	.9131	.9066	.8970	.8832	.8635	.8354	.7945	.7344	.6469
3556.8	5200	.9172	.9132	.9068	.8973	.8838	.8646	.8373	.7977	.7399	.6558
3583.3	5250	.9172	.9132	.9069	.8976	.8844	.8657	.8391	.8008	.7451	.6642
3609.8	5300	.9172	.9133	.9071	.8980	.8850	.8668	.8409	.8038	.7501	.6723
3636.3	5350	.9172	.9133	.9072	.8983	.8856	.8678	.8426	.8067	.7549	.6799
3662.8	5400	.9172	.9134	.9073	.8985	.8861	.8687	.8442	.8094	.7594	.6872
3689.3	5450	.9172	.9134	.9075	.8988	.8867	.8697	.8458	.8121	.7637	.6942
3715.8	5500	.9172	.9134	.9076	.8991	.8872	.8706	.8473	.8146	.7679	.7009
3742.3	5550	.9172	.9135	.9077	.8994	.8877	.8714	.8488	.8170	.7718	.7072
3768.8	5600	.9172	.9135	.9079	.8996	.8882	.8723	.8502	.8193	.7756	.7133
3795.4	5650	.9172	.9136	.9080	.8999	.8886	.8731	.8516	.8216	.7792	.7191
3821.9	5700	.9172	.9136	.9081	.9002	.8891	.8739	.8529	.8237	.7827	.7247
3848.4	5750	.9172	.9136	.9082	.9004	.8895	.8747	.8542	.8258	.7861	.7300
3874.9	5800	.9172	.9137	.9083	.9006	.8900	.8754	.8554	.8278	.7893	.7350
3901.4	5850	.9172	.9137	.9084	.9008	.8904	.8761	.8566	.8297	.7923	.7399
3927.9	5900	.9172	.9138	.9085	.9011	.8908	.8768	.8577	.8316	.7953	.7446
3954.4	5950	.9172	.9138	.9086	.9013	.8912	.8775	.8589	.8334	.7981	.7490
3980.9	6000	.9172	.9138	.9087	.9015	.8916	.8782	.8599	.8351	.8008	.7533
4007.4	6050	.9172	.9139	.9088	.9017	.8920	.8788	.8610	.8367	.8035	.7574
4033.9	6100	.9172	.9139	.9089	.9019	.8924	.8794	.8620	.8383	.8060	.7613
4060.4	6150	.9172	.9139	.9090	.9021	.8927	.8800	.8630	.8399	.8084	.7651
4086.9	6200	.9172	.9140	.9091	.9023	.8931	.8806	.8639	.8414	.8108	.7688
4113.4	6250	.9172	.9140	.9092	.9025	.8934	.8812	.8648	.8428	.8130	.7723
4140.0	6300	.9172	.9140	.9093	.9027	.8937	.8817	.8657	.8442	.8152	.7756
4166.5	6350	.9172	.9141	.9094	.9029	.8941	.8823	.8666	.8456	.8173	.7788
4193.0	6400	.9172	.9141	.9095	.9031	.8944	.8828	.8674	.8469	.8193	.7820
4219.5	6450	.9172	.9141	.9096	.9032	.8947	.8833	.8682	.8482	.8213	.7850
4246.0	6500	.9172	.9141	.9097	.9034	.8950	.8838	.8690	.8494	.8232	.7879
4272.5	6550	.9172	.9142	.9097	.9036	.8953	.8843	.8698	.8506	.8250	.7906
4299.0	6600	.9172	.9142	.9098	.9037	.8956	.8848	.8706	.8518	.8268	.7933
4325.5	6650	.9172	.9142	.9099	.9039	.8958	.8852	.8713	.8529	.8285	.7959
4352.0	6700	.9172	.9143	.9100	.9040	.8961	.8857	.8720	.8540	.8302	.7984
4378.5	6750	.9172	.9143	.9100	.9042	.8964	.8861	.8727	.8551	.8318	.8008
4405.0	6800	.9172	.9143	.9101	.9043	.8967	.8866	.8734	.8561	.8334	.8032
4431.5	6850	.9172	.9143	.9102	.9045	.8969	.8870	.8740	.8571	.8349	.8054
4458.0	6900	.9172	.9144	.9103	.9046	.8972	.8874	.8747	.8581	.8363	.8076
4484.6	6950	.9172	.9144	.9103	.9048	.8974	.8878	.8753	.8590	.8377	.8097
4511.1	7000	.9172	.9144	.9104	.9049	.8976	.8882	.8759	.8599	.8391	.8118
4537.6	7050	.9172	.9144	.9105	.9050	.8979	.8885	.8765	.8608	.8405	.8138
4564.1	7100	.9172	.9145	.9105	.9052	.8981	.8889	.8770	.8617	.8418	.8157
4590.6	7150	.9172	.9145	.9106	.9053	.8983	.8893	.8776	.8625	.8430	.8176
4617.1	7200	.9172	.9145	.9107	.9054	.8985	.8896	.8782	.8634	.8442	.8193
4643.6	7250	.9172	.9145	.9107	.9056	.8988	.8900	.8787	.8642	.8454	.8211
4670.1	7300	.9172	.9145	.9108	.9057	.8990	.8903	.8792	.8650	.8466	.8228
4696.6	7350	.9172	.9146	.9108	.9058	.8992	.8907	.8797	.8657	.8477	.8244
4723.1	7400	.9172	.9146	.9109	.9059	.8994	.8910	.8802	.8665	.8488	.8260
4749.6	7450	.9172	.9146	.9110	.9060	.8996	.8913	.8807	.8672	.8499	.8276
4776.1	7500	.9172	.9146	.9110	.9061	.8998	.8916	.8812	.8679	.8509	.8291
4802.6	7550	.9172	.9146	.9111	.9062	.9000	.8919	.8816	.8686	.8519	.8306
4829.2	7600	.9172	.9147	.9111	.9064	.9002	.8922	.8821	.8693	.8529	.8320
4855.7	7650	.9172	.9147	.9112	.9065	.9003	.8925	.8825	.8699	.8539	.8334
4882.2	7700	.9172	.9147	.9112	.9066	.9005	.8928	.8830	.8706	.8548	.8347
4908.7	7750	.9172	.9147	.9113	.9067	.9007	.8931	.8834	.8712	.8557	.8360
4935.2	7800	.9172	.9147	.9113	.9068	.9009	.8933	.8838	.8718	.8566	.8373

APPENDIX IV. PROGRAM "VIS"

This program calculates the minimum and maximum intensities and Michelson fringe visibility for multiple-beam interference in a thin dielectric film on a metal substrate. These quantities are calculated through Eqs. (A-20), (A-21) and (A-22), respectively, for angles of incidence that can be changed in any increment. The criterion for the optimum angle of incidence for monochromatic light is that the fringe visibility is equal to one, or equivalently the minimum intensity is equal to zero. The optimum angle varies with wavelength only because the optical constants of the film and substrate are functions of wavelength. Thus, a single wavelength is part of the input along with coefficients for a linear approximation to the real and imaginary parts of the refractive index of the substrate and either the refractive indices or refractometer scale readings of the film at several wavelengths through the visible spectrum. Further details on the calculation of the optical constants have been given in Appendix II.

A list of program variables and a description of the data input are presented first. A sample output follows the program.

Variables in Program "VIS"

Variable	Symbol	Description
A,ASQ B,BSQ	A, A^2 B, B^2	Intermediate variables to calculate amplitude reflection coefficients and phase changes (interface 1), Eqs. (A-4) and (A-5).
AMN	ϕ(deg)	Initial angle of incidence.

Variable	Symbol	Description
CK1,CK2 CN1,CN2		$k = CK1 + CK2\ (\lambda - 3800)$. $n = CN1 + CN2\ (\lambda - 3800)$. Coefficients for a linear approximation of the complex refractive index of the substrate, $n_c = n - ik$.
CX	$\cos\phi'$	COS(PHIPR)
FILM1,FILM2, FILM3,FILM4		Name of film to be printed in output.
LAMBDA	λ(Å)	Single wavelength to be used in the program.
MINT(J,1),MINT(J,2)	I_{min}	Minimum intensity in multiple-beam interference for s and p polarizations, Eq. (A-20).
MXINT(J,1),MXINT(J,2)	I_{max}	Maximum intensity in multiple-beam interference for s and p polarizations, Eq. (A-21).
NTOT		Number of angles of incidence (one more than the number of increments added to initial angle of incidence).
PHI	ϕ(rad)	Angle of incidence (interface 3).
PHID	ϕ(deg)	Angle of incidence (interface 3).
PHIPR	ϕ'(rad)	Angle of refraction (interface 3), Eq. (A-1). Also, angle of incidence (interface 1).
R(J,1),R(J,2)	$r_{1,s}, r_{1,p}$	Amplitude reflection coefficients for s and p polarizations (interface 1), Eqs. (A-6) and A-7).
RI(N)	n_1	Refractive index of dielectric film at a specified wavelength in the input.
RID	n_1	Refractive index of dielectric film calculated from function RIC(WAVLTH) at wavelength, LAMBDA.
RL(J,1),RL(J,2)	$r_{3,s}, r_{3,p}$	Amplitude reflection coefficients for s and p polarizations (interface 3), Eqs. (A-2) and (A-3).

Variable	Symbol	Description
SBSTRA1,SBSTRA2		Name of substrate to appear in output.
SCALE(N)		Refractometer scale reading of liquid film material (Bausch and Lomb precision refractometer with prism, 749-1).
STEPS	$\Delta\phi$(deg)	Increment of change of angle of incidence
SX	$\sin\phi'$	SIN(PHIPR)
TN,TK	n,k	Real and imaginary parts of the complex refractive index of the metal substrate, $n_c = n - ik$.
TX	$\tan\phi'$	SX/CX
VISIB(J,1),VISIB(J,2)	V	Michelson fringe visibility for s and p polarizations, Eq. (A-22).
WAVLTH(N)		Wavelength associated with the variation of the refractive index of the film material with wavelength in the input.

Input for Program "VIS"

Explanations of these input variables have been given in the list of variables.

Card	Variable	Units	Column and Format
1	SUBSTRA1,SBSTRA2		1-20,2A10
2	FILM1,FILM2, FILM3,FILM4		1-40,4A10
3	CN1	Dimensionless	1-10,F10.7
	CN2	1/Å	11-20,F10.7
	CK1	Dimensionless	21-30,F10.7
	CK2	1/Å	31-40,F10.7
4	AMN	Degrees	1-10,F10.2
	STEPS	Degrees	11-20,F10.2

Card	Variable	Units	Column and Format
	NTOT		21-23,I3*
5	LAMBDA	Å	1-5,F5.0
6	WAVLTH(N)	Å	1-5,F5.0
	RI(N)	Dimensionless	6-15,F10.5
	SCALE(N)	Dimensionless	16-25,F10.5
7 to 19**	Same as card 6		

*Integers must be written at the far right of the field.

**See footnote for program "HUE". If one card is used, then the value of WAVLTH(1) should be equal to LAMBDA in the input.

```
      PROGRAM VIS (INPUT,OUTPUT,TAPE 98, PLOT, TAPE 99=PLOT)
C
C
C     THIS PROGRAM CALCULATES THE MICHELSON FRINGE VISIBILITY FOR LIGHT
C     REFLECTED FROM A DIELECTRIC FILM(NON-ABSORBING) COVERING A METAL
C     (ABSORBING) SURFACE.  THE INTENSITY OF REFLECTED LIGHT IS A PER-
C     IODIC FUNCTION OF FILM THICKNESS AT EACH WAVELENGTH AND ANGLE OF
C     INCIDENCE.  THE MAXIMUM AND MINIMUM INTENSITIES AND FRINGE VISI-
C     BILITY ARE CALCULATED AT ANGLES OF INCIDENCE BETWEEN ZERO AND
C     NINETY DEGREES FOR MONOCHROMATIC LIGHT.  PROVISION IS MADE TO IN-
C     CORPORATE THE VARIATION OF OPTICAL CONSTANTS OF BOTH THE FILM AND
C     SUBSTRATE WITH WAVELENGTH.
C
C
      REAL RSQ(100,2),R(100,2),RL(100,2),LAMBDA,MXINT(100,2),MINT(100,2)
     X,VISIB(100,2)
      DIMENSION WAVLTH(50),RI(50),W(50),RESID(50),S(1),AI(20,6),BI(20),
     XTWVLTH(52),TRI(52),SCALE(50)
      COMMON/RICOM/BI,NO
      COMMON/CCPOOL/XMIN,XMAX,YMIN,YMAX,CCXMIN,CCXMAX,CCYMIN,CCYMAX
C
C
C     INPUTS ARE  (1) THE METAL SUBSTRATE, (2) THE FILM, (3) FOUR COEF-
C     FICIENTS FOR A LINEAR APPROXIMATION OF THE COMPLEX INDEX OF RE-
C     FRACTION OF THE METAL SUBSTRATE, (4) THE INITIAL ANGLE OF INCI-
C     DENCE, THE STEP CHANGE AND THE NUMBER OF ANGLES, (5) SINGLE WAVE-
C     LENGTH TO BE USED IN THE PROGRAM, (6) THE REFRACTIVE INDEX OR RE-
C     FRACTOMETER SCALE READINGS FOR THE FILM AT UP TO 14 WAVELENGTHS.
C
C
    1 FORMAT(2A10)
    2 FORMAT(4A10)
    3 FORMAT(4F10.7)
   31 FORMAT(10X,4A10,*FILM ON A SMOOTH, FLAT*,2A10,*ELECTRODE*)
   29 FORMAT(10X,*MAXIMUM AND MINIMUM INTENSITIES ALONG THE FILM AND MON
     XOCHROMATIC FRINGE VISIBILITY AS A FUNCTION OF ANGLE OF INCIDENCE*)
   28 FORMAT(10X,*FOR BOTH P AND S-POLARIZED LIGHT*)
   46 FORMAT(10X,*COMPLEX REFRACTIVE INDEX OF SUBSTRATE IS  NC=N-I(K).
     XN=CN1+CN2(LAMBDA-3800.)  K=CK1+CK2(LAMBDA-3800.)*)
   45 FORMAT(10X,*LAMBDA IS THE WAVELENGTH BETWEEN 3800. AND 7800. A.
     XCN1=*,F10.7,*  CN2=*,F10.7,*  CK1=*,F10.7,*  CK2=*,F10.7,//)
   40 FORMAT(10X,*WAVELENGTH IS*,F6.0,1X,*A*)
   41 FORMAT(10X,*REFRACTIVE INDEX OF FILM IS*,F7.4)
   42 FORMAT(10X,*COMPLEX REFRACTIVE INDEX OF SUBSTRATE-  N=*,F7.4,4X,*K
     X=*,F8.4,////)
   32 FORMAT(9X,*ANGLE*,18X,*MINIMUM*,25X,*MAXIMUM*,23X,*VISIBILITY*,//)
   33 FORMAT(27X,*S*,15X,*P*,15X,*S*,15X,*P*,15X,*S*,15X,*P*,//)
   34 FORMAT(10X,F5.2,6F16.5)
   22 FORMAT(2F10.2,I3)
   44 FORMAT(F5.0)
   18 FORMAT(F5.0,2F10.5)
      READ 1,SBSTRA1,SBSTRA2
      READ 2,FILM1,FILM2,FILM3,FILM4
      READ 3,CN1,CN2,CK1,CK2
      READ 22,AMN,STEPS,NTOT
      READ 44,LAMBDA
C     EITHER 1 OR MANY VALUES OF THE REFRACTIVE INDEX OR REFRACTOMETER
C     SCALE READINGS FOR THE FILM OVER THE VISIBLE RANGE OF LIGHT SHOULD
C     BE ON THE INPUT CARDS.
      DO 401 N=1,14
      READ 18,WAVLTH(N),RI(N),SCALE(N)
```

```
      IF (WAVLTH(N).EQ.0000.) GO TO 402
  401 CONTINUE
  402 MI=N-1
      NC=6
C     ENTER RI(N) OR HAVE IT CALCULATED FROM THE REFRACTOMETER SCALE
C     READING.
      DO 403 N=1,MI
      IF (RI(N).EQ.0.0) RI(N)=REFRXC(SCALE(N),WAVLTH(N))
      W(N)=1.0
  403 CONTINUE
C     IF THERE IS ONLY ONE INPUT CARD, THEN THAT REFRACTIVE INDEX AND
C     WAVELENGTH IS USED IN THE CALCULATIONS.  IT CORRESPONDS TO THE
C     INPUT WAVELENGTH(LAMBDA).
      IF (MI.LT.2) GO TO 406
      DO 404 I=1,MI
      WAVLTH(I)=WAVLTH(I)/4000.
  404 CONTINUE
C
C     LEAST SQUARE POLYNOMIAL FIT TO DETERMINE THE COEFFICIENTS FOR THE
C     POLYNOMIAL IN THE FUNCTION RIC(WAVLTH) THAT REPRESENTS THE VARIA-
C     TION OF REFRACTIVE INDEX OF THE FILM WITH WAVELENGTH.  THE RESULT-
C     ING POLYNOMIAL IS PLOTTED ALONG WITH THE SEVERAL INPUT VALUES AS A
C     CHECK ON THE ACCURACY OF THE METHOD OVER THE ENTIRE VISIBLE RANGE.
C
      CALL LSQPOL(WAVLTH,RI,W,RESID,MI,S,1,AI,BI,6)
      DO 405 I=1,MI
      WAVLTH(I)=WAVLTH(I)*4000.
  405 CONTINUE
      XMIN=3000.
      XMAX=8000.
      YMIN=1.3
      YMAX=1.4
      CALL CCGRID(5,10,6HLABELS,10,10)
      CALL CCPLOT(WAVLTH,RI,MI,6HNOJOIN,6,1)
      TWVLTH(1)=3800.
      DO 30 J=1,41
      TRI(J)=RIC(TWVLTH(J))
      TWVLTH(J+1)=TWVLTH(J)+100.
   30 CONTINUE
      CALL CCPLOT(TWVLTH,TRI,50,4HJOIN,0,1)
      CALL CCEND
      GO TO 407
C     COEFFICIENTS FOR POLYNOMIAL IN FUNCTION RIC(WAVLTH) THAT REPRE-
C     SENTS VARIATION OF REFRACTIVE INDEX OF FILM WITH WAVELENGTH-- IN
C     THE CASE THAT JUST ONE REFRACTIVE INDEX OR REFRACTOMETER SCALE
C     READING AND WAVELENGTH IS IN THE INPUT CARDS.
  406 BI(1)=RI(1)
      BI(2)=0.
      BI(3)=0.
      BI(4)=0.
      BI(5)=0.
      BI(6)=0.
  407 CONTINUE
      PRINT 31,FILM1,FILM2,FILM3,FILM4,SBSTRA1,SBSTRA2
      PRINT 29
      PRINT 28
      PRINT 46
      PRINT 45,CN1,CN2,CK1,CK2
      PRINT 40,LAMBDA
      RID=RIC(LAMBDA)
      PRINT 41,RID
      TN=CN1+CN2*(LAMBDA-3800.)
```

```
      TK=CK1+CK2*(LAMBDA-3800.)
      PRINT 42,TN,TK
      PRINT 32
      PRINT 33
C     J REFERS TO THE ANGLE OF INCIDENCE WHICH IS BEING CHANGED IN
C     INCREMENTS.
      DO 213 J=1,NTOT
      PHID=AMN+(J-1)*STEPS
C     CONVERSION OF ANGLES FROM DEGREES TO RADIANS
      PHI=0.0174533*PHID
C     EQUATION (A-1)
      PHIPR=ASIN((1./RID)*SIN(PHI))
C     DIELECTRIC FILM REFLECTION EQUATIONS(WITH THE PRESENT SIGN CONVEN-
C     TION- AT NORMAL INCIDENCE THE POSITIVE P-POLARIZATION ELECTRIC
C     FIELD VECTORS OF THE INCIDENT AND REFLECTED LIGHT DO NOT COINCIDE)
      TEMP1=COS(PHI)
      TEMP3=RID*COS(PHIPR)
C     EQUATION (A-2)
      RL(J,1)=(TEMP1-TEMP3)/(TEMP1+TEMP3)
      TEMP2=RID*COS(PHI)
      TEMP4=COS(PHIPR)
C     EQUATION (A-3)
      RL(J,2)=(TEMP2-TEMP4)/(TEMP4+TEMP2)
C
C     SEPARATION OF REFLECTION COEFFICIENT AND PHASE CHANGE AT GAS-FILM
C     INTERFACE.  PHASE CHANGE IS NOT NEEDED IN THIS PROGRAM.
C     M=1 FOR S-POLARIZED LIGHT, M=2 FOR P-POLARIZED LIGHT
C
      DO 153 M=1,2
      IF(RL(J,M)) 152,153,153
  152 RL(J,M)=-RL(J,M)
  153 CONTINUE
C
C     SECTION TO CALCULATE METALLIC REFLECTION COEFFICIENT FOR S-POLAR-
C     IZED(M=1) AND P-POLARIZED(M=2) LIGHT.  EQUATION FOR THE VARIATION
C     OF THE COMPLEX REFRACTIVE INDEX WITH WAVELENGTH WAS INTRODUCED
C     EARLIER.  COMPLEX REFRACTIVE INDEX= TN+I(TK)
C
      SX=SIN(PHIPR)
      CX=COS(PHIPR)
      TX=SX/CX
C     THE FOLLOWING EXPRESSIONS FOR A AND B ARE EQUIVALENT TO EQUATIONS
C     (A-4) AND (A-5).
      TEMP1=(TN**2-TK**2-RID**2*SX**2)**2+4.*TN**2*TK**2
      TEMP2=TN**2-TK**2-RID**2*SX**2
      TEMP3=2.*RID**2
      ASQ=(SQRT(TEMP1)+TEMP2)/TEMP3
      IF(ASQ) 110,112,112
  110 A=0.
      GO TO 114
  112 A=SQRT(ASQ)
  114 BSQ=(SQRT(TEMP1)-TEMP2)/TEMP3
C     EQUATIONS (A-6) AND (A-7)- REFLECTION COEFFICIENTS AT METAL-FILM
C     INTERFACE FOR S AND P-POLARIZED LIGHT.
      RSQ(J,1)=(ASQ+BSQ-2.0*A*CX+CX*CX)/(ASQ+BSQ+2.0*A*CX+CX*CX)
      IF(RSQ(J,1)) 125,124,124
  125 R(J,1)=0.
      GO TO 126
  124 R(J,1)=SQRT(RSQ(J,1))
  126 CONTINUE
      RSQ(J,2)=RSQ(J,1)*(ASQ+BSQ-2.0*A*SX*TX+SX*SX*TX*TX)/(ASQ+BSQ+2.0*A
     X*SX*TX+SX*SX*TX*TX)
```

```
      IF(RSQ(J,2)) 128,130,130
  128 R(J,2)=0.
      GO TO 132
  130 R(J,2)=SQRT(RSQ(J,2))
  132 CONTINUE
C
C     SECTION TO CALCULATE MAXIMUM AND MINIMUM INTENSITIES OF REFLECTED
C     LIGHT ALONG A TAPERED FILM AND THE MICHELSON FRINGE VISIBILITY AS
C     A FUNCTION OF ANGLE OF INCIDENCE.  EQUATIONS (A-20), (A-21) AND
C     (A-22) ARE USED.  AGAIN, M=1 REPRESENTS S-POLARIZED LIGHT AND M=2
C     REPRESENTS P-POLARIZED LIGHT.
C
      DO 250 M=1,2
      MINT(J,M)=((R(J,M)-RL(J,M))/(1.0-R(J,M)*RL(J,M)))**2
      MXINT(J,M)=((R(J,M)+RL(J,M))/(1.0+R(J,M)*RL(J,M)))**2
      VISIB(J,M)=(MXINT(J,M)-MINT(J,M))/(MXINT(J,M)+MINT(J,M))
  250 CONTINUE
      PRINT 34,PHID,MINT(J,1),MINT(J,2),MXINT(J,1),MXINT(J,2),VISIB(J,1)
     X,VISIB(J,2)
  213 CONTINUE
      STOP
      END
```

N=1.35 DIELECTRIC FILM ON A SMOOTH, FLAT N=2.07-I(4.40) ELECTRODE
MAXIMUM AND MINIMUM INTENSITIES ALONG THE FILM AND MONOCHROMATIC FRINGE VISIBILITY AS A FUNCTION OF ANGLE OF INCIDENCE FOR BOTH P AND S-POLARIZED LIGHT
COMPLEX REFRACTIVE INDEX OF SUBSTRATE IS NC=N-I(K). M=CK1+CM2(LAMBDA-3800.) K=CK1+CK2(LAMBDA-3800.)
LAMBDA IS THE WAVELENGTH BETWEEN 3800. AND 7800. A. CK1= 2.0700000 CM2= 0.0000000 CK1= 4.4000000 CK2= 0.0000000

WAVELENGTH IS 5892 A
REFRACTIVE INDEX OF FILM IS 1.3980
COMPLEX REFRACTIVE INDEX OF SUBSTRATE- N= 2.0700 K= 4.4000

ANGLE	MINIMUM		MAXIMUM		VISIBILITY	
	S	P	S	P	S	P
0.00	.54648	.54640	.71981	.71981	.13641	.13641
1.00	.54641	.54639	.71905	.71897	.13643	.13639
2.00	.54643	.54637	.71916	.71886	.13649	.13633
3.00	.54646	.54634	.71935	.71867	.13658	.13623
4.00	.54650	.54630	.71961	.71841	.13672	.13609
5.00	.54656	.54624	.71994	.71808	.13698	.13591
6.00	.54663	.54618	.72035	.71766	.13712	.13569
7.00	.54670	.54610	.72084	.71717	.13738	.13542
8.00	.54679	.54601	.72140	.71661	.13768	.13512
9.00	.54689	.54591	.72203	.71597	.13802	.13476
10.00	.54700	.54580	.72274	.71525	.13840	.13437
11.00	.54712	.54569	.72352	.71445	.13883	.13392
12.00	.54724	.54557	.72438	.71357	.13938	.13342
13.00	.54737	.54544	.72531	.71261	.13981	.13288
14.00	.54751	.54532	.72631	.71157	.14037	.13227
15.00	.54764	.54519	.72739	.71045	.14097	.13162
16.00	.54778	.54505	.72854	.70924	.14162	.13090
17.00	.54792	.54492	.72977	.70795	.14232	.13012
18.00	.54806	.54480	.73107	.70657	.14307	.12928
19.00	.54820	.54466	.73244	.70510	.14387	.12836
20.00	.54833	.54456	.73389	.70354	.14472	.12738
21.00	.54845	.54446	.73541	.70189	.14562	.12631
22.00	.54857	.54437	.73700	.70015	.14658	.12517
23.00	.54867	.54429	.73867	.69830	.14759	.12394
24.00	.54876	.54424	.74041	.69636	.14866	.12263
25.00	.54883	.54420	.74222	.69432	.14980	.12121
26.00	.54888	.54419	.74411	.69218	.15098	.11970
27.00	.54890	.54421	.74607	.68993	.15225	.11808
28.00	.54889	.54426	.74810	.68757	.15358	.11634
29.00	.54887	.54434	.75020	.68509	.15498	.11448
30.00	.54880	.54447	.75237	.68250	.15645	.11250
31.00	.54870	.54464	.75462	.67979	.15799	.11038
32.00	.54855	.54486	.75693	.67696	.15962	.10812
33.00	.54836	.54513	.75932	.67399	.16133	.10570
34.00	.54811	.54547	.76178	.67090	.16312	.10312
35.00	.54780	.54587	.76431	.66767	.16501	.10037
36.00	.54743	.54634	.76691	.66429	.16699	.09743
37.00	.54699	.54689	.76958	.66077	.16907	.09430
38.00	.54647	.54752	.77232	.65709	.17126	.09096
39.00	.54586	.54825	.77513	.65325	.17356	.08739
40.00	.54517	.54907	.77801	.64924	.17597	.08360
41.00	.54438	.55000	.78096	.64506	.17851	.07955
42.00	.54348	.55104	.78398	.64070	.18118	.07524
43.00	.54246	.55221	.78706	.63615	.18398	.07064
44.00	.54131	.55350	.79022	.63140	.18693	.06574
45.00	.54003	.55494	.79344	.62643	.19004	.06052
46.00	.53859	.55653	.79673	.62125	.19331	.05495
47.00	.53700	.55828	.80009	.61584	.19676	.04902
48.00	.53523	.56021	.80351	.61018	.20040	.04270
49.00	.53327	.56231	.80700	.60427	.20424	.03597
50.00	.53110	.56462	.81055	.59809	.20829	.02879
51.00	.52872	.56713	.81418	.59162	.21257	.02114
52.00	.52609	.56986	.81786	.58486	.21710	.01299
53.00	.52320	.57283	.82161	.57777	.22190	.00429
54.00	.52003	.57034	.82543	.57604	.22698	.00496
55.00	.51656	.56255	.82931	.57953	.23237	.01486
56.00	.51276	.55438	.83325	.58329	.23810	.02541
57.00	.50860	.54581	.83725	.58734	.24420	.03666
58.00	.50405	.53679	.84132	.59171	.25069	.04866
59.00	.49908	.52732	.84544	.59641	.25761	.06148
60.00	.49366	.51735	.84963	.60148	.26500	.07517
61.00	.48774	.50685	.85388	.60688	.27291	.08988
62.00	.48128	.49578	.85819	.61265	.28139	.10544
63.00	.47423	.48410	.86256	.61885	.29050	.12217
64.00	.46653	.47177	.86699	.62547	.30038	.14008
65.00	.45814	.45873	.87147	.63253	.31086	.15926
66.00	.44899	.44494	.87601	.64009	.32228	.17983
67.00	.43900	.43033	.88061	.64808	.33465	.20190
68.00	.42809	.41484	.88526	.65656	.34809	.22561
69.00	.41619	.39841	.88997	.66559	.36273	.25110
70.00	.40318	.38096	.89474	.67516	.37872	.27856
71.00	.38897	.36242	.89959	.68529	.39629	.30817
72.00	.37344	.34270	.90442	.69608	.41552	.34014
73.00	.35646	.32172	.90934	.70732	.43676	.37471
74.00	.33789	.29941	.91432	.71924	.46033	.41215
75.00	.31758	.27567	.91934	.73180	.48650	.45274
76.00	.29538	.25046	.92441	.74501	.51569	.49688
77.00	.27113	.22374	.92953	.75887	.54837	.54460
78.00	.24468	.19551	.93470	.77348	.58506	.59643
79.00	.21594	.16588	.93991	.78861	.62639	.65243
80.00	.18488	.13507	.94517	.80451	.67280	.71249
81.00	.15180	.10395	.95047	.82109	.72488	.77801
82.00	.11693	.07220	.95582	.83836	.78286	.84141
83.00	.08053	.04257	.96120	.85631	.84521	.90528
84.00	.04298	.01743	.96663	.87494	.90934	.96093
85.00	.01640	.00177	.97210	.89423	.96683	.99805
86.00	.00836	.00476	.97761	.91418	.99926	.98985
87.00	.01505	.04388	.98315	.93475	.96985	.91032
88.00	.09859	.15432	.98874	.95593	.81866	.72201
89.00	.34290	.41219	.99435	.97769	.48716	.44667
90.00	1.00004	1.00003	1.00000	1.00000	-.00002	-.00002

REFERENCES

1. F. G. Will, J. Electrochem. Soc. 110(2), 145 (1963).
2. F. G. Will, J. Electrochem. Soc. 110(2), 152 (1963).
3. E. Justi, M. Pilkuhn, W. Scheibe and A. Winsel, High-Drain, Hydrogen-Diffusion Electrodes Operating at Ambient Temperature and Low Pressure, Verl. d. Akad. d. Wissensch. u.d. Lit., Wiesbaden, 1959, p. 33.
4. R. P. Iczkowski, J. Electrochem. Soc. 111(9), 1078 (1964).
5. H. J. R. Maget and R. Roethlein, J. Electrochem. Soc. 112(10), 1034 (1965).
6. D. N. Bennion and C. W. Tobias, J. Electrochem. Soc. 113(6), 589 (1966).
7. T. Katan, S. Szpak and E. A. Grens, J. Electrochem. Soc. 112(12), 1166 (1965).
8. V. P. Belokopytov, N. A. Aladzalova, N. D. Borisova, Yu. G. Chirkov, Soviet Electrochem. 4(11), 1159 (1968).
9. R. Kh. Burshtein, M. R. Tarasevich, S. F. Chernyshyov and V. V. Karasev, Societ Electrochem. 3(7), 803 (1967).
10. R. Kh. Burshtein, M. R. Tarasevich, S. F. Chernyshov and Yu. G. Chirkov, Soviet Electrochem. 4(11), 1154 (1968).
11. V. A. Shepelin, Soviet Electrochem. 3(8), 896 (1967).
12. E. N. Lightfoot, J. Electrochem. Soc. 113(6), 614 (1966).
13. V. Ludviksson and E. N. Lightfoot, A. I. Ch. E. Journal 14(4), 674 (1968).
14. E. N. Lightfoot and V. Ludviksson, J. Electrochem. Soc. 113(12), 1325 (1966).

15. Yu. A. Chizmadzhev and V. S. Markin, Soviet Electrochem. 2, 1246 (1966).

16. S. V. Chesnokov, Soviet Electrochem. 4, 1354 (1968).

17. S. V. Chesnokov, Soviet Electrochem. 5, 113 (1969).

18. Yu. G. Chirkov, V. S. Markin and V. S. Chesnokov, Soviet Electrochem. 6, 875 (1970).

19. S. F. Chernyshov, R. Kh. Burshtein, M. R. Tarasevich and A. V. Yalyshev, Soviet Electrochem. 6, 919 (1970).

20. R. H. Muller, J. Electrochem. Soc. 113(9), 943 (1966).

21. W. D. Bascom, R. L. Cottington and C. R. Singleterry in Contact Angle, Wettability and Adhesion, R. F. Gould, ed. (American Chemical Society, Washington D. C., 1964), p. 355.

22. J. J. Bikerman, J. Colloid Science 11(4), 299 (1956).

23. J. J. Bikerman, Kolloid Zeitschrift und Zeitschrift für Polymere 218(1), 52 (1967).

24. H. Jeffreys, Proceedings Cambridge Phil. Soc. 26, 204 (1930).

25. A. D. Read and J. A. Kitchener, SCI Monograph No. 25, p. 301.

26. B. V. Deryagin in Research in Surface Forces, A special research report translated from Russian (Consultants Bureau, New York, 1962), Vol. 2, p. 23.

27. J. H. Turney, Profiles of Supermeniscus Electrolyte Films on Partially Submerged Gas Electrodes (M. S. Thesis), LBL-171, Aug. 1971.

28. H. Gu, Ellipsometry of Surface Layers (M. S. Thesis), LBL-165, Dec. 1971.

29. H. Kubota, Interference Color in Progress in Optics, E. Wolf, ed. (Interscience Publishers, Inc., New York, 1961), Vol. 1, p. 212.

30. C. R. Brown, Interferometry of Solid Thin Films (M. S. Thesis), LBL-2264, Dec. 1973.

31. R. H. Muller, J. Opt. Soc. Am. 54(3), 419 (1964).

32. F. A. Jenkins and H. E. White, Fundamentals of Optics, 3rd ed. (McGraw-Hill Book Company, Inc., New York, 1957), p. 271.

33. W. Koenig in Handbuch der Physik, H. Geiger and K. Scheel, eds. (Springer, Berlin, 1928), Vol. XX.

34. J. R. Mowat and R. H. Muller, Reflection of Polarized Light from Absorbing Media, University of California, Lawrence Berkeley Laboratory, UCRL-11813, 1966.

35. R. W. Ditchburn, Light, 2nd ed. (Interscience Publishers, Inc., New York, 1963).

36. A. Vasicek, Optics of Thin Films (North Holland Publishing Company, Amsterdam: Interscience Publishers, Inc., New York, 1960).

37. M. Born and E. Wolf, Principles of Optics, 4th ed. (Permagon Press, New York, 1970).

38. W. D. Wright, The Measurement of Colour, 4th ed. (Adam Hilger, LTD, London, 1969).

39. The Science of Color, Committee on Colorimetry Optical Society of America, 1963.

40. K. L. Kelley, J. Opt. Soc. Am. 33(11), 627 (1943).

41. W. D. Wright, J. Opt. Soc. Am. 33(11), 632 (1943).

42. H. Kubota and T. Ose, J. Opt. Soc. Am. 45(2) (1955).

43. International Critical Tables, 1st ed., 1929, Vol. V, p. 248.

44. Landolt-Bornstein Tables, Optishe Constanten (Springer, Germany, 1962), Vol. II, pt. 8.

45. K. Vedam. W. Knausenberger and F. Lukes, J. Opt. Soc. Am. 59(1), 64 (1969).

46. G. B. Irani, T. Huen and F. Wooten, J. Opt. Soc. Am. 61(1), 128 (1971).

47. M. Otter, Zeitschrft für Physik 161, 163 (1961).

48. J. W. Seeser, App. Opt. 14(3), 640 (1975).

49. Bausch and Lomb Precision Refractometer, Catalog Number 33-45-03.

50. H. J. Mathieu, D. E. McClure and R. H. Muller, Rev. Sci. Instrum. 45(6), 798 (1974).

51. R. H. Muller, Principles of Ellipsometry in Advances in Electrochemistry and Electrochemical Engineering (John Wiley and Sons, New York, 1973), Vol. 9, p. 167.

52. L. Holland, Vacuum Deposition of Thin Films (John Wiley and Sons, 1956).

53. Handbook of Chemistry and Physics, 47th ed., p. B-280.

54. O. S. Heavens, Optical Properties of Thin Solid Films (Dover Publications, Inc., New York, 1965).

55. H. J. Mathieu, Computer Programs for Ellipsometry, LBL-1470, May 1973.

56. R. B. Bird, W. E. Stewart and E. N. Lightfoot, Transport Phenomena (John Wiley and Sons, New York, 1960), p. 70.

57. D. N. Bennion, Phenomena at a Gas-Electrode-Electrolyte Interface, Department of Chemical Engineering, University of California, Berkeley, June 1964.

TECHNICAL INFORMATION DIVISION
LAWRENCE BERKELEY LABORATORY
UNIVERSITY OF CALIFORNIA
BERKELEY, CALIFORNIA 94720